THE UNIVERSITY *of* EDINBURGH

Chapter 1

Introduction

1.1 Obesity impact and anti-obesity therapies

1.1.1 Worldwide burden of obesity

Obesity is a major health problem that has reached epidemic proportions worldwide. The World Health Organisation (WHO) defines obesity as a body mass index (BMI) greater than 30kg/m^2 and also predicts that there will be approximately 2.3 billion overweight people aged 15 years and above and over 700 million obese people worldwide by 2015 (WHO; http://www.who.int/mediacentre/factsheets/fs311/en/). Scotland has one of the highest levels of obesity (27% of adults and 15% of children) in the world, with only the USA and Mexico having higher levels http://www.scotlandgov.uk/Publications/2010/02/17140721/4). In addition to its associated adverse health consequences, obesity-associated healthcare is a serious economic burden. In Europe alone, up to €10.4 billion was spent on obesity-related healthcare in 2009 (Muller-riemenschneider *et al.,* 2009) mainly due to the expenditure on co- morbidities including Type II diabetes, cardiovascular diseases, various cancers, and the attendant increase in morbidity and mortality (Mokdad *et al.,* 2003; Brown *et al.,* 2009; Guh *et al.,* 2009).

Therapeutic intervention for obesity has proven extremely challenging. Obesity is a complex trait involving the interaction of genes involved in fundamental aspects of weight maintenance, exposure to an environment characterised by an over-abundance of food and sedentary life-style choices with limited physical activity (Poskitt 2009). A marked shift in diet has occurred worldwide (Popkin 2001) with greater saturated fat intake, reduced intake of complex carbohydrates and dietary fibre, and reduced fruit and vegetable intake (WHO 2003).

In terms of pharmacological strategies, the current anti-obesity drugs on the market are primarily concerned with reducing appetite or fat absorption in the gut. These include; *Sibutramine*, a neurotransmitter (serotonin and dopamine) reuptake inhibitor which increases the levels of these substances in synaptic

clefts, suppressing appetite by producing a feeling of satiety; *Rimonabant*, a cannabinoid receptor (CB1) antagonist, which causes decreased appetite and *Orlistat*, which acts by preventing fat absorption through inhibiting lipases (which break down triglycerides in the gut). However, serious side effects have been documented with some of these drugs, including an increased rate of cardiovascular events with Sibutramine use (Curfman *et al.,* 2010). In 2007, the Scottish Medicines Consortium removed *Rimonabant* from use in the NHS Scotland due to risks of adverse psychiatric events (Burch *et al.,* 2009). However, despite these setbacks, there have been considerable advancements in the treatment of obesity, achieved by combining pharmacological treatments with diet, exercise, behavioral approaches and surgery (gastric band surgery and liposuction). However, the prevalence of obesity continues to increase inexorably, particularly in the Asia Pacific region (Gill 2006; Low *et al.,* 2009), and thus further advancements in obesity treatment are needed, ideally avoiding invasive procedures such as surgery.

1.1.2 Interaction between adipocytes and endothelial cells: potential anti-obesity therapy?

Effective anti-obesity treatment is hindered further by the complexity of adipose biology, particularly the interaction of the plethora of factors within the adipose tissue that modulate its expansion and function. For example, obesity results from both an increase in size of the adipocyte and an increase in the number of adipocytes. A host of metabolically-active proteins secreted by adipocytes, including adipokines, affect adipose growth and many of the obesity-associated pathologies (Chaldakov *et al.,* 2003; Gimeno and Klaman 2005; Kershaw *et al.,* 2004; Ronti *et al* 2006). Moreover, adipose tissue contains non-adipose stromal-vascular cells including endothelial cells. Endothelial cells are important in blood vessel formation, primarily to regulate the blood supply to the adipose tissue, supplying both oxygen and nutrients and hence affecting adipose tissue growth. As expected, several studies have underlined the importance of these endothelial cells in the development of adipose tissue (Hutley *et al.,* 2001; Aoki *et al.,* 2003; Fukumura *et al.,* 2003) and suggest that

interaction between these two cell types represents a target to control adipose tissue growth. However, it is currently uncertain whether adipocytes primarily regulate adipose tissue blood vessel development or, conversely, adipose tissue blood vessel growth dominantly controls adipose tissue expansion.

This thesis attempts to address the relationship between endothelial cells (and associated blood vessel development) and the growth of adipose tissue during obesity. To provide the relevant frame of reference, a comprehensive review of adipocyte and blood vessel function is provided.

1.2 Adipocyte Physiology

1.2.1 Lipid storage and uptake

A fundamental role for adipocytes is storage and synthesis of fatty acids (FA), also known as lipogenesis. Lipogenesis encompasses the processes of fatty acid synthesis and subsequent triglyceride (TG) synthesis, and takes place in both the liver and the adipose. Lipogenesis is tightly hormonally regulated, in particular by insulin (Figure 1.1) in conjunction with the nutritional state (for review see Kolditz and Langin 2010). For example, lipogenesis is stimulated in the fed state, particularly by diets high in carbohydrates (via insulin) and inhibited by fasting (and dietary polyunsaturated FA). Insulin increases the uptake of glucose in adipocytes via recruitment of glucose transporters (Glut4) to the plasma membrane (Kaestner *et al.,* 1991). These effects are achieved by the binding of insulin to the insulin receptor at the cell surface, thus activating its tyrosine kinase activity and many downstream effects via tyrosine phosphorylation (Nakae & Accili 1999). Insulin also has longer-term effects on the expression of lipogenic genes via the transcription factor sterol regulatory element binding protein-1 (SREBP-1) (Hua *et al.,* 1993; Tontonoz *et al.,* 1993; Assimacopoulos-Jeannet *et al.,* 1995).

Growth hormone (GH) can also inhibit lipogenesis, which can result in a significant loss of fat and associated gain of muscle mass (Etherton 2000). This may be mediated by GH decreasing insulin sensitivity, resulting in down-regulation of fatty acid synthase expression in adipose tissue (Yin *et al.,* 1998).

Leptin is another hormone that has a key feedback inhibitory effect on adipocyte lipogenesis. Leptin, one of the most abundant adipocyte proteins, is secreted in proportion to the fat mass and signals to the hypothalamus to reduce energy intake (see section 1.3.1 on adipokines). It is also thought to affect metabolic pathways in adipose tissue by stimulating the release of glycerol from adipocytes (Siegrist-Laiser *et al.,* 1997). Leptin achieves this by both stimulating FA oxidation and inhibiting lipogenesis (Bai *et al.,* 1996), which in turn is accomplished by down-regulating the expression of genes involved in FA and TG synthesis (Soukas *et al.,* 2001). Leptin-mediated changes in expression of lipogenic genes may be mediated through a pathway involving stimulation of SREBP-1 (Hua *et al.,* 1993; Tontonoz *et al.,* 1993). SREBPs are transcription factors that regulate the expression of genes connected with cholesterol and fatty acid metabolism (Yokoyama *et al.,* 1993). However, they are not the only transcription factors involved. *In vitro* studies have established the importance of the up-stream stimulatory factors (USFs) in regulation of the fatty acid synthase promoter by insulin (Wang and Sul 1997). Another important transcription factor in adipose tissue is peroxisome proliferator-activated receptor γ (PPAR)γ, which triggers adipocyte differentiation by inducing the expression of several genes critical for adipogenesis. Indeed, a number of adipose related genes are regulated by PPARγ, including fatty acid binding protein (FATP) and acyl-CoA synthetase (Kersten *et al.,* 2000). The regulation of these adipose genes, coupled with evidence suggesting PPARγ expression is stimulated by insulin (Vidal-Puig *et al.,* 1997) and SREBP-1 (Fajas *et al.,* 2000), means PPARγ is both an adipogenic and lipogenic factor. This has been supported by clinical data which show that patients prescribed synthetic PPARγ agonists frequently gain fat mass (Fuchtenbusch 2000).

In addition to de novo lipogenesis, adipose tissue can also take up and store FFA in the form of TG. This process is mediated by two major pathways; a passive component, and a saturable component that exhibits the characteristics of a protein-facilitated process (Pohl *et al.,* 2004). A model proposed for the passive component involves the “flip-flop” of fatty acids into the inner membrane. This

hypothesis and name is based on the assumption that transfer of fatty acids across the lipid bilayers in adipocytes would occur through diffusion and is very rapid (Hamilton 1998). The second component of lipid uptake involves proteins in the plasma membrane of adipocytes, which are implicated in the facilitated fatty acid transport, including caveolin-1 (Trigatti *et al.,* 1999) and fatty acid translocase (FAT- also known as CD36). When over-expressed in fibroblasts, FAT/CD36 increases fatty acid uptake (Ibrahimi *et al.,* 1996) and FAT/CD36 deficient mice have increased serum fasting levels of non-esterifed free fatty acids (NEFA) and show reduced NEFA uptake in isolated adipocytes (Febbraio *et al.,* 1999). This confirms the essential role played by FAT/CD36 in facilitated FA transport, alongside movement of FA by "flip-flop".

Circulating FFAs taken up into the adipose tissue can be the product of TG hydrolysis by lipoprotein lipase (LPL). The enzyme is associated with the luminal side of capillaries and arteries, where it hydrolyses TG to produce FFAs. LPL converts chylomicrons to remnants and begins the cascade required for conversion of very low density lipoprotein (VLDL) to low density lipoprotein (LDL).

1.2.2 Lipolysis

In addition to the uptake of FA, one of the other major processes of WAT is lipolysis, the release of free fatty acids (FFA) and glycerol from triglycerides (TG). This process is stimulated when the organism needs to mobilize energy, such as during times of prolonged fasting or exercise. Under normal circumstances (basal), there is tight, hormonal, regulatory control of lipolysis, provided by catecholamines and insulin (Figure 1.1). However, perturbations in normal lipolysis are associated with obesity, including increased basal rates of lipolysis that contribute to the development of insulin resistance and impaired stimulation of lipolysis (Reynisdottir *et al.,* 1995; Large *et al.,* 1999). Therefore, lipolysis has an important role in energy metabolism and is vital to metabolic health.

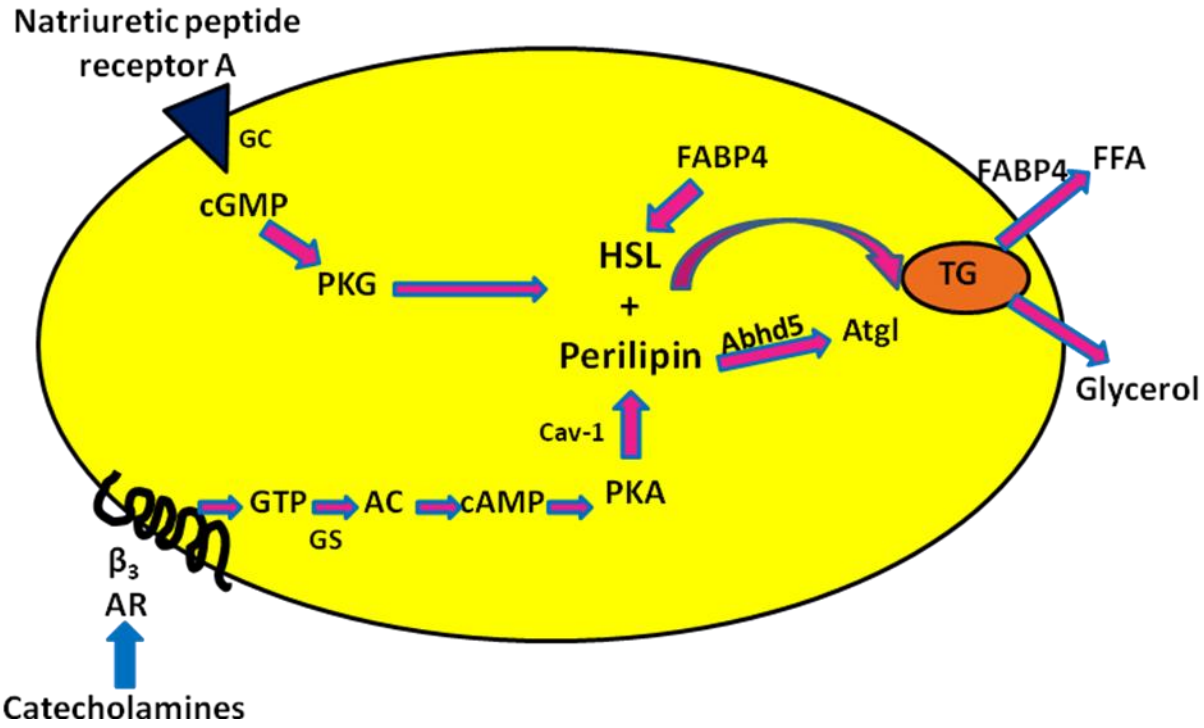

Figure 1.1: Stimulation of lipolysis in adipocytes. Signal transduction pathways for catecholamines via adrenoceptor (AR) and pathways associated with activation by natriuretic peptides. Beta (β) AR stimulation increases GTP binding to Gs, which activates adenylyl cyclase (AC), increasing cyclic adenosine monophosphate (cAMP) production. cAMP-dependent protein kinase (PKA) is activated which leads to the phosphorylation and activation of hormone sensitive lipase (HSL) and perilipin A. This promotes translocation to the surface of the lipid droplet shown in orange. Caveolin-1 (Cav-1) facilitates the interaction between PKA and perilipin. Phosphorylation of perilipin also activates ATGL through Abhd5, leading to hydrolysis of triglycerides (TG) and release of fatty acids (FA) and glycerol, produced by the hydrolysis of TG. Adipocyte lipid binding proteins (e.g. FABP4), facilitate non-esterified fatty acid (NEFA) trafficking between metabolic enzymes and membranes. FABP4 also binds to HSL in response to stimulated lipolysis. GTP, guanosine triphosphate binding protein; cGMP, cyclic guanosine monpohosphate; GC, guanylyl cyclase; PKA, protein kinase A; TG, triglycerides; FFA, free fatty acids.

Lipolysis may be stimulated by the hormone adrenaline and noradrenaline (which acts as a neurotransmitter), in response to fasting or exercise, through the activation of β_1 and β_2-adrenergic receptors (AR), and the β_3-adrenergic receptor in rodents. Coupling of the β-ARs to stimulatory guanosine triphosphate-(GTP)-binding proteins, activates adenylyl cyclase, increasing cyclic adenosine-3',5'-monophosphate (cAMP) production. A rise in cAMP activates protein kinase A (PKA). PKA activity is thought to increase lipolysis by phosphorylating two substrates; the lipid-droplet (LD) associated protein, perilipin (Peri A is the predominant perilipin isoform in adipocytes) (Greenberg *et al.,* 1993) and hormone sensitive lipase (HSL), a major lipase in adipocytes (Friedrikson *et al.,* 1981; Holm 2003; Yeaman 2004). HSL phosphorylation by PKA increases HSL activity and also, more importantly, promotes translocation of HSL from the cytosol to the LD (Egan *et al.,* 1992). This interaction between HSL, perilipin and lipid stores at the LD surface is thought to account for the majority of catecholamine-stimulated (versus basal) lipolysis (Brasaemle *et al.,* 2000). The complexity of lipolysis recently increased due to the identification of adipose triglyceride lipase protein (ATGL) (Villena *et al.,* 2004; Zimmerman *et al.,* 2004) and Abhd5, a perlipin-interacting protein (Subramanian *et al.,* 2004; Yamaguchi *et al.,* 2004) and coactivator of ATGL (Lass *et al.,* 2006). Genetic deletion of ATGL has demonstrated its importance in basal and stimulated lipolysis, as it is known to catalyse the initial step in triglyceride hydrolysis in adipocyte LDs (Zimmermann *et al.,* 2004; Haemmerle *et al.,* 2006). Further work has indicated that PKA phosphorylation of perilipin activates ATGL indirectly through its direct interactions with Abhd5 (Granneman *et al.,* 2007). Furthermore, FABP4, or adipocyte lipid binding protein, is thought to make NEFAs more soluble and facilitate their intracellular trafficking between metabolic enzymes (including HSL) and membranes (Winder 1998). FABP4 binds to HSL, in response to stimulated lipolysis (Winder *et al.,* 1990).

In human adipocytes, an additional signal transduction pathway independent of catecholamines is implicated in pro-lipolytic events. Natriuretic peptides bind type A receptors, which possess intrinsic guanylyl cyclase activity. Rises in cyclic guanosine 3',5'-monophosphate (cGMP) activate PKG, which phosphorylates

HSL and perilipin (Sengenes *et al.,* 2000) in a PKA-like manner. Stimulation of lipolysis by natriuretic peptides is of a similar magnitude to that of catecholamines and is known to be particularly prominent in exercise (Moto *et al.,* 2004; Lafontan *et al.,* 2005).

Until recently HSL was thought to be the rate limiting enzyme in lipolysis, as it is highly expressed in WAT (Holm *et al.,* 1987) and displays high hydrolytic activity for TG, diacylglycerols (DAG), monoacylglycerols and cholesterol (Fredrikson *et al.,* 1981; Grober *et al.,* 2003). However, other factors potently regulate lipolysis including lipases, cofactors and lipid associated proteins (see Zechner *et al.,* 2005 for review). One of these lipid associated proteins is caveolin-1. Caveolae are small invaginations on cell plasma membranes (Patel *et al.,* 2008), which are abundant in adipocytes (Thorn *et al.,* 2003). Expression of caveolin-1 results in increased formation of these invaginations on cell membranes (Parton *et al.,* 2006). Caveolae have several functions including participation in signal transduction (Drab *et al.,* 2001) and NEFA binding and transport (Trigatti *et al.,* 1999). Caveolin-1 is known to associate with the LDs and therefore a role in lipolysis has been implicated (Fujimoto *et al.,* 2001; Ostermeyer *et al.,* 2001; Pol *et al.,* 2001). In accordance with this, caveolin-1 deficient mice displayed a decreased lipolytic response to pharmacological stimulation of lipolysis (with the β_3 agonist CL-316, 243) (Cohen *et al.,* 2004). Perilipin phosphorylation is also decreased in the absence of caveolin-1, suggesting caveolin-1 facilitates the interaction between PKA and perilipin (Cohen *et al.,* 2004). This together suggests a pro-lipolytic function for caveolin-1, via perilipin phosphorylation (Bezaire and Langin 2009).

As well as the stimulation of lipolysis, catecholamines can also inhibit lipolysis via the activation of α_2-AR and their coupling to inhibitory GTP-binding proteins (Figure 1.2). This binding to GTP-binding protein inhibits adenylyl cyclase action and cAMP production. Therefore, AR-dependent lipolysis is dictated by the combined effects mediated by the balance of pro-lipolytic β-AR and anti-lipolytic α_2-AR (Wang *et al.,* 2008). The impairment of PKA-stimulated lipolysis

observed in obesity results from accentuated stimulation of α-AR (Jensen *et al.,* 1989; Lafontan & Berlan 1995; Stitch *et al.,* 2000).

The most potent inhibitor of lipolysis is the hormone insulin, which signals for the energy replete state and, thus, activation of energy storage pathways (see Lipogenesis 1.2.1 above). Insulin binding to its receptor activates the insulin receptor substrate 1, PI3Kinase and phosphodiesterase 3B, which degrades cAMP and consequently reduces PKA activation (for review see Carmen and Victor 2006). In addition, adenosine 5'-monophosphate-activated protein kinase (AMPK) can also inhibit lipolysis (Sullivan *et al.,* 1994; Corton *et al.,* 1995), by targeting and binding to HSL (Figure 1.2).

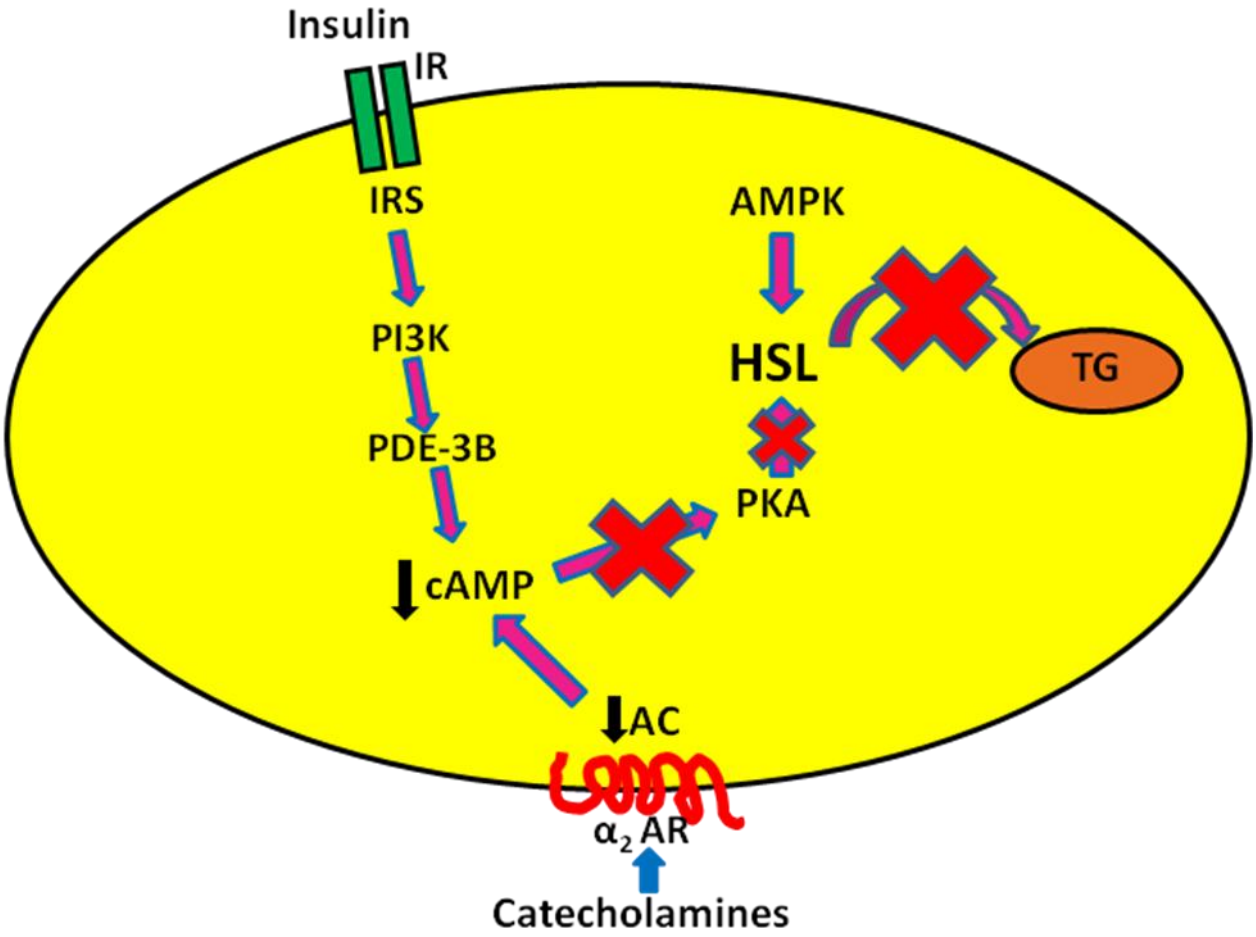

Figure 1.2: Inhibition of lipolysis in human adipocytes. Signal transduction pathways for catecholamines via adrenoceptor (AR) and insulin causing inhibition of lipolysis. α_2-AR binding to inhibitory GTP-binding protein inhibits adenylyl cyclase (AC) and decreases cyclic adenosine monophosphate (cAMP). Insulin binds to the insulin receptor (IR), activating insulin receptor substrate (IRS), phosphatidylinositol-3-phosphate kinase (PI3K) and phosphodiesterase 3B (PDE-3B), decreasing cAMP and PKA activation. Adenosine 5'-monophosphate-activated protein kinase (AMPK) inhibits lipolysis by binding to HSL. TG; triglycerides.

1.2.3 The role of adipocyte size and number in obesity

Increased lipogenesis and/or decreased lipolysis are responsible for increased adipocyte size (hypertrophy), and thus, in part, for obesity. However, this remains too simplistic a view as pharmacological activation of lipolysis has been attempted as an anti-obesity strategy. This was with the aim of reducing adipocyte hypertrophy by increasing lipolysis (Crandall *et al.,* 2006). Lipid storage by adipocytes serves a protective function, shielding the liver, pancreas and muscle against the adverse effects of ectopic lipid accumulation in these non-adipose tissues (lipotoxicity) (Dubois *et al.,* 2004; Liu *et al.,* 2006; McGarry and Dobbins 1999; Schaffer 2003). This protective function of the adipose tissue is illustrated well when there is a complete lack of adipose tissue, which is known as lipodystrophy. Lipodystrophy is associated with insulin resistance in muscle and with liver steatosis, mainly due to the lipotoxic effects of excessive ectopic storage of lipids in these tissues (Kim *et al.,* 2000; Garg 2004). However, increased adipocyte size has also been correlated with insulin resistance and increased risk of developing type 2 diabetes (Bjorntorp *et al.,* 1971; Krotkiewski *et al.,* 1983; Lundgren *et al.,* 2007). Interestingly, obese patients with fewer, large adipocytes are more glucose intolerant and hyperinsulinemic that those with the same degree of obesity but possessing metabolically active, small adipocytes (Stern *et al.,* 1972; Arner *et al.,* 2009).

Adipogenesis, the process whereby stromal preadipocytes can differentiate into adipocytes, forms a further key contribution to adipose tissue growth in obesity. Adipogenesis requires the growth arrest of proliferating preadipocytes and is initiated by the activation of several transcription factors, including peroxisome proliferator-activated receptor gamma (PPARγ) (Rosen *et al.,* 1999). This process is also accompanied by an increase in expression of adipocyte genes including adipocyte fatty acid binding protein and lipid metabolising enzymes (Gregoire *et al.,* 1998). The presence of adipogenesis throughout life has been supported by evidence showing early markers of adipocyte differentiation in very old mice (>2years) (Kirkland *et al.,* 1990). Moreover, fat cell precursors isolated from adult WAT from various species, including humans, have been

differentiated *in vitro* into mature adipocytes (Bjorntorp *et al.,* 1982; Deslex *et al.,* 1987; Gregoire *et al.,* 1995; Hauner *et al.,* 1997). Adipocyte cell number was increased when both rats and humans were fed a high-carbohydrate or high fat diet (Faust *et al.,* 1984; Miller *et al.,* 1984). Recent evidence (Spalding *et al.,* 2008) suggests that after a key phase of adipocyte number determination in early adulthood, adipocyte hypertrophy becomes the main determinant of overall obesity. This work also indicated that the rate of adipocyte turnover is slow and appears to be very tightly regulated and is, thus, a potential therapeutic target.

1.3 Adipose tissue as an endocrine organ

The simplistic view of adipose as a metabolically inert organ, which serves to synthesize and release lipids, has long been superseded. It has become clear over the last two decades that adipose tissue can also be regarded as a dynamic endocrine organ, as well as a highly active metabolic tissue (see Galic *et al.,* 2010 for review). Adipocytes produce a wide range of factors, which are involved in glucose homeostasis/insulin sensitivity (e.g. adiponectin, resistin, tumour necrosis factor (TNF-α)), inflammation (e.g. interleukin-6 (IL-6), monocyte chemoattractant protein-1 (MCP-1), macrophage inflammatory protein-1 α (MIP-1α) and TNF-α), appetite (e.g. leptin) and blood vessel development or angiogenesis (Hotamisligil *et al.,* 1993; Trayhurn and Wood 2005; Lago *et al.,* 2007). Many factors released from adipocytes may play a further role in the development and expansion of adipose tissue and its associated blood vessel development.

1.3.1. Adipokines link adipocyte function and angiogenesis

Given that a central aim of this thesis to delineate the crosstalk between adipocytes and angiogenesis in adipose tissue expansion, it is important to set a precedent for such interactions. There are many factors released by adipocytes that have additional effects upon endothelial cells. Specific examples include leptin, which acts directly in the hypothalamus as a satiety signal (Elmquist *et al.,* 1998) and has peripheral effects on the liver, pancreas, muscle and adipose

tissue (Huang and Li 2000). Genetic deletion or knockdown of leptin action leads to severe obesity, diabetes and infertility in mice (Friedman *et al.,* 1998). However, leptin is a key adipokine that affects adipose vasculature directly as it is a potent activator of angiogenesis. Leptin is known to increase vascular permeability of blood vessels and also displays a synergistic angiogenic growth effect with fibroblast growth factor-2 (FGF-2) and vascular endothelial growth factor (VEGF) (Cao *et al.,* 2001a). This pro-angiogenic role is mediated by the functional long form of the leptin receptor (OB-Rb) in endothelial cells (Sierra-Honigmann *et al.,* 1998). OB-Rb activation in endothelial cells promotes tube formation (an essential part of angiogenesis discussed below section 1.6.3) and leptin up-regulates the secretion of vascular endothelial growth factor (VEGF) via activation of the Jak/Stat3 signaling pathway (Suganami *et al.,* 2004). Leptin induces matrix metalloproteinase (MMP-2 and MMP-9) activity which can indirectly facilitate angiogenesis (Park *et al.,* 2001). Leptin also induces endothelial nitric oxide synthase-mediated vasodilatation (Tigno *et al.,* 2003) and is essential for the growing vascular demand of adipose. Therefore, in addition to being an important adipokine involved in adipose metabolism, leptin also serves as a strong mediator of endothelial function. Such evidence hints once more at a critical interaction between factors secreted during the expansion of adipose in obesity and regulation of angiogenesis within this tissue.

Resistin is another adipocyte-derived secretory factor, which has a significant role in the regulation of obesity-induced insulin resistance (Steppan *et al.,* 2001) but also can be a pro-angiogenic stimulus which affects adipose vasculature by inducing the expression of adhesion molecules (Kawanami *et al.,* 2004). This up-regulation of adhesion molecules and also chemokines in endothelial cells can then promote endothelial cell proliferation and migration (Mu *et al.,* 2006). Infusion or over-expression of resistin leads to hyperglycaemia (Banerjee *et al.,* 2004; Qi *et al.,* 2006) whereas reducing circulating resistin by gene knockout protects against obesity-induced hyperglycaemia (Steppan *et al.,* 2001).

Another important adipokine, which has dual functionality on both adipocytes and endothelial cells, is adiponectin. Adiponectin is an adipocyte-derived insulin-sensitising agent (Bouskila *et al.,* 2005) that increases fatty acid oxidation in muscle and liver, in part through the activation of peroxisome proliferator activated receptor alpha (PPARα) (Heilbronn *et al.,* 2003). Moreover, adiponectin-induced activation of adenosine monphosphate-activated protein kinase (AMPK) leads to glucose uptake via translocation of the glucose transporter GLUT4 to the cell membrane in skeletal muscle (Ceddia *et al.,* 2005). Adiponectin also inhibits the adhesion of macrophages to endothelial cells (Ouchi *et al.,* 1999) and may therefore play an important role in regulating the infiltration of adipose by macrophages that occurs during obesity. Adiponectin also has both pro-angiogenic (Denzel *et al.,* 2009; Landskroner-Eiger *et al.,* 2009) and anti-angiogenic actions in mice *in vivo* (Brakenhielm *et al.,* 2004; Man *et al.,* 2010), leaving its overall effects on adipose tissue angiogenesis in obesity uncertain. The adipokines described above are distinct examples that support the important concept that adipokines, with diverse effects on other metabolic processes, can regulate the process of angiogenesis. Identification of novel angiomodulatory factors could lead to novel therapeutic intervention strategies to target this process and reduce obesity.

1.4 Inflammatory associated proteins in obesity have angiogenic roles

Adipocytes express a large repertoire of inflammatory proteins including several chemokines (such as MCP-1, MIP-1α and interleukin-8 (IL-8), as well as the major pro-inflammatory cytokines, TNF-α and IL-6). Obesity is associated with an increased expression of these factors in the adipose tissue, leading to the concept that obesity is a chronic low-grade inflammatory state (Gimeno and Klaman 2005; Trayhurn 2005; Perman *et al.,* 2006). This inflammatory response appears to be triggered predominantly in the adipose tissue, although other sites are involved, including the pancreas and the liver (Hirosumi *et al.,* 2002; Xu *et al.,* 2003). These pro-inflammatory factors have direct effects on adipocyte metabolism; for example, the TNF-α gene knockout mouse exhibits improved

insulin sensitivity (Uysal *et al.,* 1997). TNF-α increases lipolysis in adipocytes *in vitro* (Zhang *et al.,* 2002) forming a link between adiposity, inflammation and systemic insulin resistance (Hotamisligil *et al.,* 1993). Intriguingly, TNF-α also has pro- and anti-angiogenic actions and has been shown to promote apoptosis in endothelial cells (Shih *et al.,* 2006). Notably, TNF-α promotes proliferation, migration and subsequent angiogenesis in endothelial cells and in malignant glioma cells (Nabors *et al.,* 2003). TNF-α also increases plasminogen activator inhibitor 1(PAI-1) (Birgel *et al.,* 2000). PAI-1 is elevated in obesity and pharmacological inhibition of PAI-1 reduced adipocyte differentiation and prevented the development of diet–induced obesity (Crandall *et al.,* 2006). In addition, PAI-1 is the primary physiological inhibitor of fibrinolysis (Eriksson *et al.,* 1998) and also has a pro-angiogenic effect on endothelial cells (Devy *et al.,* 2002; Schafer *et al.,* 2001). This demonstrates again the intricacy of the relationship between adipocytes in obesity and angiogenesis, where associated factors have dual or multiple functionality.

Integral to inflammatory changes in adipose tissue in obesity is increased T-cell and subsequent macrophage infiltration (Weisberg *et al.,* 2003, Xu *et al.,* 2003; Rausch *et al.,* 2008). Prevention of macrophage accumulation in adipose tissue (Weisberg *et al.,* 2006) and inhibition of macrophage function (Arkan *et al.,* 2005) prevented the development of the adverse inflammatory and metabolic phenotype. Macrophage infiltration is hypothesised to mediate clearance of dead adipocytes (Cinti *et al.,* 2005; Strissel *et al.,* 2007). However, in wound healing and tumour growth, macrophage infiltration contributes to the stimulation of angiogenesis (Sunderkotter *et al.,* 1991). Whether adipose macrophages mediate a similar angiogenic role in adipose tissue remodeling is less clear, although macrophages do play a role in normal adipose vascularisation during tissue development (Pang *et al.,* 2008).

Activated infiltrating macrophages also release cytokines and active molecules such as TNF-α, IL-6 and nitric oxide (NO) (Gordon 1998), which can exaggerate the inflammatory phenotype of the adipose tissue. These cytokines and chemokines further activate macrophages to increase lymphokine production

and secretion. Such a "feed-forward" loop eventually impairs insulin signaling within the adipocyte and causes obesity-associated insulin resistance (Grimble 2002). However, this process likely has additional effects on endothelial cells and adipose tissue angiogenesis. In addition to being released by activated macrophages, IL-6 is an important adipokine, predominantly secreted by the adipocytes and the non-macrophage adipose stromal cells (Crichton *et al.,* 1996; Fried *et al.,* 1998). IL-6 secretion is increased from adipocytes of obese humans (Mohamed-Ali *et al.,* 1997) and positively correlates with body mass and plasma FFA concentrations (Lazar 2005). Furthermore, IL-6 has a vital role in angiogenesis: it is a potent pro-angiogenic stimulus to endothelial cells, promoting proliferation and migration (Wang and Newman 2003; Nilsson *et al.,* 2005; Yao *et al.,* 2006) and also promotes neovascularisation in IL-6 transgenic mice *in vivo* (IL-6 $^{-/-}$; Campbell *et al.,* 1993).

Hypoxia may be the critical underlying factor that triggers adipose inflammation (Trayhurn and Wood 2005). Thus, as adiposity increases, clusters of adipocytes become relatively hypoxic, which initiates the release of inflammatory cytokines and angiogenic factors, including NO. This, in turn, is thought to increase blood flow, by both the stimulation of angiogenesis and vasodilatation (Trayhurn and Wood*,* 2005). Thus, a self-fulfilling cycle of events may occur in the adipose tissue in obesity whereby rapid adipocyte expansion leads to local hypoxia, which stimulates pro-inflammatory remodeling of the tissue (including angiogenesis) at the expense of reduced local insulin sensitivity and increased inflammatory signaling. If this process remains unbalanced, infiltration of macrophages to the inflamed site may become excessive, initiating a feed-forward inflammatory response that ultimately leads to systemic inflammation and insulin resistance without adequate adipose tissue blood vessel growth.

To summarise, considerable evidence has established that adipose tissue is a dynamic endocrine organ, as well as a highly active metabolic tissue. Obesity results in the increased secretion of cytokines and growth factors, which play important roles in regulating metabolic and cardiovascular processes. However, besides adipocytes, adipose is composed also of the stroma-vascular fraction

that includes pre-adipocytes, macrophages/dendritic cells and endothelial cells that have a role in the growth and maintenance of adipose tissue. It is evident that the local circulation in the tissue plays a major role in providing the metabolic substrates, as well as clearing adipose-derived products. How this process is dysregulated in an obese state remains relatively unclear.

1.5 The vasculature of adipose tissue

Most adult tissues remain a similar mass, with an associated stable vasculature (Hobson & Denekamp 1984). Adipose tissue is one of the notable exceptions, and retains the capacity for dynamic vascularisation. Growing adipose tissue requires an adequate oxygen and nutrient supply, and the ability of the adipose tissue vasculature to grow and regress throughout adulthood suggests it maintains an ability to recruit new capillaries. Indeed adipose tissue explants from rabbits induced neovascularisation, whereas liver and muscle did not, in the rabbit cornea angiogenesis assay (Silverman *et al.,* 1988). Within adipose tissue, each adipocyte is in close proximity to a blood capillary (Rosell and Belfrage 1979) and normal growth and maintenance of adipose is dependent on a functional blood capillary network (Crandall *et al.,* 1997). Thus, as with some tumour formations, growth of normal adipose tissue expansion may be dependent upon its vasculature (Folkman 1997). Although crucial for the development of adipose tissue, vascular density is rarely examined or assessed within the adipose tissue in obesity studies.

Although mostly overlooked, the rate of lymphatic drainage in adipose tissue is inversely related to its growth and lymphatic vessels tend to be absent where fat deposition is more abundant (Ryan 1995). Little is known about this circulatory system in adipose tissue even though it may play an important role in endothelial function and adipose expansion (Skobe and Detmar 2000).

1.5.1 The effect of nitric oxide on vascular tone

An important regulator of vascular tone within blood supply to the adipose is nitric oxide (NO). NO is a bioactive gas produced through the conversion of L-arginine to L-citrulline by any of three nitric oxide synthases (neuronal nitric oxide synthase (nNOS); endothelial nitric oxide synthase (eNOS/NOSIII) and calcium-insensitive nitric oxide synthase (iNOS); Ignarro 1990) in vascular endotheial cells. NO stimulates soluble guanylate cyclase (sGC) in vascular smooth muscle cells, increasing cytoplasmic cGMP levels. cGMP activates cGMP-dependent protein kinases (PKG) and gated ion channels to cause vascular relaxation (Moncada *et al.,* 1991). NO is a contributory factor in tumour angiogenesis and maintaining vascular tone within tumour blood vessels (including lung, prostate and cervical cancer) (Ng *et al.,* 2007; Murohara *et al.,* 1998). NOS expression (in particular iNOS) was observed in adipose tissue over ten years ago (Ribiere *et al.,* 1996; Kapur *et al.,* 1999). Reductions in nitric oxide bioavailability can also trigger other events including valscular tone alterations, thrombotic dysfunctions, smooth muscle cell proliferation and migration as well as leukocyte adhesion (Madamanchi *et al.,* 2005). Such events are also associated with an increased production of reactive oxygen species (ROS), which in turn reduce endothelial NO availability (Gao *et al.,* 2009).

Another important regulator in hypoxic conditions in addition to NO, is hypoxia-inducible factor (HIF). HIF-1 is a basic helix-loop helix transcription factor, which induces the expression of many genes including iNOS and VEGF (Melillo *et al.,* 1995; Forsythe *et al.,* 1996). HIF contains an α and a β subunit; the β subunits are constitutive and it is the α subunits that are unique to the hypoxic response. HIF acts as an oxygen-sensing mechanism and is recruited through the stabilisation of the α subunit. The C-terminus of the HIF-1α/HIF-2α interacts with the CH1 part of the transcriptional coactivator CBP/P300. In the presence of oxygen, the HIF asparaginyl hyroxylase FIH adds an atom of oxygen to the β–carbon of Asn803, which in turn, prevents the recruitment of CBP/P300. In the presence of oxygen, HIF prolyl hydroxylases add an atom of oxygen to Pro403 and/or Pro564, converting the residue to 4-hydroxyproline (Semenza *et al.,* 1997). The interaction with HIF-α I is mediated by the von Hippel-Lindau (VHL)

protein. The multiprotein E3 ligase complexed with VHL leads to polyubiquitylation of the HIF α subunit, which is then destroyed by proteasomes. Three different HIF prolyl hydeoxylases have been identified: PHD1 (prolyl hydroxylase domain 1), PHD2 and PHD3 (Maxwell 2005).

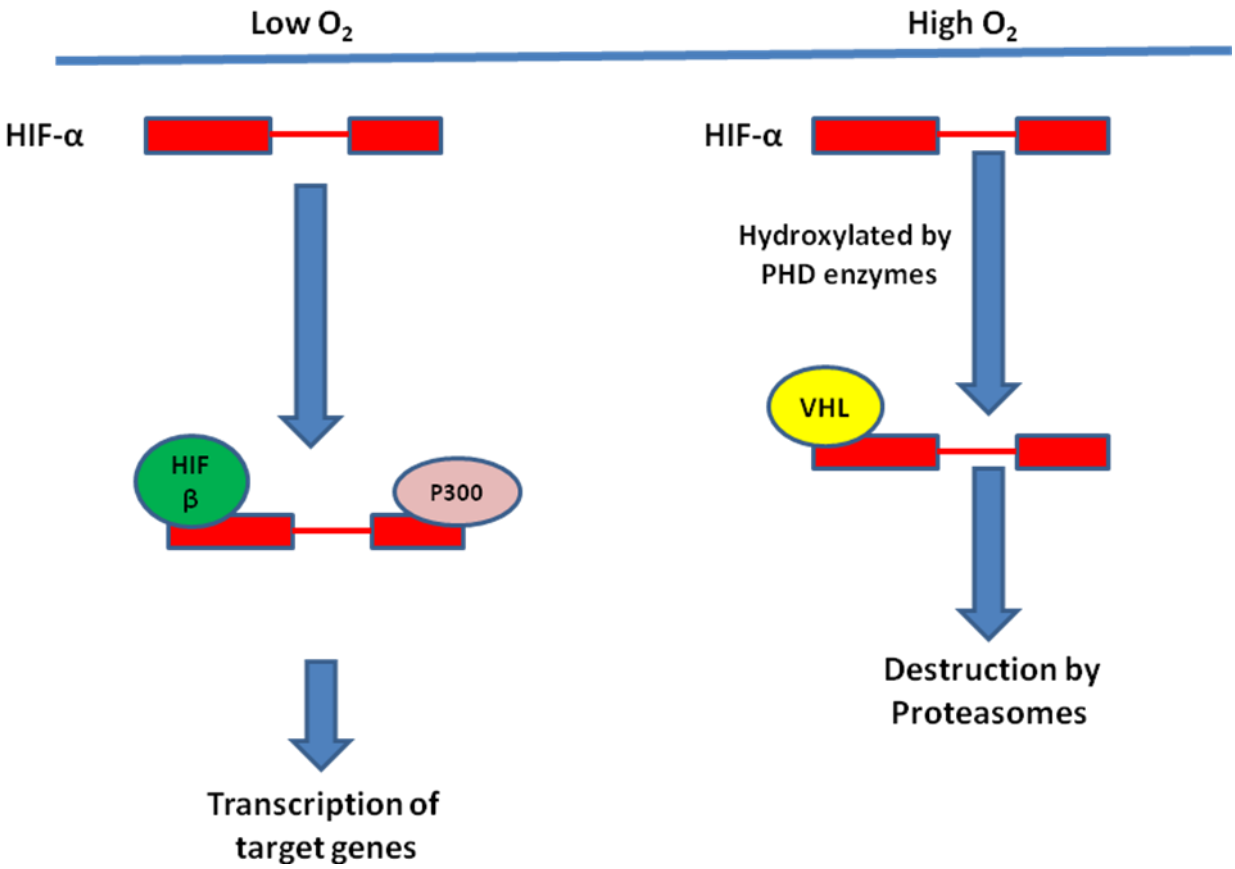

Figure 1.3: Regulation of hypoxia inducible factor complex by oxygen is through hydroxylation of the α- subunit. In low oxygen, C-terminus of HIF-α interacts with transcriptional coactivator CBP/P300, causing transcription of target genes. In presence of oxygen, HIF-α is hydoxylated by prolyl hydroxylase domain (PHD) enzymes. The prolyl hydroxylation allows capture by von-Hippel-Lindau (VHL) protein, leading to ubiquitylation and destruction.

1.5.2 The role of endothelial cells in adipogenesis

The maturation of adipocytes is an essential process that allows the growth of an adipose tissue depot. Importantly, endothelial cells promote the differentiation of pre-adipocytes in a co-culture of mature adipocytes and endothelial cells (Aoki *et al.,* 2003). Furthermore, an anti-angiogenic compound (anti-VEGFR2 antibody) which inhibited blood vessel formation, led to a significant reduction of adipogenesis of preadipocytes when injected subcutaneously in mice (Fukumura *et al.,* 2003). Endothelial cell proliferation was also present in expanding adult adipose tissue (Crandall *et al.,* 1997). Thus, the adipocyte-endothelial cell interaction is very important.

1.6 Angiogenesis

An understanding of the systems that co-ordinate and regulate blood vessel development and regression in angiogenesis must be addressed to fully understand the adipocyte-endothelial cell interaction. Moreover, it is this balance between angiogenesis inducers and inhibitors in the microenvironment that really controls the rate of new blood vessel formation. Tipping this balance determines the angiogenic environment within a tissue.

The term angiogenesis refers to the formation of blood vessels from pre-existing capillaries and post-capillary venules (Carmeliet and Jain 2000). Angiogenesis is involved in many aspects of normal physiological function, particularly embryogenesis. It is also involved in menstruation, wound healing and particularly in muscle during exercise. However, in the adult, excess and/or impaired angiogenesis is central to the pathology of many diseases (Folkman 1995) including coronary heart disease, ischaemic heart disease, critical limb ischaemic, arthritis and tumour development in cancer (Griffioen 2000).

1.6.1 The angiogenic cascade

Angiogenic events are tightly regulated by growth factors and inhibitors of neovascularisation (Conway *et al.,* 2001). The process of angiogenesis can be divided into four serially occurring events: initiation, proliferation, migration/stabilisation and regression (Figure 1.3):

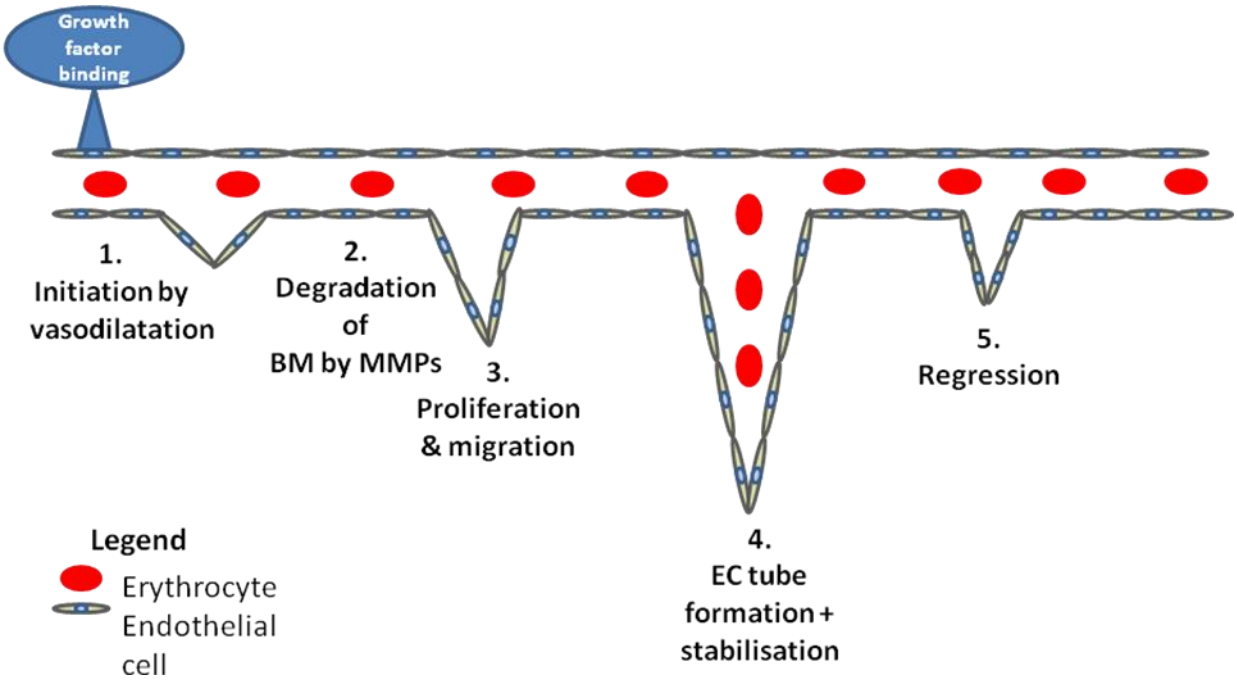

Diagram 1.4: The angiogenic cascade. Diagram representing the five main components of the angiogenic cascade. Growth factor-receptor binding activates signaling pathways within endothelial cells, causing vasodilatation and the release of proteolytic enzymes that degrade the basement membrane surrounding the parent vessel. Endothelial cells proliferate and sprout out of basement membrane, then migrate using cell surface adhesion molecules. MMPs then dissolve the surrounding tissue matrix and tubes begin to form. New blood vessels mature and blood flow begins. Finally, vessels enter the stage of regression, which involves apoptosis of endothelial cells. BM, basement membrane; MMPs, matrix metalloproteinases (For review, refer to Carmeliet and Jain 2000).

1.6.2 Initiation of angiogenesis

The initial phase of angiogenesis is endothelial cell activation, which is a prerequisite for endothelial cells to enter the angiogenic cascade (Griffoen 2000). This occurs primarily by alteration of gene expression (Zardi *et al.,* 2005). The transcription factor hypoxia-inducible factor (HIF)-1α regulates numerous cellular responses to states ranging from hypoxia to oxidative stress, associated both with physiological states and with the development and progression of many pathophysiological states (Haddad 2005). HIFs act on HIF-binding sites (HBSs) within the hypoxia-response elements (HREs) of oxygen-regulated genes (Camenisch *et al.,* 2001). Vascular endothelial growth factor (VEGF) is the most prominent HIF-1α target protein involved in vascularisation. Additionally, the reactive nitrogen species (RNS) pathway may also regulate the stability and activity of HIF-1α, showing that the expression of nitric oxide synthase could cause HIF-1α accumulation (Haddad 2002).

1.6.3 Proliferation

Following activation, endothelial cell penetration into new areas of the body occurs by degradation of the basement membrane by extracellular proteinases, including MMPs (Griffoen 2000). MMPs are a family of zinc-dependent endopeptidases that are collectively capable of degrading all components of the extracellular matrix (Coussens *et al.,* 2002). Most MMPs are expressed through the actions of growth factors, cytokines, hormones, physical stress and oncogenic cellular transformation (Szabo 2004).

In addition to basement membrane degradation by MMPs, the VEGF family and its receptors play a central, specific role in mediating endothelial cell proliferation and migration, as well as increasing vascular permeability (Carmeliet *et al.,* 1996). VEGF-A is a secreted glycoprotein, with at least eight known human isoforms that bind to an extracellular domain. This activates the tyrosine kinase domain of both VEGF receptor-1 (VEGFR-1) and VEGFR-2 on endothelial cells. Inhibitors of the tyrosine kinase domain effectively inhibit angiogenesis *in vitro* and *in vivo*, and are currently in clinical trials to treat gastrointestinal stromal tumours and renal cancer (Morabito *et al.,* 2006).

Another secreted protein from endothelial cells that also has a binding affinity to the tyrosine kinase receptor, is angiopoietin-1 (Ang-1). The tyrosine kinase receptor or Tie2, binds Ang-1 which tightens junctional molecules within the vessel (Thurston *et al.,* 2000) and thus promotes interaction between endothelial cells and mural cells (vascular smooth muscle cells and pericytes) as an adhesive protein (Carlson *et al.,* 2001). Studies using gene knockouts of either Ang-1 or Tie 2 have demonstrated their importance in developmental angiogenesis as they experienced embryonic lethality, particularly in the heart (Yancopoulos *et al.,* 2000). This is indicative of a vital role of Ang-1/Tie 2 in the development of blood vessels. Another endothelial growth factor that induces both proliferation and migration and has similar potent angiogenic effects to VEGF, is hepatocyte growth factor (HGF). HGF synergistically augments the angiogenic effects of VEGF *in vivo* (Van Belle *et al.,* 1998), which is mediated by the Ets family of transcription factors, leading to the expression of VEGF and MMPs. Fibroblast growth factor (FGF) is another major growth and differentiation factor. FGF-1 can induce endothelial cell proliferation and endothelial tube formation in collagen (Kanda *et al.,* 1996). In addition, FGF inhibitors reduce angiogenesis, for example shark cartilage and its derivatives inhibit FGF-induced angiogenesis (Gonzalez *et al.,* 2001).

1.6.4 Migration and stabilisation

Following proteolytic degradation of the extracellular matrix, "leader" endothelial cells start to migrate through the degraded matrix. They are followed by proliferating endothelial cells, which are stimulated by a variety of growth factors, some of which are released from the degraded extracellular matrix, including VEGF and FGF (Liekens 2001). There is then an interaction of endothelial cells with the extracellular matrix and smooth muscle cells to form capillary tubes, which involves a host of pro-angiogenic factors including VEGF, FGF and interleukin-8 (IL-8) (Fidler & Ellis 2000). Recruitment of pericytes in small vessels or smooth muscle cells in larger vessels is required. Platelet derived growth factor (PDGF) is among the most potent stimuli for smooth muscle cell migration and proliferation *in vitro* (Heldin *et al.,* 1998).

Differentiation of precursor cells into pericytes and smooth muscle cells is believed to be initiated upon endothelial cell contact. In response, transforming growth factor β (TGF-β) is released by endothelial cells and is activated in a plasmin mediated manner. Activated TGF-β acts on myofibroblasts and pericytes, which may contribute to the formation of the vessel (Griffioen 2000).

The immature tube then forms and vessel stabilisation begins, which marks the end of growth factor dependence (Darland *et al.,* 1999) (see section 1.7.4). Once tube formation occurs, flow commences and local oxygen levels increase, resulting in a decrease in VEGF levels (Beck *et al.,* 1997). Also, TGF-β can alter integrin profiles and stimulate basement membrane production and accumulation (Enenstein *et al.,* 1992). The presence of the basement membrane may provide a long-term signal that supports vessel stabilisation. Furthermore, evidence suggests that Ang-1 plays a role in vessel stabilisation as its absence lead to defects in vessel remodeling (Beck *et al.,* 1997).

The processes of cell invasion, proliferation and migration/stabilisation not only depend on angiogenic enzymes, growth factors and their receptors, they are also mediated by cell adhesion molecules. These can be classified into four families depending on their biochemical and structural characteristics and include the integrins, the immunoglobulin supergene family, the cadherins, and the selectins (Bischoff 1997). The integrin family functions in a variety of cell-matrix and cell-cell interactions in the vasculature and, as they are expressed on endothelial cells, participates in endothelial cell migration and formation of capillary-like tubes *in vitro* (Luscinskas and Lawler 1994). Besides integrins, cadherins including VE-cadherin are expressed throughout vascular development and are localised at points of cell-to-cell contact (Breier *et al.,* 1996). Based upon its expression on angiogenic blood vessels and its localisation, platelet endothelial cell adhesion molecule-1 (PECAM-1/CD31) is also implicated in angiogenesis (Berger *et al.,* 1993).

1.6.5 Regression of vessels

Once assembled in new vessels, endothelial cells become quiescent and have an extremely low turnover rate (Engerman *et al.,* 1967). This process of becoming quiescent is important as reduced survival of endothelial cells caused vascular regression in the embryo (Carmeliet *et al.,* 1999). Endothelial apoptosis is a natural mechanism of vessel regression, seen in the retina and ovary, and is a frequently observed effect of exogenously-administered angiogenesis inhibitors, including endostatin (O'Reilly *et al.,* 1997). The angiogenic balance needs to be tipped towards the anti-angiogenic side to induce endothelial cell apoptosis (Jain *et al.,* 1998) and factors responsible for causing a shift towards an anti-angiogenic environment include endostatin, thrompospondin-1 (TSP-1), vasohibin and caveolin-1 (Good *et al.,* 1990; Taraboletti *et al.,* 1992; Vogel *et al.,* 1993; O'Reilly *et al.,* 1997; Liu *et al.,* 1999; Watanabe *et al.,* 2004). In addition, angiopoietin-2 is also known to play a role in vessel regression by blocking the vessel stabilisation action of angiopoietin-1 (Holsash *et al.,* 1999). Haemodynamic forces are also essential for vascular maintenance (Nisoli *et al.,* 1998; Yamauchi *et al.,* 2007).

In summary, angiogenesis is tightly controlled through a balance of many pro- and anti-angiogenic factors. In healthy tissue, the balance weighs heavily to the anti-angiogenic side until new vessels are needed. New vessels either enter an apoptotic stage to prevent angiogenesis. Some of these factors are summarised in Figure 1.4:

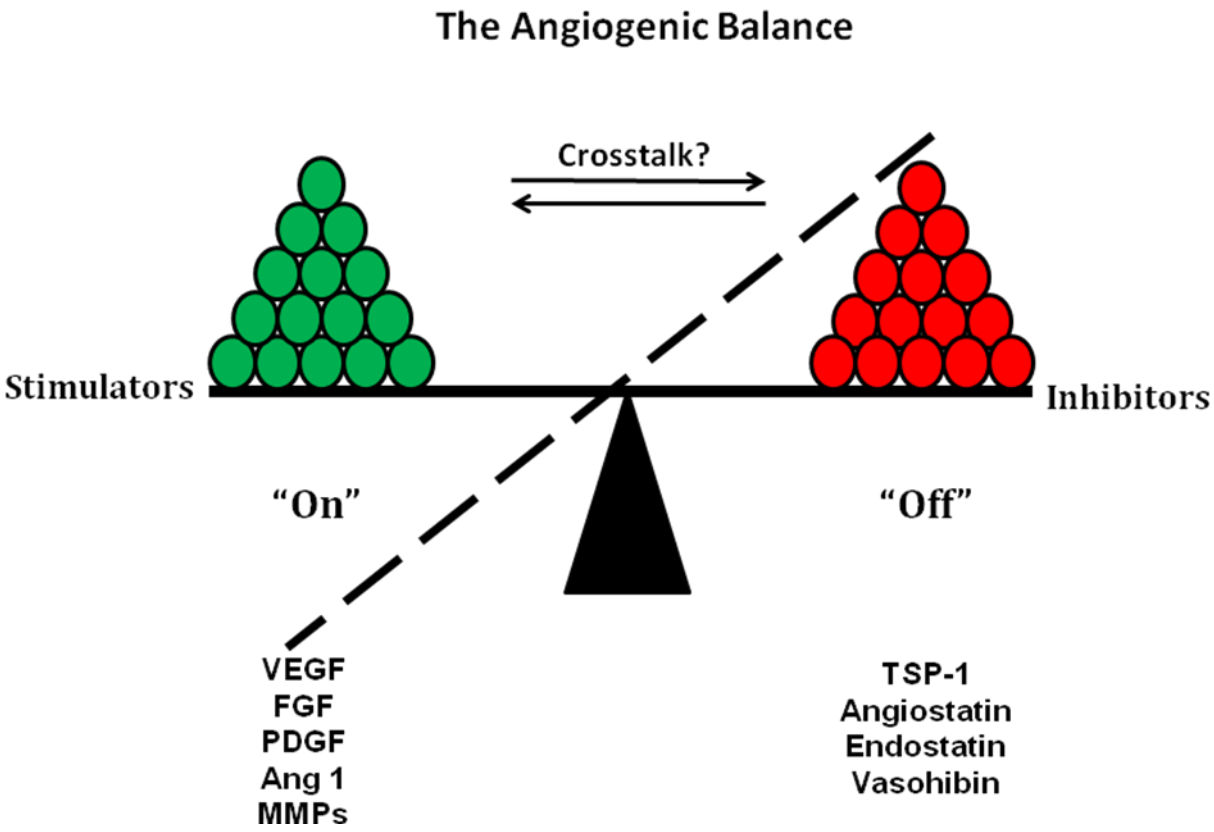

Figure 1.5: The effect of pro- and anti-angiogenic factors upon angiogenesis. A tip in the angiogenic balance towards pro-angiogenic environment induces angiogenesis. Tipping the angiogenic balance towards an anti-angiogenic environment inhibits angiogenesis. Feedback mechanisms between pro- and ant-angiogenic factors will modulate angiogenesis as well. Pro-angiogenic factors include vascular endothelial growth factor (VEGF); fibroblast growth factor (FGF); hepatocyte growth factor (HGF); platelet derived growth factor (PDGF); angiopoietin-1 (Ang 1); and the matrix metalloproteinases (MMPs). Anti-angiogenic factors include thrombospondin-1 (TSP-1); angiostatin; endostatin; and vasohibin.

1.7 Influence of adipocytes upon angiogenesis

It is evident that extensive crosstalk occurs between adipocytes and endothelial cells, which is likely to play a role in coordinating angiogenesis and adipogenesis. This creates a potential avenue for therapeutic intervention in the treatment of obesity through targeting the adipose vasculature. Indeed, an inhibitor of angiogenesis, TNP-470, prevented the development of obesity in $Lep^{ob/ob}$ mice (Rupnick *et al.,* 2002). TNP-470, a synthetic analog of fumagillin (antimicrobial agent isolated from Aspergillus fumigates), is a well-characterized, selective inhibitor of endothelial cell growth and angiogenesis (Kusaka *et al.,* 1994). Similar results were also obtained using TNP-470 with the high fat diet-induced obesity model (Brakenhielm *et al.,* 2004), strengthening the case for manipulation of angiogenesis in the treatment of obesity. Moreover, an apoptosis-inducing agent specifically targeted to adipose vasculature (using an *in vivo* phage display to isolate a peptide motif that homes to white fat vasculature), showed the reversion of obesity in mice (Kolonin *et al.,* 2004). The injection of dominant negative PPARγ-transfected preadipocytes led to the inhibition of blood vessel development at the site of injection (Fukumura *et al.,* 2003), suggesting that cells incapable of normal adipocyte differentiation are unable to recruit vessels. This body of evidence re-emphasises the direct role adipocytes play in the development of their own vasculature. In accordance, there are many angiogenic factors that have emerging roles on adipose function. VEGF, alongside its role in regulating endothelial cell proliferation and migration in angiogenesis (Carmeliet *et al.,* 1996), also accounts for the major portion of the angiogenic activity of media conditioned by adipocytes (Zhang *et al.,* 1997). In addition, adipose tissue VEGF expression and secretion is known to be induced by hypoxia and insulin (Mick *et al.,* 2002; Zhang *et al.,* 1997). Inflammatory cells that have infiltrated adipose, including macrophages, and adipose stromal cells, can also contribute to VEGF production (Cho *et al.,* 2007; Rehman *et al.,* 2004).

Other members of the VEGF family are also implicated in adipose tissue development. Placental growth factor (PlGF) impairs adipose tissue growth, which is due to defective angiogenesis rather than altered adipogenesis (Christiaens *et al.,* 2006; Lijnen *et al.,* 2006). Furthermore, studies *in vitro* have confirmed that HGF is released by cultured adipocytes (Saiki *et al.,* 2006) and preadipocytes (Silha *et al.,* 2005). VEGF, Ang-1 and -2, as well as Tie2 receptors, are also known to play a significant role in the sprouting and branching of vessels in angiogenesis. However, with the exception of a study of Ang-2 gene expression in preadipocytes and Lep $^{Ob/Ob}$ adipose tissue (Cohen *et al.,* 2001), there are very few studies of adipose tissue angiopoietins. Taken together these studies implicate VEGF and other growth factor family members in the modulation adipose tissue growth via the vascular system. However, factors that have important angiogenic effects (Lijnen *et al.,* 2006; Lijnen 2011) may not have any effect upon adipogenesis or, potentially, on adipose tissue angiogenesis (Christiaens *et al.,* 2006).

Another strong contender in the modulation of adipose angiogenesis is thrombospondin 1 (TSP-1). TSP-1 is a potent anti-angiogenic factor, which is produced by both resting and activated macrophages (DiPietro and Polverini 1994). TSP-1 suppressed angiogenesis in the cornea pocket assay and inhibited growth in the chicken chorioallantoic membrane (CAM) assay (Armstrong and Bornstein 2003; Iruela-Arispe *et al.,* 1999). TSP-1 also has subsequent effects upon the regulation of inflammation and wound healing (Bornstein 2001). Increased TSP-1 expression has been reported in the adipose of rats (Hida *et al.,* 2000) and is elevated in the plasma and renal tissue of diabetic patients (Bayraktar *et al.,* 1994). Thus, a role for TSP-1 seems plausible in regulating vascular growth in adipose.

Adipose tissue also produces several MMPs including MMP-2 and MMP-9 (MMPs are also to be produced by macrophages and endotheial cells (Galis *et al.,* 1995; Taraboletti *et al.,* 2002)). These have been postulated to affect preadipocyte differentiation and maturation by modulating the extracellular matrix (Bouloumie *et al.,* 2002). Furthermore, deletion of tissue inhibitor-1 of

MP (TIMP-1) leads to a reduction of adipose mass in mice fed a high-fat Western diet (Lijnen *et al.,* 2003). MMP inhibitors, as well as MMP and TIMP gene knockouts, markedly inhibit adipose development in conjunction with, and even independent of, angiogenesis (Croissandeau *et al.,* 2002). Collectively, MMPs and TIMPs play a role in controlling adipogenesis, potentially through the modulation of angiogenesis.

In summary, many established angiomodulatory factors are altered in adipose tissue and in obesity. Many adipocyte-derived factors exert effects upon endothelial cells and vice versa. Further examination of the endothelial-adipocyte crosstalk occurring during adipose expansion may expose new avenues for therapeutic intervention.

1.8 Hypothesis and Aims:

The overarching hypothesis of this thesis is that obesity compromises angiogenic potential in adipose tissue and leads to the detrimental metabolic phenotype.

The specific aims of this thesis were:

- To determine whether angiogenesis is altered in obesity;
- To identify novel angiomodulatory genes in adipose tissue associated with obesity in a unique polygenic model of fatness (Fat; F) versus leanness (Lean; L);
- To functionally characterise angiomodulatory genes with respect to their effects on endothelial cells and adipocytes and fat mass *in vitro* and *in vivo*;
- To determine the effects of altered nutritional status (obesity, weight loss) on adipose vasculature and angiomodulatory genes *in vivo*.

Chapter 2

Materials and Methods

2.1 Animals

2.1.1 Mouse lines and housing

2.1.1.1 *Fat and Lean mice:*

A polygenic model of obesity (Fat) and leanness (L) was employed to investigate changes in angiogenic potential in obesity. Fat and Lean mouse lines were selected from a three-way cross of two inbred lines (JU and CBA) and one outbred line (CFLP), as described in detail (Bunger and Hill 1999). Briefly, selection of the first twenty generations was on the ratio of gonadal fat pad weight to body weight of ten-week old males and subsequently on dry matter content of males at fourteen weeks of age. Inbred lines were initiated from a single family of each of the lines after forty-seven generations of divergent selection and maintained by full sibling mating (Bunger and Hill 1999). Mice were fed standard chow (Rat and Mouse no 3; Special Diet Services, Essex, UK) from weaning. Animals were housed in standard cages with controlled lightening (12-h light, lights on at 07.00), with relative humidity of 50±10% and under pathogen free conditions, at a room temperature of 23±2°C.

2.1.1.2 Lep$^{Ob/Ob}$ mice:

Another model of genetic obesity, the leptin deficient mouse ($^{Ob/Ob}$), was also used. Seven week old, male Lep$^{Ob/Ob}$ mice were obtained from Jackson Laboratories (Jackson Laboratories, Bar Harbour, ME, USA) (n=6). Age-matched, male mice with a pure C57BL/6J background were bred from a colony from The University of Edinburgh (n=6) and used as controls. Both types of mice were housed in standard cages as described above.

2.1.1.3 Diet-induced obesity in C57BL/6J mice:

Diet-induced obesity was investigated using C57BL/6J mice. Six week old male C57BL/6J mice (n=12) supplied by Charles River (Kent, London, UK). C57BL/6J is the most widely used inbred strain for these studies as they are susceptible to diet-induced obesity, type 2 diabetes and atherosclerosis (Winzell and Ahren 2004). This time period is sufficient to cause obesity and the associated

metabolic phenotype, for example insulin resistance and associated islet dysfunction (Black *et al.,* 1988). The animals were randomly assigned to two different dietary groups: Control and high fat diet (HF) and singly housed as described above.

2.1.1.4 Pair-feeding in C57BL/6J mice

The effect of pair-feeding on angiogenesis was also examined. Six week old male C57BL/6J mice (n=18) supplied by Charles River (Kent, London, UK), were randomly assigned to two different dietary groups as described in 2.1.2: Control and high fat diet (HF) and were singly housed as described above (n=6 for each group).

2.1.1.5 Diet-induced obesity with associated minipump implantation in C57BL/6J mice

The effect of a thrombospondin 1 analogue (ABT-510; Abbott Laboratories, Abbott Park, IL, USA) upon angiogenesis in high fat fed mice was also investigated. Five week old male C57BL/6J mice (n=24) supplied by Charles River (Kent, London, UK) were randomly assigned to two different dietary groups as described in 2.1.2: Control and high fat diet (HF) and had minipumps containing ABT-510 inserted (described below).

2.1.2 Dietary manipulation

2.1.2.1 Fat and Lean mice

Fat and Lean mice were either placed on a high-fat diet (50% kcal energy as saturated fat D12331; Research Diets, New Brunswick, NJ) or a calorie-matched control diet (11% kcal energy as saturated fat, D12328; Research Diets, New Brunswick, NJ) for eighteen weeks. The mice had free access to their respective food and water throughout the study. It must be noted that there are marked differences, other than caloric content, of high fat and chow diets. Energy intake can be broken down into gross, digestible and metabolisable energy content. Gross energy is the complete energy contained within the food itself. Digestible

energy is the gross energy minus the energy lost in faecal matter. The metabolisable part is the digestible minus the energy lost in urine.

2.1.2.2 Diet induced obesity in C57BL/6J mice

The control animals were fed a standard pelleted diet (2014 Teklad Global 14% Protein Rodent Maintenance Diet, Harlan, UK) containing 20% of energy as proteins, 67% of energy as carbohydrates (5% sucrose, 62% starch) and 13% energy as fat by dry weight, for a period of twelve weeks. The HF group (n=12) were fed a high fat diet (58% calories as fat) over the same period. The mice had free access to their respective food and water throughout the study. Body weights and food intake were monitored weekly.

2.1.2.3 Pair fed C57BL/6J mice

The control animals were fed a standard pelleted diet (see above), while the HF group (n=12) were fed a high 58% calories as fat, as before, for a period of twelve weeks. After this time on either diet, mice either continued control (n=6), HF diet *ad libitum* (n=6) or HF diet restricted to the amount of calories (kcal/ [g body weight]) that the Control group had consumed the previous week (*pair-fed* model), as described (Howard *et al.,* 1999). In order to distinguish between fat depot loss through pair-feeding and that caused by primary inhibition of angiogenesis, it was important to have controls that are still high fat fed. Respective diets were continued for a further three weeks, where body weight and food intake were recorded daily (until mice were 21 weeks old). The HF and control mice had free access to their respective food and water throughout the study.

2.1.2.4 *Diet-induced obesity with associated minipump implantation in C57BL/6J mice*

C57BL/6J mice were randomly assigned to two different dietary groups: Control and high fat diet (HF) as described before for a period of eight weeks. The mice had free access to their respective food and water throughout the eight week study. Body weights and food intake were monitored weekly.

2.1.3 Surgical Procedures

All mice were killed by asphyxiation (to preserve aortas) in carbon dioxide. All animal experiments were carried out in accordance with the British Home Office Animals (Scientific Procedures) Act 1986.

2.1.3.1 Sponge implantation

The sponge implantation model has been routinely used to measure vascularity (Hague *et al.,* 2002). Thus, as an established means of measuring angiogenesis, the sponge implantation model was employed throughout this thesis. Mice were anaesthetized using isoflurane (2-2.5 l/min), weighed and administered analgesic subcutaneously (buprenorphine; 0.1mg/kg body weight; Reckitt & Colman Pharmaceuticals Inc, Richmond, London, UK). The lower back of the animals was shaved, a small incision made, and a subcutaneous pocket produced on the right hand side underneath the dorsal skin by blunt dissection. This process was repeated until the pocket was large enough to insert a sterile (sponges autoclaved prior to experimentation) polyurethane sponge (1 cm x 0.5 cm; eFoam Bilston, England, UK). The lesions were closed using Reflex 9mm skin closure clips. Animals were singly housed immediately after surgery and maintained for a further 3 weeks.

Twenty-one days after sponge implantation mice were killed by asphyxiation in carbon dioxide, and aortas, adipose and sponges collected for further analysis. Sponges were rapidly excised with underlying connective tissue, and bisected. One half of each sponge was transferred to a 1.5 ml Eppendorf and immediately frozen on dry ice for further experiments. The second half of the sponge was fixed in 10% formalin.

2.1.3.1.1 Sponge processing and staining

For analysis of vascularity, formalin-fixed sponges were processed into paraffin wax using a Tissue Tek Vacuum Infiltration Processor (VIP) and embedded in paraffin wax. Excess paraffin wax was trimmed from the surface and 5µm transverse sections were taken from the cut surface of each sponge. Sections were collected on to poly-l-lysine-coated slides (Sigma-Aldrich, UK) using a

flotation bath to ensure firm adhesion. Slides were oven dried (37ºC) overnight. The following day slides were dewaxed using xylene (Sigma Aldrich, UK), and rehydrated through graded strengths of ethanol (99%, 90%, and 70%) for five minutes each. Sections were then stained by haematoxylin and eosin (H&E; Sigma Aldrich, UK) for five minutes, rinsed in distilled water, dipped (two seconds) in acid alcohol (1% hydrochloric acid in 50% ethanol; Sigma Aldrich, UK) and rinsed in distilled water for a further fifteen minutes. Slides were then immersed in eosin for one minute and rinsed in distilled water once again. Finally, slides were dehydrated prior to cover slipping by one minute immersions in 95% and 100% ethanol, and then xylene for five minutes.

2.1.3.1.2 Quantification of sponge vascularity

Sponge sections were examined by light microscopy using KS300 imaging software (Karl Zeiss Axissop) as described below. The vascularity of the explanted sponges was determined by Chalkley counting (Fox *et al*., 1995). Vascular density was determined using a 25-point Chalkley eyepiece graticule at x40 magnification (covering an area of 0.5 mm^2 at this magnification). For each sponge, three non overlapping counts were performed in the areas with the highest vascularity. These areas were subjectively identified under low magnification (10x). The graticule was rotated in the eyepiece to where the maximum number of vessels was overlain by the graticule grid. Individual blood vessel density was then obtained by taking the mean of three graticule counts. Blood vessels were identified morphologically, with or without erythrocytes apparent in the lumen. The mean of the three counts gave the overall Chalkley score.

2.1.3.1.3 Haemoglobin content as an index of angiogenesis

Neovascularization was also assessed by measuring the concentration of haemoglobin in the enclosed sponge implants (Majima *et al.,* 1997). Sponges were implanted as described above (Section 2.1.3.1) in C57BL/6J mice. The sponges were taken immediately after death at Days 4, 7, 13 and 21 days after

implantation. After the sponges were weighed, they were cut into several pieces with scissors and 2mls of Drabkin's reagent (Sigma Aldrich, UK) were added and the samples homogenized with a Polytrone homogenizer (Kinematica GMBH, Luzern, Switzerland). Samples were then centrifuges for fifteen minutes at 10,000 x *g*. The supernatant was filtered through a 0.22 m filter (Milipore Ltd, Watford, UK) and the haemoglobin concentration in the supernatant, obtained was determined using a spectrophotometer (OPTImax Tunable Reader, Molecular Devices, CA, USA) absorbance read at 540 nm) and standards made from cyanmathemoglobin (Sigma Aldrich, UK; made from making 180 mg/ml standard solution in Drabkin's reagent). The concentrations of haemoglobin in the granulation tissues were expressed as mg/g wet tissue. This was then compared to histological examination (counting individual blood vessels in H&E stained sponge section by the Chalkley method) of the other half of the same sponge.

2.1.3.2 Mini pump insertion

The continous subcutaneous delivery of a thrombospondin-1 analogue (ABT-510) or saline into C57BL/6J mice was achieved using implanted osmotic minipumps (Model 1004: Alzet, Palo Alto, CA). Mice were anaesthetised with isoflurane (2-2.5 l/min), weighed and administered appropriate analgesia (buprenorphine (0.1 mg/kg body weight) by subcutaneous injection). The lower back of the animals was shaved, a small incision made, and a subcutaneous pocket formed on the right flank with blunt-ended scissors. This process was repeated until the pocket was large enough to insert the osmotic pump on the left hand side. The lesions were closed using Reflex 9 mm skin closure clips. The pumps delivered saline or ABT-510 continuously at a rate of 0.25 µl per hour for twenty eight days. Animals were monitored closely for infection and local irritation throughout the course of the experiment.

Twenty eight days post-implantation mice were tail-tip bled and then killed by asphyxiation in carbon dioxide, and aortas, adipose and sponges collected for

further analysis. Osmotic minipumps were weighed, examined for residual drug and then snap frozen.

2.1.3.3 Intraperitoneal Glucose Tolerance Test

Mice were fasted overnight. The test was initiated by the intraperitoneal injection of glucose (2 mg/g body weight- 25% stock solution in saline) (Morton *et al.,* 2001). Blood samples were collected from the tail tip at 0 (before) and at 5, 15, 30, 60 and 120 min after injection. Blood glucose concentration was determined immediately using an Accu-Chek Instant Plus blood glucose monitor (Roche Diagnostic, Burges Hill, UK). Blood samples were centrifuged at 3000 x *g* for 10 minutes (4^{o}C) and aliquots of 20 µl plasma were frozen. 5 µl aliquots of each plasma sample in duplicate to determine the plasma insulin, using an Insulin ELISA kit (Crystal Chem, Downers Grove, IL, USA). Briefly, after preparation of 0.1, 0.2, 0.4, 0.8, 1.6, 3.2, 6.4 and 12.8 ng/ml insulin standards in distilled water, samples were bound to a 96 well micro-titre plate, incubated and then subjected to 2 washes with wash buffer. After incubation and 5 washes in wash buffer, enzyme substrate was added, followed by the addition of 100 µl of secondary antibody. The reaction proceeded at room temperature and was stopped after 40 minutes with the specific stop buffer supplied in the kit and absorbance at 550 nm measured on a Molecular Devices Spectra 340 microplate reader (USA). Standard curves using insulin standards were generated using linear regression as shown in Figure 2.1.

2.1.3.3 Standard curve generated using insulin standards

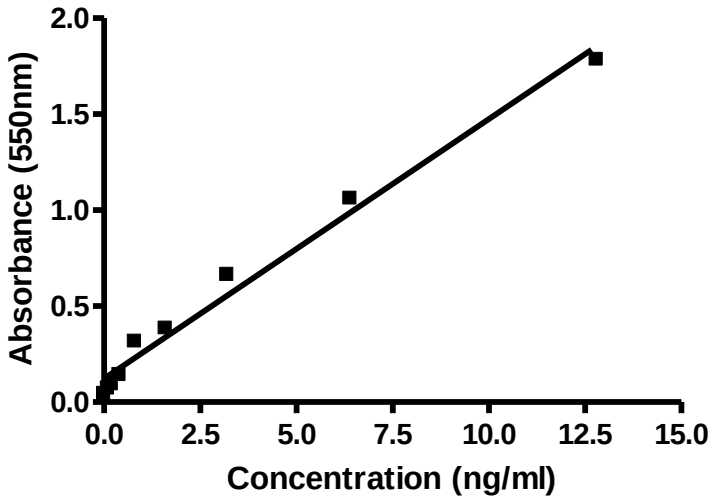

Figure 2.1: Standard curve for insulin measurements. Insulin standards used included 0.1, 0.2, 0.4, 0.8, 1.6, 3.2, 6.4 and 12.8 ng/ml used by linear regression to obtain real-time, insulin values.

2.1.3.4 Measurement of fasting non-esterified free fatty acids (NEFA)

The colorimetric determination of non-esterified fatty acids (NEFA) in plasma was achieved using a NEFA C kit (Wako Chemicals, Nuess, Germany). Tail-blood was collected into an eppendorf with no anticoagulant, at approximately 2pm after a 6 hr fast, in C57BL/6J mice. This was then centrifuged (3000 x *g,* 10 min, 4^{o}C) and an aliquot (~20 µl blood plasma) was taken and kept on ice. Reagents A and B supplied by the manufacturer (Wako Chemicals, Nuess, Germany) were prepared as according to manufacturer's instructions. Reagent A (50 µl) was added to a 96-well plate and then 5 µl of plasma was added and incubated at 37°C, for ten minutes. Reagent B (100 µl) was then added and left at 37°C for a further ten minutes. The concentration of NEFAs within the plasma were measured on a spectrophotometer (OPTImax Tunable Microplate Reader, Molecular Devices, CA, USA) at 550 nm, using a linear regression obtained from a NEFA standard curve to calculate unknown NEFA concentrations.

2.2. Microarray Analysis

2.2.1 F&L exon array experiment

RNA from subcutaneous adipose from Fat and Lean mice were analysed using a GeneChip 2.0 Affymetrix array experiment. Subcutaneous adipose ribonucleic acid (RNA) from age-matched male Fat and Lean mice placed randomly on either a high fat or control diet, from inbred lines of generations 58-65 (n=4 per group) at approximately nine months of age were used. Total RNA for microarray analysis from mouse subcutaneous adipose from Fat and Lean mice on a high fat and control diet was prepared using the TRIzol® kit (modified from procedure originally described by Chomczynski and Sacchi 1987). Four samples for each category (fat and high fat fed (FF); fat and control fed (FC); lean and high fat fed (LF); lean and control fed (LC) were prepared. RNA quality was assessed using an Agilent 2100 Bioanalyser, which is a microfluidics-based platform to test RNA quality. RNA from each sample was loaded onto a specialised chip, which in turn can allow electrical current to pass and their electrical output a determinant of their RNA quality. RNAs were then processed

for hybridisation through standard Affymetrix protocols, with one round of cDNA amplification using standard Affymetrix protocols (which are standard measurements used for further quality assessment namely noise and background). Processed RNAs were hybridised to Affymetrix Mouse Exon 1.0 ST Arrays. Scanning was on an Affymetrix GeneChip scanner. The GeneChip Mouse Exon 1.0 ST Array core probeset had 16654 non-control probe sets. RNA quality control and processing were carried out by Ark Genomics, Roslin, Edinburgh. Further analysis and database preparation were by Dr Donald Dunbar of the Bioinformatics Team at the Centre for Cardiovascular Science (CVS). The criteria used for determining whether changes were significant was calculated by Limma and adjusted by Benjamini and Hochberg. Fold changes, greater than 1.5 and associated adjusted p-values less than 0.05, were used to select genes.

Data were extracted through the GeneChip® Operating Software (GCOS) software and cell intensity file (CEL) files were used for further data processing. CEL files were imported into OneChannelGui software (Sanges *et al.,* 2007), normalised by RMA with background subtraction in the Affy (Gautier *et al*., 2004) module, and statistically analysed with the Limma (Wettenhall and Smyth 2004) package and the Rank Products (RankProd) package (Breitling *et al.,* 2004). Gene ontology (Ashburner *et al.,* 2000) and Kyoto Encyclopaedia of Genes and Genomes (KEGG) pathway enrichment analysis were performed using the Webgestalt (Zhang *et al*., 2005) and Database for Annotation, Visualisation and Integrated Discovery (DAVID) (Dennis *et al.,* 2003).

Analysed microarray data, along with probe annotation, were imported into a custom built MySQL database (www.mysql.com) with a web-based query interface (built in PHP: php.net) by the Cardiovascular Science Bioinformatics Team. The query interface allows searching by gene annotation and gene expression data and is available to registered users at (http://ddunbar.mvm.ed.ac.uk/nmorton/). Microarray data will be archived in the ArrayExpress data repository (www.ebi.ac.uk/arrayexpress) before publication.

2.2.2 Realtime PCR

RNA was isolated from subcutaneous adipose of mice, using RNAeasy columns (RNeasy Mini Kit, Qiagen, UK). Briefly, 100 mg of adipose tissue were homogenised with a polytrone homogenizer (Kinematica GMBH, Luzern, Switzerland) in 700 µl Buffer RLT, supplied by the manufacturer (Qiagen, UK). The homogenate was then left at room temperature (15°C-25°C) for five minutes. Chloroform (200 µl) was then added and eppendorf vortexed for fifteen seconds. Samples were then centrifuged at 12,000 x *g* for fifteen minutes at 4°C. The upper, aqueous phase was then transferred to a new, sterile eppendorf and 600 µl ethanol added, which was mixed by vortexing. The samples were then transferred to an RNeasy Mini spin column (Qiagen, UK) and placed in a 2 ml collection tube (supplied by the manufacturer). These were then centrifuged for fifteen seconds at 10,000 x *g* at room temperature and afterwards, the flow-through was discarded. Buffer RW1 (700 µl) was then added to the RNAeasy Mini spin column and centrifuged for fifteen seconds at 10,000 x *g*, with the flow-through being discarded. Buffer RPE (500 µl) was added to the RNAeasy Mini spin column and centrifuged for fifteen seconds at 10,000 x *g*, with the flow-through discarded. The membrane of the column was then dried by placing the column into a new collection tube and centrifuged at 10,000 x *g* for one minute. To elute the RNA from the column, 30 µl of RNase-free water (supplied by manufacturer) was added directly to the column membrane and centrifuged at 10,000 x *g* for one minute. RNA was also isolated from cell cultures using TRIZOL reagent (Invitrogen, Paisley, UK) as described (Morton *et al.,* 2001). Briefly, medium was removed from cell cultures and TRIZOL was added according to the size of well the cells were grown in; 6 well, 1ml of TRIZOL; 12 well, 0.5 ml of TRIZOL. Cells were then scraped and removed and immediately frozen until use. RNA extraction protocol described above was then followed. Total RNA from both methods was quantified by spectrophotometry at 260 nm (Nanodrop ™ 2000, Thermo Fisher Scientific Inc, Essex, UK). Levels of specific mRNAs were measured by real-time PCR. A total of 1 µg RNA was treated with deoxyribonuclease I (amplification grade; Invitrogen Ltd, Paisley, UK) subsequently and transcribed to cDNA using oligo

(deoxythymidine)$_{20}$ and Superscript III (Invitrogen, Paisley, UK) according to the manufacturer's instructions. Real-time PCR was performed on a Roche Lightcycler using Master Mix (Roche, Burgess Hill, UK) and primer/probe sets from Applied Biosystems (Foster City, CA) as shown (Table 2.1). Beta-Actin, cyclophilin and GAPDH mRNA levels were used as internal controls (Table 2.1).

Gene	**Assay ID**
Angpt1	Mm00456503_m1
Angpt2	Mm00545822_m1
Angiotensin receptor like 1	Mm00442191_s1
VEGFA	Mm00437304_m1
FGF	Mm00523992_g1
Thrombospondin	Mm00449032_g1
Interleukin 8	Mm00438258_m1
Interleukin 2	Mm00434256_m1
MMP11	Mm00485048_m1
MMP9	Mm00442991_m1
MMP2	Mm00439508_m1
PDGF	Mm00435546_m1
Endostatin	Mm00487131_m1
HGF	Mm00434924_m1
CD36	Mm01135198_m1
B-Actin	Mm00462402_m1
Cyclophilin	Mm02342430_g1
GAPDH	Mm99999915_g1

Table 2.1: Real-time PCR primer/probes identifications from Applied Biosystems. Angpt1, angiopoietin 1; Angpt2, angiopoietin 2; VEGFA, vascular endothelial growth factor A; MMP11, matrix metalloproteinase 11; MMP9, matrix metalloproteinase 9; MMP2, matrix metalloproteinase 2; PDGF, platelet derived growth factor; HGF, hepatocyte growth factor; B-Actin, beta actin; GAPDH, glyceraldehydes 3-phosphate dehydrogenase.

2.2.3 Western Blot analysis

Thrombospondin 1 protein levels were measured by Western blot. Protein was extracted from subcutaneous adipose tissue. Briefly, approximately 100 mg of adipose tissue was homogenised using a polytrone homogenizer (Kinematica GMBH, Luzern, Switzerland), in lysis buffer containing 20 mM Tris (pH7.5), 150 mM NaCl, 1 mM EDTA, 1 mM EGTA, 1% Triton X-100 and a protease inhibitor (Roche, UK). Lysates were solubilised for fifteen minutes at 4°C and centrifuged at 16,000 x *g* for ten minutes to clear lysate. The adipose tissue protein extract was then removed and frozen until needed. Protein concentrations were determined by the Bradford assay. Briefly, Bradford reagent (Sigma Aldrich, UK) was diluted fivefold (1part Bradford: 4 parts dH_20) and filtered through a Whatman 540 filter paper. Adipose tissue protein extract (1 µl) was then added to the diluted Bradford reagent (100 µl) on a 96 well plate and the blue colour formed was measured with a spectrophotometer (OPTImax Tunable Microplate Reader, Molecular Devices, CA, USA) at a wavelength of 595nm. A standard curve was also prepared and measured using a serial dilution series of (0.1-1.0 mg/ml) protein bovine serum albumin (BSA; Sigma Aldrich, UK). Samples were incubated for five minutes at 95°C and 50µg protein from each sample were separated by SDS-PAGE (Sigma Aldrich, UK) on a 10 % running gel. The proteins were transferred overnight onto nitrocellulose filters in 20 % methanol, 200 mM glycine, 25 mM Tris buffer (pH 7.8; Sigma Aldrich, UK). The membrane was then blocked in 1 X Blotto and 5 % BSA (Sigma Aldrich, UK) for two hours at room temperature. The membrane was then washed in 1 X Tween TBS (TTBS) and incubated in 1 X Tris-buffered saline (TBS) (Tris-hydrochloric acid and 3 M NaCl; Sigma Aldrich, UK), 0.5 % BSA and thrombospodin-1 antibody (Santa Cruz Biotechnology Inc, CA, USA, sc-12312) for two hours at room temperature. Excess antibody was removed by several washes in 1 X TTBS. Monoclonal antibody against mouse thrombospondin-1 (TSP-1), raised in rabbit was used at 1:1000 dilution, according to manufacturer's guidelines (Santa Cruz Biotechnology Inc, CA, USA, sc-12312). Specific binding was visualized using an enhanced chemiluminescence system (Amersham, Buckinghamshire, United

Kingdom). Uniform transfer of proteins was visually determined by Ponceau red staining of the membrane. Briefly, after electrophoresis, the membrane was blotted in 5 ml of Ponceau stain for five minutes (0.1 % Ponceau stain in 1 % acetic acid; Sigma Aldrich, UK). The membrane was then transferred to 5 % acetic acid (Sigma Aldrich, UK) for a further five minutes. The membrane was then washed twice in distilled water for five minutes each and if successful transfer has occurred, proteins were visible in red. The membrane can then subsequently be blocked as normal.

2.3 *In vitro* methods of assessing angiogenesis

2.3.1 Mouse aortic ring assay

Angiogenesis was studied by culturing rings of mouse aorta in three-dimensional collagen gels (Small *et al.*, 2005) based on modifications of the method originally reported for the rat aorta (Nicosia *et al.,* 1990). This assay uses a matrix-rich product (Matrigel) prepared from Engelbreth–Holm–Swarm (EHS) tumor cells whose primary component is laminin (Madri *et al.,* 1988; Grant *et al.,* 1994). Matrigel is liquid at 4ºC, but solidifies to gel at 37ºC. Aortic rings derived from rodents are placed into the gel under appropriate culture conditions to stimulate growth of endothelial tube-like structures. The gel provides a 3D matrix for sprouting vessels from the cultured aortas. Although several methods of assessing *in vitro* angiogenesis are in use, including cell proliferation, migration and tube formation assays (discussed in Appendix 7.1), this assay was selected as it is currently considered to be the most accurate *in vitro* method of simulating *in vivo* angiogenesis (Auerbach *et al.,* 2003).

2.3.2 Culture Conditions and tissue harvesting for aortic rings

Matrigel (BD Biosciences, UK) was allowed to equilibrate to temperature from solid (-20ºC) to liquid (4ºC) overnight. 1ml filter pipette tips and 24 well plates were also allowed to equilibrate to temperature (-20ºC) overnight. All culture was performed in a class II tissue culture hood (ICN microflow). Matrigel (100 µl) was added to each well of the uncoated tissue culture plate ensuring air bubbles were not introduced into the gel (this is essential as gaps in the Matrigel

do not allow tube formation and, therefore, introduce a systematic error). Plates were incubated for 20 min at 37ºC in order to allow the gel to set. Mice were then killed by asphyxiation in carbon dioxide. A thoraco-abdominal midline incision was made and skin pulled back to prevent the entry of fur into the peritoneal cavity. Thoracic aortas were removed and preserved in EBM-2 serum free/basal medium (EBM-2 serum free media supplemented with aliquots of ascorbic acid, heparin and GA1000 (antibiotic; Cambrex Biosciences, UK). The peri-aortic fibroadipose tissue was carefully removed with fine micro-dissecting forceps and iridectomy scissors, taking care not to damage the aortic wall. Aortic rings (1-2 mm in length; approximately 8 per aorta) were isolated and rinsed in basal EBM-2. Single aortic rings were then placed into each Matrigel-containing well. A further 100 µl of Matrigel was layered on top of the aortic rings, and incubated for 20 min at 37ºC. Basal EBM-2 (1 ml; Cambrex BioScience, Wokingham, UK) was then added to each well and the plate was returned to the incubator. Medium was changed every 48 hours with new media incubated at 37ºC for 30-60 min before addition to the wells. Experiments were all performed in triplicate and aortic rings were cultured for a period of ten days.

Further experimentation explored the possibility of changing the medium used in HUVEC culture (EBM-2) to medium used in adipocyte culture (DMEM) as co-culture of both cell types was desirable. Therefore, DMEM medium with 10 % FCS (FCS contains growth factors essential for cell growth) and 2 mM glutamine (common amino acid also essential for growth of HUVECs) was employed. This was shown to induce TLS formation in aortic rings (refer to Appendix section 7.2.8).

2.3.3 Vessel Quantification

Quantification can be achieved by the measurement of the length and/or the abundance of tube-like structures from the aortic ring (Auberbach *et al.,* 2003). Abundance rather than length was taken as a measurement of aortic ring angiogenesis in this thesis as it was discovered that length did not necessarily

reflect growth (Figure 2.2). Quantification of tube like structure (TLS) abundance was performed every two days under an Olympus CK40 inverted light microscope at 40x magnification from day 2 to day 10 of culture. Images were captured daily using a coolsnap photometrics camera and analysed for area of vessel abundance using MCID software (Imaging Research Inc.).

2.3.3 Aortic ring vessel quantification of tube like structures (TLS)

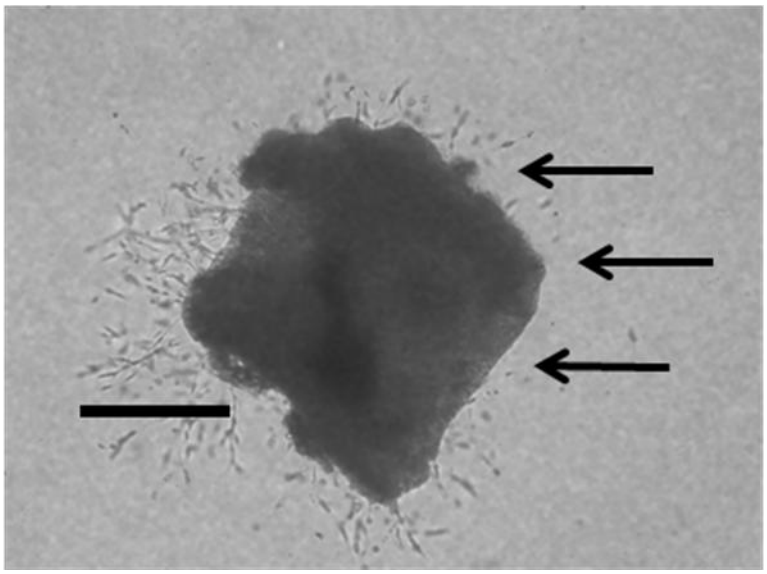

Figure 2.2: Quantification of tube like structures (TLS) from aortic rings. Length of TLS was not representative of growth from aortic ring, as shown by the thick, black line compared to no growth shown by black arrows.

2.3.4 Dil-Ac-LDL incorporation into aortic rings

Aortic rings were removed and sectioned and cultured for 2, 4, 6, 8 and 10 days (as described in section 2.3.1). Rings were then stained for four hours at 37°C with 10 μg/ml fluorescent acetylated low density lipoprotein (Dil-Ac-LDL, acetylated low density lipoprotein labelled with 1,1-dioctadecyl-3,3,3,3-tetramethylindocarbocyanine perchlorate; Biomedical Technologies, Stoughton, MA), which is selectively taken up by endothelial cells (Voyta *et al.,* 1984). Aortic rings were then examined by fluorescent microscopy using rhodamine excitation and emission filters, and white light; with representative images captured (Nikon inverted microscope TE2000-U C1; magnification x 10). Dil-Ac-LDL had no effect on endothelial cell growth rate at the concentration used for labelling cells (data not shown).

2.4 *In vivo* methods of assessing angiogenesis

2.4.1 Optical projection tomography (OPT) of polyurethane sponges

Optical projection tomography (OPT) is a 3D imaging technique (Sharpe *et al.,* 2002), which is comprised of a diffuse light source, illuminating a rotating, biological sample, suspended in a refractive index matching solution (Bioptonics 3001, Bioptonics, UK). Adjustable optics focus light from a plane of interest in the sample onto a charged coupled device (CCD), which captures intensity data to a connected computer (Dell Inc, UK) for acquisition and reconstruction. This technique was used to visualise the specific, genetic labelling of endothelial cells in blood vessels that infiltrated implanted sponges expressing yellow fluorescent protein (YFP) in mice. As an incorporated YFP endothelial cell specific signal would be detectable within vessels that infiltrate the sponge, then no additional antibodies would be required for OPT analysis. Sponges were implanted into YFP mice for 21 days as previously described (section 2.1.3.1). Sponges were removed, fixed in 2 % formalin (rather than 10 %, to prevent quenching of the YFP signal) and then were suspended in filtered 1.5 % low melting point agarose (Sigma Aldrich, UK) on magnetic mounts. Blocks were then trimmed, dehydrated for 24 hours in methanol. After this time, blocks were placed in a 1:2 solution of benzyl alcohol (BA, Acros Organics) benzyl benzonate

(BB, Acros Organics) to clear the agarose. The optical projection tomograph (Bioptonics 3001, Bioptonics UK) was prepared for scanning and samples attached via a magnet were centred to the axis of rotation. Magnification was set to 1 pixel = 6 µm, scans were performed using UV light, and raw data were acquired at increments of 0.9°.

2.4.2 Thrombospondin-1 enzyme-linked immunosorbent assay (ELISA)

Thrombospondin-1 immunoassays were performed on plasma using human Thrombospondin-1 ELISA kits (Quantikine, R&D Systems, UK). Tail blood was collected from two C57BL/6J mice, aged 10 weeks and centrifuged for 15 minutes at 1000 x *g* within an hour of collection. The plasma supernatant was then collected and kept on ice. Human plasma was diluted 1:75 in calibrator diluents RD1-56 prior to the assay. Murine plasma was used undiluted. Assay diluent RD1-56 (100 µl) was first added to each well, followed by 50 µl of standard, control or sample, as appropriate and the plate incubated at room temperature (2 hrs). Each well was then washed 4 times using wash buffer. Diluted human thrombospondin-1 conjugate (200 µl) was then added to each well and the samples were allowed to incubate (2 hr, room temperature). At the end of this period the wash step was repeated and substrate solution (200 µl) added to each well. The plate was then protected from light, and left to incubate at room temperature for 30 mins. Finally, stop solution (50 µl) was added to each well and the optical density of each well was calculated using a plate reader set to 450 nm/540 nm. All solutions were provided by the manufacturer (Quantikine, R&D Systems, UK).

2.4.3 Isolation of adipose tissue stromal vascular fraction by fluorescent activated cell sorting (FACS)

Subcutaneous adipose tissue was isolated from mice immediately after asphyxiation in carbon dioxide. Tissues were handled using aseptic technique and were placed into warm Krebs solution (115 mM NaCl, 5.9 mM KCl, 1.2 mM $MgCl_2$, 1.2 mM NaH_2PO_4, 1.2 mM Na_2SO_4, 2.5 mM $CaCl_2$, 25 mM $NaHCO_3$ and 10 mM glucose, pH 7.4) immediately after removal. Tissues were weighed and

minced into fine (<10 mg) pieces using sterile scissors. Minced samples were placed in 2 mg/ml collagenase Type I solution, containing phosphate buffered saline (PBS), 0.5 % bovine albumin (BSA) and Type I collagenase (Sigma-Aldrich, UK). The samples were incubated at 37°C on an orbital shaker (215 Hz) for 45 minutes. Once digestion was complete, samples were passed through a sterile 250 µm nylon mesh (PlastOK, Meshes and Filtration Ltd, Birkenhead, UK). The suspension was centrifuged at 18 x *g* for ten minutes. The pelleted cells (the stromal vascular fraction (SVF)) were collected, and the floating cells (the adipocyte-enriched fraction) were removed. The SVF was resuspended in 10 ml PBS containing 0.5 % BSA and passed through a 0.45 µm filter (MACS, Miltenyi Biotec, Surrey, UK). This filter was then washed with PBS (10 ml) and the cell suspension was centrifuged again (18 x *g*, for 10 minutes). Erythrocyte lysis buffer was incubated at room temperature for five minutes. Erythrocyte-depleted SVFs were centrifuged (500 x *g* 5 min), and the pellet was resuspended in 1ml of FACS buffer (PBS containing 5 mM EDTA and 0.5 % BSA; MACS, Miltenyi Biotec, Surrey, UK).

SVF cells isolated from adipose tissue samples were cooled on ice and counted using a hemocytometer. After counting, cells were centrifuged (500 *g*, 5 min) and re-suspended in FACS buffer (MACS, Miltenyi Biotec, Surrey, UK) at a concentration of 7×10^6 cells/ml. Cell suspensions were incubated in the dark at 4°C on a bidirectional shaker for 30 minutes in FcBlock (20 µg/ml) (BD Pharmingen, San Jose, California, USA). Cells isolated from YFP mice were washed twice in 1ml FACS buffer then centrifuged (500 x *g*, 5 min) and re-suspended in 1 ml FACS buffer (MACS, Miltenyi Biotec, Surrey, UK). Cells isolated from C57BL/6J mice after the FcBlock were incubated for an additional 50 min with fluorophore-conjugated relevant primary antibodies (rat monoclonal CD31 antibody; IgG1, 130-092-654; 5 µg/ml; Abcam) or isotype control antibodies, as appropriate. Following incubation with CD31 primary antibody, 1 ml FACS buffer (MACS, Miltenyi Biotec, Surrey, UK) was added to the cells. Cells were centrifuged (500 x *g*, 5 min) and re-suspended in 1 ml FACS buffer (MACS, Miltenyi Biotec, Surrey, UK). The wash was repeated twice. Cells

from both C57BL/6J and YFP mice were analyzed on a FACSCalibur and analysis was performed using CellQuest software (Becton, Dickinson and Co., Franklin Lakes, New Jersey, USA). Briefly, all cells were visualized on forward scatter/side scatter, and the appropriate population was gated on the basis of size and granularity. The gated population was then plotted with Forward scatter on the Y axis, and CD31-PE (FL-2 channel). Positive cells were those in the upper right and lower right quadrants. Percent positive cells were calculated based on collection of 10,000 events.

2.5 Cell culture

2.5.1 Mouse 3T3L1 adipocyte cell line

Mouse 3T3-L1 preadipocytes were obtained from American Type Culture Collection (USA). Cells were cultured in basal medium, which consists of Dulbecco's modified Eagle's Medium (DMEM), 10 % newborn calf serum (Gibco, Invitrogen, UK), 500 units/ml Penicillin and 200 mM L-Glutamine (Cambrex, Wokingham, UK). Cells were passaged using trypsin (0.25 %) exposure for 2 minutes at 37°C when at 80 % confluence. Trypsin was neutralised with an equal volume of basal medium and cells were centrifuged for five minutes at 1000 rpm.

3T3L1 pre-adipocytes passages 2-12 (P2-P12) were seeded onto 6-well collagen-coated plates for differentiation, at a density of 2.5 x 10^5 cells/well. Cells were cultured for 48 hours until confluent, then basal medium was replaced with differentiation medium 1, which consisted of DMEM, 10 % fetal calf serum, 500 units/ml penicillin, 200 mM L-glutamine, 0.5 mM 3-isobutyl-1-methylxanthine (IBMX), 0.25 μM dexamethasone and 1 μg insulin (Sigma Aldrich, UK).

Following a further 48 hour incubation, the medium was replaced by differentiation medium 2, which is similar to differentiation medium 1, but lacks dexamethasone and IBMX. Similarly, after 48 hours incubation, the medium was replaced by differentiation medium 3- DMEM containing 10 % fetal calf serum

(FCS), 500 units/ml penicillin and 200 mM L-glutamine. The cells were cultured until they were lipid-filled, which was assessed morphologically (with the counting of lipid droplets observed within random adipocytes within field of view) and confirmed by staining, as described below (section 2.5.3). Fully differentiated cells, with numerous lipid droplets within the adipocytes, were apparent from 10-12 days after initial seeding. For cell treatments, mature 3T3L1 cells were incubated overnight at 37°C (5 % CO_2 and 97 % humidity) in DMEM medium made with charcoal-stripped FCS before treatments commenced. Stripped FCS was prepared as described below: FCS (500 ml) was heat-inactivated at 56°C for twenty minutes in a waterbath. In a sterile hood (ICN Microflow), ten grams (10 g) of dextran coated charcoal (Sigma Aldrich, UK) was added to the FCS and sealed, stirring overnight at 4°C with a magnetic stirrer. After this time, FCS was transferred to 50 ml falcon tubes in the hood and centrifuged at 3,300 rpm for 15 minutes. The supernatant was removed and filtered twice through each of the following syringe filters; 0.5 µm, 0.45 µm and 0.22 µm (Millipore, Watford, UK) and then aliquoted in 10 ml falcon tubes and stored at -20°C.

2.5.2 Manipulation of 3T3L1 adipocytes

Once adipocytes had been incubated overnight with stripped FCS, medium was removed and replaced with fresh stripped FCS (refer to section 2.5.1). This was used as the medium to dissolve any chemical compounds in further experimentation. Experiments were conducted on 6, 12 or 24 well plates, for a period of six hours. After this time, both medium and cells (scraped from the collagen coated plates) were removed for analysis.

In order to assess the effect of various compounds upon adipocyte function (lipolysis or lipid uptake), it was necessary to include positive controls that were known to stimulate these processes. For example, insulin is a known, potent inhibitor of lipolysis (Sekar *et al.,* 1996) and was used subsequently as a positive control to demonstrate this. Concentration response curves (1, 10 and 100 nM; Sigma Aldrich, UK) were used to determine the most effective

concentration of insulin to use in subsequent experiments. Conversely, CL 316,243 (Pharmacia Biotech, UK) is a β_3-adrenoceptor agonist and is known to stimulate the release of free fatty acids (Hoffstedt *et al.,* 1996). Concentration-response curves (1, 10 and 100 nM) were constructed to determine the optimum concentration of CL 316,243 agonist to use in subsequent experiments. This agonist has potent lipolytic effects at 10 nM (Largis *et al.,* 1994). To elucidate the mechanisms of thrombospodin-1 (TSP-1) on adipocyte function, various concentrations of the Type I repeat analogue of TSP-1, ABT-510, were used (1, 10 and 100 nM) as these were optimal for inhibiting endothelial cell function at these concentrations (Good *et al.,* 1990; Iruela-Arispe *et al.,* 1991). ABT-510 was dissolved at 100 X concentration in sterile phosphate buffered sulphate for all experiments (PBS).

Pathways that are known to be activated and associated with TSP-1 action on endothelial cells were also investigated. The p38 inhibitor, SB203580 (1, 10 and 100 nM), the PI3K inhibitor, Wortmannin (1, 10 and 100 nM) and the p38 activator, anisomycin (3, 30 and 300 nM) were used. Inhibitory doses for the p38 MAPK were optimal with 10nM SB203580, and this was used in the ABT-510 dose-response to find optimal concentration (Egelman *et al.,* 1998). Wortmannin is a potent PI3 kinase inhibitor in rat adipocytes at a concentration of 100 nM (Castan *et al.,* 1999), thus an ABT-510 concentration response-curve was conducted with this dose. Anisomycin, a known stimulator of p38 MAPK (Barros *et al.,* 1997) was used as a positive control for this pathway (30 nM).

Stimulation of nitric oxide production was reported with addition of 10 µm myristate acid (Zhu *et al.,* 2005). TSP-1 inhibits myristic acid uptake into endothelial cells (Isenberg *et al.,* 2007). To investigate if this was a potential mechanism, inhibition of nitric oxide production by the nitric oxide synthase inhibitor, L-N^{G}nitro-arginine methyl ester (L-NAME) was employed. L-NAME inhibits nitric oxide production in adipocytes (300 µM; Nisoli *et al.,* 1998) and thus the ABT-510 concentration-response curve was conducted with 300 µM L-NAME.

2.5.3 Lipid accumulation in 3T3L1 adipocytes

Lipid accumulation in adipocytes was measured by Oil Red O staining in 96-well plates. Cells to be tested were fixed in 10% formalin overnight. Cells were then washed with 100 µl distilled water (dH_2O), and washed with 100 µl 70% ethanol. Oil Red O stock solution (Sigma Aldrich, UK) was diluted 6:4 in dH_2O, filtered through a 0.2 micron filter, and 50µl of this filtered oil red O solution used to stain the cells for twenty-five minutes. Cells were then rinsed again in ethanol and dH_2O, as described above. Photographs were taken at this stage using an Olympus CK40 light microscope at 10 x magnification and a coolsnap photometrics camera to observe lipid accumulation with oil red O staining. IGEPAL (4 %; Sigma-Aldrich, UK) was prepared in isopropanol and added to the adipocytes for one hour, causing the cells to lyse and release oil red O. Finally, the absorbance was read on a plate reader at 550 nm (a measure of the oil red accumulation in the adipocytes). In addition to Oil red O staining, molecular markers of adipocyte differentiation could be investigated to confirm complete differentiation including leptin, fatty acid binding protein (FABP) or perilipin.

2.5.4 Non-esterified free fatty acid assay for 3T3L1 adipocytes

When performing colorimetric tests on cell culture supernatants, cells are usually grown in phenol-free DMEM, as the colouring in the phenol (red) can interfere with the assay. Free fatty acid (FFA) assays were performed using the HR Series NEFA-HR (2) kit (Wako Diagnostics, VA, US). Briefly, 100 µl reagent 1 was added to 50 µl of sample then incubated at 37°C for 10 mins. After this time, 50 µl of reagent 2 was added and the absorbance of the solution was read at 550 nm.

2.5.5 Primary 3T3L1 adipocyte conditioned medium

Subcutaneous fat pads from 12 week old, male Tie2/YFP mice were excised and minced in PBS containing 0.5 % BSA. Tissue suspensions were centrifuged at 500 x *g* for five minutes to remove erythrocytes. Collagenase (1 mg/ml; Sigma-Aldrich, UK) was added to the tissue suspensions and incubated at 37°C for 45 minutes with shaking. The cell suspension was filtered through a 100 µm filter

(Millipore, UK) and then spun at 300 x *g* for five minutes to separate floating adipocytes from the SVF pellet. The adipocytes were then washed three times in PBS to remove any remaining collagenase from the cells. Isolated, floating adipocytes (approximately 1 ml) were then cultured in 2 ml eppendorf containing 1 ml of basal medium. Cells were then kept at 37^{o}C in a humidified atmosphere of 5 % CO_2, 97 % humidity and cultured for 24 hours. The adipocyte- conditioned medium containing factors released by the primary adipocytes was then collected. Culture medium without adipocytes was incubated in the same way and used as a control medium.

2.5.6 Measurement of palmitate uptake in 3T3L1 adipocytes

Pre-adipocytes (Passage 8 - Passage 11) were seeded onto 12 well plates at a density of 2.5 x 10^5 cells/well. Adipocytes were then fully differentiated, as described (section 2.5.1), and incubated with stripped FCS overnight prior to experimentation. Drug combinations (ABT-510 1-100 nM; dissolved in sterile PBS) were incubated with the adipocytes for 6 hours at 37^{0}C.

Palmitate uptake was measured by the addition of unlabelled palmitate (1.2 nM), dissolved at 100X concentration in 100% ethanol, and radiolabelled [^{3}H] palmitate (0.3 µCi) in a 0.1 % BSA solution. The reaction was allowed to continue for 6 hours in an incubator at 37°C. Medium-associated radioactivity was obtained by removing medium (1 ml) and adding it to 2 ml of aqueous scintillation fluid (Amersham Pharmacia Biotech). Radioactivity of these samples was then measured in a Beckham LS330 scintillation counter. Cell-associated radioactivity was obtained by washing the cells several times in medium to remove any unbound palmitate and scraping cells with 1 ml 10 % sodium dodecyl sulphate (SDS; Sigma Aldrich, UK) and adding it to 2 ml of aqueous scintillation fluid (Amersham Pharmacia Biotech) in a Beckham LS330 scintillation counter.

Palmitate uptake in adipocytes was optimised prior to experimentation with ABT-510. A time-course experiment was designed to monitor the movement of [^{3}H] palmitate into the adipocytes. Initial experiments examined palmitate

uptake between 5-30 seconds as described in previous publications (Bonen *et al.,* 1998; Guthmann *et al.,* 1999; Coburn *et al.,* 2000). However, no differences in uptake were observed (data not shown). Longer experiments had previously been designed for 18 hours and 24 hours (Yu *et al.,* 2006; Xi *et al.,* 2007), with the reassurance that there was no de-tritiation of palmitate until day two of incubation (Carnicero 1984). Therefore, prolonged incubation of palmitate was examined. The time-course that revealed a shift in uptake into the adipocyte ranged from 5, 15, 30, 45, 60, and 180 and 360 minutes, whereby increased cellular translocation was observed at 360 minutes (6 hours) as shown below (Figure 2.3).

2.5.6 Preliminary time course palmitate uptake experiment in 3T3L1 adipocytes

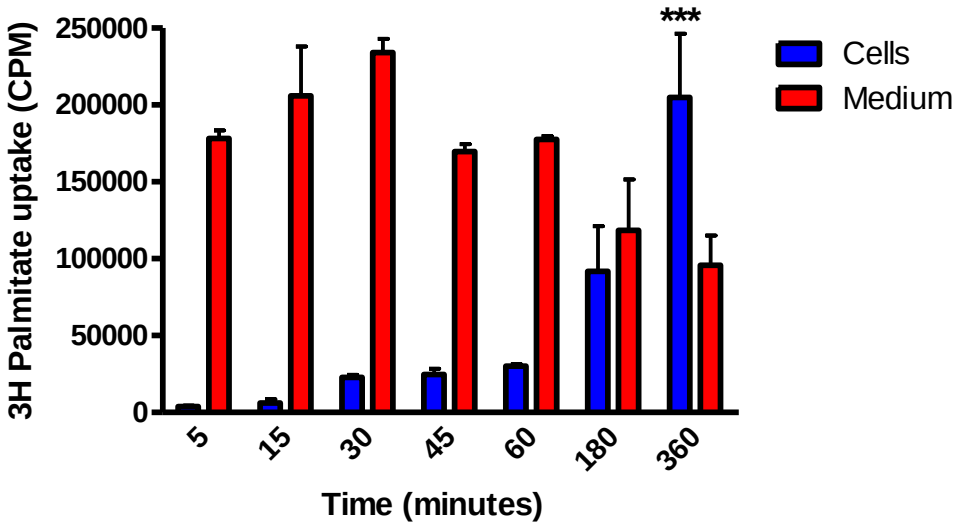

Figure 2.3: ^{3}H palmitate uptake in fully mature 3T3L1 adipocytes. ^{3}H palmitate uptake into the adipocytes was evident at 360 min (6 hours). Higher concentrations of ^{3}H palmitate were evident in the medium and not the adipocyte cells until this point. Data are expressed as mean ± SEM; n=6 for all groups. Data analysed by two way ANOVA followed by Bonferroni correction; **p<0.01.

2.5.7 Intracellular cGMP measurement in 3T3L1 adipocytes

Pre-adipocytes (P10-P14) were seeded onto 24 well plates at a density of 2.5 x 10^5 cells/well. Adipocytes were then fully differentiated with the above protocol (section 2.5.1) and then changed to stripped fetal calf serum overnight prior to experimentation. Cells were then treated in stripped fetal calf serum medium with myristic acid (10 µM) and ABT-510 (100 nM-100 µM).

After five minute incubation (Nisoli *et al.,* 1998; same reference for myristic acid concentration), medium was removed, cells lysed, and intracellular cGMP was determined by ELISA assay (Cell Biolabs; San Diego, USA). The assay protocol was as follows: 50 µL of cell lysate or standard was added to the goat anti-rabbit cGMP coated plate. 25 µL of diluted peroxidase cGMP tracer conjugate was then added to each well. 50 µL of diluted rabbit anti-cGMP polyclonal antibody was then added to each well and incubated (2 h, room temperature) with continuous shaking. The wells were then emptied and each microwell strip was washed 5 times with 250 µL of 1X wash buffer per well, with thorough aspiration between each wash. After the last wash, the wells were tapped on paper towels to remove excess buffer. 100 µL of substrate solution were then added to each well and incubated for 15 minutes on an orbital shaker. The reaction was stopped by adding 100 µL of the stop solution to each well. Absorbance was read immediately on a spectrophotometer using 450 nm as the primary wave length. All solutions were provided by the manufacturer (Cell Biolabs; San Diego, USA).

2.5.8 Nitrite quantification in 3T3L1 adipocytes by the Griess Assay

3T3L1 pre-adipocytes passage 10-14 (P10-P14) were seeded onto 24 well plates at a density of 6.0 x 10^4 cells/well. Adipocytes were then fully differentiated with the above protocol (section 2.5.1) and then changed to stripped fetal calf serum medium overnight prior to experimentation. Cells in stripped FCS medium were then exposed to TNF-α (0.5 ng/ml; mouse recombinant), L-NAME (300 µM) and/or ABT 510 (1-100 µM) as indicated below. Previous work had demonstrated that 0.8 mM DEA/NO inhibited stimulated nitric oxide production from adipocytes (Klatt *et al.,* 2000) and that

TNF-alpha mediated NO production that facilitates lipolysis at a concentration of 0.5 ng/ml (Lien *et al.,* 2009).

L-NAME and DEA/NO were incubated with 3T3L1 adipocytes for 1 hour before experimentation, to allow the inhibitors to act prior to incubation with compounds. The drug combinations described above were then incubated with the adipocytes for a further 4 hours, and the medium was removed and assessed for nitrite production by the Griess assay. Briefly, 50 µl of Griess reagent (1 % sulphanilamide and 0.1 % naphthyl-ethylenediamide in 5 % phosphoric acid; Sigma Aldrich, UK) were added to 50 µl of medium on a 96 well plate. After a 15 minute incubation at room temperature, optical density was measured at 540nm using a microplate reader (Molecular Devices Spectra 340 microplate reader, USA). Calibration curves were made with 0.1 M $NaNO_2$ (1, 10 and 100 nM- results obtained by linear regression; Sigma Aldrich, UK) dissolved in stripped fetal calf serum media.

2.5.9 CD36 receptor knockdown in 3T3L1 adipocytes by siRNA

RNA interference, guided by small interfering RNA (siRNA), is an effective method to target and suppress the expression of specific genes (Bernstein *et al.,* 2001). We attempted to knockdown the CD36 receptor with siRNA ablation in 3T3L1 adipocytes. Both 3T3L1 pre-adipocytes and fully mature adipocytes were transfected using the DeliverX kit (Panomics, Freemont, CA). DeliverX combines siRNA in nanoparticles which are capable of diffusing through the plasma membrane of adipocytes and release the siRNA within the cell. Four different CD36 specific siRNAs (Shanghai GenePharma, Shanghai, China) were used to increase the chance of successful knockdown, as they coded different parts of the CD36 receptor in adipocytes. Different concentrations (1- 30 nM) were used to optimise the specific concentration required for successful knockdown and as recommended in manufacturer's guidelines (Shanghai GenePharma, Shanghai, China). The siRNA IDs were: **CD36-216** (sequence (5' -> 3') – sense: CAG AUG ACG UGG CAA AGA ATT); antisense: UUC UUU GCC ACG UCA UCU GGG); **CD36-826** (sequence (5' -> 3') – sense: CGC UGU GUU CGG AUC

UGA TTT); antisense: UUC AGA UCC GAA CAC ACA GCG TAT); **CD36-837** (sequence (5' -> 3') – sense: GAU CUG AAA UCG ACC UUA ATT): antisense: UUA AGG UCG AUU UCA GAU CCG) and **CD36-954** (sequence (5' -> 3') – sense: CCA AUA ACU GUA CAU CUT ATT): antisense: UAA GAU GUA CAG UUA UUG GAG. GAPDH siRNA (Shanghai GenePharma) (sequence (5' -> 3') - sense: GUA UGA CAA CAG CCU CAA GTT); antisense: CUU GAG GCU GUU GUC AUA CTT), was used as a positive control for knockdown, as according to the manufacturer's instructions had successful knockdown in 3T3-L1 cells (Shanghai GenePharma, Shanghai, China). Scrambled sequences supplied by the manufacturer were also used as negative controls. The adipocytes (both pre and mature adipocytes) were grown to approximately 70 % confluency (Passage 3- passage 12). The DeliverX transfection reagents were sonicated for five minutes prior to use for the proper formation of the complex used for transfection. The 5 µM (1 µl for 12-well collagen coated plate) working stock siRNA was combined with the transfection reagent (49 µl for 12-well collagen coated plate), vortexed and incubated for 20 minutes at 37°C. Working siRNA transfection complexes (1, 10 and 30 nM) were then prepared by adding complex dilution buffer to prepared concentrated siRNA transfection complexes and sonicated again for five minutes. Adipocytes were transfected at Day 6 of differentiation and also at the pre-adipocyte stage in 12-well plates. First, cells were washed with PBS, then transfection reagent (50 µl) was added for five minutes (this reagent has no serum or antibiotics). After this time, serum and antibiotics (100 µl) were added and, after 4 hours incubation at 37°C in 5 % CO_2 and 97 % humidity, DMEM medium was added up to 0.5 ml and incubated for 72 hrs. After this period, Trizol (Invitrogen, UK) was added and RT-PCR was performed to verify that the transfection had worked.

2.5.10 Human endothelial cell culture

Human umbilical vein endothelial cells (HUVECs- Promocell; Heidelberg, Germany) were cultured at 37^{o}C in 75 cm^{3} flasks using endothelial cell culture medium (EGM-2 BulletKit - basal medium containing human epidermal growth factor, hydrocortisone, gentamicin, ampherotericin B, fetal bovine serum,

vascular endothelial growth factor, human fibroblast growth factor B, insulin-like growth factor 1, ascorbic acid and heparin - Lonza Walkersville; Maryland, USA). When cells had grown to confluence they were passaged by first removing the culture medium and then washing the cells twice with 3 ml HEPES-buffered saline solution (Reagent Pack Subculture Kit – Lonza Walkersville; Maryland, USA). HUVECs were then incubated with 3 ml trypsin/EDTA solution (Reagent Pack Subculture Kit - Lonza Walkersville; Maryland, USA) at 37°C for 5 minutes, and the sides of the flask were gently tapped to lift cells from the culture surface. 5 ml trypsin neutralising solution (Reagent Pack Subculture Kit - Lonza Walkersville; Maryland, USA) was then added to the cells to prevent cell lysis. The cell suspension was then split equally between four new flasks, 15 ml culture mediums were added and the flasks were incubated at 37°C. Cells up to passage 6 (P6) were used for experimentation.

2.5.11 Assessment of cell viability: Typan blue exclusion

HUVEC viability was assessed using the Trypan blue exclusion techniques (Cook and Michell, 1989). HUVECs (200,000 cells/well in 1.8 ml growth medium) were plated onto 6 well plates and incubated (2 hours, 37°C, 97 % humidity) to allow adhesion to the well surface. These were then incubated (under standard culture conditions section 2.5.10) with ABT 510 solution (100 µM; 2 ml final volume in serum free cell culture medium) for 6 and 24 hours. Briefly, the HUVECs were washed and trypsinised (section 2.5.10) and an aliquot (10 µl) of the cell suspension was mixed with 90 µl Trypan Blue. Live cells exclude the stain and appear white when examined microscopically, using a at x10 magnification (Olympus CK40 light microscope and coolsnap photometrics camera). Dead cells cannot exclude the stain and, therefore, appear dark blue. Live and dead cells were counted using a haemocytometer in one field of view; the number of dead cells was expressed as a percentage of total cells counted.

2.5.12 In vitro tube formation assay in HUVECs

Twenty-four well plates were initially coated with Matrigel (250 µl; BD Biosciences, UK) as previously described (section 2.3.3). HUVECs (Passage 2-

passage 6) were rinsed with Hepes solution, trypsinised and neutralised by the addition of Trypsin Neutralising Solution (TNS) (All obtained from Cambrex, UK). A suspension of 4.0 x 10^4 cells/ml was prepared in basal medium, containing only EBM-2, ascorbic acid, heparin and GA1000. Aliquots (1 ml) of the cell/medium suspension were then added to each of the required number of wells of the pre-coated Matrigel plate. Plates were incubated at 37°C, and images were acquired at 4, 8 and 20 hours. Tube-like structures were viewed using a Karl Zeiss Axioskop inverted light microscope at X 40 magnification. Images were then viewed using the Microcomputer Imaging Device (MCID) and a live-feed camera. Capillary connections were counted by marking all branch points between tube-like structures, which was done manually using a cell counter (Volin *et al.,* 1999). Each image was blinded prior to counting.

Experiments involved the addition of 100 nM of ABT-510 (Abbott Laboratories, Abbott Park, IL, USA) dissolved in sterile PBS were incubated on HUVECs prepared as described above to observe tube-like development. Control (PBS only) was incubated also.

2.6 Immunohistochemistry

2.6.1 CD31 immunohistochemistry

Frozen sections of subcutaneous adipose tissue (10 μm) from 10 week, male C57BL/6J mice were cut in the cryostat chamber at a temperature of -30 to -35°C and stored at -80°C until further processing. Fixation of adipose tissue sections was in 10 % formalin for 10 mins, followed by three successive washes in phosphate buffered solution (PBS). Sections were then dehydrated though graded strengths of ethanol (70 %, 80 %, 90 % and 100 %). Immunohistochemical staining for CD31 was undertaken using the streptavidin–biotin–peroxidase method using the Vectastain Avidin-Biotin-Complex (ABC) kit for peroxidase (rat IgG) (Vector Laboratories, UK) according to the manufacturer's protocol. Incubation with the primary antibody, which was rat anti-mouse CD31 (BD Pharmingen) at a dilution of 1:50 in PBS, was performed overnight (according to the manufacturer's protocol). Sections were

washed twice in PBS, and then developed with DAB (100 µl- allowing the brown colour to develop for ≤5 minutes; Vectors Laboratories, UK). Sections were counterstained with haematoxylin and eosin (H & E), cleared with xylene, and mounted using DPX mounting medium.

2.6.2 Haematoxylin and eosin staining of mouse adipose tissue

Epididymal and subcutaneous adipose tissue sections (10 µm thick) were cut in a cryostat and mounted on glass slides. Sections were then formalin fixed (10 %) overnight. The following day slides were dewaxed using xylene, and rehydrated through graded strengths of ethanol (99 %, 90 %, and 70 %) for five minutes each. Sections were then stained by haematoxylin and eosin (H&E) for five minutes, rinsed in distilled water, dipped (two seconds) in acid alcohol (1 % hydrochloric acid in 50 % ethanol; Sigma Aldrich, UK) and rinsed in distilled water for a further fifteen minutes. Slides were then immersed in eosin (Sigma Aldrich, UK) for one minute and rinsed in distilled water once again. Finally, slides were dehydrated prior to cover slipping by one minute immersions in 95 % and 100 % ethanol, and then xylene for five minutes.

2.6.3 Determination of mouse adipocyte size

For quantification of the size of adipocytes, the areas of adipocytes in the haematoxylin and eosin-stained preparations were analysed. Mature white adipocytes were identified by their characteristic unilocular (honeycomb) appearance (Nechad *et al.,* 1983) (Figure 2.4). Total areas of adipocytes were traced manually and were examined by under light microscope (Karl Zeiss Axissop) at X 10 magnification. The whole section of adipose tissue on a field of view was analysed, using MCID software (Imaging Research Inc.). Fully formed adipocytes were counted in each section. Any adipocytes which had incomplete cell membranes were not counted.

2.6.2 Haematoxylin and eosin staining of mouse adipose tissue

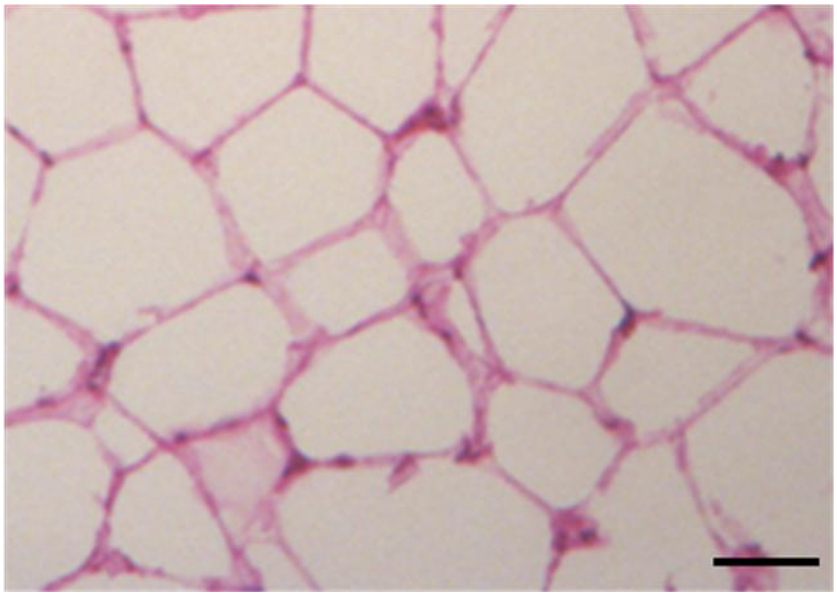

Figure 2.4: H&E stained adipose tissue section. Adipose tissue section demonstrating the clear unilocular or honeycomb appearance of adipocytes. Scale bar represents 5 μm.

2.6.4 Determination of media/adventitia ratio of blood vessels in mouse adipose

For quantification of the media/adventitia ratio, the areas of both the media and adventitia in the haematoxylin an eosin-stained preparations were analysed. Blood vessels were identified within adipose tissue sections. Total tunica media (usually thickest layer of blood vessel and rich in vascular smooth muscle) and tunica adventitia (outside of the blood vessel, made completely of connective tissue) areas of blood vessels were traced manually and were examined under light microscope (Karl Zeiss Axissop) at X 10 magnification. These were then analyzed with MCID software (Imaging Research Inc.). Data were then expressed as ratios (media area divided by adventitia area).

2.7 Data analysis and statistics

All statistical analyses were carried out using Minitab 2005 (Minitab Inc. Chicago, IL, USA) and GraphPad 2007 (PRISM, GraphPad Software, San Diego, CA, USA) for windows. Data are given as mean ± SEM unless otherwise indicated. Linear regression, paired t-tests, one–way and two-way ANOVA followed by Bonferroni *post hoc* or Dunnett's multiple comparison post hoc test where appropriate, were used to detect significant effects between data. Differences were considered significant when $p<0.05$. Asterisks indicate a significant difference: *$p<0.05$; **$p<0.01$; ***$p<0.001$. NS indicates a non-significant result.

Chapter 3
Identification of key adipose tissue angiomodulatory genes and the impact of obesity on angiogenesis *in vitro*

3.1 Introduction

3.1.1 Proposed pro-angiogenic environment in obesity

Adipogenesis and angiogenesis are functionally linked (see Chapter 1; Introduction 1.7). This stems predominantly from the ability of adipose tissue to act as an endocrine organ that produces and secretes multiple cytokines and growth factors (Coppack *et al.,* 2001), which can affect angiogenesis, as well as adipocyte function (Trayhurn *et al.,* 2008).

Angiogenesis is thought to occur within the expanding adipose tissue in obesity, facilitating the provision of adequate oxygen and nutrients to the tissue (Carmeliet and Jain 2000). Accordingly, many pro-angiogenic factors have been linked to obesity (see Chapter 1.7). These include, for example, platelet-derived growth factor (PDGF) (Heldin *et al.,* 1998; Pang *et al.,* 2008), interleukin 8 (Straczkowski *et al.,* 2002), hepatocyte growth factor (HGF) (Bussolino *et al.,* 1992; Rehman *et al.,* 2004; Jung *et al.,* 2009), vascular endothelial growth factor (VEGF), (Miyazawa-Hoshimoto *et al.,* 2003) and the angiopoietins (Ang 1 and 2; Koblizek *et al.,* 1998; Etoh *et al.,* 2001). Of particular interest to this chapter regarding high fat feeding, were the studies concerning the pro-angiogenic matrix metalloproteinases (MMPs). Treatment of high fat fed mice with galardin, a broad spectrum inhibitor of MMPs and, subsequently, angiogenesis, reduced fat deposits (Lijnen *et al.,* 2003). Similarly, accelerated development of high-calorie diet-induced obesity was observed in MMP-3 deficient mice (Maquoi *et al.,* 2003). Supporting the notion that expanding adipose tissue requires an increase in pro-angiogenic factors, Ang 2 is up-regulated during adipose tissue growth (Silha *et al.,* 2005; Voros *et al.,* 2005). Other pro-angiogenic factors have also been positively correlated with body mass index (BMI; Asano *et al.,* 2001; Silha *et al.,* 2005), thus there is substantial evidence to indicate that an increase in pro-angiogenic factors is required for the development of obesity.

Conversely, circulating levels of some anti-angiogenic factors, such as endostatin and ceramide kinase, are also elevated in obesity (Silha *et al.,* 2005; Wu *et al.,* 2007). Increased anti-angiogenic activity would be consistent with the demonstration that obese mice have lower adipose tissue capillary density (rarefaction, also known as capillary drop out) than controls (Lijnen *et al.,* 2006). Preclinical studies are consistent with this model and imply that obese adipose tissues are hypoxic (Ye *et al.* 2007). Although the hypothesis that adipose tissue rarefaction might precede hypoxia remains untested, it is interesting to note that adipose tissue is also known to produce pro-angiogenic factors including VEGF, leptin, tumour necrosis factor-α (TNF-α), and plasminogen activator inhibitor 1 (PAI-1) in response to hypoxia (Scannell *et al.,* 1995; Fitzpatrick *et al.,* 1998). Furthermore, the tip region of the adult epididymal adipose is extremely hypoxic, and expresses high levels of pro-angiogenic factors including VEGF, VEGF receptors and MMPs (Cho *et al.,* 2007). This gives further credence to the concept that there is increased expression of pro-angiogenic factors in adipose tissue in obesity.

Given the growing body of evidence for this altered angiomodulatory status in obesity, and the weight of evidence suggesting increased angiogenic drive in obese, potentially hypoxic adipose tissue, it was hypothesised that there would be an increase in angiogenesis in adipose tissue in obesity. Specifically, it was proposed that the expanding adipose requires increased vascularity to supply the tissue with oxygen and nutrients.

3.1.2 Adipose gene expression profiling in obesity

To determine the overall angiogenic balance in adipose, angiomodulatory genes within the adipose tissue of lean and obese mice were examined. As obesity is a multi-gene/factorial environment-determined trait/condition, it is highly unlikely that a single (angiomodualtory) gene could explain the development of this complex disease. Thus, there are over two hundred genes that, when mutated or expressed as transgenes in the mouse, result in phenotypes that affect body weight and adiposity (Chagnon *et al.,* 2002). In addition, the number

of quantitative trait loci (QTL) reported from animal models, when last assessed, reached over four hundred (Rankinen *et al.,* 2006). This included the identification of the four major obesity QTLs in a unique mouse line selected for divergent fat mass- the Fat mouse line (Horvat *et al.,* 2000). In this chapter, the polygenic Fat model of obesity was challenged with dietary fat in order to recapitulate a gene/environment phenocopy of idiopathic human obesity that might serve as a good source of altered, and perhaps more readily 'translational', angiomodulatory genes (compared to monogenic obesity). An added power of this model was that the major obesity QTLs had been determined in previous studies as outlined below.

The identification of candidate-genes accounting for the effect of obesity QTLs can be pursued in a number of ways. One approach is by performing microarray analysis of gene expression. Changes in gene expression are then related with QTL position of the gene to strengthen causal likelihood. Microarrays are now widely used, enabling the simultaneous analysis of thousands of genes in a single experiment (Brown and Botstein 1999; Moreno *et al.,* 2001). Some studies have used cultured, clonal, human adipocytes (Soukas *et al.,* 2001; Permana *et al.,* 2004) to gain insight into obesity mechanisms. However, cultured cells have important differences to primary adipose obtained directly from experimental animals or humans. Notably, clonal adipocytes lack the endothelial vasculature that control important aspects of lipid metabolism such as LPL activity (Ailhaud *et al.,* 1992). Microarray profiling of adipose tissue from Pima Indians, a population with one of the highest rates of prevalence of obesity and Type II diabetes (Lillioja and Bogardus 1988), shed light on many potential candidate genes for the susceptibility to obesity (Lee *et al.,* 2004). Similar work conducted on adipose from other obese subjects highlighted many adipokines (see section 1.2.5) that contribute to the pathogenesis of obesity (Baranova *et al.,* 2005). These large scale genomic studies emphasise that the gene expression profile of adipose tissue differs considerably between lean and obese subjects. Improved understanding of these differences could lead to the identification of key mechanisms contributing to obesity.

This chapter employed gene expression profiling, in particular focussing on angiomodulatory factors (i.e. using a global gene array more strictly as a pathway focussed array) within the adipose tissue, to specifically address the idea that angiogenesis within adipose tissue plays a major role in the pathogenesis of obesity. Microarray chip analysis of subcutaneous adipose tissue from the polygenic mouse model Fatness (F) and Leanness (L) exposed to standard chow and high dietary fat was used to model the complex trait found in human obesity. This model was created by selecting Fat and Lean mouse lines from a three-way cross of two inbred and one outbred line (Bunger and Hill, 1999). This polygenic model has the advantage, as in human obesity, of deriving from a multigenic complex trait rather than a single gene mutation. Upon high fat feeding, F mice showed the anticipated increase in fat accumulation, particularly in the subcutaneous fat depot (Morton *et al.,* 2005). Therefore, these mice provided an excellent means to gain insight into the altered angiogenic response in adipose tissue with obesity. Increased expression of pro-angiogenic factors likely gives rise to an obese phenotype evidenced by the profound effect of broad spectrum angiogenesis inhibitors on the development of obesity (Brakenhielm *et al.,* 2004). This approach serves to help identify angiomodulatory 'causal' genes for the obesity phenotype. This may allow more accurate and therefore more effective obesity treatments with specific angiogenesis inhibitors.

3.1.3 Angiogenesis as assessed by angiogenic assays in obesity

In addition to investigation into angiomodualtory gene profiling in adipose tissue, specific assays were required to observe angiogenesis in obesity. Two well-established angiogenic assays were employed to assess the angiogenic response in obesity; 1. the *in vitro* aortic ring assay (Nicosia & Ottinetti 1990) and 2. the *in vivo* sponge implantation model (Andrade *et al.,* 1987, Hu *et al.,* 1995; Hague *et al.,* 2002). These assays would be used on a number of murine obesity models to test for broad species-wide effects on angiogenesis. The following models were employed: 1. a polygenic model of obesity, Fat (F) mice and their comparator lean strain, the Leanness, (L) mice; 2. a monogenic model

of morbid obesity, the Ob/Ob mouse, which is deficient in leptin (Friedman and Halaas 1998) and finally 3. a gene/environment model of obesity the diet-induced C57BL/6J mouse strain was also studied.

3.2 Experimental hypothesis

The experiments described in this chapter were designed to validate the hypothesis that obesity increases angiogenesis and is associated with an increase in adipose tissue pro-angiogenic factor gene expression.

3.2.1 Aims

Specifically the chapter aimed to:

- Determine whether angiogenesis-associated genes were altered in adipose tissue of Fat versus Lean mice.
- Identify any key, differentially-expressed and validated factors across the obesity models that could be taken forward for further functional analysis.
- Determine whether angiogenesis-associated changes in genes are reflected in altered angiogenesis in a number of key models of obesity (F, Ob/Ob mice and high fat diet-induced obesity).

3.3 Experimental Protocol

3.3.1 Fat and Lean mouse models

Polygenic models of obesity (Fat) and leanness (L) were employed to investigate changes in angiogenic potential in obesity. Fat and Lean mouse lines were selected from a three-way cross of two inbred lines (JU and CBA) and one outbred line (CFLP), as described in detail (Bunger and Hill 1999). Briefly, selection of the first twenty generations was on the ratio of gonadal fat pad weight to body weight of ten-week old males and subsequently on dry matter content of males at fourteen weeks of age. Inbred lines were initiated from a single family of each of the lines after forty seven generations of divergent selection and maintained by full sibling mating (Bunger and Hill 1999).

For microarray analysis, subcutaneous adipose tissue RNA from age-matched male Fat and Lean mice placed randomly on either a high fat or control diet, from inbred lines of generations 58-65 (n=4 per group) at approximately nine months of age was analysed (Morton *et al.,* unpublished). Mice were fed standard chow from weaning. For high fat diet experiments, mice were switched to a high-fat diet (58 % kcal as fat) or a calorie-matched control diet (11 % kcal as fat, calories substituted with sucrose) for a further eighteen weeks. The mice had free access to their respective food and water throughout the study.

Total RNA for microarray analysis from same subcutaneous adipose from Fat and Lean mice on a high fat and control diet was prepared using the TRIzol method. RNA from four samples for each category (fat and high fat fed (FF); fat and control fed (FC); lean and high fat fed (LF); lean and control fed (LC) was prepared and hybridised to Affymetrix Genechip 2.0 microarray chips as described in section 2.2.1. RNA was isolated from same subcutaneous adipose tissue used in the microarray of F and L mice for real-time PCR validation using RNAeasy columns (see section 2.2.2).

Fat (6-7 months of age; n=4-5) and Lean (6-9 months of age; n=4-5) mice were also used for sponge implantation and removal of aortic rings. Detailed methods

describing sponge implantation, removal and analysis and aortic ring removal can be found in section 2.1.3.1 and 2.3.1 respectively. Epididymal adipose was also removed for histological analysis using Haematoxylin & Eosin (H & E) (see section 2.6.2). Once stained, blood vessels within sections were identified and areas of the media and internal lamina of each blood vessel in the adipose were measured and a ratio derived (see section 2.6.4).

3.3.2 Use of other models of obesity

A model of genetic obesity, the leptin deficient mouse (Lep $^{ob/ob}$), was also used for sponge implantation, removal of aortic rings and investigation into gene expression changes in subcutaneous adipose tissue. Seven week old, male ob/ob mice were obtained from Jackson Laboratories (n=6). Age-matched, male mice from an in-house C57BL/6J colony from The University of Edinburgh (n=6) were used as controls.

Diet-induced obesity was also investigated using C57BL/6J mice. C57BL/6J is the most widely used inbred strain for these studies as they are susceptible to diet-induced obesity, type 2 diabetes and atherosclerosis (Winzell and Ahren 2004). This time period is adequate to cause obesity and the associated adverse metabolic phenotype (Black *et al.,* 1988).

Six week old male C57BL/6J mice (n=12) were singly housed and randomly assigned to two different dietary groups: control and high fat diet (HF). The control animals were fed a standard pelleted diet (containing 20 % of energy as proteins, 67 % of energy as carbohydrates with 5 % sucrose, 62 % starch and 13 % energy as fat by dry weight). The HF group (n=12) were fed a high fat (58 % kcal as fat) as before, for a period of twelve weeks.

RNA was isolated from subcutaneous adipose tissue of Lep$^{Ob/Ob}$ and three month high fat-fed mice with the use of RNAeasy columns.

3.4 Results

3.4.1 Microarray analysis of subcutaneous adipose tissue from Fat and Lean mice

In order to identify broad angiomodulatory changes in adipose tissue from Lean and Fat mice, with or without a further dietary obesity challenge, RNA was obtained from subcutaneous adipose (the most divergent in mass in response to diet: Morton *et al.,* 2005) and used for microarray analysis. Angiogenesis gene ontology (Ashburner *et al.,* 2000) and KEGG pathway enrichment analysis was performed using Webgestalt (WEB-based Gene SeTAnalysis Toolkit) (Zhang *et al*., 2005) and DAVID (Database for annotation, visualisation and integrated discovery) (Dennis *et al.,* 2003; Huang *et al.,* 2009). The differential expression of angiogenesis-related genes were analysed for significant changes in a custom built MySQL database. qRT-PCR was used to validate gene expression changes indicated by the microarray pathway analysis. Validation was performed on a selection of genes that were either up- or down-regulated and were chosen to represent key stages of different pathways. This included some genes from the angiogenic pathway that were differentially expressed and subsequently became the focus of this thesis. The analysis revealed that F and L mice display a divergent angio-modulatory gene expression pattern with distinct responses to the high fat challenge as described below.

3.4.1.1 Differential expression of angio-modulatory genes

Microarray data identified genes that were affected by strain, by diet or by the combination of strain and diet (Figure 3.1). A greater number of pro-angiogenic factors were significantly changed by obesity in the Fat mice ($p<0.05$). For example, angiopoietin-2 (Ang-2; Figure 3.1A), angiotensin-like receptor 1 (Figure 3.1B) fibroblast growth factor-13 (FGF-13; Figure 3.1C) and platelet derived growth factor (PDGF; Figure 3.1D) all showed increased expression in the F strain. There was no effect on expression of angiopoietin-like 4 (Figure 3.1E) and matrix metalloproteinase-11 (MMP11; Figure 3.1F) in the F mice. Conversely, other pro-angiogenic factors, including angiopoietin-1 (Ang-1; Figure 3.1G), fibroblast growth factor-2 (FGF-2; Figure 3.1H) and matrix

metalloproteinase-9 (MMP9; Figure 3.1I) were all significantly lower in Fat mice.

The anti-angiogenic factors ceramide kinase (Figure 3.1J) and vasohibin (Figure 3.1K), were elevated in Fat mice. However, there was no significant effect of diet within the strains. Interestingly, an increase in expression of the anti-angiogenic factor thrombospondin-1 (TSP-1) (Figure 3.1L) was observed in the F strain compared to the L. Furthermore, TSP-1 expression within the F strain was also upregulated when fed a high fat diet

Therefore, an overall increase in pro-angiogenic factors was observed in the Fat mice. However increases in anti-angiogenic factors also highlight that both a pro-and anti-angiogenic tone is increased in obesity, as expected for this complex homeostatic process (see section Introduction 1.6).

3.4.1.1 Divergent angio-modulatory gene expression responses in Fat versus Lean mice

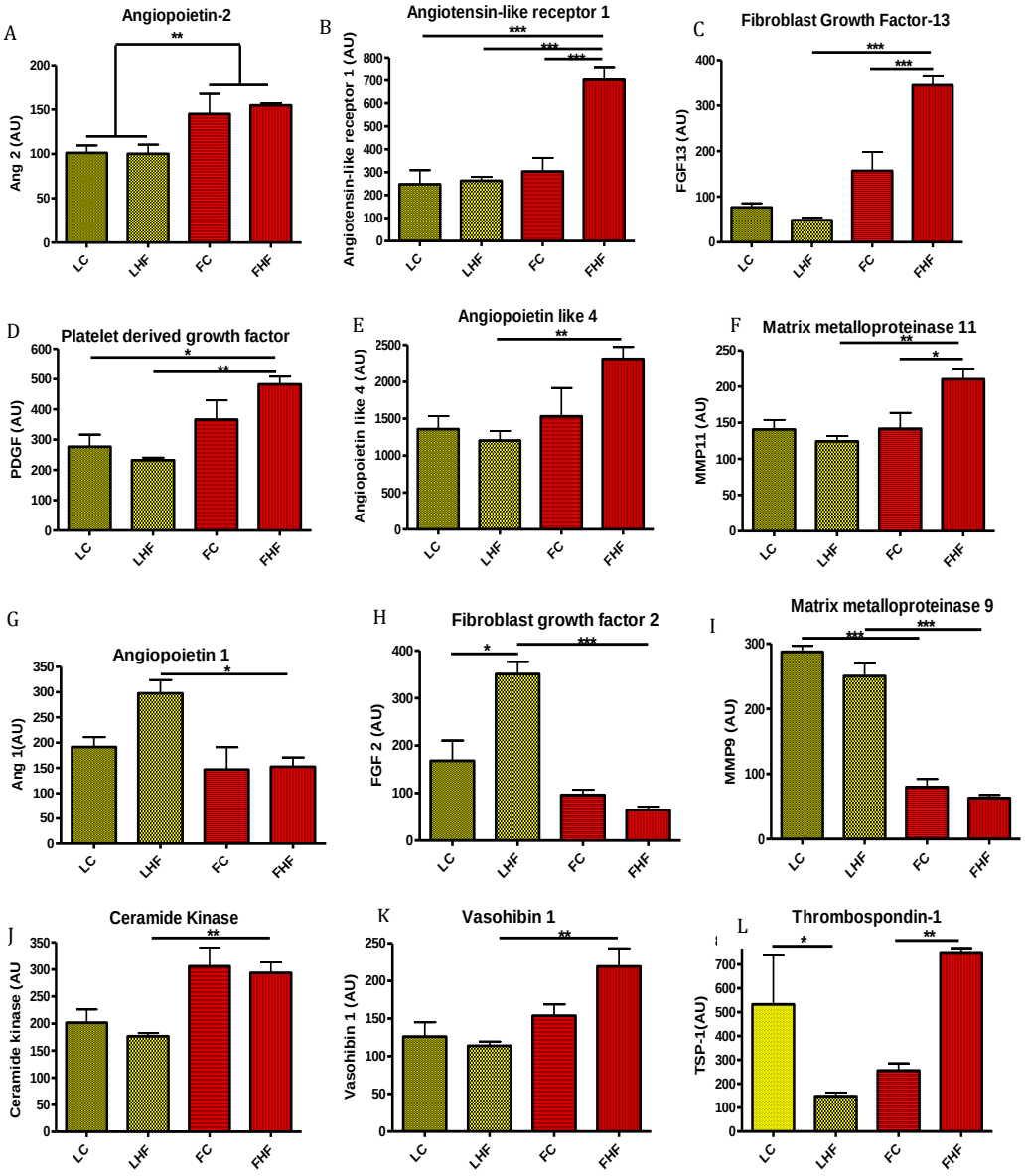

Figure 3.1: Divergent changes in expression of genes involved in angiogenesis: microarray chip analysis in Lean and Fat mice on control or high fat diet. Proangiogenic genes that were differentially expressed in the Fat mouse strain included angiopoietin-2 (Ang-2; **A**); angiotensin-like receptor 1 (**B**); fibroblast growth factor-13 (FGF-13; **C**); platelet derived growth factor (PDGF; **D**); angiopoietin like 4 (AL4: **E**) and matrix metalloproteinase-11 (MMP-11; **F**). Proangiogenic genes affected by diet in the Fat strain included angiopoietin-1 (Ang-1; **G**) and fibroblast growth factor 2 (FGF2; **H**); metalloproteinase-9 (MMP-9; **I**). Anti-angiogenic genes that were differentially expressed in Fat mice included ceramide kinase (**J**) and vasohibin-1 (**K**). An antiangiogenic factor affected by high fat diet in Fat mice was thrombospondin-1 (TSP-1; **L**). LC, Lean control; LHF, lean high fat; FC, fat control and FHF, fat high fat. Lean control/high fat n=4; Fat control/high fat n=4. **p<0.01; Two way ANOVA with *Bonferroni* post hoc test.

3.4.1.2 Validation and confirmation of angio-modulatory gene expression in adipose of Lean and Fat mice

To validate the angiomodulatory gene expression changes seen in the microarray, RNA was extracted from subcutaneous adipose tissue from the complete cohort (n=6 from each strain and dietary constraint) in order to increase statistical power over the microarray (see section 2.2.1). The expression of the housekeeping gene, glyceraldehyde-3-phosphate dehydrogenase (GAPDH) did not differ within and between groups when used (data not shown). Therefore, transcript levels of this gene were used for normalisation of most target genes. However, because of their relatively low expression levels matrix metalloproteinase-11 (MMP-11) and fibroblast growth factor 13 (FGF-13) could not be fully validated, as a suitable internal control with both a comparable expression level (cycle number) and stable expression across groups could not be found.

Ang-1 and MMP-9 levels were reduced in Fat mice (Figure 3.2A & B). The only increase in expression of a pro-angiogenic factor was FGF-2 (Figure 3.2C) in the Fat mice, in contrast to the microarray result. The anti-angiogenic factor TSP-1 (Figure 3.2D) was elevated in Fat mice on a high fat diet, confirming the microarray. Therefore, there was an apparent, overall shift in angiogenic tone towards an anti-angiogenic environment in adipose tissue of Fat mice. Microarray changes in Ang-2 and PDGF expression were not reproduced by RT-PCR (Figure 3.2E &F respectively).

3.4.1.3 Identification of obesity QTL-associated in angiomodulatory genes

The main QTLs in obesity in Fat and Lean F2 crosses have already been described (Horvat *et al.,* 2000). This facilitated identification of potentially causal genes for obesity of the Fat mice (Horvat *et al.,* 2000). The majority of genes that were differentially expressed were mapped to obesity QTLs (FOB chromosomal regions), which included both pro- and anti-angiogenic factors (Table 3.1B). These included Ang-1, angiotensin like receptor 1, ceramide kinase, FGF13, MMP9, PDGF, vasohibin and TSP-1. Four pro-angiogenic factors

were not mapped to obesity QTLs (Figure 3.1A); Ang-2, angiopoietin like 4, FGF-2 and MMP-11, reducing their likelihood for causality for obesity in Fat mice.

3.4.1.4 Confirmation of established angio-modulatory genes

As well as the factors outlined above, there was a wide array of factors involved in angiogenesis that were not shown to be differentially regulated in the microarray experiment of F and L strains (Table 3.2). This was somewhat surprising given previous evidence demonstrating their association in obesity (see section 1.6). It was important to investigate these genes as the power of the microarray experiment was relatively low and thus subtle, significant changes in angiogenic profile may not have been apparent. Therefore, some of these factors were examined by real time quantification (Figure 3.3).

Increased gene expression of the pro-angiogenic vascular endotheial growth factor (VEGF) was observed in F mice on a high fat diet. VEGF expression was suppressed in L mice on high fat diet (Figure 3.3A). There was no effect upon expression of other pro-angiogenic factors including interleukin-8 (IL-8) and MMP-2 (Figure 3.3B & C). Hepatocyte growth factor was unchanged (HGF; Figure 3.3D). The anti-angiogenic factor endostatin was elevated in the adipose tissue of the F mice (Figure 3.3E).

These genes were normalised to TATA binding protein (TBP) instead of GAPDH as additional RNA was needed and therefore extracted.

3.4.1.2 RT-qPCR validation of angiomodulatory genes in Fat and Lean adipose tissue

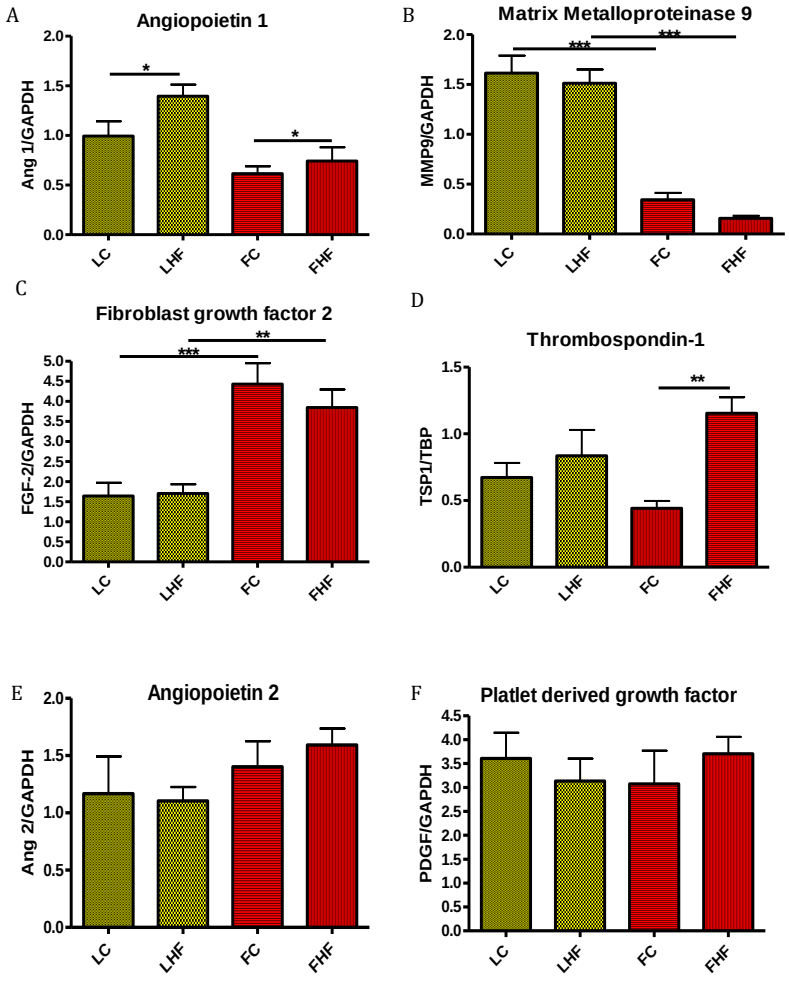

Figure 3.2: Validated mRNA levels of angiomodultory genes in adipose tissue from Fat and Lean mice on control or high fat diet. RT-PCR validation of angiogenesis associated genes highlighted by microarray. These include angiopoietin-1 (Ang1; **A**); matrix metalloproteinase-9 (MMP-9; **B**); fibroblast growth factor-2 (FGF-2; **C**); thrombospondin-1 (TSP-1; **D**); angiopoietin-2 (Ang-2; **E**) and platelet-derived growth factor (PDGF; **F**). LC, Lean control; LHF, lean high fat; FC, fat control and FHF, fat high fat. Lean control/high fat n=4; Fat control/high fat n=6; GAPDH; glyceraldehyde-3-phosphate dehydrogenase Two way ANOVA with *Bonferroni* post hoc test; *p<0.05; **p<0.01; ***p<0.01; NS, non significant.

3.4.1.3 Angiomodulatory genes mapping to obesity quantitative trait loci (QTLs)

A

Genes	QTL Region for Obesity
Angiopoietin 2	**N/A**
Angiopoietin like 4	**N/A**
Fibroblast growth factor 2	**N/A**
Metalloproteinase 11	**N/A**

B

Genes	QTL Region for Obesity
Angiopoietin 1	**FOB3A**
Angiotensin like receptor 1	**FOB1**
Ceramide Kinase	**FOB3**
Fibroblast growth factor 13	**FOB4**
Metalloproteinase 9	**FOB1**
Platelet-derived growth factor B	**FOB3B**
Thrombospondin- 1	**FOB1**
Vasohibin 1	**FOB2**

Table 3.1: Quantitative trait loci (QTL) region assignation for angiomodualtory genes altered in F and L mice. Angio-modulatory genes that are differentially expressed in Lean and Fat mice and whether the gene is mapped to an obesity QTL (**B**) or not (**A**). N/A; non-applicable.

3.4.1.4 Known angiomodulatory genes not differentially expressed between F and L adipose tissue in the microarray analysis

Known angiomodulatory genes that were not differentially expressed in microarray between Fat and Lean mice	
Pro-angiogenic factors	**Anti-angiogenic factors**
Adiponectin	Endostatin
Hepatocyte growth factor	Caveolin
Hypoxia-inducible factor 1 α	
Integrin alpha II and V	
Interleukin 2 & Interleukin 8	
Metalloproteinase 2	
Tie 2	
Vascular endothelial growth factor	

Table 3.2: Angiogenesis-related genes not highlighted in microarray analysis of subcutaneous adipose of Fat and Lean mice on chow or high fat diets. Pro- (in left hand column) and anti-angiogenic factors (in right hand column) not differentially expressed on the microarray analysis of fat and lean mice.

3.4.1.4 mRNA levels of angiogenesis related genes in adipose tissue of Fat and Lean mice

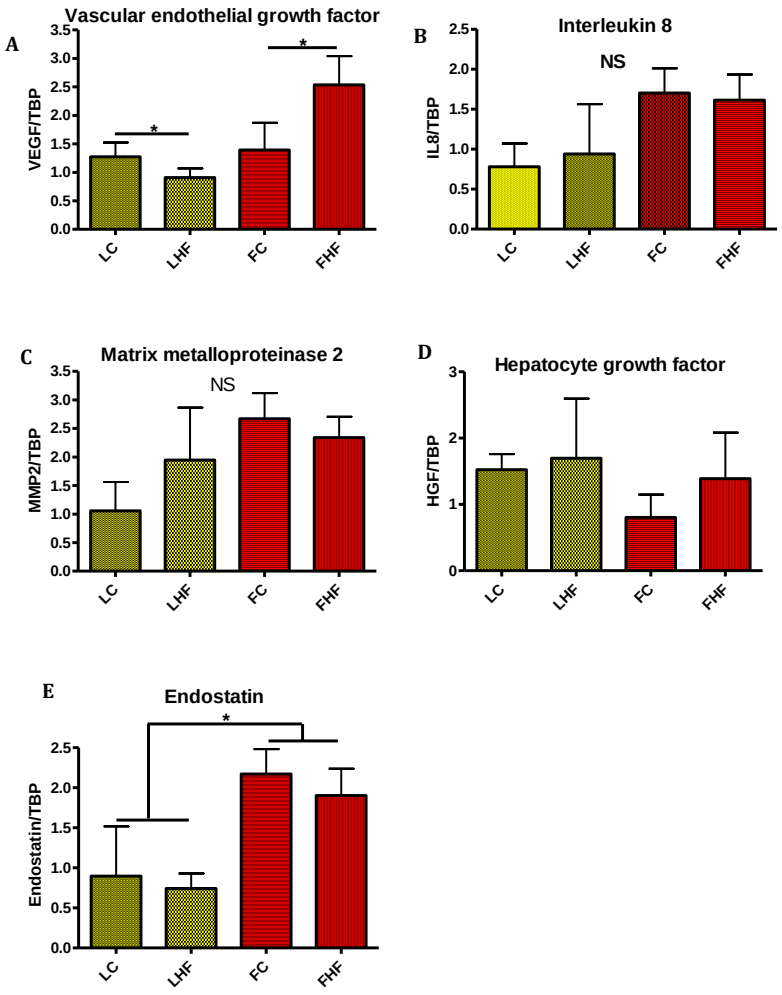

Figure 3.3: Relative expression of established angiogenesis-related genes not highlighted by microarray in Fat and Lean mice on control or high fat diet. Vascular endotheial growth factor (VEGF) (**A**), interleukin-8 (**B**), matrix metalloproteinase 2 (MMP2) (**C**), hepatocyte growth factor (HGF) (**D**) and endostatin (**E**). LC, Lean control; LHF, lean high fat; FC, fat control and FHF, fat high fat. Lean control/high fat n=6; Fat control/high fat n=6; *p<0.05; NS, non significant. TBP; TATA binding protein; Two way ANOVA with *Bonferroni* post hoc test.

3.4.1.5 Upregulation of TSP-1 expression in diet-induced and genetic obesity

Contrary to the initial hypothesis, TSP-1, an anti-angiogenic factor was upregulated in high fat fed F mice. Microarray data suggested that F mice responded to a high fat diet by increasing adipose TSP-1 expression, whereas Le mice downregulated TSP-1 on this diet. Real time PCR analysis validated this increase in Fat mice, suggesting a new hypothesis that an increased anti-angiogenic tone may be present within adipose tissue in obesity. Additionally, TSP-1 is mapped to an obesity QTL, strengthening its potential role as a candidate obesity gene.

The diet-induced increase in TSP-1 expression was investigated in alternative models of obesity in order to test this finding in a broader range of obesity models. Accordingly, TSP-1 expression was investigated in subcutaneous adipose tissue from genetically obese (the $Lep^{Ob/Ob}$ mouse - a leptin deficient, monogenic model of obesity) and high fat diet-induced obesity models (C57Bl/6J administered a high fat diet for 3 months) (Figure 3.4A-B). Crucially, both $Lep^{Ob/Ob}$ and the diet-induced obese mouse models demonstrated elevated adipose tissue TSP-1 expression.

3.4.1.5 Thrombospondin-1 (TSP-1) mRNA levels in adipose tissue from diet-induced and genetic obesity models

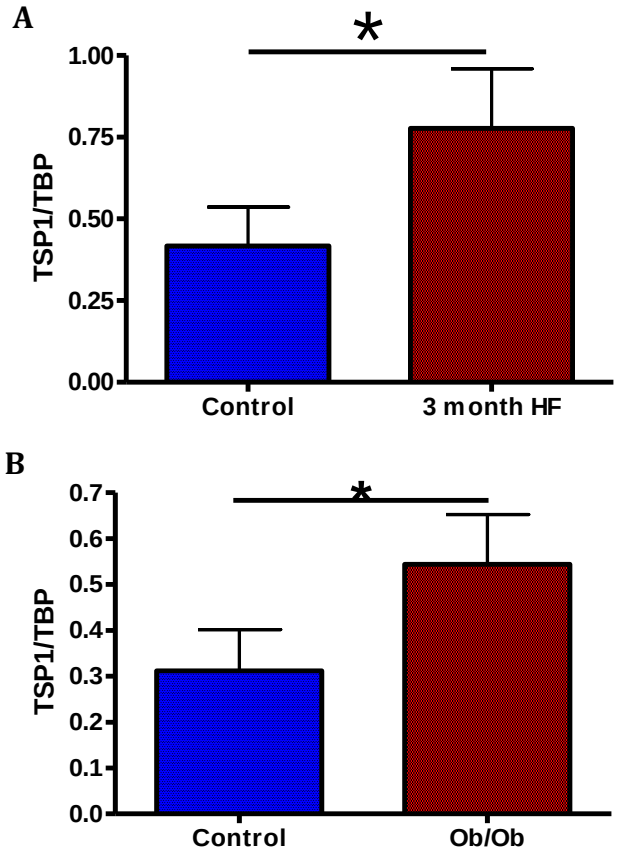

Figure 3.4: Subcutanoues adipose tissue thrombospondin-1 (TSP-1) mRNA levels in diet-induced and genetic obesity. Effect of dietary obesity using 12 week high fat fed mice (**A**) and genetic obesity using ob/ob mice (**B**), on subcutaneous adipose tissueTSP-1 expression. TBP; TATA binding protein; Data are expressed as mean ± SEM; n=6. *p<0.05; Student's t test.

3.4.2 The effects of obesity on angiogenesis *in vitro*

TSP-1 expression was increased in adipose tissue of obese animals of various models, as assessed by microarray and RT-qPCR. These data implies a decrease of angiogenesis in obesity, leading to promotion of a hypoxic environment. The effect of obesity of angiogenesis was examined using the aortic ring assay (refer to Materials and Methods 2.3.1).

Tube-like structures (TLS) could be detected after two days culture in aortic rings from all animals investigated. After 10 days in culture, some TLSs began to degrade and, therefore, analysis was performed on day 10 on all subsequent slides. TLS were quantified every two days under an inverted light microscope at 40x magnification from day 2 to day 10 of culture and analysed using MCID software (see section 2.3.1).

3.4.2.1 Aortic tube-like structure number (TLS) development is reduced in obesity

Aortic rings from F, $Lep^{Ob/Ob}$ and high fat fed obese mice consistently demonstrated diminished TLS formation when compared to chow fed C57BL/6J controls (Figure 3.5 D, E & F respectively)

3.4.2.2 Lean (L) and C57BL/6J mice have comparable aortic tube-like structure (TLS) number

No significant difference in TLS number was observed between L mice and C57BL/6J mice throughout the 10 day period ($p>0.05$) (Figure 3.6).

3.4.2.1 Tube like structure formation was reduced on Day 10 from F, Lep $^{ob/ob}$ and 3 month high fat-fed mice aortic rings

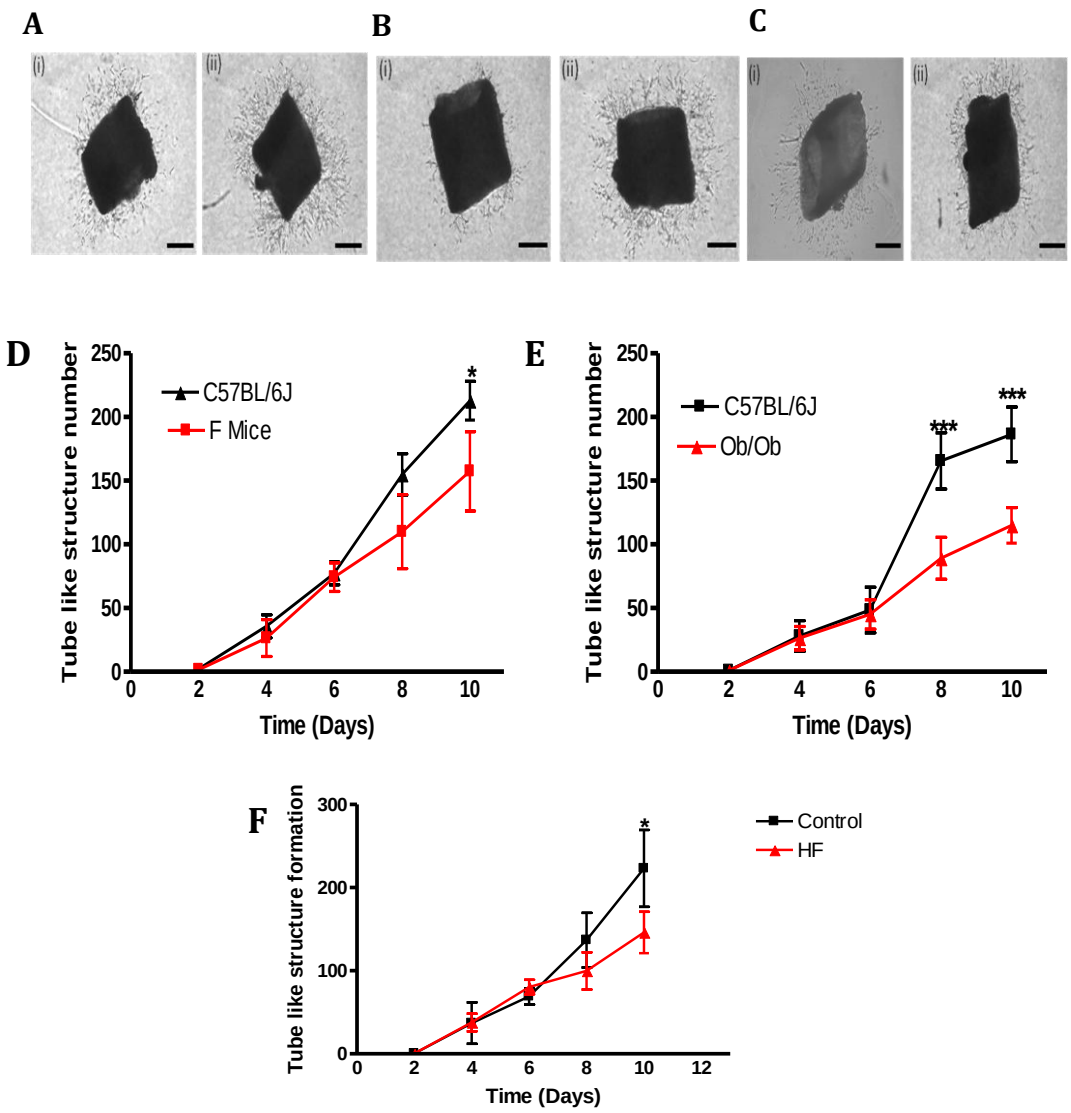

Figure 3.5: Tube-like structure (TLS) formation in aortic rings cultured from Fat, Lep $^{ob/ob}$, diet-induced obese and C57BL/6J mice. TLS formation as assessed by manual counting under light microscopy. New vessel formation was noted after the first 2 days in culture, and rapidly increased for the next 8 days in all groups. A: TLS formation from aortic rings of (i) Fat and (ii) C57BL/6J mice. B: TLS formation from aortic rings of (i) Lep $^{Ob/Ob}$ and (ii) C57BL/6J mice. C: TLS formation from aortic rings of (i) 3 month high fat fed and (ii) C57BL/6J mice. TLS formation was quantified in Fat (D), Lep $^{Ob/Ob}$ (E) and 3 month high fat fed mice (F). Data are expressed as mean ± SEM; n=4-5, Scale bar represents 0.2 mm. Data were analysed by repeated measures ANOVA followed by Bonferroni corrections; *p<0.05; ***p<0.001; HF; high fat fed mice.

3.4.2.2 Tube like structure formation was comparable in Lean versus C57Bl/6J mice aortic rings

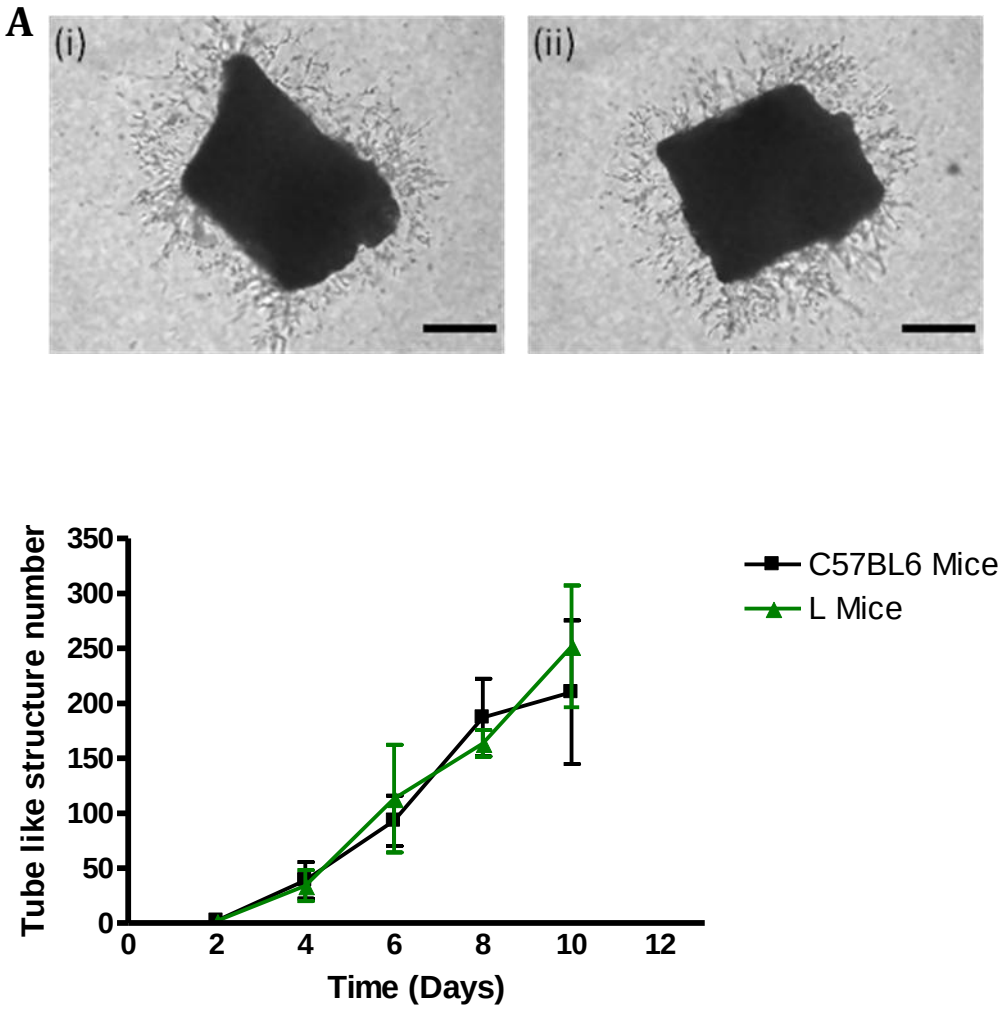

Figure 3.6: Tube-like structure (TLS) formation in aortic rings cultured from Lean and C57BL/6J mice. A: TLS formation was assessed by manual counting under light microscopy from (i) Lean and (ii) C57BL/6J mice. New vessel formation was noted after the first 2 days in culture, and rapidly increased for the next 8 days in both groups. **B:** TLS numbers from Lean and C57BL/6J mice were quantified. Data are expressed as mean ± SEM; n=4-5, Scale bar represents 0.2 mm. Data were analysed by repeated measures ANOVA followed by Bonferroni corrections.

3.4.3 *In vivo* examination of angiogenesis in obesity

In vitro studies demonstrated diminished angiogenesis in the aortic vasculature of obese animals. To determine whether this reduction in angiogenesis was observed specifically in the adipose of obese animals, histological analysis of epididymal fat depots from Lean chow-fed, Lean high-fat fed, Fat chow fed and Fat high fat-fed mice were examined by H&E, as described in section 2.6.2. The epididymal adipose depot was chosen as the subcutaneous depot had been harvested for real time PCR and the mesenteric adipose depot in Lean mice was too small to cut and stain. Furthermore, to investigate the role of obesity in angiogenesis *in vivo*, three week subcutaneous implantation of sponges in C57Bl/6J mice after three months administration of high fat diet were histologically assessed for vessel density.

3.4.3.1 High fat feeding increased media/adventitia area in blood vessels of Fat and Lean mice

Epididymal adipose tissue from both L and F mice on control (Figure 3.7A & C respectively) and high fat diets (Figure 3.7B & D respectively) were sectioned and stained with Haematoxylin and Eosin (H&E). Vessel numbers were unchanged between strains (Figure 3.7E). However, high fat feeding in both F and L mouse models induced an increased media/adventitial area within the blood vessels of the adipose (Figure 3.7F). For example, both L and F chow fed mice exhibited lightly stained blood vessels (shown in pink- individual adipocytes are shown as thinner walled, delicate, unilocular pink structures). High fat fed L and F mice exhibited markedly stained blood vessels, with an associated increase in adventitial area within the blood vessels of the adipose.

3.4.3.2 Obesity is associated with increased vascularity in subcutaneous sponges

To complement the H & E staining of adipose and assess adipose vascularity, the sponge model of angiogenesis was used. Sponges were implanted into F and C57BL/6J mice and also high fat-fed and chow fed C57BL/6J mice for a period of three weeks (see sections 2.4.1, 2.4.2 & 2.4.3). Due to a failure in L line breeding, analogous experiments in Lean mice were not performed. Vascularisation

occurred in all sponges. Sponges implanted into F mice demonstrated increased vascularity compared with C57Bl/6J controls (Figure 3.9). There was increased vascularity ($p=0.04$) in sponges of HF fed C57Bl/6J mice (Figure 3.9).

3.4.3.1 Vascular density and media/adventitia area in blood vessels in high fat fed Fat and Lean mice

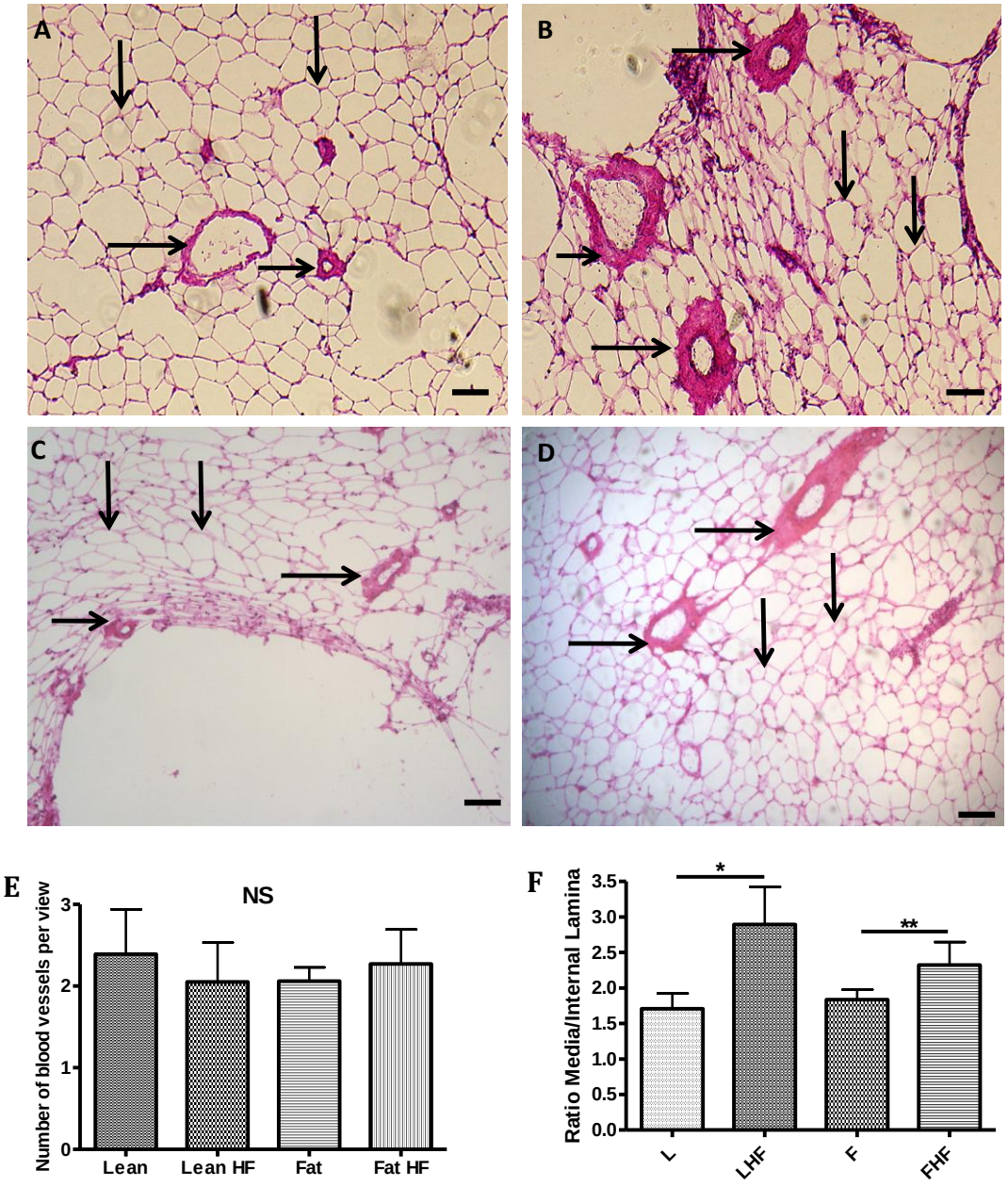

Figure 3.7: Assessement of blood vessels within epidiymal adipose tissue of F & L mice on chow or high fat (HF) diets. Photomicrographs (x 40) of H & E stained blood vessels in epididymal adipose tissue from F and L mice, on either a high fat or chow diet. **A**: Adipose tissue from Fat control–fed mice; **B**: Adipose tissue from Fat high fat fed mice; **C**: Lean control adipose tissue and **D**: Adipose tissue from Lean high fat fed mice. Quantification of the number of blood vessels within adipose tissue (**E**). Quantification of media/lamina areas within blood vessels of adipose tissue (**F**). Measurements of individual blood vessels within adipose were made using MCID software. Horizontal arrows indicate adventitia and vertical arrows indicate adipocytes. Data are expressed as mean ± SEM; n=4-6. Scale bar represents 10 μm. Data analysed by repeated measures ANOVA followed by Bonferroni corrections; NS; non-significant; *p<0.05; **p<0.01.

3.4.3.2 Vessel infiltration into sponges of Fat mice

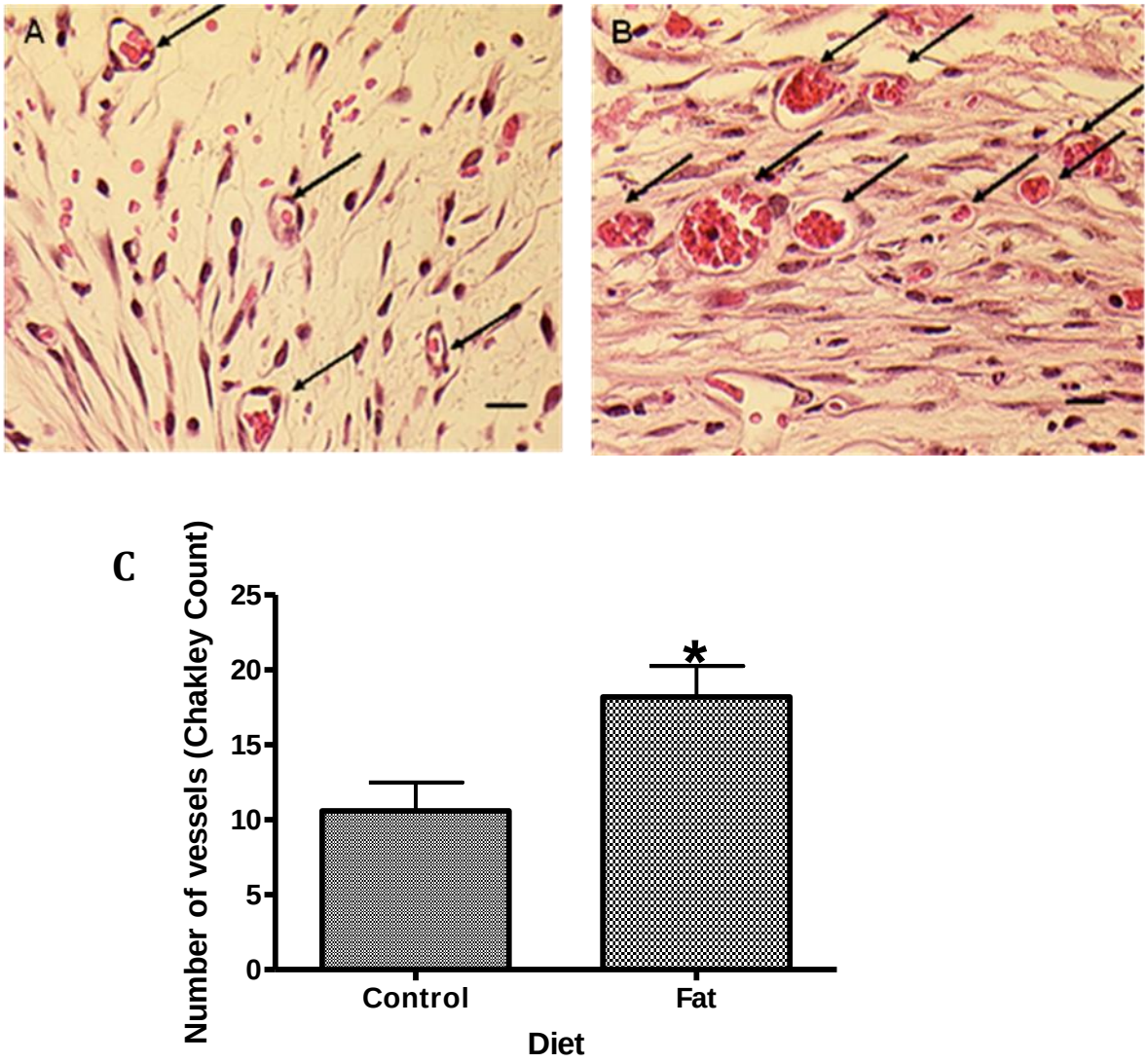

Figure 3.8: Blood vessel infiltration in sponges excised from Fat mice compared to C57BL/6J controls. Photomicrographs (40x) of H&E stained sponges from control (C57BL/6J) (**A**) and Fat mice (**B**). Blood vessels were identified morphologically, with or without erythrocytes present in the lumen and quantified using Chalkley counting (**C**). Scale bar represents 10 µm. Arrows indicate blood vessels. Data are expressed as mean ± SEM, and data were analysed by Student's t test; n=6; * $p<0.05$.

3.4.3.2 Vessel infiltration into sponges of 3 month high fat-fed mice.

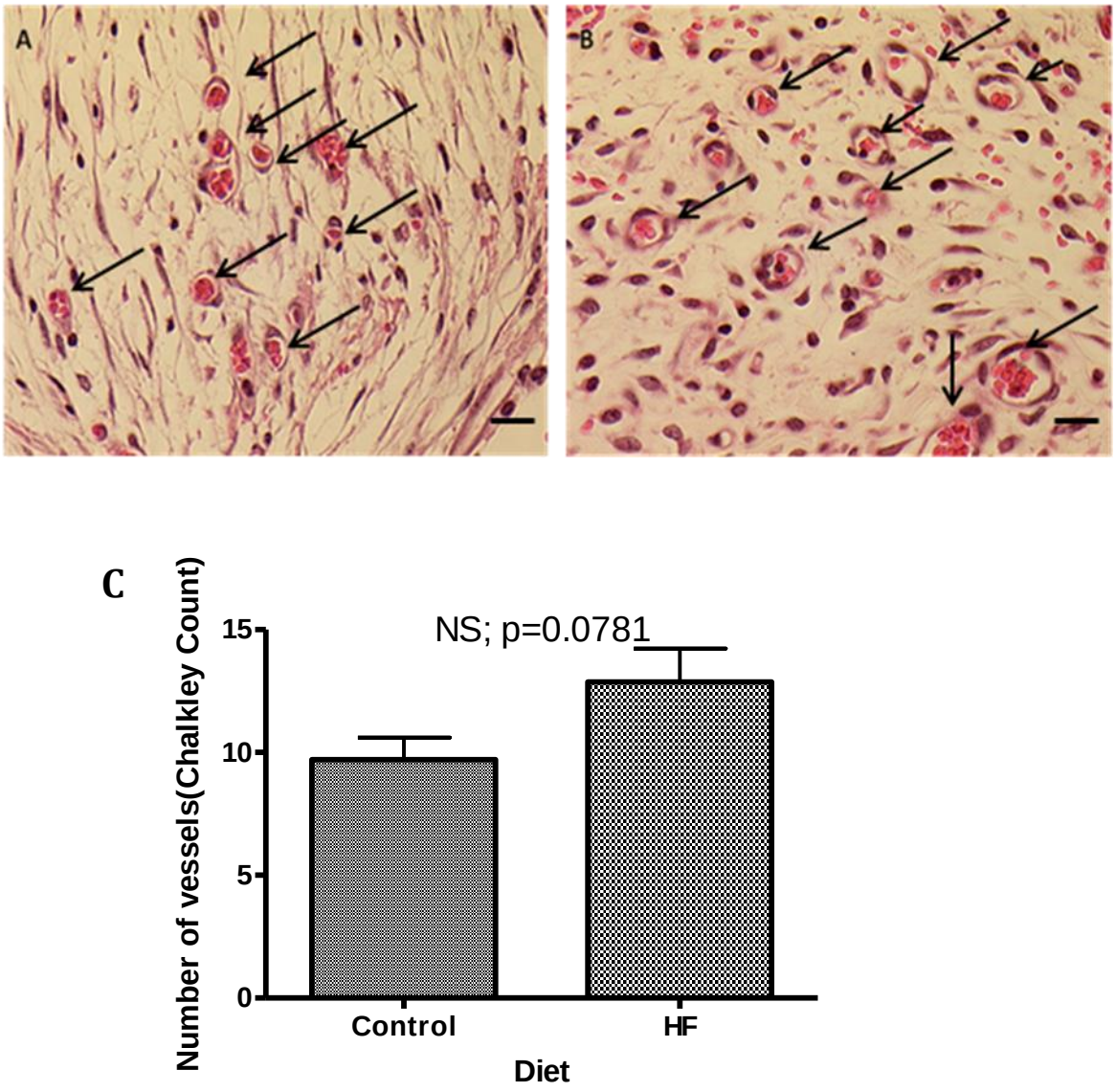

Figure 3.9: **Blood vessel infiltration in sponges excised from 3 month high fat fed C57BL/6J mice compared to chow fed C57BL/6J mice.** Photomicrographs (40 X) of H&E stained sponges from control (C57BL/6J) (**A**) and 3 month high fat mice (**B**). Blood vessels were identified morphologically, with or without erythrocytes present in the lumen and quantified using Chalkley counting (**C**). Scale bar represents 10 μm. Arrows indicate blood vessels. Data are expressed as mean ± SEM, and data were analysed by Student's t test; n=6.

3.5 Discussion:

This chapter tested the hypothesis that genetic and diet-induced obesity is associated with increased angiogenesis in adipose tissue. The overall finding was that obesity is associated with both increased pro- and anti-angiogenic tone. Furthermore, a novel anti-angiogenic factor thrombospondin-1 (TSP-1) was a candidate obesity gene that may generally modulate adipose tissue angiogenesis across a number of key obesity models.

3.5.1 Divergent angiogenic response by Fat and Lean mice from microarray

A large body of evidence exists highlighting the importance of angiogenesis in the development of obesity (Crandall *et al.,* 1997; Zhang *et al.,* 1997; Rupnick *et al.,* 2002). For example, the angiogenesis inhibitor, TNP-470, prevented the development of obesity in ob/ob mice (Rupnick *et al.,* 2002) and in other mouse models of obesity (high-fat diet-induced obesity in C57BL6 mice) (Brakenhielm *et al.,* 2004). Despite this contention, little experimental data exists regarding adipose tissue vessel density quantification in obesity. It was therefore hypothesised that an increase in adiposity should be accompanied by an increase in vascularity, to provide adequate oxygen to the growing adipocytes.

In order to address the original hypothesis that obesity was associated with elevated angiogenesis, a direct, gene profiling approach was adopted to reveal any such change towards a pro-angiogenic environment. Given the hypothetical framework of altered angiogenic processes within adipose tissue and its strong support from the previous studies (Rupnick *et al.,* 2002), a human-like obesity phenocopy model was exploited, the polygenic Fat mice, in order to look at broad angiomodulatory gene expression changes using microarray analysis.

In accordance with the original hypothesis and previous literature, there was increased expression of pro-angiogenic factors Ang 2, MMP11 and PDGF in obesity (Fat mice) by the microarray. However these changes could not be replicated by qPCR (potential reasons discussed in section 3.5.3). Moreover, contradictory results were obtained for FGF-2. Real time PCR experimental

results were favoured over microarray due to the greater sensitivity and statistical power (section 3.5.3). Thus, the increased FGF-2 expression supports our original hypothesis that obesity is associated with an increase in adipose tissue pro-angiogenic factors. Conversely, decreased expression of the pro-angiogenic factor angiopoietin-1 (Ang-1) was confirmed by real time validation. Ang-1 upregulation has been previously reported in experimental adipose tissue growth (Dallabrida *et al.,* 2003) and mapped to the obesity FOB3A QTL on chromosome 15. Decreased Ang-1 therefore represents another angiomodulatory factor that would be important to follow in future work; Ang-1 may be a potential causal obesity gene. Although this is an important observation, it is not necessarily a novel finding, and investigation into the role of Ang-1 in obesity by various groups was underway at the time this research was conducted. Furthermore, a striking upregulation of TSP-1, a factor whose role in obesity research was less apparent this time, was observed. For these reasons, the role of TSP-1 in obesity was investigated, and Ang-1 was not pursued in this thesis.

3.5.1.1 Identification and validation of a QTL-associated angiomodulatory factor in obesity

Angiogenesis is controlled by a balance between pro- and anti-angiogenic factors (see section 1.6). Simply, an increase in pro-angiogenic factors may logically result in the decrease of anti-angiogenic factors to promote vessel development within the adipose tissue. This hypothesis was somewhat challenged, as clear elevation of anti-angiogenic gene expression such as angiotensin-like receptor 1 and TSP-1 (both mapped to obesity QTLs) in Fat mice placed on a high fat diet was apparent; an observation validated by real time PCR. These results may represent a compensatory upregulation of anti-angiogenic factors in adipose tissue in obesity.

A reduction in angiogenesis may in fact contribute to the hypoxic environment of the adipose tissue (Ye *et al.,* 2007). Therefore, the data demonstrate an increased expression of both pro-angiogenic and anti-angiogenic factors in adipose tissue in obesity. Given that the overall effect on vessel formation is

dependent on this complex balance *in vivo*, this may explain the discrepant responses demonstrated by the angiogenic assays and this serves as a critical caveat for the interpretation of these commonly employed experimental approaches (see below), to what may be occurring within any given organ *in vivo*.

3.5.2 Angiogenic response across different models of obesity suggest increased anti-angiogenic environment

As both pro-and antiangiogenic effects had been observed in angiogenesis profiling studies in obese models, it was important to obtain information concerning the effect of this imbalance on adipose-related angiogenesis. This chapter shows that angiogenic responses are complex and may be different depending on the assay employed to assess it. This could be explained with respect to the *in vitro* methods applied to an artefactual effect of *ex vivo* cell culture, or indeed to a divergent response between adipose tissue vessels and sponge-associated neovascularisation and those of the aorta. Nevertheless, Fat mice, Ob/Ob mice and three month high fat-fed obese mice had a consistently reduced capacity for the development of aortic tube-like structures. This impressive observation that vessels removed from an obese environment can still maintain reduced angiogenic capacity was contrary to our initial hypothesis and it was concluded that aortic angiogenesis is impaired in obesity. Decreased aortic angiogenic response is in line with previous studies using aortas from Ob/Ob mice (Gealekman *et al.,* 2008) and also Zucker diabetic fatty rats (Brodsky *et al.,* 2004), which is reassuring. These results are also consistent with the lower capillary density (also known as capillary drop out) and decreased VEGF (Pasarica *et al.,* 2008) in adipose tissue of obese mice. Furthermore, the observed decrease in angiogenesis may also be further evidence to indicate a hypoxic environment present in obesity, as it is known that obese mouse adipose tissue is hypoxic (Ye *et al.,* 2007). Therefore, decreased aortic angiogenesis appears to be a good reporter model for reduced angiogenesis associated with adipose tissue in obesity.

Whilst an excellent means of measuring angiogenesis *in vitro,* the aortic ring model does not directly test whether obesity alters adipose tissue angiogenesis. Therefore, analysis of the number of vessels within adipose was performed using H & E staining of adipose sections. There was no significant change between F and L mice on either diet yet analysis of the blood vessels within these sections did lead to an interesting observation, that the high fat-diet caused the formation of enlarged media surrounding the vessels in both animal lines. Future work will be necessary to dissect the exact composition and function of this increased media to internal lamina area ratio. It is speculated that the mechanism of this thickening in high fat feeding may be angiogenesis, and certainly diet-related.

No difference in blood vessel number between F and L mice is not in accordance with the altered angiogenic profile observed in adipose gene expression. This may mean that the lack of effect is a result of a technique fraught with technical problems including differences in length, shape, path of growth or plane of adipose section. This in turn could underpower the data and potentially not represent adipose tissue angiogenesis in obesity. It may also be that local changes within the adipose that can be extrapolated using sensitive methods like RT-PCR, yet these changes could be missed in sections.

This direct assessment of adipose tissue angiogenesis was proving troublesome (see Appendix; Chapter 8) and thus, the *in vivo* sponge model was used as an ideal means to determine any changes in blood vessel distribution. Sponges proved to be an excellent way to examine the infiltration of small blood vessels, with erythrocytes remaining visible within the vasculature when cut and stained. However, in contrast to the aortic ring assay, obesity was associated with a significant increase in the number of vessels present in sponges from Fat mice (no significant result in high fat-fed mice). Clearly, conflicting results were being produced from the *in vitro* (aortic ring) and *in vivo* (sponge) assays. This may reflect that although *in vitro* angiogenic assays can be useful in screening for specific functions of endothelial cells, findings may not translate well. It could also be due to the sheer complexity of the angiogeneic system *in vivo*. In

addition, previous studies have shown that sponge implantation can cause non specific immune responses which, in turn, may cause a significant alteration to the angiogenic response (Auberbach *et al.* 2000).

The most direct way of examining adipose tissue angiogenesis might initially appear to be the staining of blood vessels within fat pads. This revealed no difference in vascularity. However, the increased medial thickening witnessed around the blood vessels observed with high fat feeding, may shed light on the original pro-angiogenic hypothesis. It may be argued that the medial thickening observed in adipose could relate well to the angiostatic effect witnessed in aortic rings from the obese models. This is because such thickening was not evident within the vessels of the sponges (where increased angiogenesis was observed). Thus, medial thickening may be indicative of decreased angiogenesis and strengthen the argument of an anti-angiogenic environment, as seen with increased TSP-1 expression (as discussed below). This notion is also supported by the finding that angiogenesis is not required for intimal thickening in cardiovascular disease (Khurana *et al.,* 2005), thus decreased angiogenesis evident in aortic rings from obese models may lead to thickening of vessels.

3.5.3 Care in interpretation of microarray

The discrepancies between microarray and real time validation data and also the absence of changes in some of the angiomodulatory genes may be due to the low power of the microarray chip experiment (n=4). In addition, many angiomodulatory factors are post-transcriptionally regulated, and this is not addressed in depth in mRNA level analysis. In spite of these caveats, the assumption is that the gene expression patterns generated by the microarray would provide a broad initial insight into the angiogenic biology of the adipose tissue during obesity that would allow for further investigation.

Real-time PCR analysis was performed on the same subcutaneous fat pads used in the microarray and, as for TSP-1, on additional models of genetic and diet-induced obesity. It may also have been useful to use cDNA from different cell types from within the adipose to observe whether expression changes are

conserved and confined to distinct cellular types; namely adipocytes versus endothelial cells and immune cells (T cells and macrophages), that accumulate in obesity (Weisberg *et al.,* 2003; Rausch *et al.,* 2007). All these cell types are known to produce angiogenic factors (Sumi *et al.,* 2007) and are abundant in adipose tissue and thus remain major contenders to the contribution to the regulation of the tissue vasculature.

The subcutaneous fat depot was the tissue of choice as this exhibited the greatest divergence in fat mass gain between Fat and Lean mice (Morton *et al.,* 2005). Therefore if this tissue experienced the largest increased mass, it would be hypothesised that it would demonstrate the largest differences in angiogenic gene expression. However, it must be noted that there is a higher risk of obesity-associated metabolic diseases with increased adipose tissue mass in the visceral adipose tissue, as compared with the subcutaneous area (Wajchenberg 2000). Furthermore, subcutaneous and visceral adipose are metabolically different (Vohl *et al.,* 2004) and subcutaneous adipose tissue cannot be removed from a mouse as a single identity. This may mean that there will be differences in their gene expression profiles, with regard to adipose angiogenesis. Nevertheless, fat mass divergence is comparable across fat depots between Fat and Lean mice, suggesting similar mechanisms may be at work in all adipose tissues between these lines.

3.5.4 Altered angiogenic response by Fat and Lean mice not highlighted in microarray

A broad spectrum gene array approach was essential in providing insight into angiomodulatory factors altered by obesity. However, as outlined above, many factors previously shown to influence angiogenesis were not shown to be either up- or down-regulated in Fat or Lean adipose tissue. Therefore, it was appropriate to investigate some of these established angiogenic factors by real-time analysis to investigate perhaps more limited changes in gene expression not detectable, due to the low power of the microarray. These included pro-angiogenic factors; vascular endothelial growth factor (VEGF), hepatocyte

growth factor (HGF), matrix metalloproteinase-2 (MMP-2) and interleukin-8. Alongside their effects on endothelial cells, they were also investigated as all have established effects on adipose. For example, VEGF accounts for the major portion of the angiogenic activity of media conditioned by adipocytes (Zhang *et al.,* 1997) and HGF is also known to increase fat neovascularisation (Bell *et al.,* 2007). IL-8 is an important angiomodulatory adipokine and MMP-2 is crucially involved in basement membrane degradation in angiogenesis. Expression of the established anti-angiogenic factor endostatin, which induces endothelial cell apoptosis, was also investigated (Vogel *et al.,* 1993).

There was no significant effect of VEGF in high fat fed Fat mice and IL-8 expression in Fat compared to Lean mice. HGF showed no significant changes between either Fat or Lean mice. In agreement with a general increase in the expression of angiomodulatory genes, endostatin was increased in Fat mice. This highlights the complexity of compensatory systems which are in operation in adipose tissue in obesity and further highlights the over simplification perhaps of the original hypothesis with regards to angiogenic biology in this context. Notably, hypoxia within adipose tissue may occur intermittently suggesting that changes in highly localised vascular angiomodulatory tone may not be reflected in whole adipose tissue depot mRNA profiling studies.

3.5.5 Enhanced TSP-1 expression in obesity

Of particular interest from both the microarray and real time analyses was the divergent response shown by thrombospondin 1 (TSP-1). As described above, TSP-1 is an anti-angiogenic factor, which maps within the obesity QTL (FOB1). The data suggested that the Fat mice respond to a high fat diet by increasing levels of TSP-1, whereas the Lean mice reduce expression of TSP-1 on this diet. These changes parallel fat pad mass, which was shown to increase in high fat-fed Fat mice, but to decrease in high fat-fed Lean mice (Morton *et al.,* 2005). Intriguingly, from a genetics perspective, this increases the likelihood that an angiomodulatory mechanism may be causal to the obese phenotype of the Fat

mice (Raniken *et al.,* 2006). TSP-1 changes were replicated in the Fat but not the Lean strain, further highlighting the importance of secondary validation.

Moreover, TSP-1 expression was also elevated in commonly-used dietary and genetic models of obesity strengthening the case that TSP-1 case is an angiomodulatory gene increased in obesity. Unfortunately due to the large size of the TSP1 protein (450kDa) Western blot analysis to validate this change at the protein level was unsuccessful, a finding reported by others (Voros *et al.,* 2005; Varma *et al.,* 2008).

Reassuringly during the course of this thesis, TSP-1 expression was reported to be elevated in the adipose tissue of obese rodents (Hida *et al.,* 2000; Voros *et al.,* 2005, Varma *et al.,* 2008), although it has never been implicated as a potential causal obesity gene, something that is explored more fully in later chapters of this thesis. Encouragingly, circulating TSP-1 levels were also increased in obese, insulin-resistant subjects and were correlated with adipose inflammation (Varma *et al.,* 2008), confirming our results may translate well into human obesity.

3.5.6 Concluding remarks

In summary, the data in this chapter suggests that, in accordance with the original hypothesis, obesity is associated with an increase in pro-angiogenic factors. However, this hypothesis was overly simplistic, as increases in anti-angiogenic factors were also revealed, confirming that the angiogenic balance is altered by obesity. In accordance with the complex balance of angiomodulatory genes in obesity, different angiogenic assays achieved different results in models of obesity. Therefore, both angiogenic assays were taken forward to be used for future work/chapters in order to have a broad platform of methodology as possible with which to test our specific hypotheses.

Critically, of the genes that were regulated differentially in adipose tissue, one key anti-angiogenic factor that also maps to a major obesity QTL in Fat mice was validated and was in accordance with concurrent reports in the literature on

obesity. As a validated candidate obesity gene with anti-angiogenic properties, it was decided to take TSP-1 forward to develop a further refined hypothesis on its role in adipose tissue in obesity.

Chapter 4

Regulation of adipocyte thrombospondin-1 and the direct effects of ABT-510 on adipocytes *in vitro*

4.1 Introduction

We identified increased gene expression of thromspondin-1 (TSP-1) in adipose of diet-induced and genetic obesity, as well as a relationship between obesity and altered angiogenic potential (see Chapter 3). TSP-1 is elevated in human adipose tissue with obesity (Varma *et al.,* 2008) and in addition, TSP-1 levels were augmented in humans and mice with certain cancers (Nathan *et al.,* 1994; Volpert *et al.,* 1998). However, the overall effect of an increase in an endogenous angiogenesis inhibitor on the expanding adipose (or indeed a tumour) remains unclear. What is clear is that TSP-1 has an established anti-angiogenic effect in endothelial cells (Good *et al.,* 1990; Iruela-Arispe *et al.,* 1991; Taraboletti *et al.,* 1992; Vogel *et al.,* 1993; Tolsma *et al.,* 1993; DiPetro *et al.,* 1994; Volpert *et al.,* 1995). Therefore, this chapter aimed to examine the direct influence of TSP-1 on adipose tissue by identifying factors that may increase TSP-1 expression in adipocytes and to delineate the signalling pathways activated by TSP-1 in the adipocyte.

4.1.1 TSP-1 structure and function

There is already an established role of TSP-1 and its effects on endothelial cells. TSP-1 is a large (450kDa), multimeric, extracellular matrix protein, that is secreted by a variety of cell types (Frazier 1991; Lahav 1993), including platelets, from which it is released to maintain haemostasis (Bonnefoy *et al.,* 2008). TSP-1 is an anti-angiogenic factor in endothelial cells and, at supra-physiological concentrations (>20 nM which is about forty times that seen in normal plasma; approx 0.5 nM) (Saglio & Slayter 1982; Browne *et al.,* 1996), TSP-1 inhibits endothelial cell proliferation (Good *et al.,* 1990; Taraboletti *et al.,* 1992; Vogel *et al.,* 1993) and migration (Good *et al.,* 1990; Taraboletti *et al.,* 1990; 1992; Tolsma *et al.,* 1993; Volpert *et al.,* 1995) as well as their ability to form lumens (Tolsma *et al.,* 1997) and tubes (Iruela-Arispe *et al.,* 1991; DiPetro *et al.,* 1994). In accordance with its anti-angiogenic role, TSP-1 null mice were shown to display a mildly increased vascular density in muscle (Crawford *et al.,* 1998), which would also suggest that developmental angiogenesis may be modulated by TSP-1. Similarly, transgenic mice over-expressing TSP-1 in the

epidermis exhibit delayed wound healing, which is characterised by decreased vascularity (Streit *et al.,* 2000). Conversely, TSP-1 null mice have normal vascular density in healing wounds (Agah *et al.,* 2002). This perhaps re-enforces the concept that angiogenesis requires a balance between multiple pro- and anti-angiogenic factors and, thus, knockout of a single modulatory gene may not dominantly affect vascular density (Agah *et al.,* 2002). In addition to its anti-angiogenic role, TSP-1 can act as a pro-angiogenic factor in non-endothelial cells by promoting the migration of vascular smooth muscle cells and stimulating matrix assembly by binding other matrix proteins, including MMP2 (Taraboletti *et al.,* 1990; Gao *et al.,* 1996).

4.1.2 Anti-angiogenic domains of TSP-1

These pro- and anti-angiogenic effects of TSP-1 are attributed to distinct domains of this highly complex protein. Thus, TSP-1 has a structure consisting of: (1) an N-terminal heparin binding domain; (2) a coil, which dictates not only its conformation but also participates in interchain disulphide bonds; (3) a cysteine rich sequence; (4) three Type I repeats (which are also known as thrombospondin type I repeats (TSRs) or properdin-like domains); (5) three Type II repeats; (6) Seven calcium-binding Type III repeats; and finally, (7) a C-terminal globular domain (Bornstein 1992; Adams 2001) (Diagram 4.1). The N-terminal domain is also known to mediate VEGF uptake and clearance via low density lipoprotein receptor-related protein (LRP) (Greenaway *et al.,* 2007).

The large size of TSP-1 makes it not only impractical to work with in cellular and *in vivo* models, but complicates the interpretation of the results. As the region responsible for the inhibition of angiogenesis has been mapped to the Type I repeat (Tolsma *et al.,* 1993), much interest has now surrounded these smaller fragments for their potential use as therapeutic agents in angiogenesis-dependent diseases. A structurally-modified proteolytic fragment from the Type I repeat of TSP-1 inhibited VEGF-induced endothelial cell migration *in vitro*, and decreased FGF-induced neovascularisation in a rat cornea model (Dawson *et al.,* 1999). It became apparent, however, that this heptapetide underwent rapid

clearance in rodents. Subsequently two more stable nona-papetides, ABT-510 and ABT-526 were discovered to have anti-angiogenic actions (Haviv *et al.,* 2005).

ABT-510 is derived from the second Type I repeat from the NH_2 terminal third of TSP-1 (Dawson *et al.,* 1999). ABT-510, like TSP-1, has been shown to cause endothelial cell apoptosis via activation of Fas and Src-related kinase p59 Fyn pathway, ultimately leading to endothelial cell death (Jimenez *et al.,* 2000; Quesada *et al.,* 2005). ABT-510 inhibits the migration of human microvascular endothelial cells stimulated by growth factors and decreases endothelial cell proliferation and tube assembly in fibrin gels (Reiher *et al.,* 2002; Haviv *et al.,* 2005). As a potent angiogenic mimic of TSP-1, ABT-510 was chosen for subsequent studies in this thesis with the caveat that *in vivo* levels of the endogenous TSP-1 molecule may be elevated. Therefore, our findings are interpreted cautiously with respect to the effects of increased levels of the endogenous molecule, with presumably more pleiotropic effects.

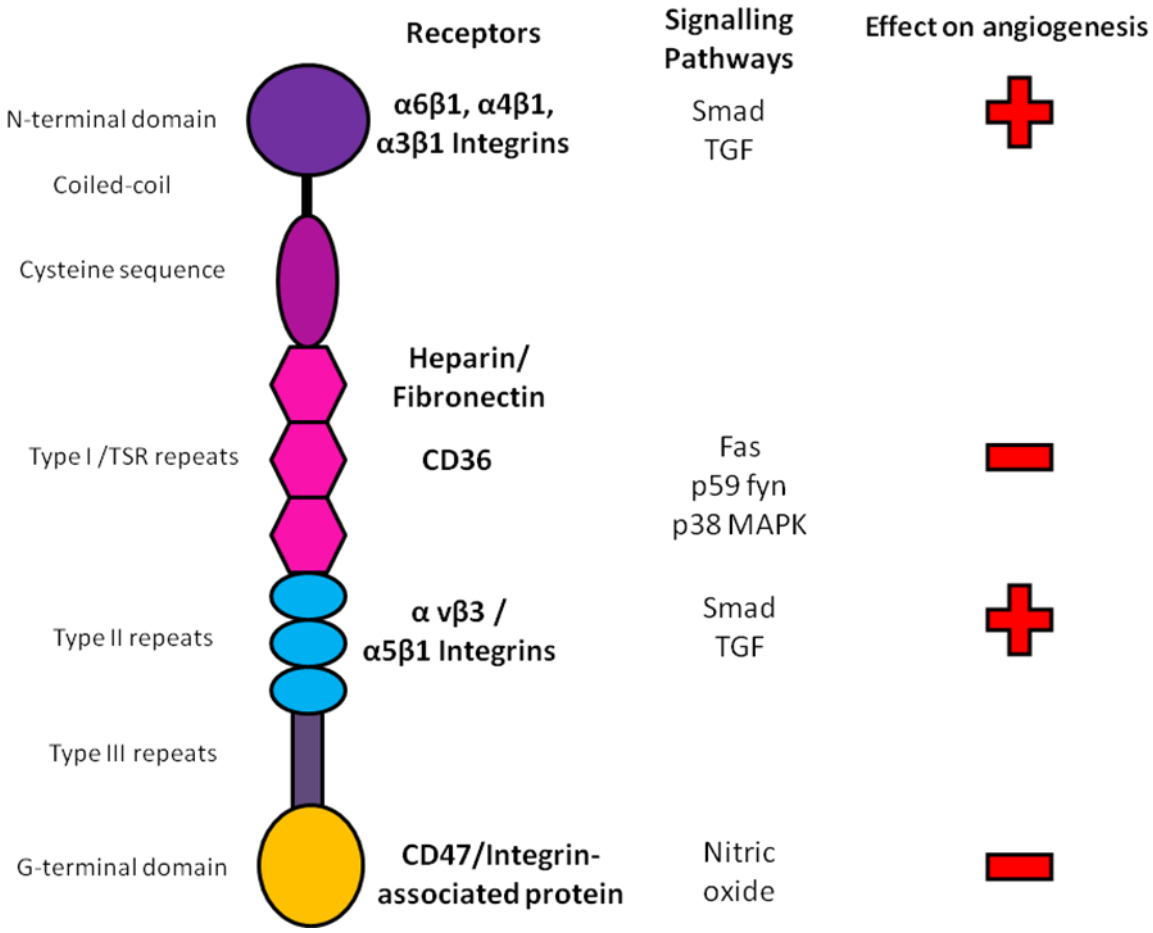

Diagram 4.1: Thrombospondin-1 (TSP-1) structure. Pro- and anti-angiogenic domains of TSP-1 acting at endothelial cell receptors. These include N-terminal domains with integrin binding, causing pro-angiogenic effects, involving proteins in the transforming growth factor (TGF) family including Smad; Type I repeats or TSR region binding CD36 and heparin causing an anti-angiogenic effect, involving Fas, p38 mitogen activated protein kinase (MAPK) and p59 fyn; region containing Type II repeats binding again some of the integrin family inducing a pro-angiogenic effect and finally a G-terminal domain which can bind CD47 causing an-anti-angiogenic effect, mediated through nitric oxide signalling pathways.

4.1.3 CD36 mediates ABT-510 anti-angiogenic activity

The mechanism by which ABT-510/Type I repeat of TSP-1 exerts its anti-angiogenic effect has been thoroughly investigated. Intact TSP-1 binds to a large number of cognate molecules; it has at least 12 different receptors (Bornstein 1995), many of which are present on the surface of the endothelial cells. These include extracellular matrix proteins, cell-surface protein receptors, and glycolipids, proteases, and growth factors/cytokines. However, the most well characterised interaction is that between ABT-510/Type I repeat of TSP-1 and CD36.

CD36 is an 88kDa cell-surface membrane protein belonging to the scavenger receptor B family. Activation of CD36 induces platelet aggregation, anti-angiogenesis, uptake of long chain fatty acids and oxidised LDL (oxLDL), cell adhesion and macrophage phagocytosis (Febbraio *et al.,* 2001). As well as being expressed on endothelial cells, CD36 is also expressed highly on adipocytes (it is known as FAT, fatty acid translocase), muscle cells, enterocytes and hepatocytes (Abumrad *et al.,* 1993; Nassir *et al.,* 2007).

The important interaction that exists between TSP-1/Type I and CD36 has been reiterated in studies using neutralising antibodies against CD36, whereby the ability of TSP-1 to inhibit migration and corneal vascularisation was blocked (Dawson *et al.,* 1997) and large vessel endothelial cells lacking CD36 failed to respond to TSP-1 *in vitro*, unless transfected with exogenous CD36 (Febbraio *et al.,* 2001). In addition, CD36 null mice were resistant to the effects of TSP-1 (Jimenez *et al.,* 2000), confirming that the anti-angiogenic activity of TSP-1 is dependent upon CD36 in endothelial cells. This was illustrated further as a CD36 null mutation in the spontaneously hypertensive rat strain has been linked to insulin resistance (Aitman *et al.,* 1999; Pravenec *et al.,* 2003), and humans lacking CD36 exhibit insulin resistance (Miyaoka *et al.,* 2001). Therefore, in addition to the effects of TSP-1 on endothelial cells through CD36, the anti-angiogenic fragment of TSP-1 may bind to CD36 and alter adipocyte metabolism, potentially altering insulin associated functions. Clearly this is a

promising link between elevated TSP-1, adipocyte lipid metabolism and obesity/insulin resistance.

4.1.4 Pathways implicated in the anti-angiogenic activity of TSP-1 in endothelial cells

Aside from the role of CD36 in lipid metabolism in adipocytes, TSP-1/Type I repeats bind CD36 on endothelial cells inducing apoptosis via caspase 3 and 8 activation (Jimenez *et al.,* 2000; Nor *et al.,* 2000). This binding increases CD36 association with the signalling intermediate Fyn, activation of which is critical for TSP-1-dependent apoptosis and inhibition of angiogenesis (Simantov and Silverstein 2003). This was demonstrated when microinjections of Fyn neutralising antibodies were shown to abolish signalling events leading to TSP-1 activated apoptosis in endothelial cells (Jimenez *et al.,* 2000). TSP-1/Type I repeat interaction with CD36 also results in the activation of p38 kinase and c-Jun-NH_2-terminal kinase (JNK) (Mirichnik *et al.,* 2008). This JNK induction is crucial as TSP-1 anti-angiogenic activity was severely compromised in JNK 1 null mice (Jimenez *et al.,* 2001). Moreover, a p38 inhibitor, SB203580, blocked TSP-1 induced apoptosis *in vitro* and restored corneal angiogenesis *in vivo* (Jimenez *et al.,* 2000). This anti-angiogenic pathway is summarised in Diagram 4.2. In addition to the pathways discussed above, the TSP-1/Type I repeat induces CD36-independent inhibition of growth in HUVECs via a p53-dependent induction of p21 (Yamauchi *et al.,* 2007).

4.1.5 Overlap of TSP-1 pathways involved in adipocyte lipolysis

Alongside its role as a dynamic endocrine organ, adipose also serves as a simple lipid and energy store. Fat cells store lipids from the diet and those exported from the liver. They release these lipids as free fatty acids when the organism is fasting by a highly regulated process; lipolysis. The importance of this function has been demonstrated in lipodystrophy, where the lack of adipose tissue is associated with muscle insulin resistance and liver steatosis, mainly due to the lipotoxic effects of excessive ectopic storage of free fatty acids (Kim *et al.,* 2000; Garg 2004). Lipolysis is stimulated via adrenergic receptor activation by

catecholamines, which in turn activate the G-protein coupled signalling system including adenylyl cyclase and cAMP-dependent protein kinase (PKA). However, there is evidence that in addition to PKA, G-protein-coupled receptors and cyclic AMP can also activate mitogen-activated protein kinase (MAPK) pathways (van Biesen *et al.,* 1996; Vossler *et al.,* 1997; Gutkind 1998). There are three parallel MAPK pathways in mammalian cells, which include stress-activated protein kinases, JNK and the p38 MAPKs. These mechanisms play a vital role in adipocyte function and, since the anti-angiogenic role of TSP-1 is mediated through the p38 MAPK system in endothelial cells, it was reasoned that there may be an overlapping or common signalling mechanism in adipocytes. This is strengthened further as β_3 adrenoceptor activation in adipocytes activates p38 MAPK as a downstream consequence of the generation of cyclic adenosine monophosphate (cAMP) and protein kinase A (PKA) in lipolysis (Cao *et al.,* 2001b).

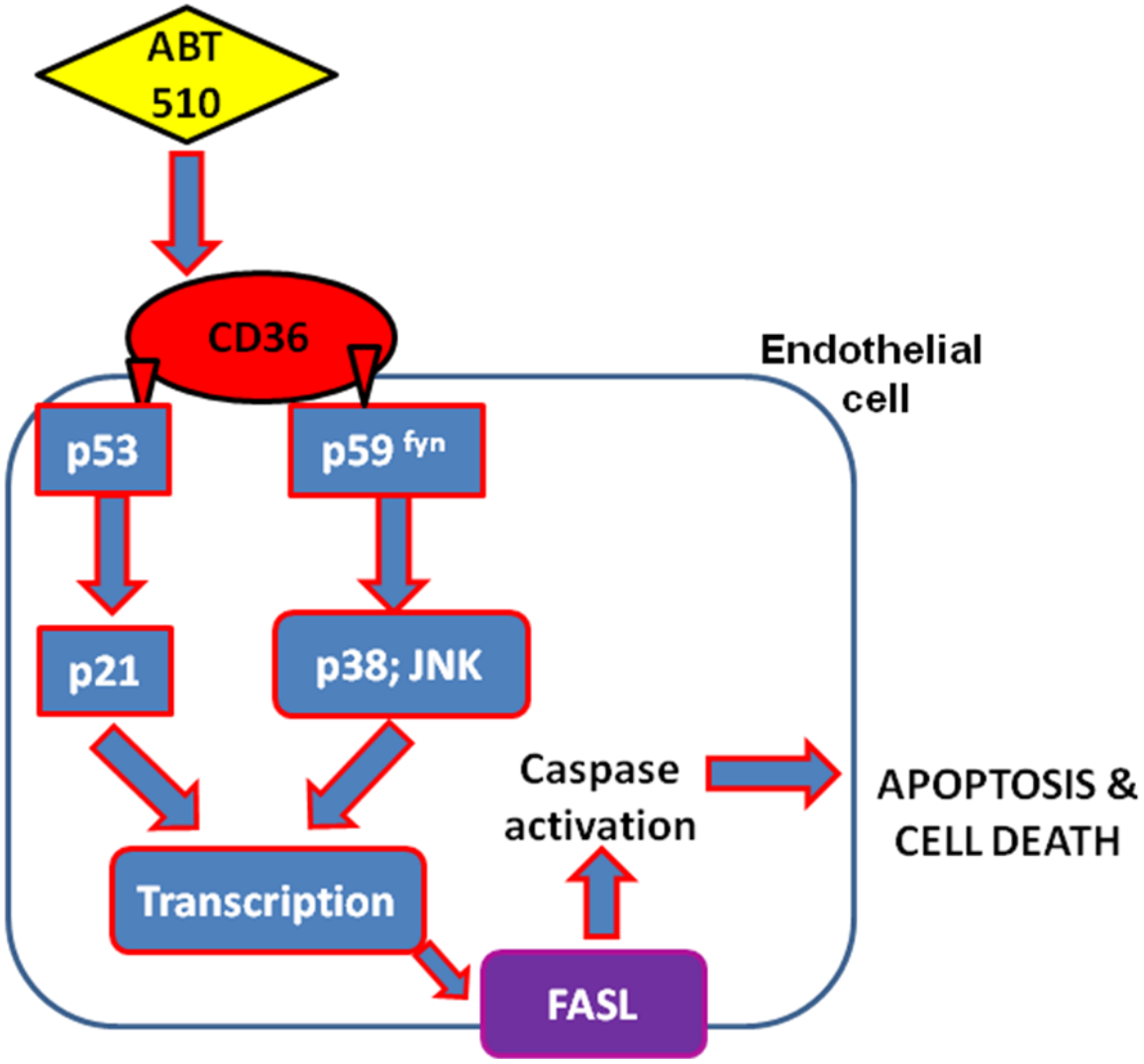

Diagram 4.2: Anti-angiogenic activity of ABT-510 upon endothelial cells. Two pathways involved after the binding of ABT-510 to CD36: to activate src-family kinases, p59fyn and p53. p38; JNK and p21 are rapidly phosphorylated, which in turn stimulate transcription and cell surface expression of FasL. Activated Fas then activates caspases and causes apoptosis. p59 fyn; proto-oncogene tyrosine-protein kinase fyn; p53; tumour protein 53; p38 MAPK; p38 mitogen-activated protein kinase; JNK; c-JunN-terminal kinase; FASL; FAS ligand.

4.1.6 Nitric oxide signalling and TSP-1

In addition to caspase-induced apoptosis, nitric oxide (NO) is implicated as a possible mediator of TSP-1 anti-angiogenic activity. As discussed in section 1.3, NO/cGMP signalling is required for angiogenesis in endothelial cells, where it can increase proliferation, adhesion and migration at relatively low concentrations (Isenberg *et al.,* 2005; 2006). TSP-1 blocked NO-stimulated increases in proliferation, adhesion and migration in endothelial cells, at picomolar concentrations (Isenberg *et al.,* 2005). Similarly, ABT-510 blocked NO/cGMP signalling in endothelial cells whereas TSP-1 null endothelial cells showed consistently increased basal levels of cGMP (Isenberg *et al.,* 2008). Thus, NO plays a vital role in endothelial function, which can be inhibited by TSP-1/ABT-510. This may be a pathway affected by ABT-510 in adipocytes.

NO also inhibits proliferation and subsequent differentiation of adipocytes (Nisoli *et al.,* 1998). Moreover, locally synthesised NO can down-regulate lipolysis in human tissue (Andersson *et al.,* 1999). In addition, NO, generated by a NO donor, impaired the lipolytic action of isoproterenol (Klatt *et al.,* 2000) and also, in obesity, reduced the rate limiting enzyme in adipocyte lipolysis, hormone sensitive lipase (HSL; Gaudiot *et al.,* 1998; Large *et al.,* 1999). Therefore, NO has many roles on endothelial cells but also is a key modulatory factor of adipocyte lipolysis and thus may potentially mediate a novel aspect of adipocyte TSP-1 action in adipocytes.

NO production is associated with many factors known to influence adipocyte function. The cytokine tumour necrosis factor-α (TNF- α) (Old 1985) inhibits insulin-stimulated glucose uptake in adipocytes (Hotamisligil *et al.,* 1996), and increases lipolysis in human, rat, and mouse adipocytes and 3T3L1 cells (Green *et al.,* 1994; Souza *et al.,* 1998; Zhang *et al.,* 2002). TNF-α can directly increase the expression of iNOS and subsequent NO production in adipose tissue (Kapur *et al.,* 1999) and this in turn suppresses lipolysis (Lien *et al.,* 2009).

The specific effect and signalling mechanisms of increased TSP-1 upon the expanding adipose in obesity has not been investigated. This chapter therefore

aimed to address the effect of the Type I repeat ABT-510 upon adipocyte function. As there is substantial evidence for the involvement of CD36, p38 and NO in the anti-angiogenic effect of TSP-1 in endothelial cells, these key signalling pathways were investigated with regard to their adipocyte function.

4.2 Hypothesis

It is hypothesised that the TSP-1/Type 1 repeat directly stimulates lipolysis in adipocytes by activation of the CD36 receptor-p38 MAPK pathway.

4.2.1 Aims

Specifically we aimed to:

- Determine the factors that may mediate increased adipocyte TSP-1 expression in obesity.
- Determine effect of the TSP-1 analogue, ABT-510, upon adipocyte differentiation.
- Determine the effect of ABT-510 on mature adipocyte lipid metabolism.
- Establish whether the CD36 receptor mediates for the effects of ABT-510 on adipocytes.
- Determine the signalling pathways mediating the effects of ABT-510 on adipocytes, including the established endothelial cell-associated CD36 mediated p38 and NO associated pathways.

4.3 Experimental Protocol

4.3.1 Differentiation of pre-adipocytes with ABT-510 incubation

As adipose has the ability to grow and regress throughout life, it was essential to assess the effect of anti-angiogenic part of TSP-1 (ABT-510) on adipocytes at both stages of their life cycle: the pre-adipocyte and differentiated adipocyte. Therefore, initial experiments were conducted upon pre-adipocytes, throughout their maturation into mature adipocytes.

Pre-adipocytes (P2-P12) were seeded onto 96-well collagen-coated plates, at a density of 2.5 x 10^5 cells/well. Cells were differentiated using specific media conditions (see section 2.5.1) with or without 100 nM ABT-510. Every two days media were replaced, again with or without 100 nM ABT-510. This continued for a period of 10-12 days. Alongside changing of media, treated and non-treated adipocytes were assessed for lipid accumulation by staining with oil red O (see section 2.5.3).

4.3.2 Manipulation of differentiated 3T3L1 adipocytes

Pre-adipocytes (P2-P12) were seeded onto 6, 12 or 24-well collagen-coated plates, at a density of 2.5 x 10^5 cells/well, for differentiation (see section 2.5.1). Cells were cultured in phenol-red free DMEM (as the phenol interferes with colorimetric assay for assessing lipolysis), until they were lipid-filled, which was assessed by eye and confirmed by staining with oil red O (see section 2.5.3). Fully differentiated cells were apparent from 10-12 days after initial seeding, and subsequently incubated overnight in medium made with stripped fetal calf serum (FCS), to starve the cells prior to experimentation. Medium was removed and replaced with fresh medium and stripped FCS containing concentrations of different compounds described below. These experiments were conducted for a period of 6 hours, as this is sufficient time for transcriptional changes to occur in the cells. After incubation, the medium (for effects on lipolysis) and cells (for changes in RNA) were removed for analysis.

As increased TSP-1 had been associated with both genetic and dietary obesity (see section 3.4.4.5), it was decided to investigate other factors that are known to be elevated in obesity and examine their effect on TSP-1 expression to try elucidate potential, causal pathways involved. For example, insulin is elevated in obesity (Reaven 1993), as are glucocorticoids (Morton and Seckl 2008). There is decreased adrenergic stimulation of obese adipose (Muzzin *et al.,* 1991) and increased circulating interleukin-6 levels (Mohamed-Ali *et al.,* 1997; Kern *et al.,* 2001). Thus, insulin, dexamethasone (glucocorticoid), beta-3 agonist (CL 316, 243; adrenergic stimulation) and IL-6 were incubated with mature Day 10 3T3L1 adipocytes and TSP-1 expression levels determined. Concentration-response curves (1, 10 & 100 nM) were used to examine the effects of physiologically relevant varying concentrations of these compounds upon TSP-1 adipocyte expression (Largis *et al.,* 1994; Shojima *et al.,* 2002; Rotter *et al.,* 2003).

To assess the effect of ABT-510 upon different aspects of adipocyte metabolism, it was important to have positive and negative controls for these functions. When examining lipolysis in mature adipocytes, insulin was used as a known, potent inhibitor (Sekar *et al.,* 1996). Concentration-response curves (1, 10 and 100 nM) were used to determine the most effective dose of insulin to use. A stimulator of lipolysis, the β_3-adrenoceptor agonist, CL 316,243, was used to stimulate the release of free fatty acids. Concentration-response curves (1, 10 and 100 nM) were used to determine the most effective dose of CL 316,243 agonist to use, as this agonist had already demonstrated lipolytic effects at 10nM (Largis *et al.,* 1994). To elucidate the mechanisms of thrombospodin-1 (TSP-1) on adipocyte function, various concentrations of the Type I repeat analogue of TSP-1, ABT-510, were used (1, 10 and 100 nM) that had already been optimised for inhibition of endothelial cell function (Good *et al.,* 1990; Iruela-Arispe *et al.,* 1991). ABT-510 was dissolved in sterile phosphate buffered saline for all experiments (PBS).

To reveal common pathways involved in ABT-510 action on adipocytes, pathways associated with TSP-1 action on endothelial cells were also

investigated. These included the p38 MAPK pathway and, thus, both an inhibitor, SB203580 (1, 10 and 100 nM), and activator of this pathway, anisomycin (3, 30 and 300 nM) were used. Concentrations needed to cause inhibition of p38 MAPK signalling pathways had been achieved with 10nM SB203580 (Egelman *et al.,* 1998). The PI3K pathway is essential for the inhibition of lipolysis through the insulin signalling pathway in adipocytes and thus a PI3K inhibitor, Wortmannin (1, 10 and 100 nM), was used. Similarly, Wortmannin can inhibit PI3 kinase activity inhibition at a concentration of 100 nM (Castan *et al.,* 1999). Finally, stimulation of nitric oxide (NO) production was achieved by addition of 10 μm myristic acid and the nitric oxide synthase inhibitor, L-N^{G}nitro-arginine methyl ester (L-NAME) was used at a concentration of 300 μm, as shown to inhibit NO production in adipocytes (Nisoli *et al.,* 1998).

Medium was collected after six hours of incubation with the respective compound and analysed for FFA content. A detailed protocol of the lipolysis assay can be found in Chapter 2 (see section 2.5.4).

In addition to lipolysis, adipocytes are involved in the uptake of fatty acids. Investigation into whether ABT-510 would have an effect on this process was necessary. A tracer fatty acid was used to track fatty acid uptake from the medium into the adipocyte. ^{3}H palmitate uptake is a reliable and accurate way to measure the rate of appearance in various cell types, including adipocytes (Jensen *et al.,* 1988). Palmitate uptake was measured in Day 10 3T3L1 adipocytes (differentiation protocol see section 2.5.1) by the addition of unlabeled palmitate (1.2 nM) with radiolabeled [^{3}H] palmitate in DMEM medium which was left for six hours for optimal uptake into the adipocytes. Cell-associated radioactivity was obtained by counting the medium extracted and cells were scraped with SDS in scintillation fluid, and counted in a scintillation counter. For optimisation studies and a detailed protocol, refer to Chapter 2 (section 2.5.6).

4.3.3 CD36 expression in differentiating adipocytes and knockdown in mature adipocytes

The established receptor on endothelial cells for ABT-510 is CD36 (Jimenez *et al.,* 2000; Febbraio *et al.,* 2001). This receptor is also expressed on adipocytes (Febbraio *et al.,* 2001) and therefore CD36 expression was examined. Firstly, CD36 expression was assessed throughout adipocyte differentiation. Next, an attempt was made to knockdown the adipocyte CD36 receptor to determine if ABT-510 was acting through this receptor. 3T3L1 adipocytes were cultured and differentiated as described before (see section 2.5.1). At days 3, 5, 7 and 10 post differentiation, medium was removed, cells were scraped and RNA isolated using TRIZOL reagent (Invitrogen) as previously described (Morton *et al.,* 2001). RNA was purified using RNAeasy columns (RNeasy Mini Kit, Qiagen, UK) (see Materials and Methods 2.2.1). cDNA was synthesised and real-time PCR was performed using CD36 primer/probe set (Mm01135198_m1; Applied Biosystems). Cyclophilin mRNA levels were used as an internal control. Finally, CD36 receptor knockdown was attempted with siRNA ablation. Both pre-adipocytes (Day 0) and fully mature (Day 10) 3T3L1 adipocytes were used as described in detail in Chapter 2 (see section 2.5.9).

4.3.4 Non-active peptide sequence

A non-active peptide sequence (NAC-Gly-Val-DIle-Thr-Arg-Ile-ArgNHEt) was used as a control to ensure that the effects of ABT-510 were specific. The potential impact of ABT-510 on lipolysis was examined by incubating 1 nM and 100 nM non-active sequence in Day 10, fully differentiated adipocytes.

4.3.5 Effect of ABT-510 upon endothelial cell function

To confirm the specific, anti-angiogenic activity of ABT-510, endothelial angiogenic assays were performed. Aortic rings were removed from eight week old C57BL/6J mice (n=6) (section 2.3.1 and 2.3.2). These rings were incubated with basal EBM-2 medium or basal EBM-2 medium + 100 nM ABT-510 for a period of 10 days, with medium replaced every two days. Quantification of tube-

like structures (TLS) throughout was quantified under an inverted light microscope as described (see section 2.3.4).

Human umbilical vein endothelial cells (HUVECs) were grown and cultured as described in Chapter 2 (section 2.5.10). HUVECs were then aliquoted into 24 well plates that had been pre-coated with 250 μl of Matrigel, at a density of 4.0 x 10^4 cells/ml. HUVECs were then incubated with basal endothelial cell medium (see section 2.5.10) with or without the incubation of ABT-510 (dissolved in PBS). HUVECs cultured on plastic produced a characteristic monolayer of cells with a "cobblestone" appearance. As expected, culturing on Matrigel (Benelli & Albini 1999) causes the cells to spontaneously form TLSs, thus generating a complex 2-dimensional network. These tubes formed rapidly, with extensive connections evident after 4 hours with a peak after approximately 8 hours in culture. HUVECs were then incubated at 37°C, and images were acquired after eight hours of culture. TLSs were viewed using a Karl Zeiss Axioskop inverted light microscope at X 50 magnification. Capillary connections were counted by marking all branch points between tube-like structures, manually using a cell counter. The counting was performed blind with respect to the treatment (vehicle or ABT-510) for each image.

4.4 Results

4.4.1 TSP-1 expression in 3T3L1 adipocytes is decreased by 10 nM interleukin-6 (IL-6) and increased by 100 nM β_3 agonist (CL316, 243) incubation but is unaffected by insulin and dexamethasone

To elucidate the factors responsible for increased TSP-1 in obese adipose tissue, factors elevated in obesity were incubated with adipocytes and TSP-1 expression determined. The effects of insulin, glucocorticoids, interleukin-6 and a beta-3 (β_3) adrenoceptor agonist (CL 316,243) on subcutaneous adipose TSP-1 expression were investigated in Day 11 3T3L1 adipocytes. Insulin and dexamethasone had no effect on TSP-1 expression (Figure 4.1 A & B). IL-6 caused a u-shaped concentration-response, whereby both 1 nM and 100 nM IL-6 did not alter TSP-1 expression, but 10nM decreased TSP-1 expression (Figure 4.1C). The β_3-agonist CL 316, 243 caused a concentration-dependent increase in TSP-1 expression (Figure 4.1D).

4.4.1 TSP-1 expression is affected by interleukin-6 (IL-6) and a β_3 agonist (CL 316, 243)

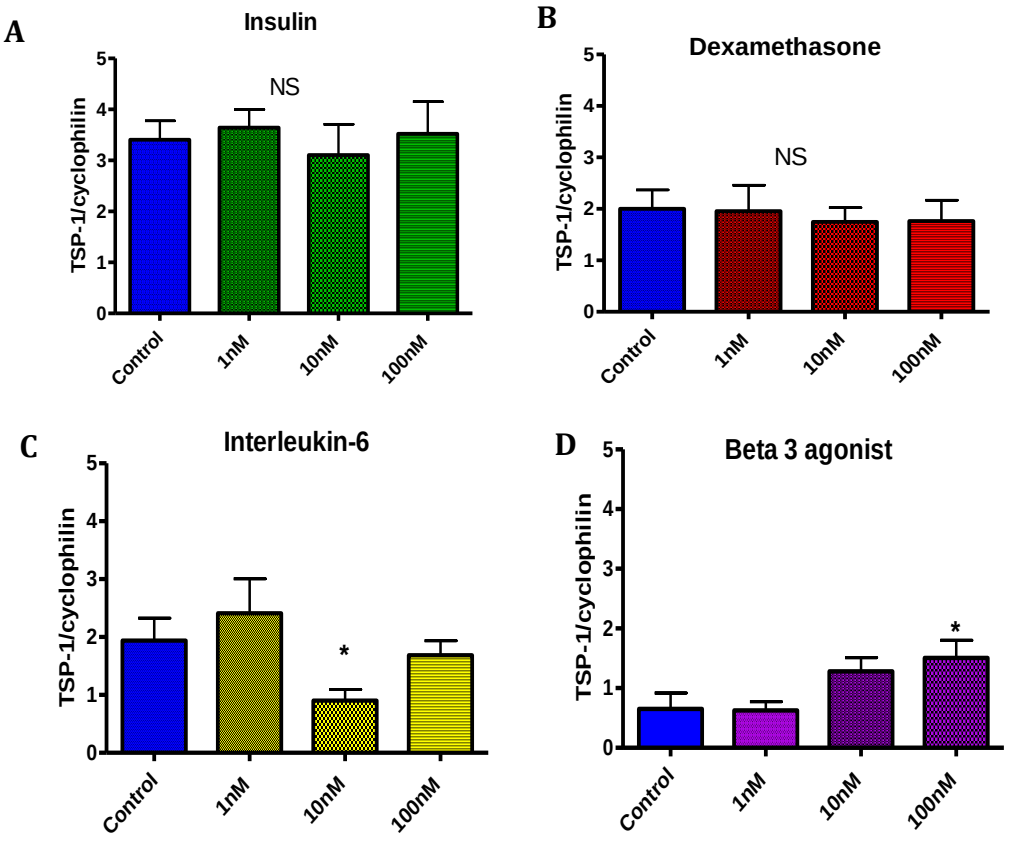

Figure 4.1: The effects of insulin, dexamethasone, interleukin-6 (IL-6) and β_3 agonist (CL 316, 243) on TSP-1 mRNA levels in 3T3L1 adipocytes. Real-time quantification of Day 11 differentiated 3T3L1 adipocytes after 6hour exposure to 1 nM, 10 nM and 100 nM insulin (**A**), dexamethasone (**B**), IL-6 (**C**) or CL 316, 243 (**D**). Data are expressed as means ± SEM; n=6 for all groups. Data analysed by one way ANOVA followed by Bonferroni corrections; *p<0.05.

4.4.2 Angiostatic effect of the TSP-1 analogue (ABT-510) on endothelial cells

In order to assess whether ABT-510 had a potent anti-angiogenic effect, two endothelial cell assays were performed. The first was the aortic ring assay, in which inhibition of growth in tube-like structure growth (TLS) had already been demonstrated (see Chapter 3), the second involved culturing human umbilical vein endothelial cells (HUVECs) on the surface of Matrigel (see section 2.5.10).

Aortic rings obtained from C57BL/6J mice and HUVECs were cultured with or without ABT-510. Tube-like structures (TLS) could be detected in aortic rings after two days in culture and TLS growth continued for the next 8 days. Tube formation analysis in HUVECs was performed at 8 hours.

4.4.2.1 ABT-510 inhibited TLS formation in aortic rings

ABT-510 (100 nM) caused an overall inhibition of TLS formation by aortic rings compared to control throughout the 10 day examination period ($p=0.00114$) (Figure 4.2). Inhibition of growth was observed as early as Day 2 and at Days 4, 8 and 10.

4.4.2.2 ABT-510 inhibited TLS formation by human umbilical vein endothelial cells (HUVECs)

Exposure to 100 nM ABT-510 inhibited TLS formation compared to controls ($p<0.001$; Figure 4.3).

4.4.2.1 ABT-510 inhibited aortic tube-like structure (TLS) growth from aortas from C57BL/6J mice

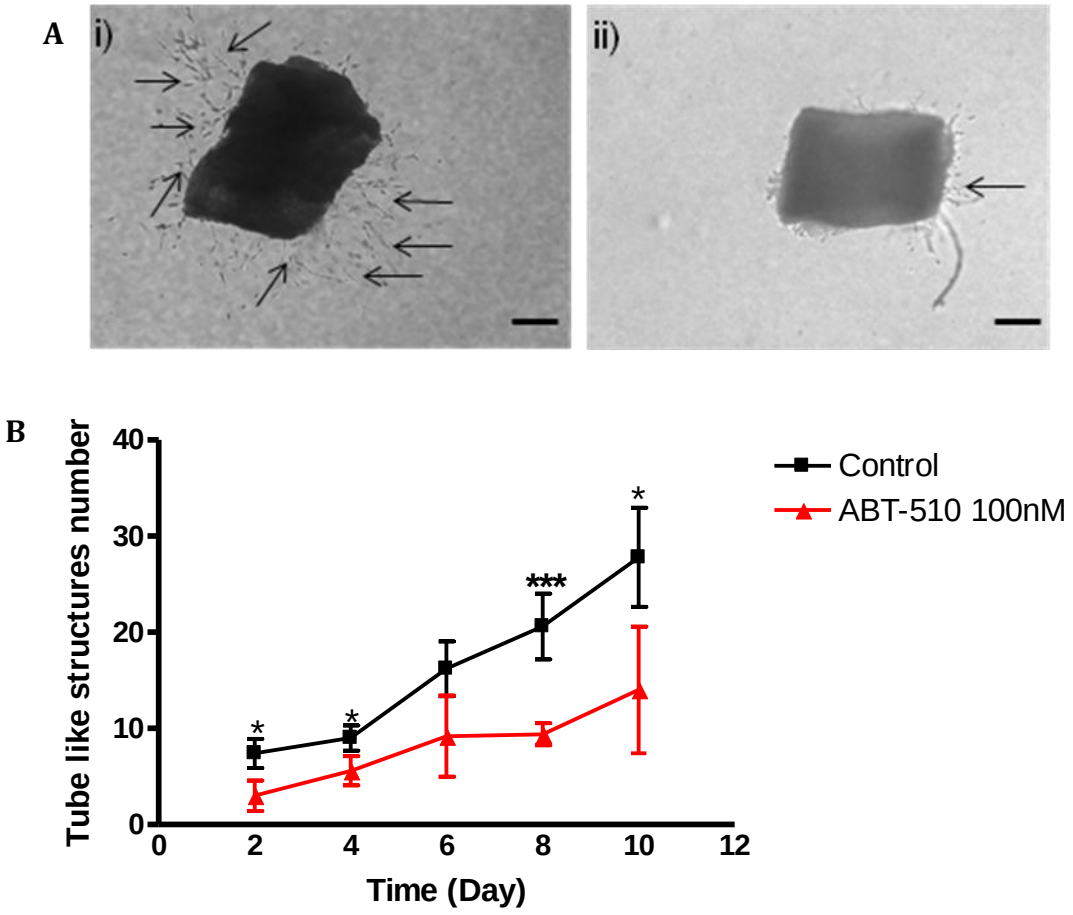

Figure 4.2: The effects of ABT-510 on aortic TLS formation from C57BL/6J mice. **A:** TLS formation from aortic rings of C57BL/6J mice was assessed by manual counting under light microscopy of (i) no ABT-510 and (ii) 100 nM ABT-510. **B**: This was quantified over a 10 day period. Arrows indicate TLS formation. Data are expressed as mean ± SEM; n=6 for all groups. Scale bars represent 0.2 mm. Data were analysed by two way ANOVA followed by Bonferroni corrections (*p<0.05; ***p<0.001).

4.4.2.2 ABT-510 inhibited tube formation by cultured human umbilical vein endothelial cells (HUVECs)

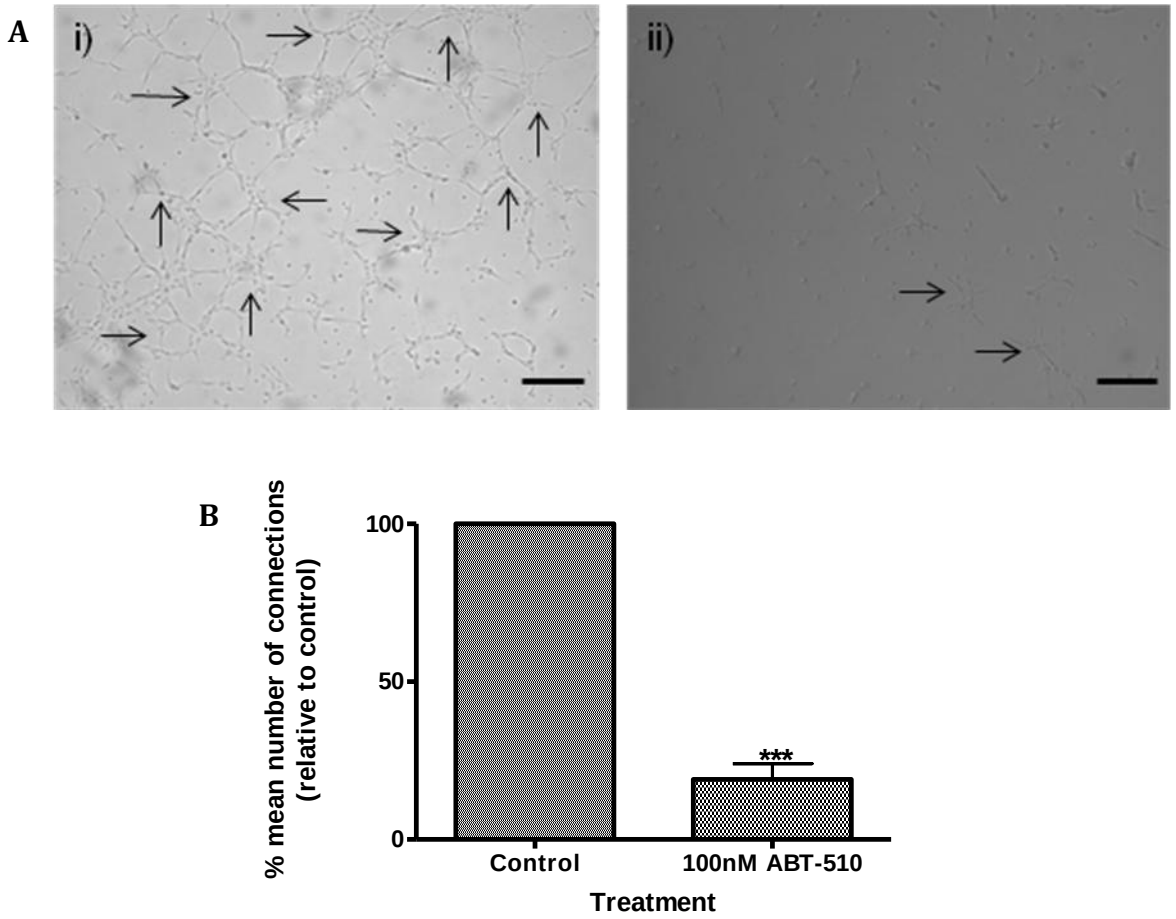

Figure 4.3: The effect of ABT-510 upon tube formation in human umbilical vein endothelial cells (HUVECs). A: Tube formation by HUVECs cultured on Matrigel was assessed by manual counting under light microscopy without (**i**) or with (**ii**) 100 nM ABT-510. Arrows indicate tubes and magnification is at X 5. These effects were analysed 8 hours after cells were seeded onto Matrigel. **B:** Quantification of tube formation in treated and untreated HUVECs. Scale bars represent 50 μm. Data are expressed as mean connections relative to the control expressed as a percentage ± SEM.; n=3 (3 well triplicates); ***p<0.001; Student's t-test.

4.4.3 Effect of ABT-510 upon 3T3L1 adipocyte physiology

The effect of ABT-510 upon on different aspects of adipocyte metabolism was assessed. As described previously (see section 1.2.3), CD36 mediates fatty acid transport in adipocytes (Abumrad *et al.,* 1993*)* and is the proposed receptor for TSP-1 function in endothelial cells (Jimenez *et al.,* 2000). Therefore, CD36 expression was examined throughout differentiation of adipocytes. As well as examining the effects of ABT-510 on the differentiation of fat cells from fibroblastic preadipocytes, fatty acid uptake and lipolysis (two major functions of adipocytes) was measured in mature adipocytes. As adipose is unique in its ability to grow throughout a lifespan, it was important to monitor the effects of ABT-510 on both preadipocytes and mature adipocytes.

4.3.3.1 Adipocyte differentiation is associated with increased CD36 expression but is not affected by ABT-510

3T3L1 adipocytes were exposed to a range of concentrations of ABT-510 (0.1 nM – 100 nM) throughout ten days of differentiation (see section 4.3.1). ABT-510 had no effect upon lipid accumulation and, subsequently, differentiation throughout the ten day differentiation period, as assessed by oil red O accumulation every two days ($p=0.3664$) (Figure 4.4 A & B).

As differentiation progressed, there was an increase in CD36 expression which reached significance on Day 7 and continued to Day 10 (Figure 4.5).

4.4.3.2 ABT-510 caused a concentration-dependent increase in [^{3}H] palmitate uptake

In order to assess the effect of ABT-510 on lipid uptake, tritiated palmitate (for optimisation, see section 2.5.6) was used to trace fatty acid uptake into adipocytes and whether this might be altered by ABT-510. ABT-510 caused concentration-dependent biphasic effect on [^{3}H] palmitate uptake in fully mature 3T3L1 adipocytes (Figure 4.6). Thus, fatty acid uptake was decreased in the presence of 0.1 nM and 1 nM ABT-510, but increased at the higher concentrations ($p<0.01$).

4.4.3.3 ABT-510 inhibited beta-3(β_3)-mediated lipolysis and non-active peptide sequence of ABT-510 did not

In addition to uptake, adipocytes also participate in the regulated release of fatty acids (lipolysis). The effect of ABT-510 on this process was assessed. ABT-510 had no significant effect on basal lipolysis (Figure 4.7A). CL-316,243, a potent β_3-adrenoreceptor agonist was used to stimulate lipolysis and insulin was used a potent physiological inhibitor of lipolysis. As anticipated, CL-316,243 increased ($p<0.05$) and 100nM insulin inhibited lipolysis ($p<0.01$) (Figure 4.7B). However, the CL-316,243-mediated lipolysis was abolished in the presence of even the lowest concentrations of ABT-510 (Figure 4.7B). ABT-510 had no additional effect on the inhibition of lipolysis with insulin (data not shown).

To ensure that the effects of ABT-510 were specific, a non-active peptide, A-317473 (sequence: NAC-Gly-Val-DIle-Thr-Arg-Ile-ArgNHEt) was supplied by Abbott Laboratories and tested on stimulated 3T3L1 adipocyte lipolysis. The non active peptide had no significant effect upon stimulated lipolysis (Figure 4.8).

4.4.3.1 ABT-510 had no effect on 3T3L1 adipocyte differentiation

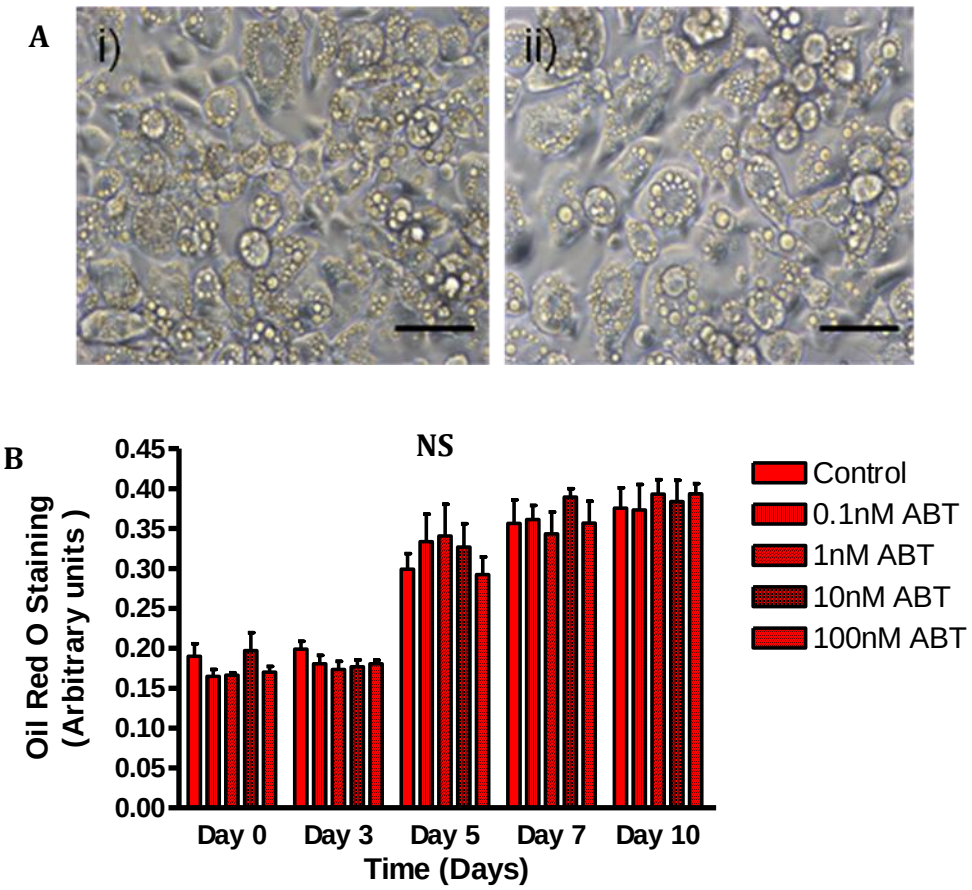

Figure 4.4: The effect of ABT-510 throughout 3T3L1 adipocyte differentiation on lipid accumulation. A: Light microscopy pictures at x 10 magnification showing oil droplet as a marker of lipid accumulation and distribution between control (i) and 100 nM ABT-510 treated adipocytes(ii). **B:** Quantified lipid accumulation in cells treated with ABT-510, using oil red O staining from days 0 to 10. Scale bar represents 0.5 µm. Data are expressed as mean ± SEM; n=6 for all groups. Data were analysed by two way ANOVA followed by Bonferroni correction.

4.4.3.1 Increased expression of CD36 with 3T3L1 adipocyte differentiation

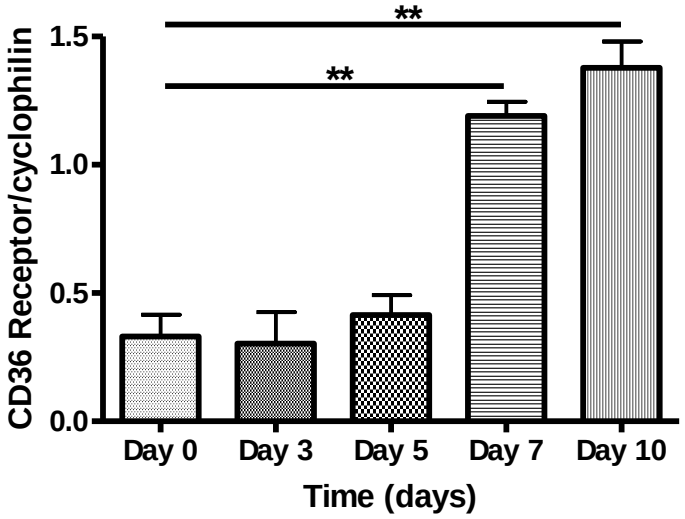

Figure 4.5: CD36 receptor mRNA levels in 3T3L1 adipocytes throughout differentiation. Real-time quantification of CD36 receptor expression in 3T3L1 pre-adipocytes throughout differentiation. Data are expressed as mean ± SEM; n=4 for all groups. Data were analysed by one way ANOVA followed by Bonferroni correction; **p<0.01.

4.4.3.2 ABT-510 has a bi-phasic effect on palmitate uptake into adipocytes

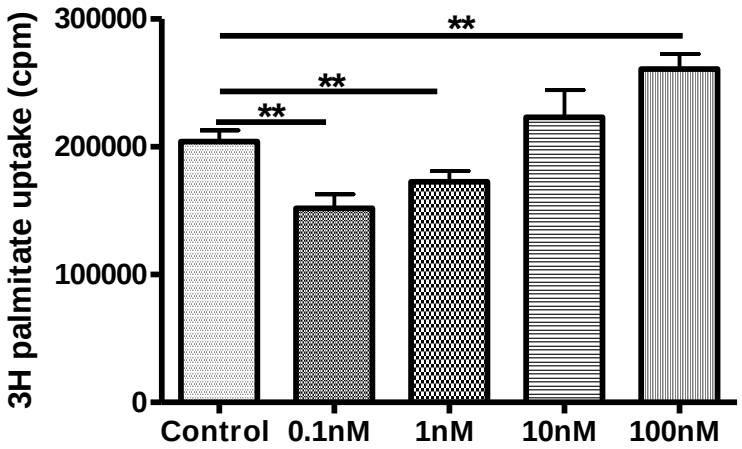

Figure 4.6: The effect of ABT-510 upon palmitate uptake into 3T3L1 adipocytes. Effect of ABT-510 (1, 10 & 100 nM) upon [^{3}H] palmitate uptake in fully differentiated adipocytes Day 10). Data are expressed as mean ± SEM; n=6 for all groups. Data were analysed by one way ANOVA followed by Bonferroni correction; **p<0.01.

4.4.3.3 No effect of ABT-510 on basal lipolysis but potent suppression of β_3-stimulated lipolysis in 3T3L1 adipocytes

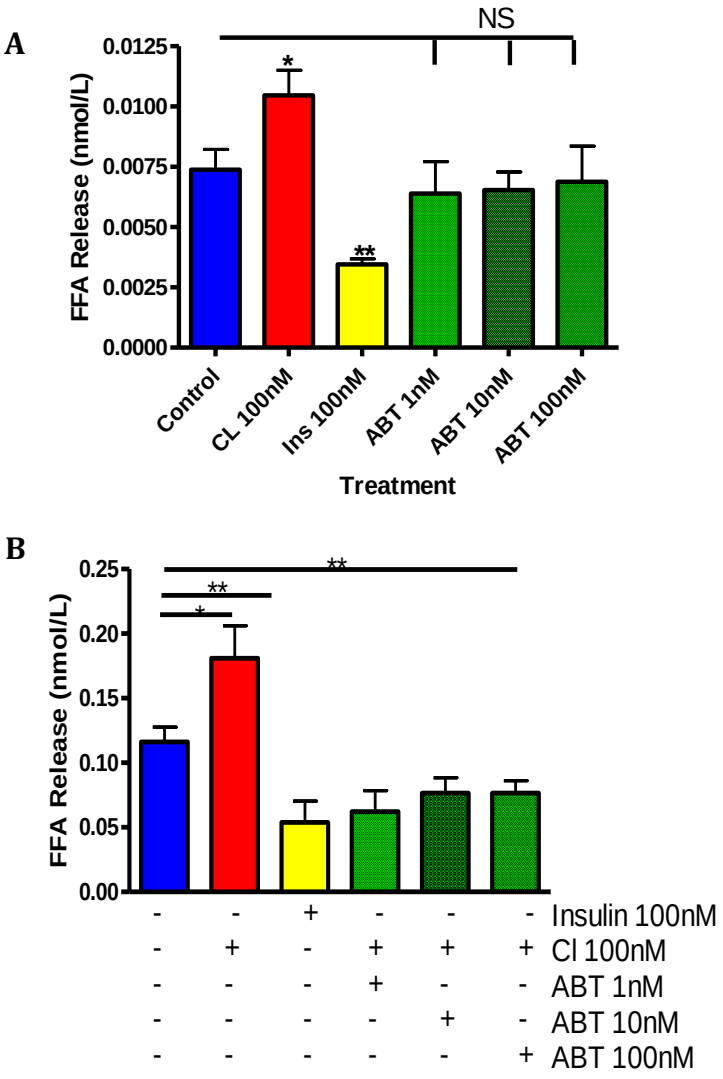

Figure 4.7: The effect of ABT-510 upon basal and β_3-stimulated lipolysis on Day 12, 3T3L1 adipocytes. A: ABT-510 effect upon basal lipolysis, including a positive stimulator- (β_3 agonist-CL 316, 243) and inhibitor (insulin) of lipolysis. **B**: ABT-510 effect upon β_3-stiumlated lipolysis including a positive stimulator (β_3 agonist-CL 316, 243) and inhibitor (insulin) of lipolysis. Data are expressed as mean ± SEM; n=6 for all groups. Data were analysed by one way ANOVA followed by Bonferroni correction; *p<0.05; **p<0.01.

4.4.3.3 No effect of non-active peptide sequence A-317473 upon 3T3L1 adipocyte lipolysis

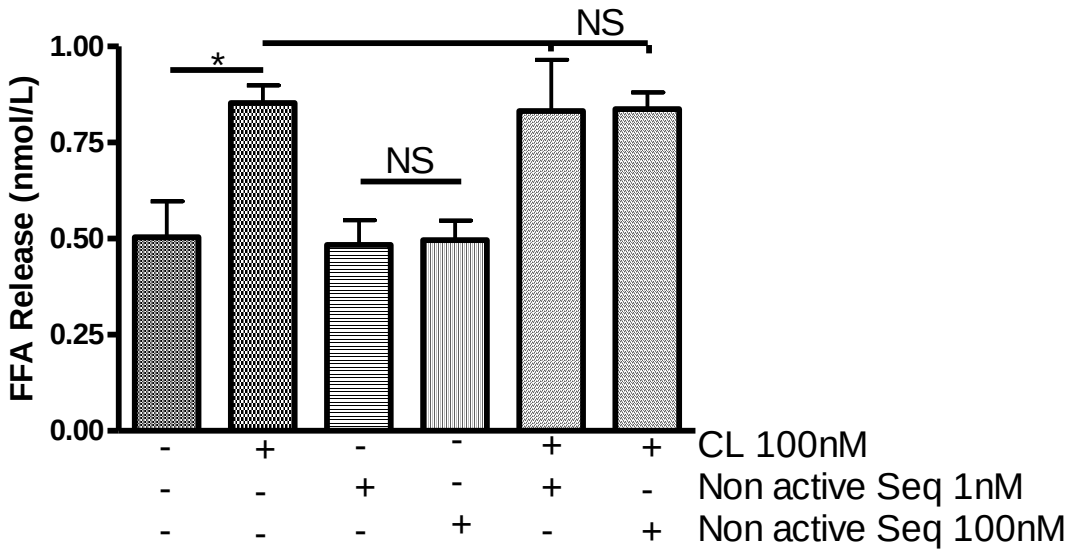

Figure 4.8: The effect of non active peptide sequence A-317473upon 3T3L1 adipocyte lipolysis. Assessment of non-active sequence (1 & 100 nM) upon lipolysis as assessed by free fatty acid (FFA) release in Day 10 3T3L1 adipocytes. Data are expressed as mean ± SEM; n=6 for all groups. Data were analysed by one way ANOVA followed by Bonferroni correction; *p<0.05; **p<0.01.

4.4.4 siRNA down regulation of CD36

To confirm that CD36 was mediating the action of ABT-510 on adipocytes, siRNA-mediated down-regulation of CD36 was attempted. Different siRNAs directed against distinct coding regions of the CD36 receptor gene (designated 1, 2, 3 and 4 below) were used to determine which would be the most effective at knocking down the gene. Furthermore, different concentrations (10 and 30 nM) of each siRNA were used during optimisation (see section 2.5.9). As a transfection control, siRNA for glyceraldehyde 3-phosphate dehydrogenase (GAPDH) and a scrambled sequence negative control (-ve) were also included. Cyclophilin and tata binding protein (TBP) was used as an internal control to correct for cellular gene expression. To verify the transfection of adipocytes using the DeliverX protocol, real-time quantitative PCR was performed on adipocytes. As shown in Figure 4.9A, knockdown of the CD36 receptor was unsuccessful and GAPDH was also not ablated compared to controls in Day 10 adipocytes. Successful knockdown of the CD36 receptor was achieved in Day 0 pre-adipocytes using 30 nM of CD36-2 and the internal control GAPDH (Figure 4.9B). However, when these cells were continued to Day 10 of differentiation, the CD36 receptor down-regulation was not reproducible (Figure 4.9C).

4.4.4 The effect of down-regulation of CD36 by siRNA on preadipocytes and mature adipocytes

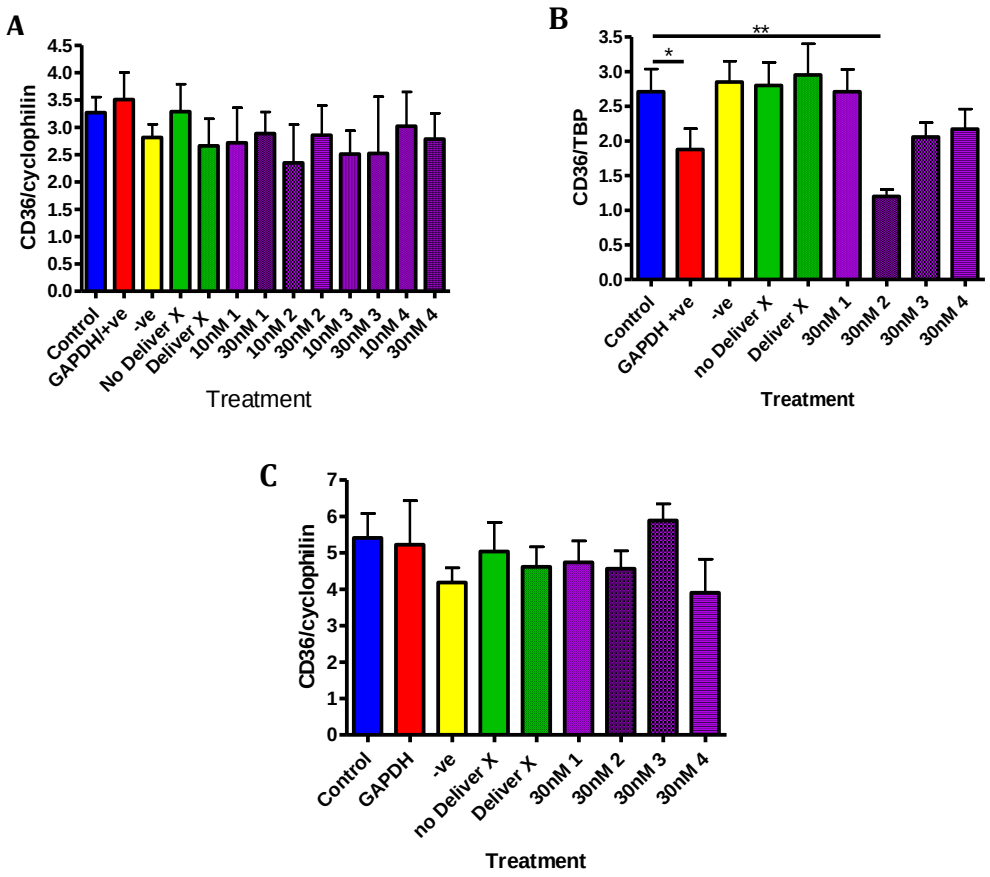

Figure 4.9: The effect of CD36 receptor siRNA transfection on preadipocytes and mature adipocytes on CD36 mRNA expression. A: RT-PCR mRNA concentrations from first attempt to transfect Day 10 3T3-L1 adipocytes with CD36 receptor specific siRNA, relative to cyclophilin expression. **B:** RT-PCR mRNA concentrations from the second attempt to transfect Day 0 3T3-L1 adipocytes with CD36 receptor specific siRNA, relative to TATA binding protein (TBP) expression. **C:** Same adipocytes as in **B** were allowed to differentiate to Day 10 and analysed for CD36 receptor knockdown. Data are expressed as mean ± SEM; n=6 for all groups. Data were analysed by two way ANOVA followed by Bonferroni correction; **p<0.01.

4.4.5 Anti-lipolytic effect of ABT-510 involves p38 MAPK and is independent of PI3K

To determine the mechanism of the novel lipid-retaining effects of ABT-510, the CD36 and insulin signalling pathways were investigated. Insulin signalling was examined as the anti-lipolytic effects of ABT-510 were comparable to this most potent anti-lipolytic hormone which also works through PI3K. This was achieved by using Wortmannin (100 nM) and SB203580 (100 nM) for a period of 6 hours, to inhibit the PI3-kinase and p38 pathways, respectively, with quantification of FFA release as the functional readout for the effect. Anisomycin, a known stimulator of p38 MAPK (Barros *et al.,* 1997) was used as a positive control for this pathway. Wortmannin (Figure 4.10) and SB203580 (Figure 4.11) did not affect the inhibition of the CL-mediated lipolysis by ABT-510 ($p>0.05$). Interestingly, stimulation of the p38 MAPK pathway using anisomycin (3 nM), caused a reversal of the ABT-510 induced inhibition of CL-mediated lipolysis ($p=0.004$) (Figure 4.12).

4.4.5 No reversal of the ABT-510-induced inhibition of β3-stimulated lipolysis by the PI3K inhibitor, Wortmannin

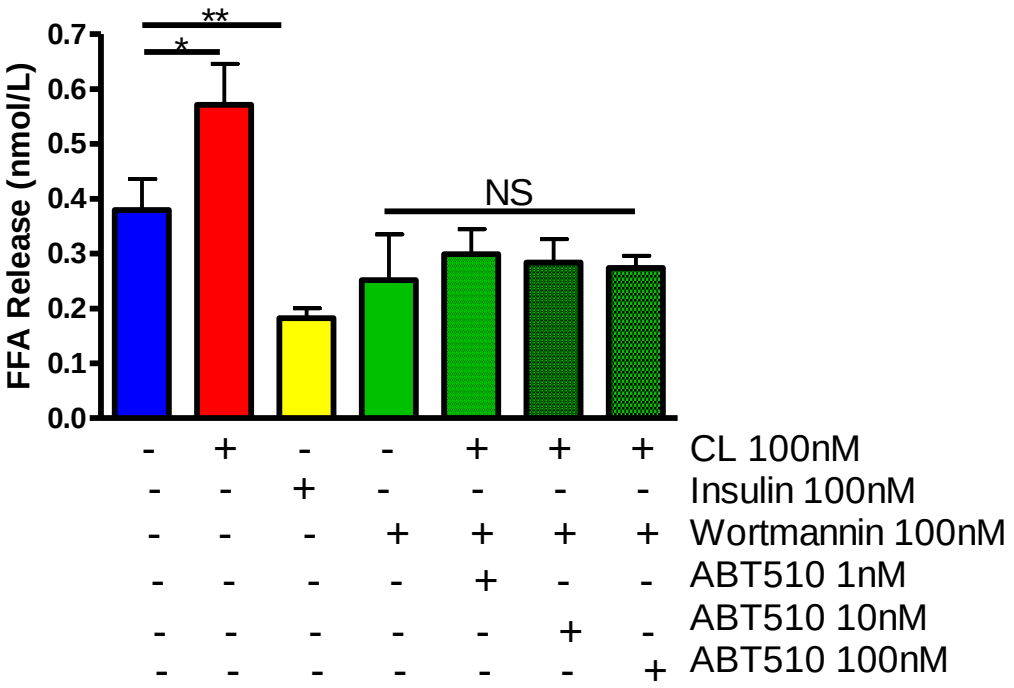

Figure 4.10: The effect of PI3K inhibitor upon β_3-stimulated lipolysis in 3T3L1 adipocytes. Effect of PI3 kinase inhibitor (Wortmannin) and ABT-510 upon basal and β_3 stimulated lipolysis as assessed by free fatty acid release (FFA) in Day 10 3T3L1 adipocytes. A positive stimulator-(β_3 agonist-CL 316, 243) and inhibitor (insulin) of lipolysis were also used. Data are expressed as mean ± SEM; n=6 for all groups. Data were analysed by one way ANOVA followed by Bonferroni correction; *p<0.05; ***p<0.001; NS= non-significant; CL= CL316, 243.

4.4.5 No reversal of the ABT-510-induced inhibition of β_3-stimulated lipolysis by the p38 MAPK inhibitor, SB203580

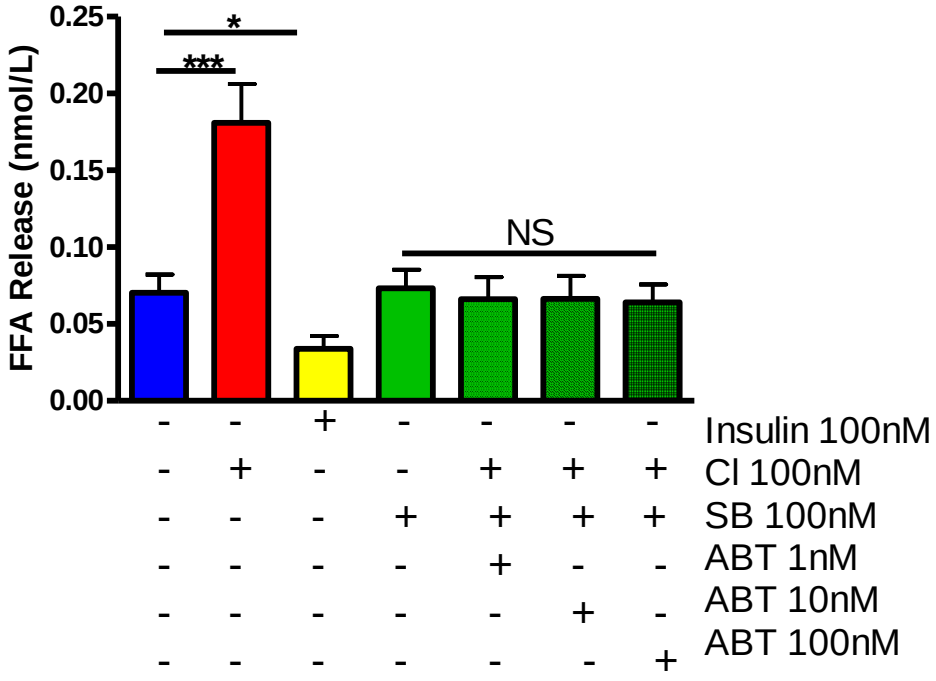

Figure 4.11: The effect of p38 MAPK inhibition on β3-stimulated lipolysis in 3T3L1 adipocytes. Effect of p38 MAPK inhibitor (SB 203580) and ABT-510 upon basal and β_3 stimulated lipolysis as assessed by free fatty acid release (FFA) in Day 10 3T3L1 adipocytes. A positive stimulator-(β_3 agonist-CL 316, 243) and inhibitor (insulin) of lipolysis were also used. Data are expressed as mean ± SEM; n=6 for all groups. Data analysed by one way ANOVA followed by Bonferroni corrections; *p<0.05; ***p<0.001; NS= non-significant; CL= CL316, 243; SB= SB203580 on legend.

4.4.5 Reversal of the ABT-510-induced inhibition of β_3-stimulated lipolysis by p38 MAPK activation

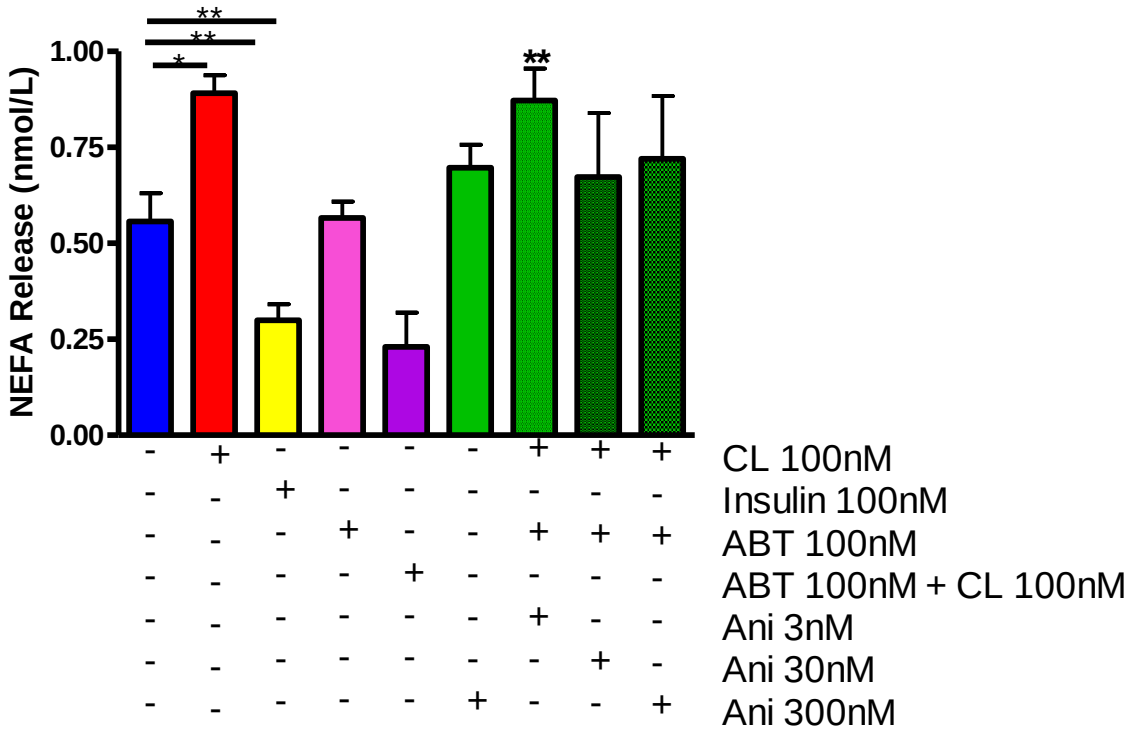

Figure 4.12: The effect of the p38 MAPK activator anisomycin on β_3-stimulated 3T3L1 adipocyte lipolysis. Effect of p38 MAPK activator (anisomycin) and ABT-510 upon basal and β_3 stimulated lipolysis as assessed by free fatty acid release (FFA) in Day 10 3T3L1 adipocytes. A positive stimulator-(β_3 agonist-CL 316, 243) and inhibitor (insulin) of lipolysis were also used. Data are expressed as means ± SEM; n=6 for all groups. Data analysed by one way ANOVA followed by Bonferroni corrections; *p<0.05; ***p<0.001; NS; non-significant. CL; CL 316, 243; SB= SB203580 on legend.

4.4.6 ABT-510-mediated inhibition of β_3 stimulated lipolysis is independent of nitric oxide pathways

Nitric oxide (NO) signalling is crucial for both endothelial cells and adipocyte function. TSP-1 and ABT-510 inhibit NO signalling in endothelial cells (Isenberg *et al.,* 2005; Isenberg *et al.,* 2008). This, coupled with the knowledge that NO also inhibits proliferation and subsequent differentiation of adipocytes (Nisoli *et al.,* 1998) and causes a decrease in lipolysis (Andersson *et al.,* 1999), may link the novel anti-lipolytic effect of ABT-510 observed in adipocytes.

Myristic acid is a fatty acid capable of activating NO production (Zhu *et al.,* 2005) and TSP-1 inhibits myristic acid uptake into endothelial cells (Isenberg *et al.,* 2007). Thus, the effect of ABT-510 inhibition of β_3-mediated lipolysis in the presence of myristic acid was investigated with the reasoning that suppression of a nitric oxide response could be involved in the anti-lipolytic mechanism (note that TNF-alpha mediated NO production facilitates lipolysis (Lien *et al.,* 2009)). Both cGMP and nitrite production were examined with myristic acid incubation to give an indication of the amount of NO produced. NO stimulates soluble guanylate cyclase (sGC), increasing cytoplasmic cGMP levels (Moncada *et al.,* 1991) and nitrite is also an important source of nitric oxide (Zweier *et al.,* 1995). However, when both cGMP synthesis (Figure 5.13A) and nitrite production (Figure 5.13B) were investigated, there was no effect of myristic acid when incubated with any of the concentrations of ABT-510. As well as the stimulation of NO production, inhibition of NO production was investigated. The nitric oxide synthase inhibitor L-NAME (L-N^G-nitro-arginine methyl ester) was used to inhibit NO production during stimulation of lipolysis. As may be predicted from the lipolytic effects of TNF-α mediated by NO, L-NAME incubation caused a reduction in lipolysis in adipocytes (Figure 4.14). This reduction was also mirrored when L-NAME was incubated in the presence of the β-agonist CL316, 243 and when both CL316, 243 and 100 nM ABT-510 were incubated in addition to 300 µM L-NAME. However, it must be pointed out that there was no additional effect with incubation of L-NAME to suppress lipolysis when ABT-510 was co-incubated.

4.4.6 No effect of myristic acid and ABT-510 on production of nitrite or cGMP by adipocytes

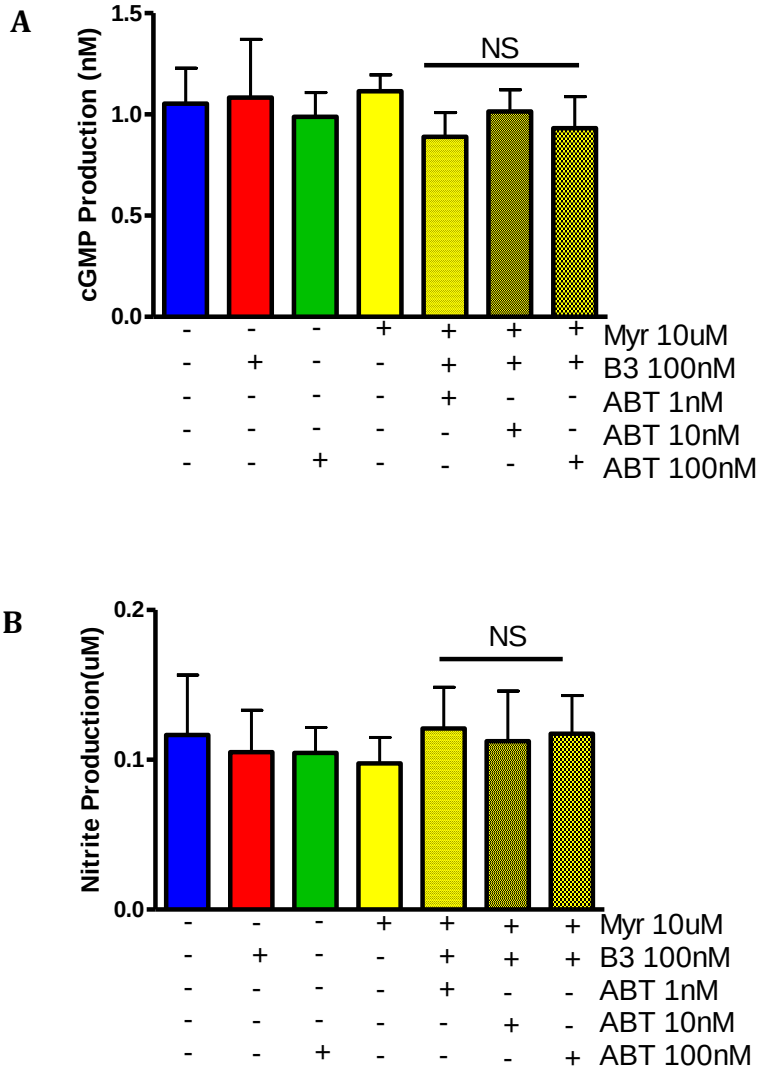

Figure 4.13: The effect of myristic acid and ABT-510 on adipocyte nitrite and cGMP production. A: cGMP production in Day 10 3T3L1 adipocytes with incubation of myristic acid and ABT-510 as assessed by the cGMP ELISA. **B:** Nitrite production in Day 10 3T3L1 adipocytes with incubation of myristic acid and ABT-510 as assessed by the Griess assay. Data are expressed as mean ± SEM; n=6 for all groups. Data were analysed by one way ANOVA followed by Bonferroni correction; *p<0.05; **p<0.01; NS; non-significant; Myr; myristic acid CL; CL 316, 243.

4.4.6 Effect of nitric oxide synthase inhibitor L-NAME on stimulated lipolysis

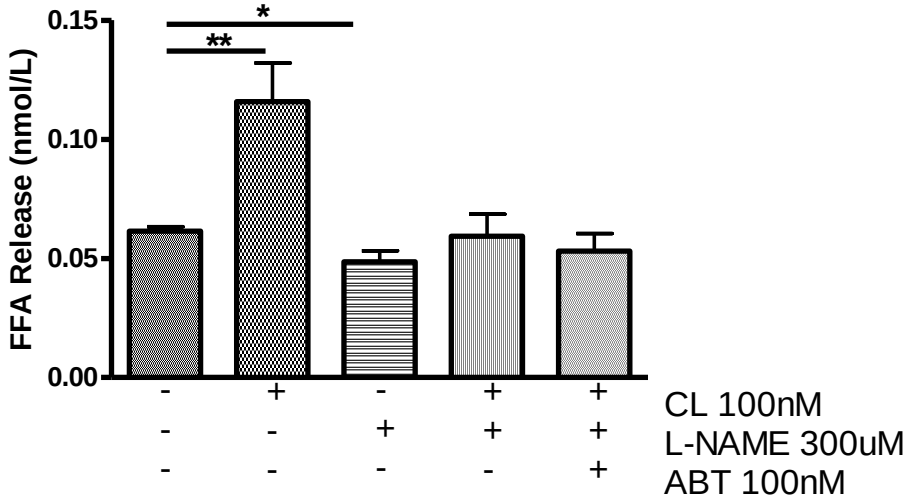

Figure 4.14: The effect of the nitric oxide synthase inhibitor L-NAME on ABT-510-mediated suppression of lipolysis in adipocytes. Effect of L-N^G-nitro-arginine methyl ester (L-NAME) and ABT-510 upon basal and β_3 stimulated lipolysis as assessed by free fatty acid release (FFA) in Day 10 3T3L1 adipocytes. A positive stimulator-(β_3 agonist-CL 316, 243) was also used. Data are expressed as mean ± SEM; n=6 for all groups. Data were analysed by one way ANOVA followed by Bonferroni correction; *p<0.05; **p<0.01; L-NAME; L-N^G-nitro-arginine methyl ester CL; CL 316, 243.

4.5 Discussion

This chapter tested the hypothesis that the anti-angiogenic activity of TSP-1 has a direct effect upon adipocyte function, through similar mechanisms involved in its anti-angiogenic action in endothelial cells. This was investigated using a synthetic, mimetic peptide of the second Type I repeat of TSP-1, ABT-510.

4.5.1 Elevated TSP-1 in obesity is also associated with other obesity-related factors

The effects of other factors known to be elevated in adipose during obesity on TSP-1 expression were examined, focussing on four key factors associated with obesity. The effects of insulin, which is elevated due to insulin-resistance (for review see Reaven 1993); increased intra-adipose glucocorticoid action (via 11β-HSD1 in obesity; Morton and Seckl 2008); decreased adrenergic stimulation of obese adipose (Muzzin *et al.,* 1991) and, finally, a locally elevated adipocytokine (interleukin-6) associated with the chronic adipose inflammation observed in obesity (Mohamed-Ali *et al.,* 1997; Kern *et al.,* 2001) were investigated. Of note, the TSP-1 receptor, CD36, has been directly linked to insulin resistance in adipocytes (Aitman *et al.,* 1999; Pravenec *et al.,* 2003) and, thus, it was hypothesied that TSP-1/ABT-510 may mediate direct effects through CD36, which is the pathway known to inhibit angiogenesis in endothelial cells (Jimenez *et al.,* 2000; Nor *et al.,* 2000; Simantov and Silverstein 2003).

TSP-1 levels had previously been correlated with increased insulin levels (result of insulin resistance) in humans (Varma *et al.,* 2008). Similarly, as excess glucocorticoid production is also associated with obesity and diabetes (Morton and Seckl 2008) and short-term administration of a synthetic glucocorticoid, dexamethasone, leads to reversible insulin resistance, hyperinsulinemia and impaired glucose tolerance in healthy individuals (Tappy *et al.,* 1994; Schneiter *et al.,* 1998), the effects of insulin and dexamethasone on TSP-1 expression were also investigated. TSP-1 expression was not affected by increasing doses of insulin or dexamethasone in adipocytes. This was surprising as dexamethasone

induces TSP-1 expression in trabecular meshwork mouse and human cells (Flugel-Koch *et al.,* 2004). Therefore, although contrary to previous results, it was concluded that increased TSP-1 expression is not mediated by increasing concentrations of insulin or dexamethasone.

Attention then turned towards adipokines and, in particular, interleukin-6 (IL-6). IL-6 is elevated in obesity (Mohamed-Ali *et al.,* 1997) and inhibits the expression of lipoprotein lipase (LPL) on adipocytes (Feingold *et al.,* 1992; Greenberg *et al.,* 1992). The typical "bell-shaped" response observed with IL-6 incubation has been reported previously and with other cytokines (Aarden 1989; Van dam *et al.,* 1993). Thus transition from the active IL-6 tetrameric form to an inactive receptor complex (Groetzinger *et al.,* 1999) could in part explain the u-shaped dose effects with IL-6.

The β_3-adrenoreceptor agonist elevated TSP-1. Thus, the adrenergic system may alter expression in obesity. β_3 agonists have remarkable anti-obesity and anti-diabetic effects in rodents (De Souza *et al.,* 1997; Ghorbani *et al.,* 1998; Liu *et al.,* 1998; Weyer *et al.,* 1998). However, catecholamine-stimulated lipolysis is reduced in obesity (Arner 1996).

4.5.2 The anti-angiogenic activity of TSP-1 may be detrimental to adipocyte function

Confirmation that the ABT-510 sequence was the specific, endothelial, anti-angiogenic part was essential. As expected, ABT-510 showed potent inhibition of endothelial cell function, including migration observed in the aortic ring preparation and tube formation in the HUVEC preparations. A non-active sequence was without effect, proving specificity for the type I repeat effects.

As ABT-510 caused no alteration of differentiation from pre-adipocyte to the fully mature adipocyte, our attention then turned towards other functions of the mature adipocyte. The likelihood of a role in mature fat cells was re-enforced by the observation that TSP-1 receptor, CD36, increased as the adipocytes became mature (>Day 7). Moreover, a novel anti-lipolytic effect of ABT-510, where ABT-

510 abolished β_3-adrenoceptor-stimulated lipolysis, was demonstrated. This, coupled with increased fatty acid uptake at high ABT-510 concentrations, could mean elevated TSP-1 in obesity promotes further lipid storage by simultaneously increasing fatty acid uptake and inhibiting free fatty acid release from the adipocyte. This may make increased adipose tissue TSP-1 production ultimately detrimental through specific actions on fatty acid movement in adipocytes in obesity. However, as alluded to previously, TSP-1 anti-lipolytic effect on adipocytes may be masked in obesity as β_3 signalling is down-regulated.

4.5.3 Study Limitations

The increase in palmitate uptake by ABT-510 was demonstrated after a six hour incubation. As discussed in the Introduction (Chapter 1), uptake of fatty acids occurs both via a carrier-mediated method (e.g. CD36) or a passive flip-flop, which is based on the assumption that fatty acids are transferred across lipid bilayers (Hamilton 1998; Stump *et al.,* 2001). Therefore, it may be argued that the movement of palmitate into the adipocytes by ABT-510 was not mediated by the proposed receptor (CD36) but this simple diffusion across the membranes. This is a valid point, however preliminary time-course experiments (see section 2.5.6) dictated 6 hours was a valid time point for investigation.

The evidence for CD36 mediating the anti-angiogenic activity of TSP-1 in endothelial cells is substantial. CD36 receptor expression was observed throughout adipocyte differentiation. However, there was no definite proof that the effects observed with ABT-510 on adipocytes were through CD36 receptor. Attempts to address this were performed by manipulation of CD36 by siRNA down-regulation. No successful knock down was observed in mature adipocytes and thus CD36 involvement in ABT-510 effect on adipocytes was not confirmed. Alternatively, an inhibitor of CD36 was considered. Sulfo-*N*-succinimidyl oleate (SSO), is an oleic acid derivative that specifically binds to and cross-links CD36 on the plasma membrane, which results in an inhibition of transport by CD36 (Coort *et al.,* 2002). This would have been ideal to examine ABT-510 effects at

least on fatty acid transport, if not CD36 signalling. Unfortunately, SSO is not commercially available and these experiments were not feasible within the time limit of the thesis.

4.5.4 The anti-lipolytic effect of ABT-510 is independent of PI3K, yet dependent upon p38 MAPK signalling

The inhibition of lipolysis by ABT-510 was equipotent to that of insulin, which is an established anti-lipolytic agent (at any dose used; 1, 10 and 100nM). Insulin exerts such an effect primarily through phosphorylating and activating phospodiesterase type 3B (PDE3B), leading to a reduction in cAMP-dependent protein kinase (PKA). Phosphoinositide-3-kinase (PI3K) is important in the anti-lipolytic insulin signalling pathways (Okada *et al.,* 1994; Rahn *et al.,* 1994). Therefore, the PI3K inhibitor, Wortmannin (Hausdorff *et al.,* 1999), was used in order to determine if ABT-510 effects were mediated through PI3K. Wortmannin reversed the anti-lipolytic effect of insulin but not ABT-510, suggesting the anti-lipolytic effect of ABT-510 is not through PI3K.

In addition to PI3K, p38 MAPK is also an established pathway that is activated by ABT-510 (Mirichnik *et al.,* 2008). p38 MAPK is also involved in glucose disposal by insulin in both muscle and adipose, whereby it causes the activation of a glucose transporter (GLUT4) (Michelle *et al.,* 2003). Moreover, β-adrenergic receptor-mediated adipocyte lipolysis and inflammation has been shown to activate p38 MAPK (Mottillo *et al.,* 2010). Thus, p38 MAPK seemed the ideal candidate as a potential mediator of ABT-510 effects on adipocytes. However, the p38 inhibitor had no additional effect upon the novel anti-lipolytic effect observed by ABT-510. Curiously, stimulation of the p38 MAPK pathway using anisomycin caused a reversal of the inhibition of β_3-induced lipolysis by ABT-510. This may indicate that ABT-510 exerts its anti-lipolytic effect through decreased p38 MAPK activation, which is completely opposite to its action in endothelial cells.

Another mediator that may potentiate ABT-510 effects on adipocytes is NO. NO inhibits basal lipolysis (Andersson *et al.,* 1999), impairs stimulated lipolysis

(Klatt *et al.,* 2000) and inactivate HSL (Gaudiot *et al.,* 1998). To determine whether ABT-510 was mediating the inhibition of lipolysis through NO signalling, experiments were conducted using mediators important in this pathway. Myristic acid causes activation of eNOS in a CD36 and AMP kinase dependent manner (Zhu and Smart 2005). In addition, myristic acid treatment of endothelial cells showed similar biochemical responses as exposure to an NO donor and these responses were inhibited by TSP-1 mimetic Type I peptides (Isenberg *et al.,* 2007). However, this chapter has presented evidence to show myristic acid incubation did not alter nitrite and cGMP production. Yet nitrite and cGMP production were also not affected by β_3-induced lipolysis which is opposite to what would be expected (predicted decrease in cGMP and nitrite production). Therefore, this may highlight a lack of sensitivity in both assays to observe differences in NO by-product production. More specific NO assays could be employed and although technical, the amperometric microelectrode assays now offer the potential to measure small amounts of NO (10^{-20} M) from single cells (Archer 1993). No evidence of fluctuations in nitrite and cGMP levels may also re-inforce that NO signalling is not a mechanism employed by myristic acid in adipocytes and thus further experimentation investigating another stimulator of NO production could be used. In addition to stimulation of NO production, inhibition of NO was achieved using L-N^G-nitro-arginine methyl ester (L-NAME). Contrary to previous literature (Gaudiot *et al.,* 2000), L-NAME suppressed lipolysis. The decrease was not further affected by the addition of ABT-510. This may indicate that either NO may not be involved in the stimulated anti-lipolytic effect of ABT-510 or that suppression of a lipolytic effect of NO, as shown with TNF-α (Lien *et al.,* 2009) might be a potential anti-lipolytic mechanism of ABT-510.

4.5.5 Future studies

Identifying mechanism(s) for ABT-510 effects upon adipocytes has proven difficult. However, down-stream targets of the p38 MAPK pathway would warrant further investigation. In particular, the nuclear factor-κB(NF-κB) signalling pathway has been implicated in the regulation of adipogenesis in

murine cells (Hauner 2005) and, more importantly to this research, has been proposed to mediate in part TNF-α-stimulated lipolysis (Bouwmeester *et al.,* 2004). This pathway may then be down-regulated in the inhibition of stimulated lipolysis by ABT-510. In addition, future studies may include co-culture of both adipocytes and endothelial cells and the effect of ABT-510 assessed. This approach would allow both cell types and their interactions to be examined.

Although no substantial effect was observed on NO or cGMP production with incubation of ABT-510, it may be interesting to assess vascular tone of adipose vessels in response to ABT-510 by myography.

Chapter 5

In vivo evaluation of the effects of thrombospondin analogue ABT-510 upon weight gain, metabolism and angiogenesis

5.1 Introduction

Synthesised antiangiogenic substances have the potential to prevent development of the vasculature and are used in the treatment of cancer. As shown in Chapter 4, ABT-510 has an additional, anti-lipolytic effect upon stimulated lipolysis in adipocytes. The potent inhibitory role of ABT-510 on angiogenesis was observed in syngeneic and xenograft mice, where tumour growth was suppressed (Jimenez *et al.,* 2001; Reiher *et al.,* 2002). Furthermore, apoptosis of solid tumour endothelial cells in mouse cancer models increased with ABT-510 administration (Haviv *et al.,* 2005). In addition, ABT-510 decreased circulating endothelial cell and endothelial progenitor cells in TSP-1 knockout mice and mice bearing lung tumours (Shaked *et al.,* 2005). These strong preclinical data have contributed to the entry of ABT-510 into Phase I and Phase II clinical trials for cancer involving adults with advanced solid malignancies (Ebbinghaus *et al.,* 2007; Markovic *et al.,* 2007). These studies have been in line with pre-clinical results whereby ABT-510 prevented tumour growth and formation; however, clinical trials demonstrated no tumour regression (Hoekstra *et al.,* 2005). Examination of the direct effect of ABT-510 upon adipose (see Chapter 4) and weight gain has not been addressed previously. This warrants further investigation particularly since, TNP-470 a synthetic analogue of fumagillin, inhibits endothelial cell growth and angiogenesis (Kusaka *et al.,* 1994) and prevented the development of obesity of both genetic and diet-induced obesity (Rupnick *et al.,* 2002; Brakenhielm *et al.,* 2004). Although it was not clear whether TNP-470 acted directly upon the adipose tissue to inhibit expansion, there was evidence to show reduced vascularity within the adipose and decreased circulating levels of lipoprotein lipase (LPL) (Rupnick *et al.,* 2002). Consistent with this observation, other inhibitors of angiogenesis, including angiostatin and endostatin, also prevented genetic obesity in mice (Rupnick *et al.,* 2002).

As these studies did not clarify the mechanism of anti-angiogenic effects upon adipose tissue and whole body physiology, it was important to investigate the effect of ABT-510 effect upon adipose tissue metabolism to establish whether

direct effects on adipose tissue was causing the alteration in weight. As highlighted previously (Chapter 4), ABT-510 is the second Type I repeat of the specific anti-angiogenic region of TSP-1. In order to appreciate the *in vivo* action of ABT-510 on metabolism, clues may be gathered from work using TSP-1. Increased TSP-1 levels have been associated with obesity and insulin resistance (Boden 2001) and with the accelerated development of atherosclerotic lesions and restenosis in diabetes (Stenina *et al.,* 2003). Moreover, as TSP-1 is synthesised by endothelial cells and adipocytes as well as platelets, it was interesting to note that endothelial cells increased TSP-1 production when incubated with high glucose (Tada *et al.,* 2001). These studies indicate that aberrant glucose metabolism may be a driver of elevated adipose TSP-1. This coupled with the fact that CD36 is main receptor mediating the anti-angiogenic activity of TSP-1 (Dawson *et al.,* 1997) (see Chapter 4) hints at a strong relationship between TSP-1 and insulin resistance. In addition, CD36 mutation in the spontaneously hypertensive rat strain has been linked to insulin resistance (Aitman *et al.,* 1999; Pravenec *et al.,* 2003) and humans lacking CD36 also exhibit insulin resistance (Miyaoka *et al.,* 2001). It was therefore important to monitor glucose homeostasis after ABT-510 administration.

Previous work has suggested at high concentrations, ABT-510 induced fatty acid uptake by adipocytes *in vitro* and potently inhibited catecholamine-stimulated lipolysis (Chapter 4). Thus, alongside its established response in inhibiting endothelial cell angiogenesis, ABT-510 may also cause fat retention by adipocytes. The work described in this chapter addresses the hypothesis that administration of high doses of ABT-510 will act directly on adipocytes to cause fat retention, thus re-instating weight gain and countering the beneficial effects of inhibition of ABT-510-mediated angiogenesis in diet-induced obesity.

5.2 Experimental hypothesis

The experiments described in this chapter were designed to address the hypothesis that administration of the TSP-1 analogue ABT-510 at high doses will increase fat uptake into the adipose tissue, directly counteracting its beneficial effects to curtail angiogenesis and associated fat expansion.

5.2.1 Aims

Specifically this chapter aimed to determine whether:

- Subcutaneous administration of ABT-510 by minipump would alter angiogenesis
- Subcutaneous administration of ABT-510 by minipump would increase high fat diet-induced weight gain at high doses.

5.3 Experimental Design

Six week old C57BL/6J mice were fed either chow (n=6) or high fat diet (n=18) for a period of four weeks (see section 2.1.1). After this time, minipumps administering vehicle (saline) or Type I repeat analogue of thrombospondin-1 (ABT-510) at low (0.6 mg/kg/day) or high (60 mg/kg/day) were inserted, alongside polyurethane sponges. High fat or control diets were continued for a further 4 weeks. After 7 weeks of high fat feeding, insulin sensitivity was assessed in control (C), high fat vehicle (V), low dose ABT-510 (AL) and high dose ABT-510 (AH) mice using glucose tolerance test (see section 2.1.3.3). Body weights were monitored throughout the 8 week study period. Twenty eight days post-implantation, mice were killed and aortas, adipose and sponges collected for further analysis (Diagram 5.1).

The use of osmotic minipumps allowed the continuous administration of high or 100-fold lower (though still angiostatic *in vitro*) doses of ABT-510 to mice as they gained weight with high fat diets. The use of minipumps has many advantages over other methods of delivery. For example minipumps are known to deliver drugs at a constant, controlled rate and reduce researcher intervention during the experimental period. With regard to concentration, minipump administration of ABT-510 at a concentration of 60 mg/kg/day for 7 days decreased angiogenesis and inflammation in a model of inflammatory bowel disease (Punekar *et al.,* 2007). Specifically, the main objective was to examine the influence of ABT-510 upon adipose vascularity when mice were gaining weight during obesity.

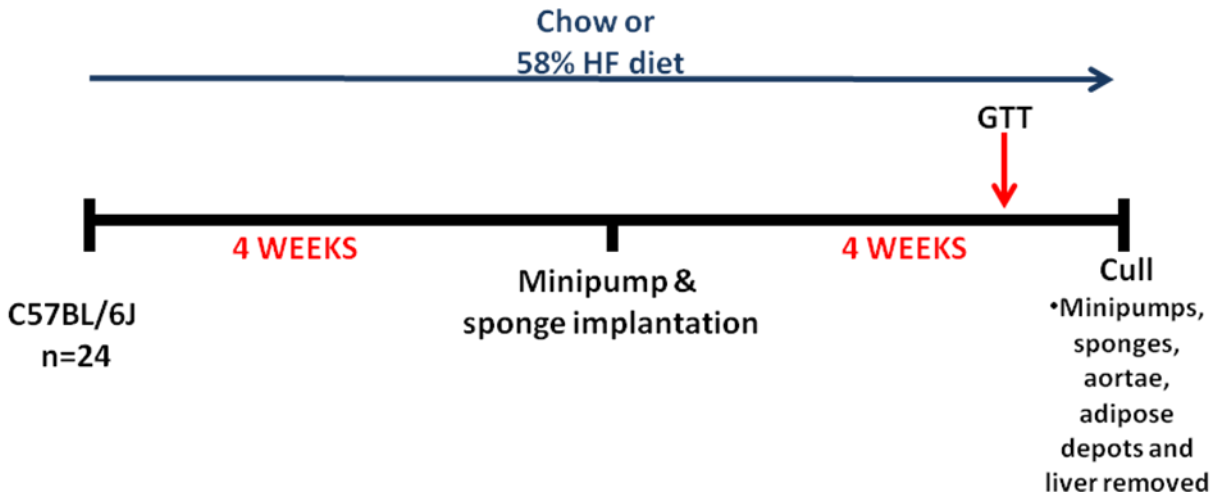

Diagram 5.1: Time line for *in vivo* ABT-510 minipump experiment. C57BL/6J mice were control or high fat fed for a period of 8 weeks. After 4 weeks of respective diet, osmotic minipumps containing either vehicle control, low and high concentration of Type I sequence repeat of thrombospondin-1 (ABT-510) were implanted, alongside sponges. ABT-510 dissolved in PBS. 7 weeks into the experiment, glucose tolerance tests (GTT) were performed. Mice were culled at 8 weeks and minipumps, sponges, adipose depots and livers removed and analysed.

5.4 Results

5.4.1 Weight gain and tissue harvesting

5.4.1.1 Divergent response in body weight exhibited by low and high doses of ABT-510

C57BL/6J mice (n=24) were fed either chow or 58% high fat diet for 4 weeks. Subcutaneous implantation of minipumps administering vehicle (saline), or ABT-510 at low (0.6 mg/kg/day) or high (60 mg/kg/day) doses were employed alongside polyurethane sponges (see section 2.1.3.1). High fat or chow diets were continued for further 4 weeks. At the beginning of the study the mice were randomly assigned to their groups: control diet (C) bodyweight: 20.2 ± 0.4 g; high fat vehicle (V): 19.7 ± 0.8 g; low ABT-510 (AL): 19.5 ± 0.8 g and high ABT-510 (AH): 20.9 ± 0.5 g. Exposure to a high fat diet for 8 weeks caused a significant ($p<0.001$) increase in body weight in the vehicle-treated (V) mice (34.0 ± 0.7 g) compared with chow fed (C) controls (30.8 ± 0.5 g) (Figure 7.1). This increase was maintained in mice exposed to high dose ABT-510 (AH; 35.0 ± 1.2 g, $p<0.001$ compared with C) but was blocked by administration of low dose ABT-510 (AL; 30.9 ± 0.6 g) (Figure 5.1).

5.4.1.2 Administration of low ABT-510 reduces all adipose depot weights but not liver weight

Subcutaneous, epididymal and mesenteric adipose depots were excised and weighed. High fat feeding caused an increase in subcutaneous, epididymal, mesenteric and liver weight in V mice, compared to C mice (Figure 5.2 A, B, C & D respectively). An increase in adipose weight was also observed in AH mice but not AL mice. Note the reduction in adipose weight did not completely mimic the reduction in body weight observed in AL mice (Figure 5.1). AL mice did not exhibit reduced liver weights compared to AH mice ($p>0.05$) (Figure 5.2 D).

5.4.1.3 Low ABT administration reduces adipocyte size

Histological examination by haematoxylin and eosin staining of adipocytes in epididymal tissue was used to assess the effects of ABT-510 on adipocyte size.

The epididymal adipose tissue was used as this depot was larger in size than the mesenteric depot and the subcutaneous adipose tissue was used for molecular investigations including real-time PCR. Adipose tissue sections were examined under a light microscope (Karl Zeiss Axissop) at X10 magnification, their perimeters traced manually and analyzed with MCID software (Imaging Research Inc.) to calculate total adipocyte area (see section 2.6.3). Increased body weight was accompanied by increased adipocyte size in both V (1.43 ± 0.51 μm^2) and AH (1.17 ± 0.60 μm^2) mice compared to C mice (0.37 ± 0.25 μm^2) (Figure 6.3). AL adipocyte size (0.68 ± 0.074 μm^2) remained larger in size than C mice (0.37 ± 0.25 μm^2) (Figure 5.3).

5.4.1 Low dose ABT-510 prevented the development of obesity whereas high dose ABT-510 did not

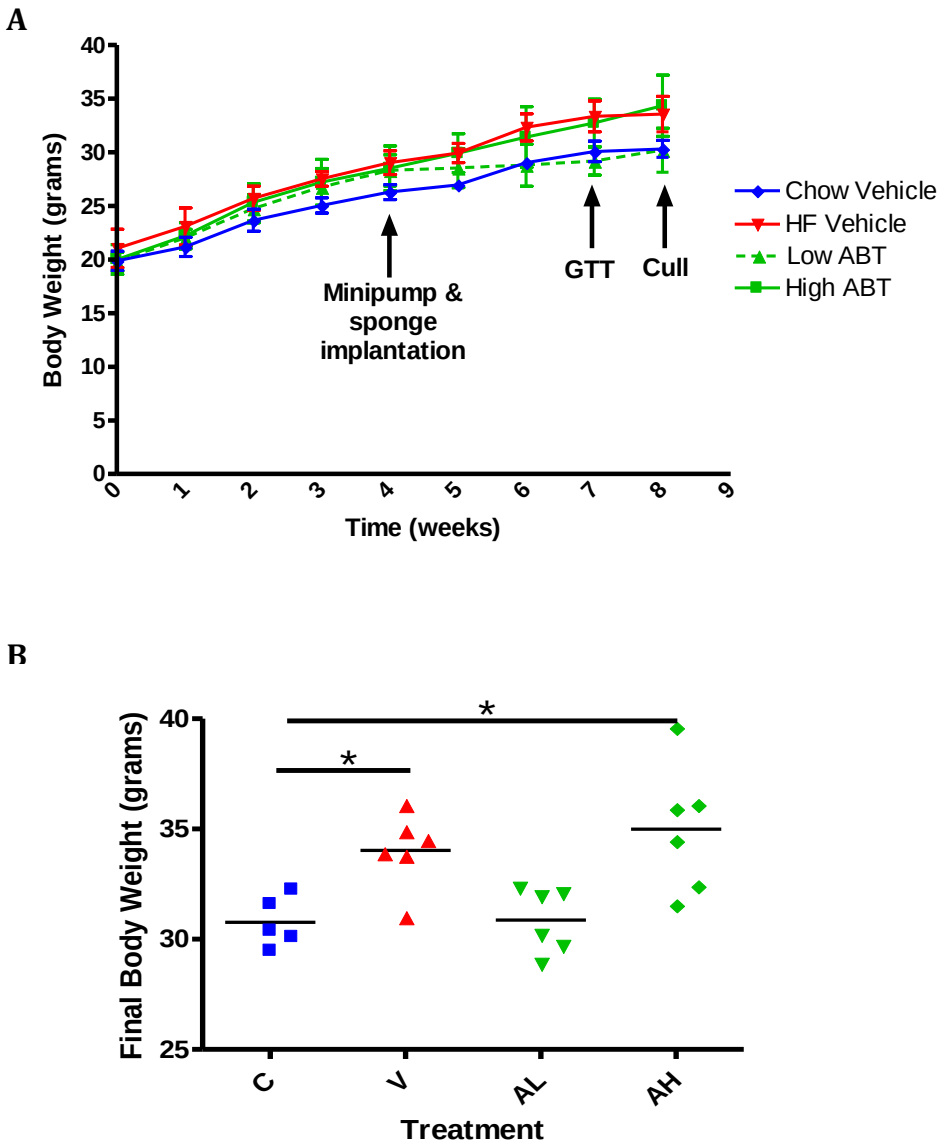

Figure 5.1: Subcutaneous minipump administration of ABT-510 in chow or high fat (HF) fed C57BL/6J mice. A: Mice placed on high fat diet (V, AL and AH) increased body weights until week 4. Subsequent minipump and sponge implantation at week 4, caused a reduction in body weight in AL mice which continued to week 8. Both V and AH increased their body weights further till the end of the 8 week study period. **B:** Final body weights of C, V, AL and AH mice. V and AH had significantly increased body weights compared to both AL and C. Results are expressed as mean weight ± SEM of 6 mice from each diet group. Two way ANOVA; Bonferroni Multiple comparison post hoc test. *$p<0.05$; C; control vehicle; V; high fat vehicle; AL; high fat low dose ABT-510; AH; high fat high dose ABT-510.

5.4.2 Low dose ABT-510 decreased all adipose weights but not liver weight

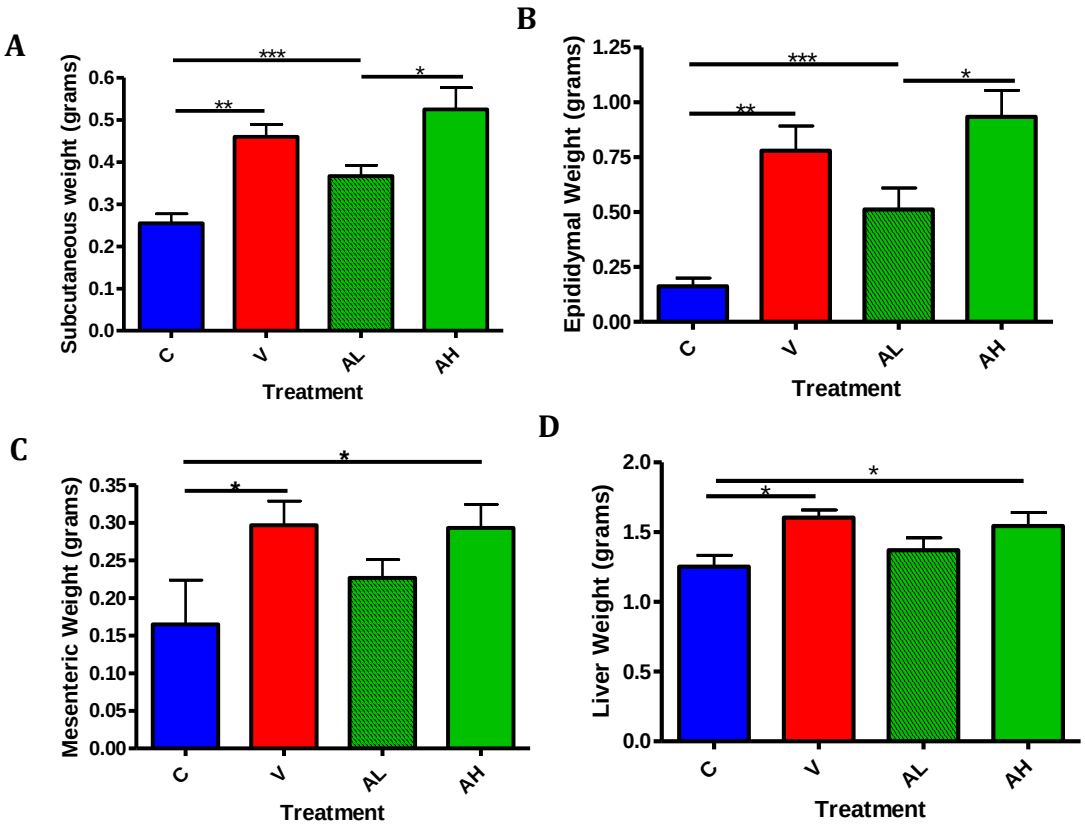

Figure 5.2: Subcutaneous, epididymal, mesenteric and liver weights from ABT-510 infusion into C57BL/6J mice. V and AH mice showed an increased subcutaneous (**A**), epididymal (**B**), mesenteric (**C**) and liver (**D**) weights compared to C mice. AL mice exhibited reduced subcutaneous (**A**), epididymal (**B**) and mesenteric (**C**) adipose tissue weights. AL did not decrease liver weight (**D**). Data are expressed as mean ± SEM; n=6 for all groups. Data analysed by one way ANOVA followed by Bonferroni corrections; *p<0.05; **p<0.01; ***p<0.001.

5.4.3.3 Low dose ABT-510 decreases adipocyte size

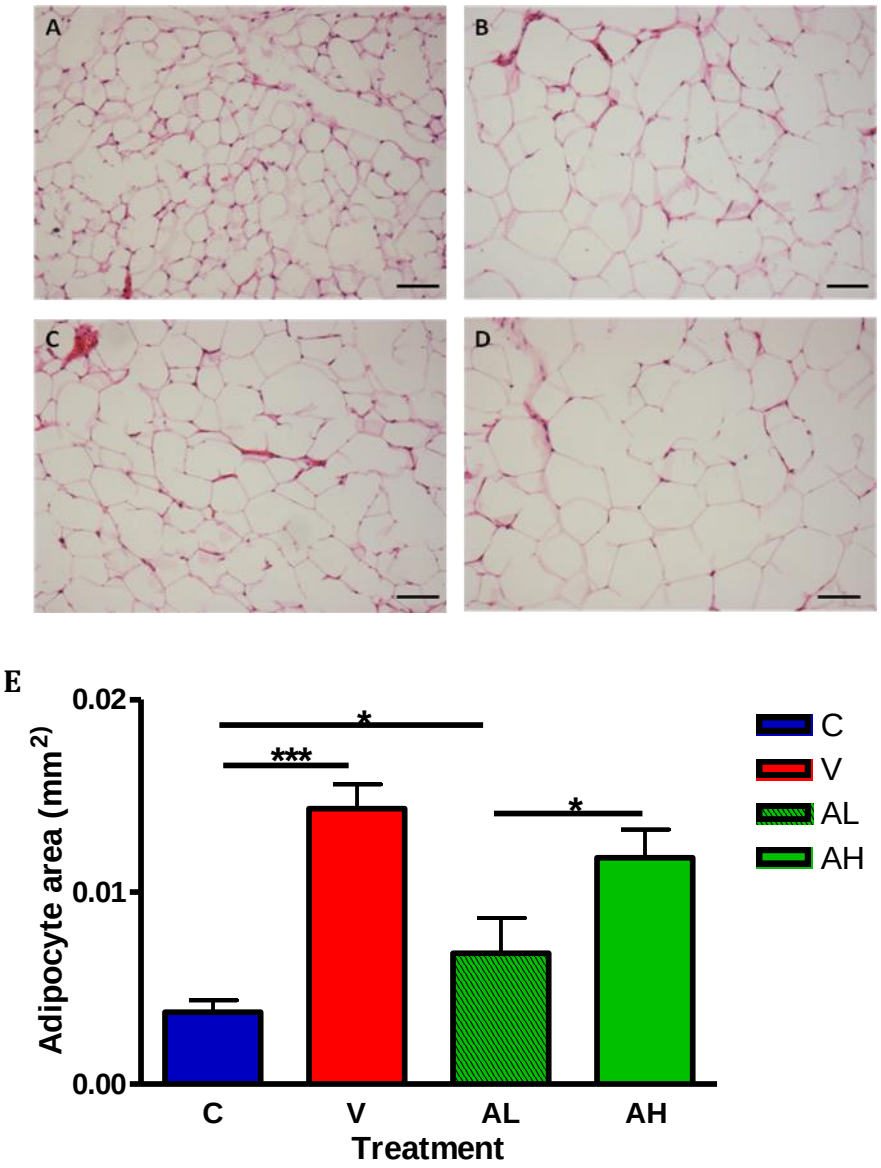

Figure 5.3: Adipocyte area in epididymal adipose from ABT-510 infused C57Bl/6J mice. A-D, Epididymal adipose sections from C, V, AL and AH mice. Photomicrographs of H & E stained adipocytes at x 10 from C (**A**), V (**B**), AL (**C**) and AH (**D**). V and AH increased adipocyte size compared to C mice (**E**). AL caused a decrease in adipocyte size in comparison to AH but not to the extent of C mice (**E**). Scale bar represents 10 μm. Data are expressed as means ± SEM; n=6 for all groups. Data analysed by one way ANOVA followed by Bonferroni corrections.

5.4.2 Low concentration ABT-510 infusion by minipump corrects glucose intolerance

In order to assess the effect of ABT-510 upon glucose homeostasis, glucose tolerance tests (GTT) were performed at week 7. Glucose was injected (2 mg/g) intraperitnoneally and blood glucose was measured from tail venesection over a 2 hour period, using an instant glucose meter (see section 2.1.3.3). V, AL and AH (all high fat fed groups) showed higher basal fasting glucose levels, indicative of insulin resistance (V: 12.03 ± 0.37 mmol/l; AL: 10.65± 0.53 mmol/l; AH: 11.85 ± 0.78 mmol/L; Figure 5.4A). Notably, AL exhibited a greater impairment of glucose tolerance than C despite having a lower bodyweight and reduced fat mass (C: 8.7 ± 0.88 mmol/l; AL; 9.68 ± 0.21 mmol; Figure 5.4A). AH, producing comparable weight gain as V, had impaired glucose tolerance (V; 14.63 ±1.58 mmol/l; and AH, 14.85 ± 0.96 mmol/l).

The higher glucose concentrations observed in the V and AH mice were associated with increased stimulated plasma insulin concentrations, observed at basal, 0 minutes (V; 1.22 ± 0.28 nmol/l and AH; 1.35 ± 0.067 nmol/l) compared to C mice, 0.23 ± 0.092 nmol/l. Throughout the 120 min time course, AL mice once again had comparable plasma insulin concentrations (0.36 ± 0.11 nmol/l) to C mice ($p<0.05$) (Figure 5.4B). Fasting (6 hours) free fatty acid (FFA) levels were also measured from blood plasma (see section 2.1.3.4) and both V (1.57 ± 0.12 mmol/l) and AH (1.74 ± 0.11 mmol/l) exhibited an elevation in fasting FFA compared to C mice, 1.18 ± 0.09 mmol/l (Figure 6.4C). Curiously, AL mice also exhibited elevated fasting FFA (1.69 ± 0.07 mmol/l) compared to C mice, converse once again to what was expected from their reduction in body weight.

5.4.2 Low ABT-510 infusion by minipump corrects glucose and insulin intolerance in C57BL/6J mice

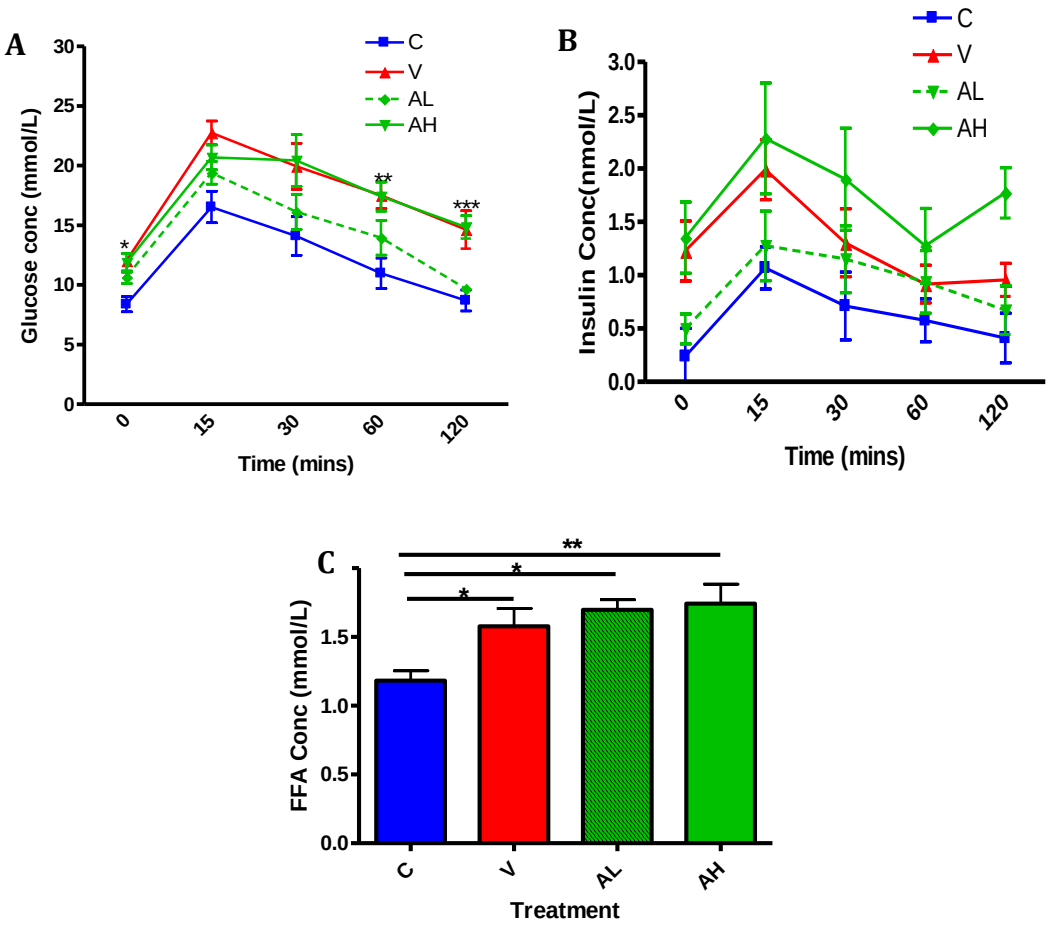

Figure 5.4: Intraperitoneal glucose tolerance testing and associated insulin excursion in ABT-510 infused C57BL/6J mice. Mice were fasted overnight and given an intraperitoneal injection of 2 mg/g of body weight of glucose in saline (25 % weight/volume). Tail-vein blood was collected at each time-point indicated and analysed by either a glucose meter (**A**) or insulin ELISA (**B**). **A**: Both V and AH had impaired glucose tolerance compared to C throughout the examination period, whereas AL reversed this. **B:** Basal insulin levels were higher in V and AH groups compared to AL and C mice. Final readings also indicate increased insulin concentrations in AH mice compared to AL and C mice. **C**: Fasting tail-vein blood was also collected and plasma removed to measure FFA. Fasting FFA levels were elevated in V, and AH mice compared to vehicle C, mice with a notable lack of effect of AL upon fasting FFAs. Control (C); high fat vehicle (V); low dose ABT-510 (AL) and high dose ABT-510 (AH). Data are expressed as means ± SEM n=6 for all groups. Data analysed by two way ANOVA followed by Bonferroni corrections (*p<0.05; **p<0.01; ***p<0.001).

5.4.3 *In Vitro* and *in vivo* angiogenesis studies: Mouse aortic ring and subcutaneous sponge implantation assays

ABT-510's effect upon angiogenesis was examined using both the aortic ring assay and the subcutaneous implantation of sponges. Tube like structure (TLS) formation could be detected after 2 days in aortic rings isolated from C, V, AL and AH mice and cultured in Matrigel (see section 2.3.1, 2.3.2 & 2.3.3). Growth continued for the next 8 days. After 10 days, some TLSs began to degrade. Therefore analysis was performed on day 10. This occurred in all treatment groups. Sponges were implanted at the same time as minipumps and removed 4 weeks later (see section 2.1.3.1). Vascularisation occurred in all sponges.

5.4.3.1 Low dose ABT-510 inhibited TLS formation compared to high fat vehicle controls *in vitro* at day 10

AL and AH had comparable suppressive effects on TLS formation form aortas (Figure 5.5).

5.4.3.2 ABT-510 did not affect angiogenesis in subcutaneous sponges

There was no difference in sponge weight between the four treatment groups: C; 0.27 ± 0.001 g; V; 0.31 ± 0.21 g; AL; 0.25 ±0.07 g and AH; 0.25 ± 0.02 g (Figure 5.6C). When vascularity within each sponge was examined, high fat vehicle (V) (Figure 5.6B) exhibited higher vessel density than Control (C) (Figure 5.6A). It also appeared, through histological examination, that both AL (Figure 5.6C) and AH (Figure 5.6D) had augmented vessel infiltration into the sponge compared to control (C).

5.4.3.1 Low dose ABT-510 minipump infusion suppressed aortic tube like structure (TLS) formation

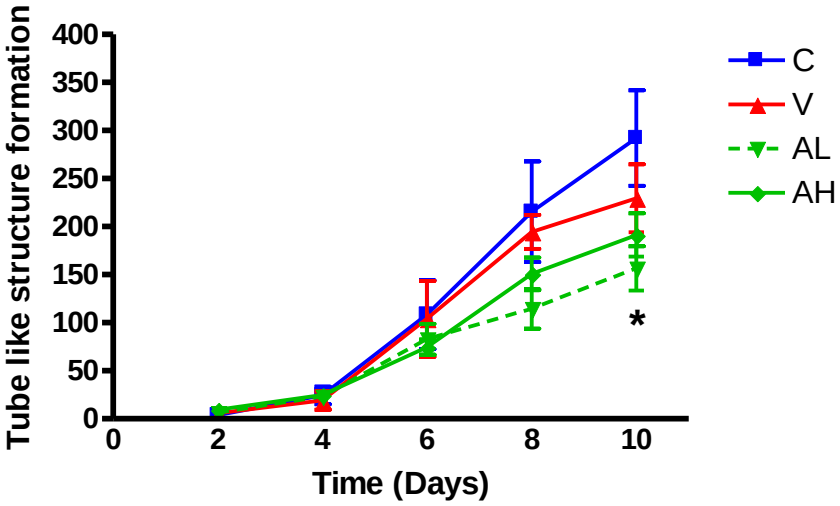

Figure 5.5: Tube like structure formation (TLS) in aortas from ABT-510 infused C57BL/6J mice. V did not alter TLS formation over the 10 day period. AL inhibited TLS growth on Day 10 compared to V. TLS formation was assessed by manual counting under light microscopy. New vessel formation was noted after the first 2 days in culture, and rapidly grew for the next 8 days in all treatment groups. Data are expressed as means ± SEM; n=6 for all groups. C control (C); high fat vehicle (V); low dose ABT-510 (AL) and high dose ABT-510 (AH).Data analysed by repeated measures ANOVA followed by Bonferroni corrections (*$p<0.05$).

5.4.3.2 Low dose ABT-510 tends to reduce sponge vascularity

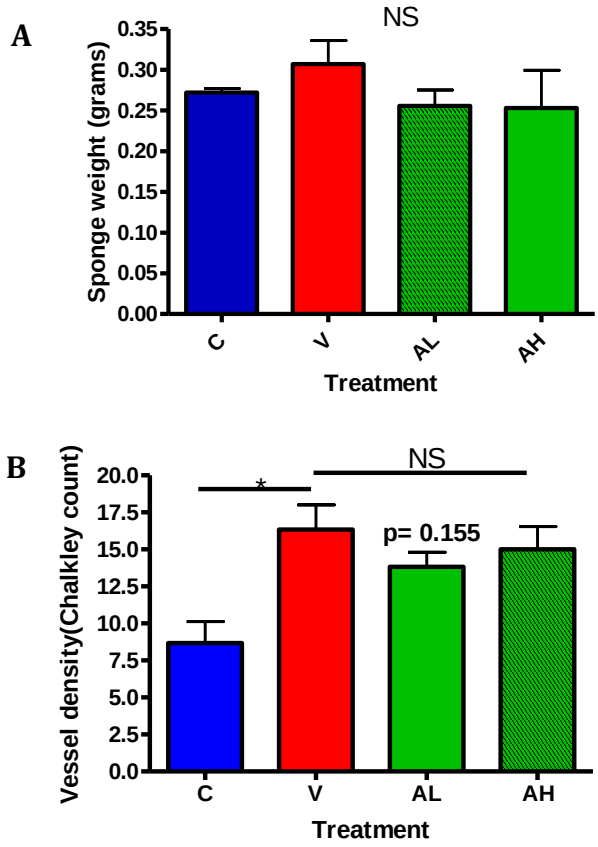

Figure 5.6: Assessment of vascularity and weight of subcutaneous sponges implanted in ABT-510 infused C57BL/6J mice. H&E stained sponges excised from C, HF, AL and AH were weighed and analysed. No difference in sponge weights from V, AL or AH mice compared to C animals (**A**). V elevated sponge vascularity compared to C mice, which was also observed when assessed by Chalkley counting (**B**). Data are expressed as means ± SEM; n=6 for all groups. Control (C); high fat vehicle (V); low dose ABT-510 (AL) and high dose ABT-510 (AH). Data analysed by one way ANOVA followed by Bonferroni corrections; NS= non-significant.

5.4.4 Opposing effects of ABT-510 upon expression of pro-angiogenic factors in subcutaneous adipose

5.4.4.1 ABT-510 suppressed fibroblast growth factor (FGF) expression and did not alter vascular endothelial growth factor (VEGF)

To observe whether the anti-angiogenic ABT-510 would alter the expression of pro-angiogenic factors, both fibroblast growth factor (FGF) and vascular endothelial growth factor (VEGF) were investigated. RNA was extracted from subcutaneous adipose (see section 2.2.2) of C, HF, AL and AH animals. Real-time quantitative PCR was used to analyse FGF and VEGF expression. The housekeeping gene, GAPDH, was used as a reliable normalisation factor. High fat vehicle (V) increased the expression of FGF ($p<0.05$), however this response was completely abolished in both ABT-510 treatment groups (Figure 5.7A). There was no effect of high fat-diet or ABT on VEGF expression ($p>0.05$) (Figure 5.7B). A similar pattern of elevated expression in high fat vehicle (V) animals was observed ($p=0.081$). This may signify a power issue ($n=6$) with this particular data set.

5.3.4.1 ABT-510 infusion decreased fibroblast growth factor (FGF) expression and had no effect upon vascular endothelial growth factor (VEGF) in subcutaneous adipose

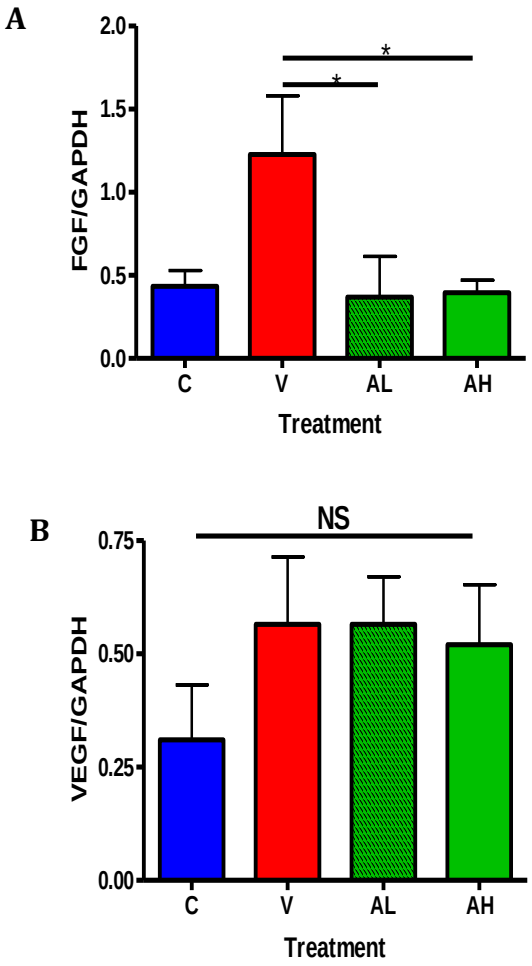

Figure 5.7: mRNA levels of fibroblast growth factor (FGF) and vascular endothelial growth factor (VEGF) in subcutaneous adipose of ABT-510 infused C57BL/6J mice. RNA extracted from subcutaneous adipose tissue of C, V, AL and AH animals was analysed for (A) FGF and (B) VEGF expression. **A:** V increased FGF expression compared to vehicle mice. Both AL and AH caused a reduction in FGF in comparison to V. **B:** There were no significant changes in VEGF mRNA levels between all groups investigated. Data are expressed as means ± SEM; n=6 for all groups. Control (C); high fat vehicle (V); low dose ABT-510 (AL) and high dose ABT-510 (AH). Data analysed by one way ANOVA followed by Bonferroni corrections (*$p<0.05$).

5.5 Discussion

Administration of anti-angiogenic agents can inhibit angiogenesis and prevent obesity (Rupnick *et al.,* 2002; Brakenhielm *et al.,* 2004). However, we have previously shown that the specific anti-angiogenic analogue of TSP-1 (ABT-510) acts directly upon the adipocyte, to inhibit lipolysis and potentially promote lipid uptake. Therefore the hypothesis that high dose administration of an inhibitor of angiogenesis (the thrombospondin-1 related peptide, ABT-510) would have a dual effect, increasing fat mass by causing an increase in lipid uptake into the adipocyte, whilst decreasing angiogenesis was tested. We chose two doses in order to dissect the fat accumulation response to an obesogenic stimulus, from the angiostatic fat reducing effects (Chapter 4).

5.5.1 Low ABT-510 concentrations reversed weight gain and its associated glucose intolerance

Previous *in vivo* experiments using ABT-510 addressed tumour size and progression (Haviv *et al.,* 2005; Rusk *et al.,* 2006) and effects on body weight and metabolism were over-looked. Clinical trials of ABT-510 in humans reported side effects which included the onset of diabetes mellitus in one patient and anorexia in three patients (Hoekstra *et al.,* 2005). However, no other metabolic or body weight effect of ABT-510 has been reported before in humans. Notably, these patients had advanced cancers and so the effect of ABT-510 in normal subjects is not known.

This chapter has demonstrated low doses of ABT-510 inhibited weight gain associated with diet-induced obesity. Interestingly, high doses of ABT-510 caused no reduction and maintained weight gain at a similar level as high fat fed vehicle treated mice. This maintenance in weight was associated with apparent insulin resistance, as indicated by glucose intolerance and elevated circulating free fatty acid (FFA) levels.

In addition to normal weight gain associated with high fat feeding, high dose ABT-510 increased liver weight whereas low doses of ABT-510 did not. This argues for a general curtailment of lipid accumulation and could feasibly be due

to an averse effect on food intake. However, if this was the mechanism for weight reduction in low dose ABT-510 treated mice, then a greater effect would be expected at higher doses. In addition, all animals administered high fat diet had elevated FFAs. This phenomenon of dyslipidemia with high fat feeding has been well documented (Ginsberg 1991; Boden 2001) and the severity of obesity is often associated with the degree of dyslipidemia. Therefore, normalisation of body weight and glucose homeostasis by low dose ABT-510 without normalisation of the lipid profile was surprising. The low dose ABT-510 did cause a small, but significant, increase in adipocyte size relative to control animals, so it is possible that this maintenance of hypertrophy contributed to higher NEFA release despite the normalisation of glucose intolerance. Alternatively, reduction in fat storage in the adipocytes may promote insulin resistance and glucose tolerance through ectopic accumulation in non-adipose tissues e.g. liver or muscle (Unger 1995). The elevated NEFA concentrations for the ABT-510-treated groups also argue against the role for ABT-510 as an anti-lipolytic agent in obesity. However, it should be noted that this effect was from catecholamine-stimulated lipolysis, which is known to be reduced in obesity (Arner 1996). Thus, the anti-lipolytic effect of ABT-510 may be masked by the down-regulation of adrenergic signalling when the animals become obese. There is also the possibility of a direct effect of ABT-510 upon hepatic triglyceride metabolism, where NEFA uptake may be altered. However since liver weights were comparable across the ABT-510/high fat treated groups this phenomena was not investigated further (but could for potential, future studies).

5.5.2 Low ABT-510 decreased aortic angiogenesis and had no effect upon sponge angiogenesis

This thesis has previously shown a novel anti-lipolytic effect of ABT-510 (potentially acting through p38 MAPK) on adipocytes. This was also coupled with a divergent effect upon lipid uptake, whereby increased uptake was observed with high doses and a reversal of this was observed with low doses of ABT-510 (Chapter 4). In addition to this action upon adipocytes, ABT-510 also

had an angiostatic effect upon endothelial cell growth in *in vitro* assays. In accordance with this role as an antiangiogenic factor, low dose ABT-510 showed a decrease in aortic angiogenesis. However, this decrease in vascularity could not be reproduced in implanted sponges for either dose of ABT-510 yet an overall increase in sponge vascularity was observed. Limitations in both *in vitro* and *in vivo* assays have already been addressed (Chapter 3) and the lack of effect in the ABT-510 sponges may not necessarily reflect angiogenic changes within the adipose tissue. This may also indicate that the aortic ring assay is more sensitive to changes in angiogenesis than the sponge assay, as there was a intrinsic decrease in TLS formation compared to the sponges, where they were exposed to constant delivery of ABT-510 and yet no decrease in vascularity. Differences in the assays may also indicate that ABT-510 may have not been active within the adipose. Evidence to support adequate drug delivery comes both from the demonstration that (i) the minipumps were reduced in weight and (ii) both doses of ABT-510 attenuated the increased expression of fibroblast growth factor (FGF) induced in subcutaneous adipose by high fat feeding, independent of weight gain differences. This effect appears to be specific to FGF; however it may be argued that a significant pattern may have emerged with vascular endothelial growth factor (VEGF) subcutaneous adipose expression, but due to the power of this experiment, the results never reached significance.

Interestingly, both doses of ABT-510 caused an enlargement in individual adipocyte area in comparison to controls. As we have previously found that ABT-510 augmented fatty acid uptake into the adipocyte, it may be argued that ABT-510 is also increasing uptake *in vivo*, causing them to become enlarged in comparison to the controls, even in the presence of reduced angiogenesis. Thus the expression of factors regulating fatty acid uptake, including CD36, could be examined in future work to observe whether ABT-510 was having an effect upon this particular process. If ABT-510 was having a direct fat retaining effect on adipocytes, this must be reconciled with the elevated NEFA. The most likely explanation, aside from increased fatty acid uptake and suppression of lipolysis, is that direct effects on FFA clearance by e.g. the liver, may have a role.

5.5.3 Study Limitations

As shown (Chapter 4), a divergent response from both a low and high (100 fold higher) dose of ABT-510 was observed. Initially it was agreed that the high dose should be 100 mg/kg/day as this has also been shown to inhibit angiogenesis (Greenaway *et al.,* 2009; Campbell *et al.,* 2010). However, due to solubility problems at such a high concentration, a concentration of 60 mg/kg/day was chosen. The anti-lipolytic effect may not be apparent *in vivo* at this lower concentration.

Shorter infusion times using ABT-510 have been shown to exert anti-angiogenic effects upon endothelial cells (Rusk *et al.,* 2006; Punekar *et al.,* 2007). However, extended exposures to ABT-510 are essential for measurable responses in human studies (Rusk *et al.,* 2006). There are also reports of delayed responses to ABT-510 in clinical trials (Westpha 2004), which would support the argument in prolonging the length of time the minipump was implanted. In addition to lengthening the minipump study, it would also be interesting to investigate ABT-510 effects upon adipose development in an already obese model (Lep$^{ob/ob}$ mouse). TSP-1 is elevated in obesity and thus ABT-510 application to an already obese model may worsen the obese phenotype. In addition, key control groups could also be added, such as control diet groups, receiving ABT-510 treatment. This would confirm the effect upon normal weight gain and ABT-510 infusion.

5.5.4 Concluding Remarks

The data in this chapter suggest that ABT-510 has biphasic effects on weight gain with high fat feeding. Low doses of ABT-510 constrain weight gain and cause glucose intolerance. High dose ABT-510 causes a weight gain to levels comparable to the high fat fed mice. These findings may suggest elevated concentrations of TSP-1 observed in obesity could initially limit adipose expansion through angiostatic properties, but at higher levels may promote lipid retention by adipocytes.

Chapter 6

The effects of high fat diet-induced weight gain and subsequent calorie-controlled weight-loss on neovascularisation

6.1 Introduction

Tumour growth in some cancers may be dependent upon angiogenic factors (Folkman 1985; Folkman 1989). Whilst this thesis does not directly address the neovascularisation process in tumour growth, there are clear mechanistic parallels between angiogenic mechanisms in tumours and in expanding adipose tissue. For example, obesity is associated with an increased incidence of some cancers both in humans and in rodents including breast, cervical, colon, kidney, liver, ovarian and pancreatic cancer (http://www.obesity.org/information/cancer_obesity.asp). Moreover, individuals that are 25 % above normal body weight have a 33 % greater cancer risk than those who maintain ideal body weight (Kritchesky 2003). Such associations imply that obesity may have a direct impact upon the angiogeneic balance. This may predispose obese individuals to an adversely altered angiogeneic response, subsequently leading to tumour growth in cancer.

Obesity results from a positive energy balance and often involves excessive caloric intake (see section 1.2). Despite the known genetic influences in susceptibility to obesity, and given the clear role of over-nutrition (e.g. leptin and Fto polymorphisms- see Chapter 3), dietary intervention is still the first, key strategy employed for combating obesity and its metabolic consequences. The impact of dietary intervention on angiogenic changes within the fat and on neovascularisation *per se* (with its potential implications for cancer risk) is not well understood.

Caloric limitation or calorie controlling (usually achieved by pair-feeding in rodents) is a commonly used intervention in obesity-related research that ensures animals receive fewer calories than *ad libitum*-fed controls. As far back as 1914, it was suggested that pair-feeding might inhibit tumour growth in mice by delaying tumour angiogenesis (Rou 1914). More recently, caloric restriction extended life span and delayed cancer development in rhesus monkeys (Colman *et al.,* 2009), and is the most potent, broadly-acting dietary intervention for preventing carcinogenesis in rodent models (Hursting *et al.,* 2007). Indeed, pair-

feeding was shown to have powerful anti-angiogenic and pro-apoptotic effects on rapidly growing mouse and human brain tumours (Mukherjee *et al.,* 2004). Although data in humans is limited, the benefits of pair-feeding appear to translate well into humans as caloric restriction during premenopausal years decreased postmenopausal breast cancer risk in women (Howell 1993). Thus, limited caloric intake may be beneficial in decreasing the angiogenic response which in turn may affect adipose angiogenesis.

Alongside caloric restriction, inhibitors of angiogenesis have been advocated in the treatment of some cancers by disrupting the endothelial cell cycle in angiogenesis. Relevant inhibitors include thalidomide and TNP-470 (synthetic analogue of fumagillin (Kusaka *et al.,* 1994)), which exhibit broad-spectrum anticancer activity in animal models (D'Amato *et al.,* 1994; Benny *et al.,* 2008) and are currently undergoing clinical trials. Intriguingly, inhibition of angiogenesis with TNP-470 also prevents fat accumulation and corrects insulin resistance in genetically obese mice (Rupnick *et al.,* 2002; Brakenhielm *et al.,* 2004). This weight loss was associated with no alterations in food intake (and thus caloric intake between the groups). However, it remains unclear how these angiogenesis inhibitors can correct insulin resistance in the face of calorie excess, and indeed whether the effects upon adipose expansion and insulin sensitivity were secondary to their angiostatic effects. However, if metabolism does adapt to cope with disposal of excess nutrients, this suggests that inhibition of angiogenesis may be a useful therapeutic intervention that could prevent obesity and its metabolic consequences – even when obesity is already established (Rupnick *et al.,* 2002).

It is not clear if the susceptibility to regain weight in these previously obese mice when angiogenesis inhibition is ceased. It is not uncommon for humans to rapidly regain weight (rebound) previously lost through dieting. The rate of weight loss often decreases and reaches a plateau due to changes in resting metabolic rate, and recent research has shown that levels of some hormones, including leptin and ghrelin, can predict the regain of weight after dieting (Crujeiras *et al.,* 2010). However, functional changes within adipose tissue

angiogenesis may also contribute to the difficulty in losing more weight. One hypothesis this chapter set out to test was whether the increased angiogenic response experienced during obesity is maintained with calorie controlled weight loss and that this in turn might provide an adipose tissue-specific mechanism that supports the subsequently accelerated weight gain.

6.2 Experimental hypothesis

This chapter hypothesised the following:

- High fat feeding (ad libitum, overnutrition) increases angiogenesis.
- Pair feeding of high fat diet to a control diet fed group, will reverse the angiogeneic process with increased expression of the anti-angiogenic factor TSP-1.

The hypotheses were tested using both the aortic ring and sponge implantation assays (see section 2.3.1 and 2.4.1 respectively). In addition, given its prominent role in adipose angiogenesis (see Chapter 3), dynamic changes in expression of subcutaneous adipose thrombospondin-1 (TSP-1) in response to pair-feeding was also investigated, hypothesising a decrease in expression in calorie controlled animals, as an increase in TSP-1 was observed in obesity.

6.3 Experimental Protocol

Six week old male C57BL/6J mice (n=18) supplied by Charles River (Kent, London, UK), were individually housed and randomly assigned to two different dietary groups: Control and High fat diet (HF) (n=6 for each group). The control animals were fed a standard pelleted diet (2014 Teklad Global 14 % Protein Rodent Maintenance Diet, Harlan, UK) containing 20 % of energy as proteins, 67 % of energy as carbohydrates (5 % sucrose, 62 % starch) and 13% energy as fat by dry weight, while the HF group (n=12) were fed a high 58% kcal of fat as before for a period of twelve weeks. After this time on either diet, mice either continued control (n=6), HF diet ad libitum (n=6) or HF diet restricted to the amount of calories (kcal/ [g body weight]) that the Control group had consumed the day before (*pair-fed* model), as previously described (Howard *et al.,* 1999). In order to distinguish between fat depot loss through pair-feeding and that caused by primary inhibition of angiogenesis, it will be important to have controls that are still high fat fed. Respective diets were continued for a further three weeks, where body weight and food intake were recorded daily (until mice were 21 weeks old). The timeline for this experiment is depicted in Diagram 6.1.

All mice had subcutaneous sponges implanted (see section 2.1.3.1) for a period of three weeks beginning at week twelve. At the end of the fifteen week study period, subcutaneous, epididymal and mesenteric adipose depots, as well as liver and sponges were excised and weighed. Aortas were also removed to assess aortic angiogenesis.

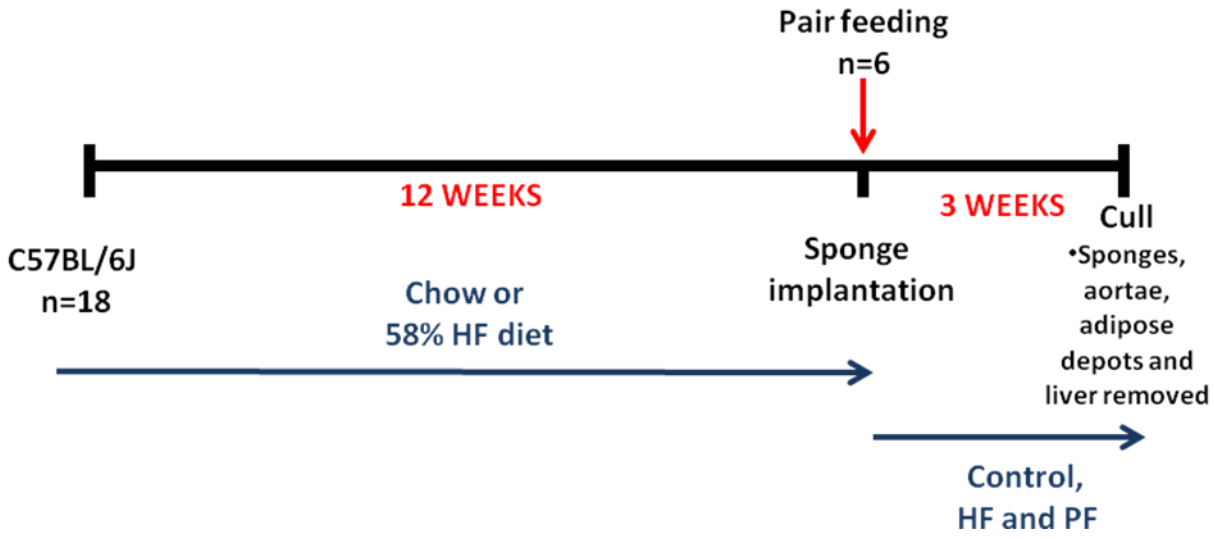

Diagram 6.1: Timeline for pair feeding experiment. C57BL/6J mice were fed a control or high-fat diet for 12 weeks (n=6/group). After this time, sponges were implanted and pair-feeding (PF) commenced. Control, high-fat fed and pair fed mice continued respective diets for a further 3 weeks were they were killed and sponges, aortae, adipose depots and livers were removed. HF; high fat.

6.4 Results

6.4.1 Diet manipulation through pair feeding

Six week, C57BL/6J mice were exposed to high fat (58 % kcal (n=12)) diet or control chow (11 % kcal; n=6) *ad-libitum* for twelve weeks (see section 2.1.4). Food intake was measured weekly and converted into kilocalories by calculating kcal to gram ratio, whereby grams eaten were multiplied by these given numbers: High fat 58 %= 5.56 and Chow 11 %= 4.07 (Figure 6.1 A). As expected, the weekly calorie intake of mice on the high fat diet (141.1 ± 3.7 kcal), was higher than the weekly calorie intake of chow-fed controls (109.20 ± 4.85 kcal) throughout the study period ($p<0.001$). No differences in absolute (grams) food consumption was observed between chow or high fat diets ($p>0.05$; data not shown). Thus, the increase in body weight shown in high fat fed animals was due to an increase in calorie content, rather than an in weight of food. The average weekly control diet intake was then applied as the calorie intake for the pair-fed group by adjusting the amount of high fat 58 % diet (corrected beginning weeks 12-15) after adjusting for body weight.

6.4.2 High fat feeding-induced weight gain is corrected by 3 weeks of pair feeding

The body weight of mice on each diet was monitored during a 15 week period (Figure 6.1 B). At the beginning of the study the mice assigned the control diet had a mass of 20.2 ± 0.4 g and the high fat group 19.7 ± 0.8 g and a significant increase in body weight in the high fat fed mice was observed at week 6 ($p<0.05$). High fat feeding continued to increase body weight compared to chow fed controls until week 12, when the pair feeding intervention began. Mice that were pair fed showed a rapid decrease in body weight, which continued until the end of the three week intervention period; 29.4 ± 2.8 g compared to ad libitum high fat fed animals; 46.1 ± 1.7 g ($p<0.001$). Indeed, the final weights of the calorie controlled group were comparable to the control fed group, 31.7 ± 1.7 g, by three weeks post pair-feeding.

6.4.3 High fat feeding-induced increases in organ weight are corrected by 3 weeks of pair feeding

High fat feeding increased all adipose depot weights compared to chow-fed controls (Figures 6.2 A, B & C). Three weeks of pair-feeding corrected all adipose depot weights examined to a comparable mass as that found in the chow-fed controls. Similarly, liver weights increased with high fat feeding (3.68 ± 0.09 g) over the fifteen week period whereas pair-feeding corrected this (1.35 ± 0.12 g) to chow-fed control levels (1.45 ± 0.11 g) (Figure 6.2 D).

6.4.4 High fat feeding-induced increases in adipocyte size is corrected by 3 weeks of pair feeding

Histological examination by haematoxylin and eosin staining of adipocytes in epididymal tissue was used to assess the effects of high fat and pair-feeding upon adipocyte size. The epididymal adipose tissue was used as an easily accessible and easily processed and quantified depot whereas the subcutaneous adipose tissue was used for molecular investigations including real-time PCR to maintain consistency with earlier studies such as F and L microarray (Chapter 3). Adipocytes were examined under a light microscope (Karl Zeiss Axissop) at x10 magnification, traced manually and analysed with MCID software to calculate total adipocyte area (see section 2.6.3). High fat feeding increased adipocyte size (17.11 ± 0.14 μm^2) compared to chow-fed controls (8.57± 0.59 μm^2, $p<0.001$). 3 week pair-feeding resulted in a decrease in epididymal adipocyte size (11.75 ± 0.61 μm^2; $p<0.001$), however adipocyte size remained significantly larger than the control mice (Figures 6.3 A &D, $p<0.01$). Histological examination revealed a structural impact of pair feeding-induced weight loss on the adipocytes with clear distortion of the cell membranes.

6.4.1 High fat feeding increased body weight whilst 3 week pair-feeding corrected body to control levels

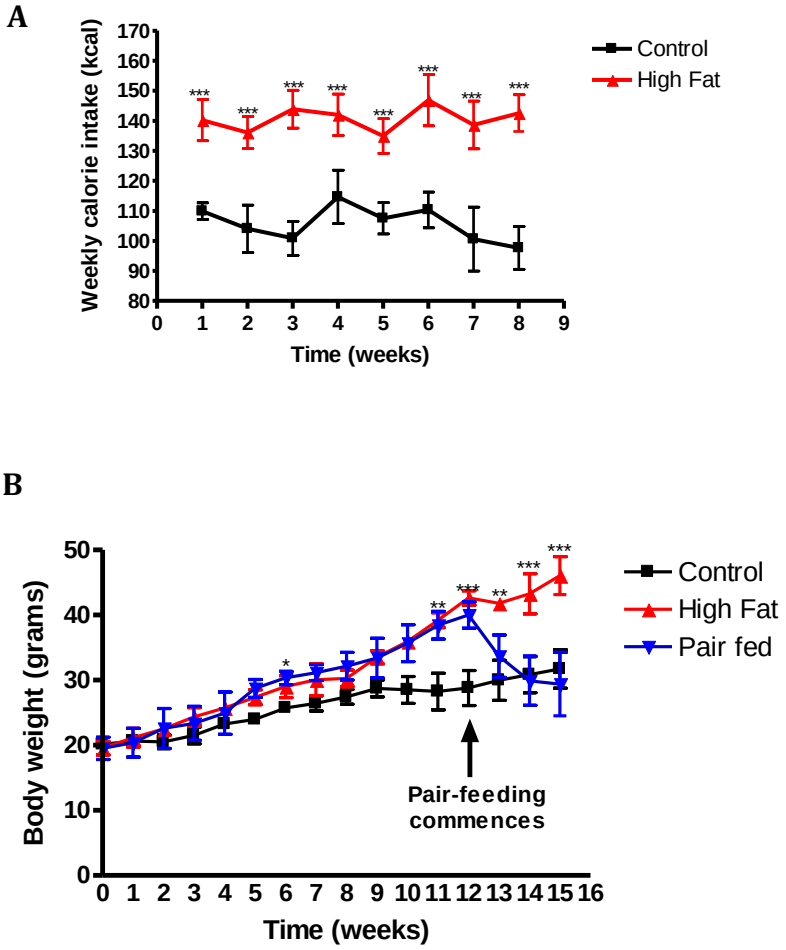

Figure 6.1: Longitudinal body weight measurements of mice placed on control diet, high fat diet and high fat with pair-feeding. A: Calorie consumption expressed as kilocalories (kcal) per week over an 8 week observation period from 6 week old C57BL/6J mice, which was used to calculate pair-fed caloric intake. **B:** Longitudinal body weight between control and pair fed groups. Pair-feeding was initiated after 12 weeks of high fat diet. Data are expressed as means ± SEM; n=6 for control; n=6 for high fat and n=6 calorie controlled. Data analysed by one way ANOVA and repeated measure ANOVA; Bonferroni Multiple comparison post hoc test; *p<0.05; ** p<0.01; ***p<0.001.

6.4.2 High fat feeding-induced increases in adipose depot and liver weights are corrected by pair feeding

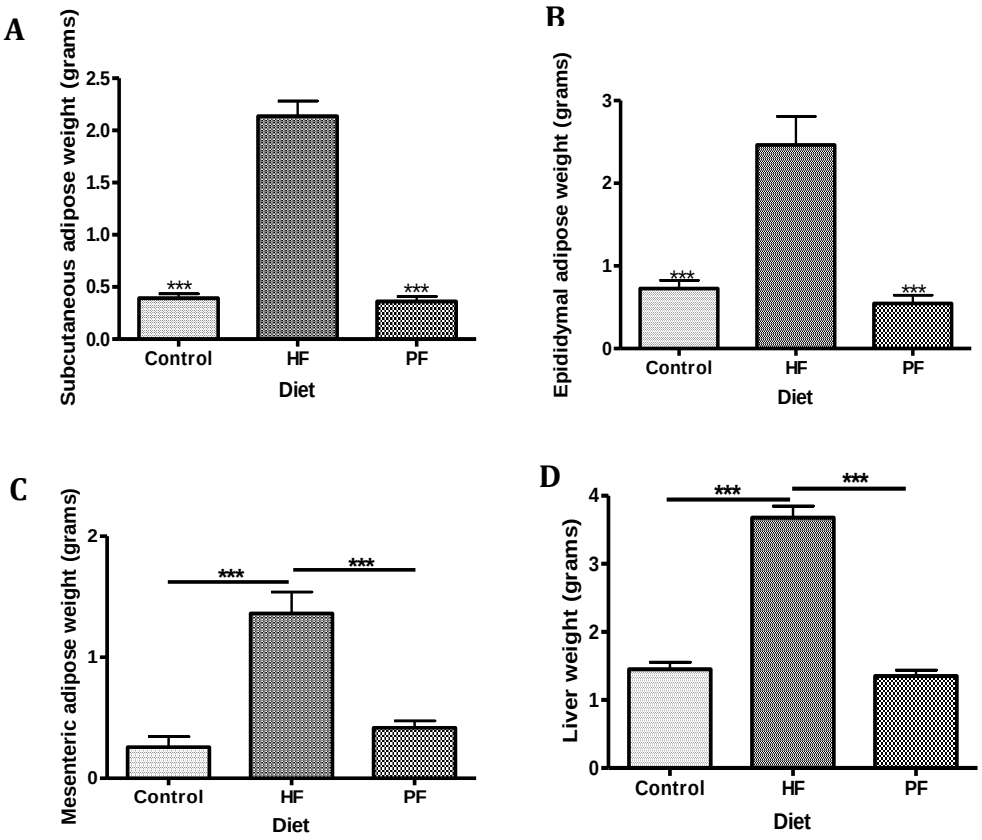

Figure 6.2: Tissue weights in control, high fat fed and pair fed mice. Weights of subcutaneous adipose (A), epididymal adipose (B), mesenteric adipose (C) and livers (D). Data are expressed as means ± SEM; n=6 for all groups. Data analysed by one way ANOVA followed by Bonferroni corrections; ***p<0.001. HF; high fat; PF; pair feeding.

6.4.4 Adipocyte size was increased with high fat feeding but only partially corrected with pair feeding

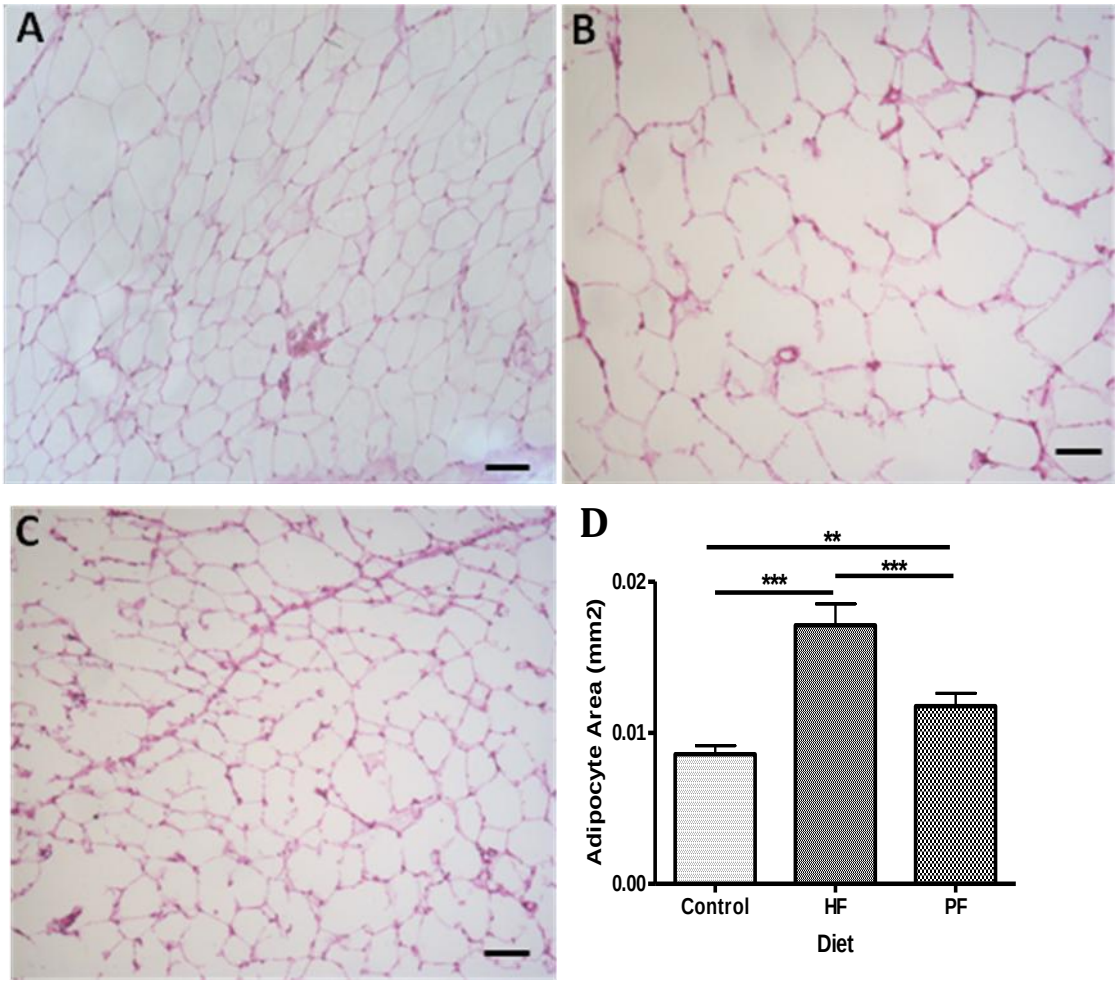

Figure 6.3: Epididymal adipocyte size from control, high fat and pair fed. Photomicrographs of H&E stained adipocytes (x10 magnification) from control (**A**), high fat (**B**) and pair-fed (**C**) mice. Quantification of adipocyte size (**D**). Scale bar represents 10 μm. Data are expressed as means ± SEM; n=6 for all groups. Data analysed by one way ANOVA followed by Bonferroni corrections; *p<0.05; ***p<0.001. HF; high fat; PF; pair feeding.

6.5 The effects of high fat feeding and pair-feeding mediated weight correction on aortic ring and subcutaneous sponge angiogenesis

To assess whether pair feeding would alter angiogenesis, both the aortic ring assay and the sponge implantation assay were employed. At the end of the study period (15 weeks) aortas were removed, cut into rings and cultured for 10 days. In addition sponges were excised and processed for histological examination (see section 2.3.1 and 2.4.1).

6.5.1 High fat and pair-feeding does not affect TLS formation *in vitro*

Tube-like structures (TLS) could be detected after two days in aortic rings from control, high fat fed and pair-fed mice. Throughout the study period, there was no effect of high fat or pair feeding upon TLS formation in aortas (Figure 6.5).

6.5.2 Pair feeding after high fat diet increases sponge vascularisation

The sponge implantation assay (see Materials and Methods 2.4.1) was used to assess the effects of pair feeding on angiogenesis *in vivo.* Vascularity tended to increase in the high fat fed group, as seen before (Chapter 3), however, this did not reach significance ($p=0.08$) (Figure 4.6). However, there was a significant increase in vessel infiltration into the sponges when the mice were pair fed high fat diet for three weeks ($p=0.02$) (Figure 4.6).

6.5.1 High fat feed and high fat, pair feeding does not affect aortic TLS formation *in vitro*

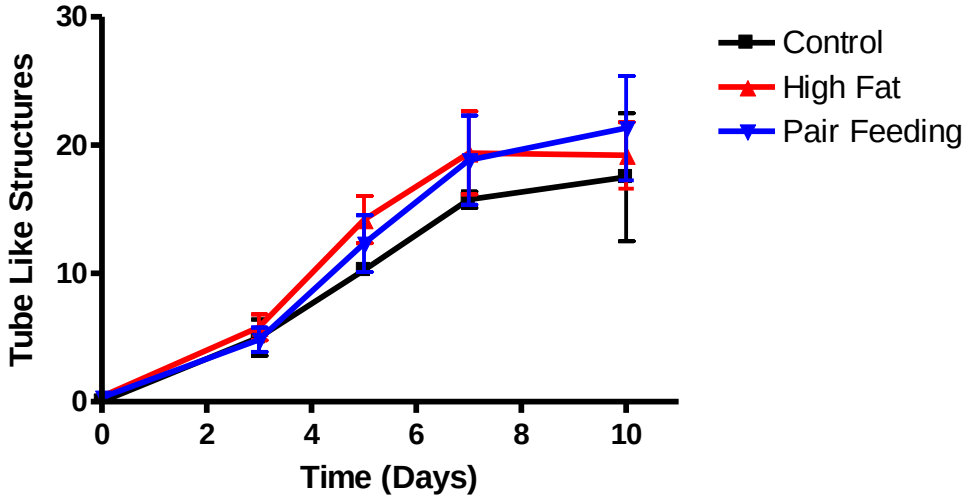

Figure 6.4: Tube like structure formation (TLS) in aortas from control, high fat fed and pair fed mice. TLS formation was assessed by manual counting under light microscopy. New vessel formation was noted after the first 2 days in culture, and grew for the next 8 days in all treatment groups. Data are expressed as means ± SEM; n=6 for all groups. Data analysed by two way ANOVA followed by Bonferroni corrections.

6.5.2 Pair feeding significantly accentuates sponge vascularity

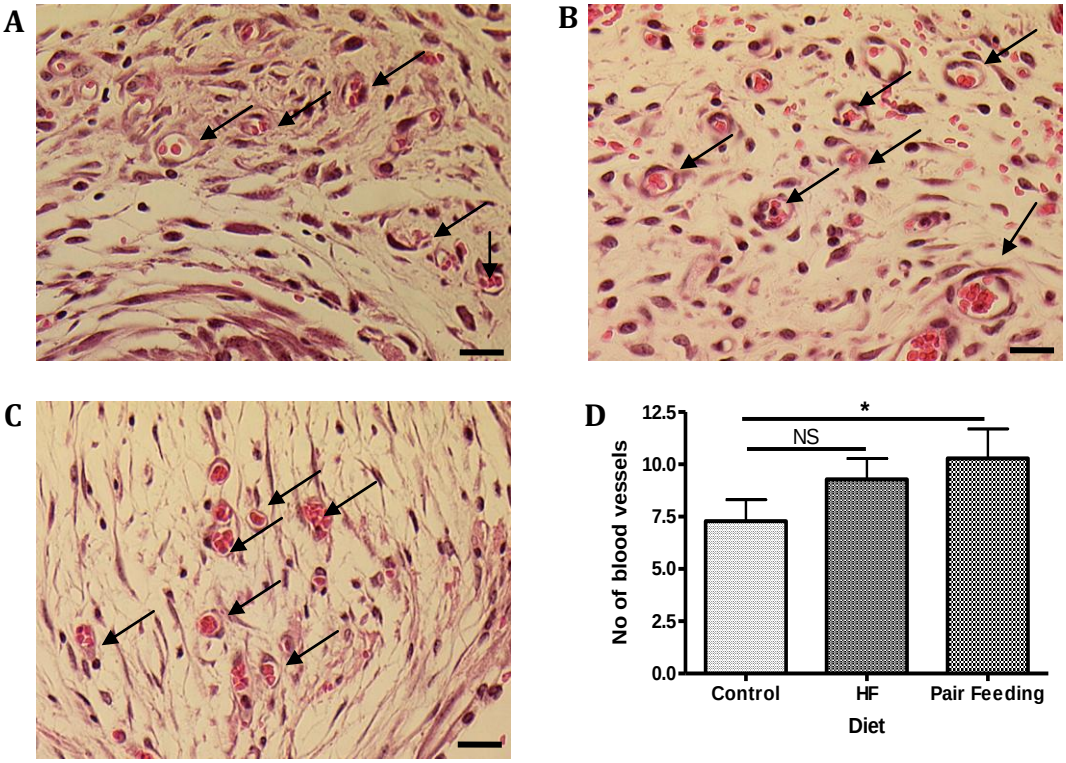

Figure 6.6: Vessel density of sponges excised 21 days after implantation from control, high fat fed and pair fed mice. Photomicrographs (x40 magnification) of H&E stained sponges from control (**A**), high fat (**B**) and pair-fed (**C**) mice. Sponge vascularity was assessed by Chalkley counting. Blood vessels were identified morphologically, with or without erythrocytes present in the lumen. Data are expressed as means ± SEM; n=6 for all groups. Data analysed by one way ANOVA followed by Bonferroni corrections; *p<0.05; NS, non-significant. Scale bar represents 10 μm. Arrows indicate blood vessels.

6.6 Effect of high fat and pair-feeding on the angiomodulatory TSP-1 levels

Both experiments described below were undertaken in order to ascertain whether pair feeding would alter the expression of the angiomodulatory marker TSP-1. A human TSP-1 ELISA was used as there was no commercially available mouse TSP-1 ELISA.

6.6.1 Human TSP1 ELISA does not cross-react with mouse TSP-1

Human TSP-1 was detected at concentrations of 869.8 ± 23.2 pg/ml from neat human plasma (n=2). Unfortunately, in neat mouse plasma (n=2) TSP-1 was not detected using the human TSP-1 ELISA despite the antigen's stated 97 % homology (Figure 6.7).

6.6.2 Pair feeding decreases TSP-1 expression in subcutaneous adipose tissue

As circulating TSP-1 was undetectable, local adipose TSP-1 gene expression (mRNA level) was investigated. RNA was extracted from subcutaneous adipose of control, high fat and pair-fed animals. The subcutaneous depot was chosen to remain consistent with the depot in which elevated TSP-1 mRNA levels had been found in obese models (see Chapter 3). Using quantitative real-time PCR (see section 2.2.1), subcutaneous adipose cDNA was analysed for TSP-1 expression. Although not significant in this cohort, TSP-1 levels showed a tendency to increase ($p=0.0754$) in agreement with the significantly increased expression we observed after 18 weeks of high fat diet (see Chapter 3). Intriguingly, pair-feeding caused a significant reduction in TSP-1 expression in subcutaneous adipose ($p<0.05$) (Figure 6.8).

6.6.1 HumanTSP-1 ELISA does not cross-react/detect murine TSP-1

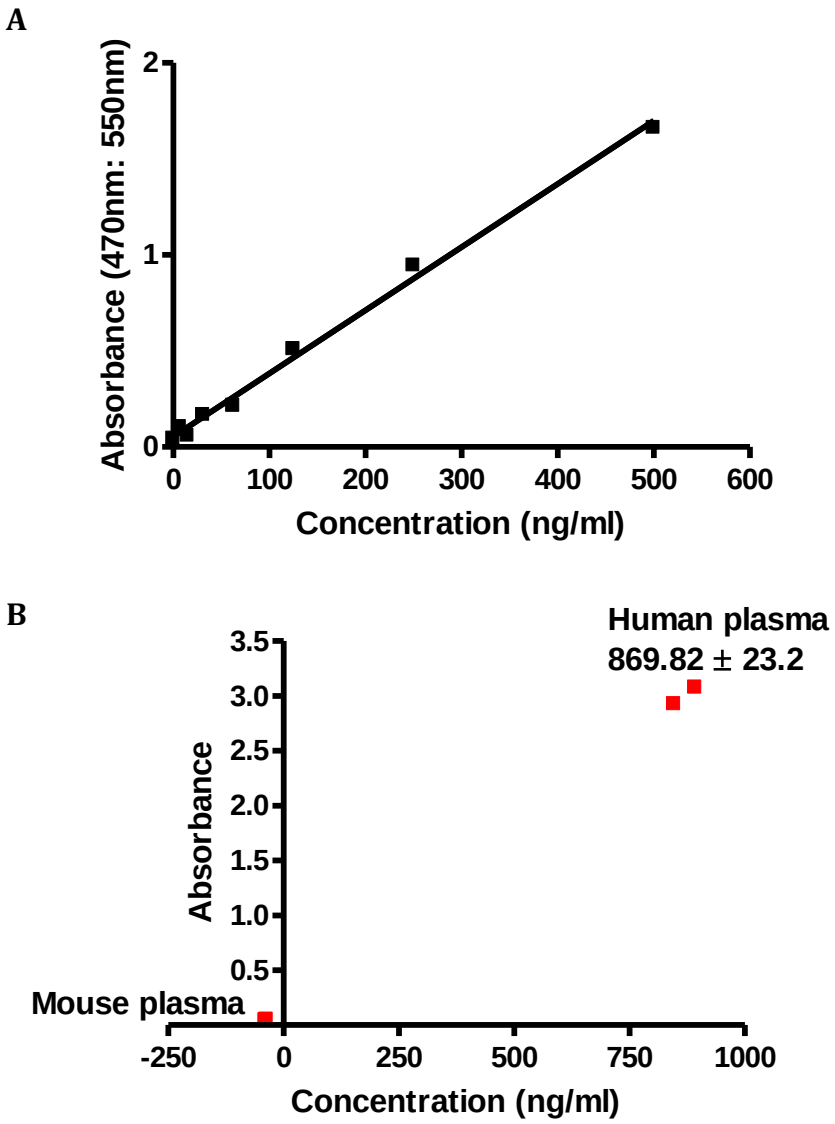

Figure 6.7: Human TSP-1 ELISA performed with human and mouse plasma. Neat human and mouse plasma were analysed by linear regression (**A**). Neat mouse and human plasma were measured on human TSP-1 ELISA (**B**). n=2 for both human and mouse samples; C57BL/6J, 10 week old mice.

6.6.2 Thrombospondin-1 (TSP-1) expression was corrected in subcutaneous adipose tissue of pair fed mice

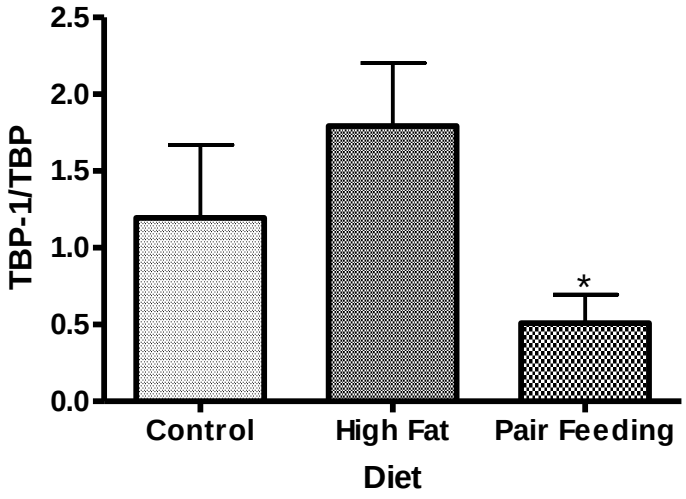

Figure 6.8: Expression of thrombospondin-1 (TSP-1) in subcutaneous adipose of control, high fat and pair fed animals. Real time quantification of TSP-1 mRNA levels of subcutaneous adipose of control, high fat fed and pair fed mice. Data are expressed as means ± SEM; n=6 for all groups. Data analysed by one way ANOVA followed by Bonferroni corrections; *p<0.05.

6.7 Discussion

The work described in this chapter examined the hypothesis that diet-induced obesity with subsequent pair feeding induced weight correction and decrease angiogenesis. Pair feeding did correct body weight yet, contrary to the original hypothesis, appeared to increase the angiogenic drive, in conjunction with reduced adipose TSP-1.

6.7.1 Pair feeding reversed weight gain, with increased sponge angiogenesis

Weight reduction through dietary control may reduce angiogenesis (Weindruch *et al.,* 1988; Hursting *et al.,* 2003; Kritchevsky 2003). Caloric restriction reduces circulating levels of certain pro-angiogenic factors (Mukherjee *et al.,* 2004); however, specific effects within adipose tissue and the effect upon adipose angiogenesis have yet to be elucidated.

We have shown that diet-induced obesity increased weight gain from after 9 weeks of high fat feeding. A subsequent three weeks of pair feeding then completely reversed the gross obesity phenotype and this was associated with decreased fat depot and organ weight, as expected. Notably, adipocyte size was partially corrected, suggesting that previous hypertrophic adipocytes may retain their hypertrophied phenotype and this may be more susceptible to future increases in lipid accumulation. Unexpected was the lack of effect of either prolonged high fat feeding or pair-feeding-induced weight correction on aortic angiogenesis *in vitro*. These results were unanticipated given the findings of previous chapters whereby obesity suppressed aortic growth (Chapter 3). Vascularity, as determined *in vivo* by implantation of sponges throughout the pair-fed dietary intervention (3 weeks), revealed a statistically significant increase in vessel density compared to chow fed controls (high fat feeding did not increase sponge vascularity as would be expected from previous work from Chapter 3 which may be due to a study, statistical power issue (n=6). These intriguing results with pair-feeding contrast with previous studies that demonstrated caloric restriction causes inhibition of angiogenesis-induced

tumour development (Hursting *et al.,* 2007; Colman *et al.,* 2009). Although a caloric restriction experiment was not conducted, pair-feeding could still be classified as a relatively similar intervention and thus may be predicted to be anti-angiogenic in its effect. Interestingly, increased vascularity in the sponges was accompanied by a decrease in TSP-1 expression in subcutaneous adipose with pair feeding, which, based on the angiostatic effects of TSP-1 on endothelial cells (Good *et al.,* 1990; Iruela-Arispe *et al.,* 1991; Volpert *et al.,* 1995), is consistent with the increased vascularity observed in the sponges. This might have also been predicted given the increase in TSP-1 expression demonstrated with obesity (Chapter 3).

The correlation between adipose TSP-1 expression and the effects observed must be approached with caution as it was not possible to measure circulating TSP-1 using the only available ELISA. Rather, decreased expression of antiangiogenic TSP-1 in pair feeding may decrease vessel regression and apoptosis. This implies that by restricting a high fat diet to the calorie intake level associated with normal growth (control diet ad libitum fed), the vasculature is not diminished but enhanced *in vivo*. Thus, applying a crash-course diet approach after a period of chronic over feeding may leave the tissue more susceptible to exaggerated (rebound) fat expansion upon subsequent exposure to obesogenic conditions. This has intriguing implications for the common practice of crash-dieting – and suggests that targeting the adipose vasculature at this critical stage could be additionally beneficial to prevent rebound weight gain. The time constraints of this thesis did not allow this to be examined further.

The reversal of weight gain observed with pair feeding with associated maintenance of sponge angiogenesis gives further insight. This indicates that the increased angiogenesis exhibited by high fat feeding (Chapter 3) is caused by the constituents of the high fat diet, independent of the calorie content. As there is very limited work regarding lipids and their affect upon angiogenesis in the literature, this remains only speculative. However, cytoplamsic lipid droplet accumulation occurs in cancer tissues (Borradaile *et al.,* 2006) and suggests

ectopic lipid accumulation may be a pro-angiogenic stimulus. Therefore the partially reduced adipocyte volume caused by pair feeding could still be indicative of a pro-angiogenic environment causing an increase in angiogenesis, as observed in the sponges.

Pair-feeding resulted in complete correction of adipose depot mass to that of control mice. However, there was only a partial reduction in adipocyte size. This may be important in the regain of weight witnessed in humans, as larger adipocytes would mean increased lipid re-uptake in the face of caloric excess. It was also apparent from histology that there was a structural impact of the rapid obese-to-non-obese transition, for example, distorted cell membranes. A recent study using caloric restriction demonstrated increased inflammation and apoptosis in mice (Patel *et al.,* 2010). This is consistent with an altered morphology caused by adipose tissue macrophages driving matrix remodelling, not only with adipocyte enlargement and adipose tissue expansion in obesity (Huber *et al.,* 2006), but in shrinking adipose tissue of the pair fed mice. Thus recruited macrophages may infiltrate the adipose during high fat feeding and reside there to combat apoptosis, if any, associated with pair-feeding. Additional examination with immunohistochemistry could be performed, including immunohistochemistry techniques using the specific macrophage marker F4/80 (Weisberg *et al.,* 2003).

A maintained vessel structure and anti-angiogenic environment with regard to TSP-1, with profound and rapid weight loss, may create a subsequently more efficient context for adipose expansion. Indeed, this notion is supported in humans whereby reducing weight by caloric restriction generally fails as most obese patients regain most of their weight thereafter – the so called rebound effect (Wadden 1993). Thus, future studies would examine local tissue and circulating levels of other angiomodulatory factors by using a general angiogenesis microarray and investigate whether a decrease in angiogenesis inhibitors was associated with pair-feeding.

6.7.2 Study Limitations

As described, measurement of circulating levels of TSP-1 was attempted using a human TSP-1 ELISA. Human TSP-1 shows a 97% homology with mouse TSP-1 (Armstrong and Bornstein 2003) suggesting that such close homology may allow the detection of mouse TSP-1 levels in plasma. Therefore, neat mouse plasma was used in order to examine TSP-1 levels. Unfortunately, this was either below the detection levels of the assay or undetectable by human TSP-1 antibodies. As this kit has not been used to measure mouse TSP-1 previously, further studies may examine other circulating angiogenic factors within the plasma, as changes in angiogenesis within the adipose may not be reflected by changes in circulating levels. These might include pro-angiogenic vascular endothelial growth (VEGF) and hepatocyte growth factor (HGF) or other anti-angiogenic factors including endostatin and interleukin-12. Measurement of TSP-1 mRNA and/or protein level in the sponge would also help link differences in TSP-1 expression in the sponge and the adipose to related angiogenic effects.

Previous methods for assessing vessel development in adipose have proven to be problematic in the context of this thesis. Therefore other means of assessing angiogenesis may be employed in order to assess blood vessel infiltration in pair fed animals. This may include a recently described immunohistological method, which allows the successful detection of both microvessels and adipocytes *in situ* (Xue *et al.,* 2010). Other means of measuring angiogenesis will be addressed in Chapter 8.

As highlighted previously, adipocyte size was not corrected fully with pair feeding. This raises questions regarding the metabolic phenotype of the pair fed mice, as prior to the caloric intervention they were obese. Thus further experimentation would test glucose tolerance and measurements of basal metabolic rates to investigate whether pair feeding altered metabolic parameters and glucose homeostasis.

6.7.3 Concluding Remarks

The present study does not provide evidence to support the initial hypothesis, that high fat feeding increased angiogenesis and pair feeding with high fat food to caloric content control diet reversed the angiogenic process. Unexpectedly, weight loss with pair feeding after initial obesity did not decrease angiogenesis. Indeed there is evidence for increased vascularity and decreased adipose expression of the anti-angiogenic factor TSP-1. Therefore, there is increased angiogenic potential with rapid weight loss after obesity. Maintained angiogenic potential (low TSP-1) and vascular architecture (sponge) with rapid weight loss may indicate a mechanistic adipose-mediated basis for rebound fat mass gain after dieting. We also describe the first, dynamic responsive regulation of adipose TSP-1.

Chapter 7

Conclusions and future aims

7.1 Experimental hypothesis and aims readdressed

The hypothesis addressed in this thesis was that obesity compromises the angiogenic potential of adipose, causing a detrimental metabolic phenotype. The work described in this thesis was designed to examine the effects of obesity on angiogenesis *in vivo* and *in vitro*. To address these aims initially, obese mouse models (both genetic and dietary) were investigated.

A consistent alteration in angiogenesis was observed, which demonstrated a novel anti-angiogenic protein, thrombospondin-1 (TSP-1), was elevated in adipose tissue in obese states. Direct effects upon adipose function were observed with an analogue of TSP-1 (ABT-510). However, this relationship between TSP-1 and obesity was more complex than originally thought, as predicted weight gain with ABT-510 administration was not witnessed.

7.1.1 Obesity affects angiogenesis differently when using different angiogenic assays

The original question driving this thesis was to investigate whether angiogenesis was affected by obesity. To answer this, both *in vitro* and *in vivo* assays were employed.

The aortic ring assay is an excellent method for evaluating the angiogenic process in an *in vitro* environment. In this assay, rings of mouse aorta are embedded in Matrigel, which then generate an angiogenic response that can be modulated with pharmacological, and/or genetic manipulation. The angiogenic process is triggered by the dissection procedure and is mediated by endogenous factors produced within the aorta (Go and Owen 2003). The use of these intact aortic explants has the advantage of including surrounding non endothelial cells (such as smooth muscle cells and pericytes) and also a supporting matrix (Staton *et al.,* 2004), an environment similar to that *in vivo*. In addition, the endothelial cells in the aortic ring are not proliferating when removed from the mouse (as they are already fully grown), which is advantageous as this mirrors a more realistic *in vivo* situation. Thus when angiogenesis is triggered, quiescent

endothelial cells respond by becoming proliferative (then migrate from existing vessels and differentiate into tubules) (Griffioen 2000).

This thesis has shown that in all obese models investigated (e.g. Fat mice, $Lep^{Ob/Ob}$ and three month high-fat fed mice), there was a diminished angiogenic response observed from aortas. This implies that obesity affects tube formation directly in the aorta. This intrinsic ability of obesity to affect vascular formation was strengthened by the observation that the polygenic model of leanness (Lean mice), did not affect aortic angiogenesis. Further examination into the angiogenic potential of Lean mice would have been desirable, however, due to breeding constraints, this was not possible.

Decreased angiogeneic responses in obesity are known; obese mice have lower capillary density (capillary drop out), decreased adipose expression of vascular endothelial growth factor (VEGF) and finally, obese adipose tissue is hypoxic (Ye *et al.,* 2007; Pasarica *et al.,* 2008). Interestingly, decreased aortic angiogenesis has also been observed the $Lep^{ob/ob}$ mouse (Gealekman *et al.,* 2008), confirming that obesity directly suppresses the ability of endothelial cells of the aorta to form tubes.

The examination of aortic ring angiogenesis has proven reliable and informative, however effects of obesity on angiogenesis *in vivo* would provide additional insight. Vessels within adipose tissue are exposed to a vast array of adipokines released by the adipocytes and also have many paracrine interactions between different cell types. This is absent in the aortic ring assay and, more importantly, adipocytes themselves are also not present. Furthermore, angiogenesis is normally a microvascular event, and thus the use of large aortic vessels does not precisely replicate the *in vivo* environment (Auerbach *et al.,* 2000). The removal of microvascular vessels is an extremely intricate procedure due to their small size and removal can result in damaged endothelium and disabled growth. For this reason, the aorta is technically

advantageous in this setting to ensure accurate examination of the angiogenic response.

Therefore, the use of an *in vivo* model, involving the subcutaneous implantation of sponges was used as a means of assessing angiogenesis in obese models. This model is another excellent means of quantifying angiogenesis as the subcutaneous insertion of polyethurane sponges elicits an angiogenic response, causing the formation and infiltration of blood vessels into the sponge, which can be analysed and quantified. This assay was chosen as it offers several advantages to the examination of angiogenesis in adipose, including implantation allowed close proximity with the subcutaneous adipose depot and therefore, exposure to adipocytes themselves. Similarly, the *in vivo* environment permitted the newly formed blood vessels to be exposed to a variety of other cell types as well as adipocytes, which may affect growth. It is not surprising that when all of these factors are present in an *in vivo* environment, that increased angiogenesis was observed in obese models (e.g. Fat mice). If reflective of events in adipose tissue, this would implicate that as the adipose depot increases in size, there is an associated increase in angiogenesis to supplement the growing metabolic demand of the adipose. Increased sponge angiogenesis also supports evidence suggesting an increase in pro-angiogenic factors in obesity. Hepatocyte growth factor (HGF) was elevated in the adipose of obese humans (Rehman *et al.,* 2003) and circulating VEGF concentrations correlated with body mass index (BMI) and visceral fat mass in obese humans (Miyazawa-Hoshimoto *et al.,* 2003).

However, this was not a simple linear relationship between increased adiposity and associated increased angiogenesis *in vivo*. Experiments were designed to directly manipulate adipose deposition to monitor the effects upon angiogenesis. Obese animals were pair-fed to decrease their body weight and the effects of the associated angiogenesis. Unexpectedly, pair-fed mice exhibited increased angiogenesis in implanted sponges.

Thus, a direct comparison between adipose angiogenesis and an *in vivo* sponge model of angiogenesis is not possible but provided invaluable clues. As stated, the sponge is implanted subcutaneously into the mouse, yet not directly into the subcutaneous adipose. Also, sponge implantation causes a non-specific immune response that may lead to an angiogenic response (Dellian *et al.,* 1996) and may account for the divergence in the angiogenic response observed.

7.1.2 Elevated TSP-1 in obesity may have detrimental effects on adipocytes

Both the *in vitro* and *in vivo* models for assessing angiogenesis were vital in confirming angiogenesis was indeed altered in obesity. To answer whether specific angiomodualtory changes were occurring in the adipose itself, an exon microarray was conducted on the subcutaneous adipose of a polygenic model of obesity (Fat mice) and Leanness (Lean mice), that had been chow or high fat fed. This demonstrated several pro- and anti-angiogenic factors to be significantly altered in obese adipose. Many of the factors that were differentially expressed had been previously reported to be affected by obesity (Bussolino *et al.,* 1992; Koblizek *et al.,* 1998; Pang *et al.,* 2008; Jung *et al.,* 2009). TSP-1 emerged as a novel anti-angiogenic factor that was elevated in Fat mice and also in genetic and diet-induced obesity. Pair feeding induced decreased TSP-1 expression in subcutaneous fat, which might have been anticipated as it was opposite to the obese models. However, we provide the first evidence for a dynamic role of TSP-1 in adipose tissue mass regulation.

Although novel at the time of investigation, it was reassuring when subsequent literature revealed a similar increase in TSP-1 expression in human obesity (Varma *et al.,* 2008). This confirmed TSP-1, an anti-angiogenic factor, as a potential obesity-related gene. However, the role of increased TSP-1 in obesity had not been explained. There were clues into the role of angiogenic factors in obesity with the use of antiangiogenic agents (for example TNP-470, a commonly used antiangiogenic factor, which caused a reduction in fat deposition, even when obesity had been established (Rupnick *et al.,* 2002). As TSP-1 had been reported to have both pro- and anti-angiogenic effects (Iruela-

Arispe *et al.,* 1991; DiPetro *et al.,* 1994; Agah *et al.,* 2002), it seemed valid to specifically scrutinise the specific antiangiogenic TSP-1 region, in line with evidence surrounding anti-angiogenic agents and obesity.

TSP-1 is a very large protein (450 kDa). To focus our studies as outlined above, the Type I repeat sequence was employed. The specific anti-angiogenic activity of TSP-1 had been mapped directly to this sequence, which was confirmed with studies examining endothelial cells (Jimenez *et al.,* 2000; Quesada *et al.,* 2005). The effect of ABT-510 upon adipocyte function had not been investigated, which was important as it had been revealed as it a potential obesity gene (in obesity QTL). ABT-510 caused inhibition of stimulated lipolysis and increased fatty acid uptake at high concentrations in mouse adipocytes. Lower concentrations decreased fatty acid uptake, suggesting that the effect of ABT-510 upon adipocytes is concentration-dependent. Therefore, it was concluded that increased TSP-1 levels observed in obesity could potentially facilitate a worsening of the metabolic state of the adipose, overcoming a beneficial constraint to adipose tissue driven by angiostatic effects by directly promoting adipocyte hypertrophy.

It was then hypothesied that, in contrast to other anti-angiogenic agents, administration of high doses of ABT-510 *in vivo* would inhibit β-stimulated lipolysis and thus cause an increase weight gain. However, this was not the case, as the hypothesised increase in body weight did not occur. The lack of such an effect *in vivo* may be attributed to the adrenergic system. β-Adrenoceptor (β-AR) stimulation causes the induction of lipolysis (see Introduction section 1.2.2). However, the adrenergic system is known to be suppressed in obesity (Arner 1996). Therefore, the inhibition of this β_3-AR-stimulated lipolysis by ABT-510, may be attenuated in our obese models and no longer be mechanistically predominant. The definite models to address this effect of ABT-510 upon adipocytes would be transgenic mouse models including; CD36 receptor knockout mouse, to clarify the role of this receptor and ABT-510 function on adipocytes, and a TSP-1 knockout mouse, to examine β-adrenergic signalling.

Angiogenesis is associated with sympathetic stimulation, as activation of β-AR increases tumour vascularisation, whereas β-AR blockers reduce vessel density (Thaker *et al.,* 2006; Lee *et al.,* 2009). However, as with the down-regulation of β-AR activation in obesity, there may be a silencing of β-adrenergic signalling in cancer, particularly prostate cancer (Yu *et al.,* 2007). Mechanistic similarities exist between cancer and obesity-associated angiogenesis that are informative to compare. For example, angiogenic factors are elevated in both cancer and obesity whilst adrenergic signalling is down-regulated in cancer and obesity (Arner 1996).

Although there was a reduction in body weight of mice administered low dose ABT-510 fed a high fat diet, the elevated circulating non-esterified fatty acids (NEFAs) were surprising. Decreasing adipose weights may be indicative that excess lipid, associated with high calorie intake of high fat food, was not being deposited appropriately. The increase in liver weight strengthens this case. When lipids are not stored safely within the adipose, they are redirected towards other organs, such as the liver, and muscle (as well as heart and pancreas) (Sethi and Vidal-Puig 2007). These tissues are not designed to store large amounts of lipid and are more susceptible to the toxic effects of excess fat accumulation (lipotoxcity). Increased circulating NEFAs reduce insulin sensitivity and insulin-stimulated glucose uptake in adipose and muscle, which increases plasma glucose (Shulman 2000). Raised fasting glucose concentrations were witnessed in low dose ABT-510 treated mice. This lipid overload to the liver, with excess influx of NEFA, produces a fatty liver and modifies various pathways of hepatic metabolism of glucose and lipids. Further examination of fat deposition by histological staining (e.g. Oil red O) within the liver would help answer the question of detrimental lipid deposition.

The inhibition of β-stimulated lipolysis by ABT-510 was of a similar magnitude to that observed with insulin. Therefore, it was plausible that ABT-510 was acting through similar pathways associated with insulin action. These included

the p38 mitogen-activated protein kinases (MAPK) and the phosphatidylinositol 3-kinases (PI3K), which were investigated using pharmacological inhibitors. Stimulation of p38 by anisomyocin reversed the anti-lipolytic effect of ABT-510 (yet inhibition did not reverse the effect). Thus, several downstream targets of p38 should be investigated to be confident this is the pathway mediated ABT-510 action upon adipocytes. These may include peroxisome proliferator activated receptor γ (PPARγ). Firstly, PPARγ expression is highest in adipose (Tontonoz *et al.,* 1994) and plays a key role in mediating both trapping of fatty acids and, consequently, fatty acid uptake through fatty acid transport protein (FTP) and CD36 (Schoonjans *et al.,* 1996; Motojima *et al.,* 1998). As previously described, the action of TSP-1 on endothelial cells is mediated through CD36 (Jimenez *et al.,* 2000; Febbraio *et al.,* 2001) and ABT-510 was postulated to act through this receptor in adipocytes. In addition, ABT-510 induced increased fatty acid uptake *in vitro* and may, therefore act on PPARγ-signalling pathways stimulating an influx of fatty acids through CD36. Moreover, PPARγ suppressed p38 MAPK phosphorylation in T cells and the PPARγ agonist rosiglitazone inhibited both the activity of MAPKs p38 and c-Jun N-terminal kinase (JNK) and NFκB, thereby decreasing the expression of pro-inflammatory genes (Desreumaux *et al.,* 2001; Jones *et al.,* 2003). This inter-linking of pathways is encouraging, as it may help find pathways responsible for the action of ABT-510.

Another downstream target of p38 MAPK is NFκB. NFκB regulates adipogenesis (Hauner 2005), which is an important process in obesity but, more interestingly, NFκB is thought to mediate TNF-α-induced lipolysis (Laurencikiene *et al.,* 2007). This pathway will have to be explored further to assess what contribution, if any it plays in ABT-510's effect upon adipocyte function. The proposed action of ABT-510 upon 3T3L1 adipocytes is summarised in Figure 7.1.

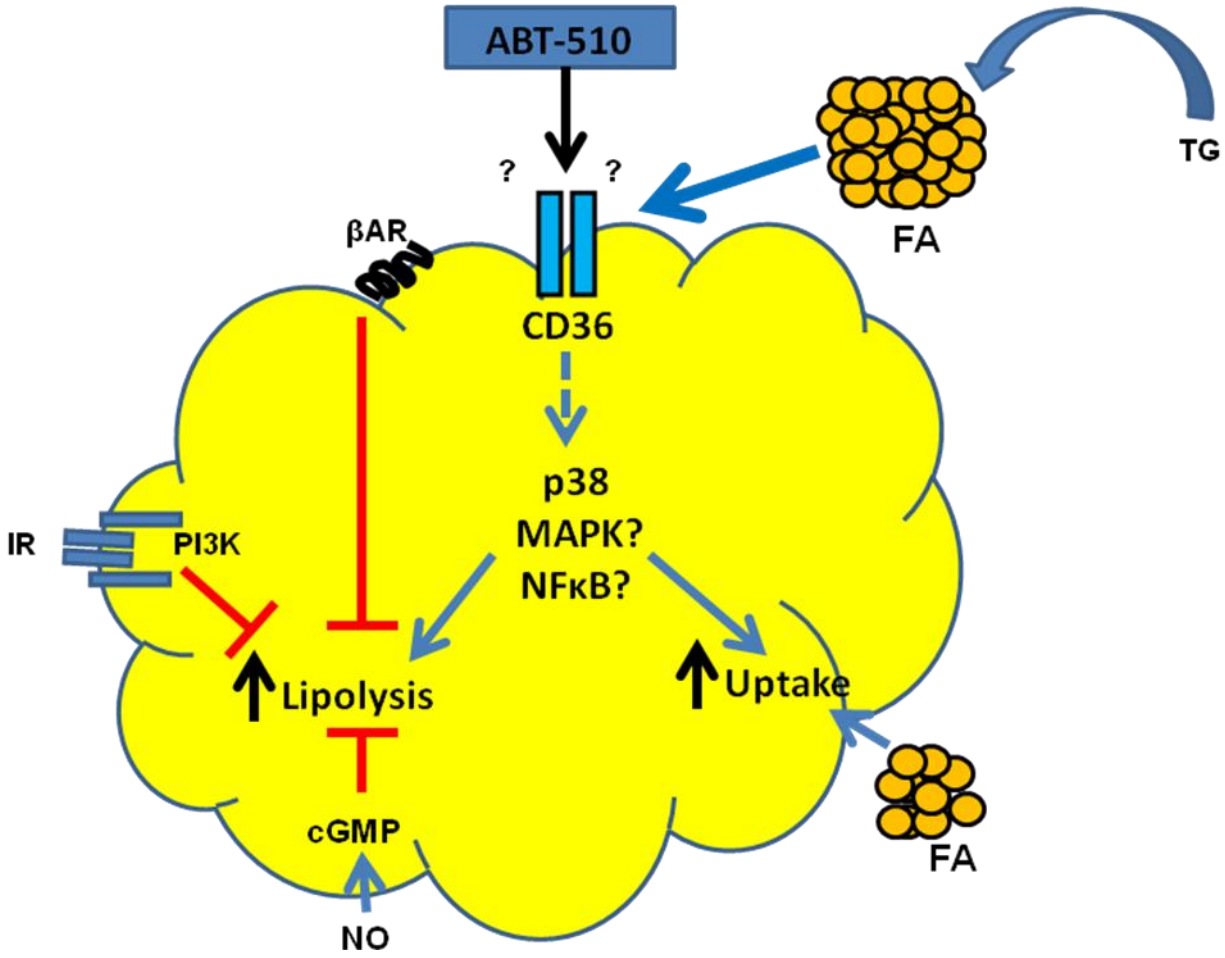

Figure 7.1: Proposed signalling pathways involved in the action of ABT-510 on 3T3L1 adipocytes. ABT-510 is thought to bind to CD36 on adipocytes where it causes i) inhibition of beta (β) adrenoceptor stimulated lipolysis, causing an increase in fatty acid in the adipocyte and ii) an increase in uptake of fatty acids, potentially through CD36, where it also increases fatty acid volume within the adipocyte. This would cause the adipocyte to become more lipid filled and be detrimental to the metabolic state of the adipocyte. β-AR; beta adrenoreceptor; FA; fatty acid; IR; insulin receptor; TG; triglycerides: NO; nitric oxide; cGMP; cyclic guanosine monphosphate. Red lines indicate inhibition; dotted lines, predicted pathway.

7.2 Future work

The research presented in this thesis has identified TSP-1 as an adipokine protein associated with obesity. The specific anti-angiogenic region of TSP-1 has helped identify a novel role for ABT-510 directly upon adipocyte function, whereby it inhibits β-stimulated lipolysis and increases lipid uptake. The complexity of the *in vivo* environment meant this anti-lipolytic role of ABT-510 was not observed.

A case for ABT-510 acting as an anti-lipolytic agent in obesity was not supported by elevated fasting NEFAs *in vivo*. As discussed above, the adrenergic system is down-regulated in obesity (Arner 1996) which may be responsible for this lack of response. Therefore, the next, key experiments would examine the effect of ABT-510 on NEFA production in the circulation of non-obese mice. This would help clarify whether the absence of β-signalling in obesity, masked the effects of ABT-510 *in vivo*.

In addition, methods for measuring the concentration of circulating ABT-510 should be developed. It would be useful to perform mass spectrometry analysis of plasma ABT-510 concentration to confirm the low and high doses administered through mini-pump were in fact achieved *in vivo*. Limitations in the amount of plasma available have hindered this investigation. As the maximum amount of procedures were planned for this experiment, residual plasma obtained from glucose tolerance testing was not sufficient to determine whether circulating ABT-510 can be measured.

Examination of specific apoptotic markers of angiogenesis within the adipose could quantify the angiostatic effect of ABT-510 upon adipose depots directly. Immunohistochemistry using antibodies for established apoptotic markers including caspase 3 and 8 (Singhal *et al.,* 2005) could be used as a surrogate for the action of ABT-510. TUNEL staining could also be used to measure apoptosis as in endothelial cells in tumours (Dings *et al.,* 2003), and thus could be applied to adipose tissue immunohistochemistry. Conversely, as there was no evidence of decreased *in vivo* angiogenesis in sponges, another means of quantifying

cellular proliferation may shed some light upon which way the angiogenic switch lies. Increased apoptosis would be associated with increased proliferation. Furthermore, PCNA and 5-bromo2'-deoxy-uridine (BrdU) staining has had excellent results for highlighting proliferation of endothelial cells in blood vessels present in tumours (Inoue *et al.,* 2003).

Mouse 3T3L1 adipocytes were used to model the mature adipocyte in obesity. However, the use of primary adipocytes from obese models may be useful to examine the role of ABT-510. These adipocytes are exposed to many cell types *in vivo*, including endothelial cells, and may therefore give more insight to the role of TSP-1 in obesity. Primary adipocytes have been successfully cultured from several species, including humans, and have some advantages over cultured cell lines (Hauner *et al.,* 1989; Kirkland *et al.,* 1990; Gregoire *et al.,* 1995). Primary cells are diploid and may, therefore, reflect the *in vivo* situation better than aneuploid cell lines (Gregoire *et al.,* 1998). They may be obtained from various adipose depots and at varying stages of development of obesity (Bjorntorp *et al.,* 1982; Deslex *et al.,* 1987).

7.3 Future aims: methods of improving evaluation of adipose angiogenesis

The need to examine and quantify adipose tissue angiogenesis directly resulted in various attempts to examine blood vessel density. This proved to be very problematic (see Chapter 8; Appendix). In addition to these methods, other *in vivo* models were considered. Established angiogenic assays including the chick choriallantoic membrane (CAM) assay and the corneal angiogenesis assays, were simply in undesirable locations and species when trying to assess adipose angiogenesis (embryo and cornea) and thus ruled out as a means of measuring adipose angiogenesis. The dorsal skinfold window chamber model seemed promising, as such a technique would allow the direct and continuous measurement of angiogenesis within a living animal (Jain 1997). Yet, the chamber window employed is very large and stretches the skin around the animal. This would then affect adipose deposition in obesity and was excluded

as a model to investigate. The generation of a mouse model (*Angiomouse*®) was also considered to observe adipose angiogenesis *in vivo,* modifying from its current use in visualising primary tumours (Hoffman 2002). The principle of *Angiomouse*® is that tumours express green-fluorescent protein (GFP), which can be visualised. Importantly, new vessels formed by angiogenesis do not fluoresce and are imaged as well-defined dark networks against the bright, green, fluorescent background of a tumour. This could be adapted to quantify the fluorescence of adipose, with associated vessel infiltration into the depot as a means of measuring angiogenesis. However, there is limited sensitivity with *Angiomouse*® due to light absorption by the surrounding tissues, particularly adipose. This was a similar problem encountered by our investigations into Tie-2 yellow fluorescent protein (YFP) mice, in which both background fluorescence in aortic rings and implanted sponges masked any signal from YFP-labelled infiltrating blood vessels (see Appendix section 8.2.1). Furthermore, it is now known that limited oxygen supplies affect GFP expression, which is the final product of a long and complex pathway involving transcription, translation and post-translational modifications, each of which can be affected by the availability of oxygen (Staton *et al.,* 2004). As this thesis has been primarily concerned with adipose angiogenesis in obese, hypoxic environments, this mouse model was ruled out as a potential tool for investigation. Finally, preliminary experiments using the insertion of Matrigel gel/plugs subcutaneously were conducted to measure how feasible this was (data not shown). Angiogenesis can be assessed from Matrigel as it forms a solid plug in which the angiogenic response can be quantified by measuring the haemoglobin content of the plug (Passanitia *et al.,* 1992). Data suggested irregularities in shape and vessel infiltration and thus was not used subsequently in this thesis.

Accomplishing quantification of angiogenesis in adipose tissue would shed further light upon this process and in alterations associated with the development of obesity. However, it has become evident during this project that the examination of angiogenesis in adipose tissue is very challenging.

It is reassuring then to know that fellow researchers have also experienced similar problems with the assessment of angiogenesis within adipose. Nevertheless, advances are being made and recently vessels and adipocytes were simultaneously detected *in situ*, using immunodetection of whole-mount, cryosectioned and paraffin-embedded adipose (Xue *et al.,* 2010). Although impressive, this technique is not without its disadvantages. Such a protocol of vascular detection in adipose cannot be performed in living adipose, as tissue must be removed from the animal. It may, therefore, be more beneficial to apply current techniques used for the detection of tumour growth in cancers in assessing adipose tissue angiogenesis. For example, quantitative reflectance optical spectroscopy methods have had success in the direct, quantitative measurement of tumour vascular oxygenation and total haemoglobin content in both preclinical and clinical models (Skala *et al.,* 2007; Vishwanath *et al.,* 2008; Bender *et al.,* 2009). These parameters of oxygenation and haemoglobin content would be indicative of tumour structure and size. This is achieved by using a technique called diffuse reflective spectroscopy, which provides a measurement of the absorption, and scattering of light from the tissue in question, and in turn provides the physiological and structural composition of a tissue (Brown *et al.,* 2009). The application of such a technique to adipose vascularisation would allow direct, *in vivo* measurements of angiogenesis in obesity. This would permit the mapping of blood vessel development or regression throughout obesity, potentially recording key points were there are alterations in angiogenesis. Increasing oxygen demand of expanding adipocytes during weight gain could be monitored in real time if the fibre optic probe conducting the diffuse reflective spectroscopy was inserted into any of the adipose depots. Thus, definitive measurements of angiogenic growth could then be assessed in obesity.

7.4 Concluding remarks

In summation, the work described in this thesis provides evidence to support our initial hypothesis. Angiogenic potential is affected by obesity, whereby *in vitro* assays indicate a suppression of angiogenesis and, conversely, *in vivo*

evidence suggests an elevation in angiogenesis in obesity. Examination of angiogenic factors by means of a microarray in a polygenic model of fatness and leanness revealed the expression of the anti-angiogenic factor thrombospondin-1 (TSP-1) was increased in subcutaneous fat in obesity. At higher doses, perhaps reflecting the increased TSP-1 expression with obesity, ABT-510 (specific anti-angiogenic Type I repeat sequence of TSP-1) dominantly promoted fat cell retention and obesity, potentially via p38MAPK signalling. *In vivo* administration of ABT-510 caused a biphasic response, whereby low doses suppressed weight gain and high doses did not. Continued studies to improve methods of the quantification of adipose angiogenesis will clarify the exact role of TSP-1 upon adipocyte metabolism and its role in obesity. Better quantification will also be beneficial in researching ABT-510 as a potential therapeutic angiogenesis inhibitor in obesity.

Chapter 8

Appendices

8.1 Quantification of angiogenesis

One of the major problems in angiogenesis research has been the difficulty of finding suitable methods for determining the angiogenic response. As with all *in vitro* assays, concern remains that results do not translate well into the effects in an *in vivo* situation. The angiogenic cascade *in vivo* is very intricate, which adds to the problem of *in vitro* analysis. However, these assays do give insight into some key angiogenic functions and there are now well established assays designed to examine each step involved in the angiogenic cascade. These include the tube formation assay, cell proliferation and motility assays.

When assessing angiogenesis the tube formation assay is more commonly used. This simply assumes the basic principle that endothelial cells form tube-like structures when cultured on a supportive matrix (Folkman 1986). This assay encapsulates at least two key steps in the angiogenic cascade, the migration and differentiation of endothelial cells. Nevertheless, this technique relies on manual counting, and lends itself to a margin of error.

Another assay examining angiogenesis, which is considered more than the tube formation assay to be a faithful *in vitro* interpretation of *in vivo* angiogenesis (Auberbach *et al.,* 2003) is the aortic ring assay (Nicosia & Ottinetti 1990). This assay allows the three-dimensional assessment of endothelial growth outward from aortic segments or rings. This assay has the added benefit of including effects mediated by non-endothelial cells on the vascular endothelium. Quantification is achieved by the time-consuming measurement of the abundance (and sometimes length) of vessel-like extensions from the aortic ring continually every two days over a ten to twelve day period. Unfortunately, the measurement of three-dimensional growths on a two-dimensional image is difficult and again manual counting contributes to a margin of error.

Several assays have been developed that permit a more realistic assessment of the angiogenic response occurring *in vivo*, which allow better interpretation of the data when all used. For example, the Matrigel plug assay, where Matrigel is injected subcutaneously into an animal, can further serve as a vehicle for cells

and compounds of interest (Passanitia *et al.,* 1992). Usually, the total haemoglobin content of the Matrigel plug is indicative of the amount of angiogenesis or sometimes the extent of vessel growth as assessed by histological means. Like most angiogenesis assays, the interpretation of this technique is not without its caveats as the histological analysis is again time-consuming and it is difficult to generate identical three-dimensional plugs, due to the consistency of the Matrigel before it sets and the movement of the animal. Another *in vivo* model, the subcutaneous implantation of a sponge, encapsulates a lot of the advantages of other techniques. This model was first described for use in measuring blood flow (Andrade *et al.,* 1987, Hu *et al.,* 1995), but was later modified to measure vascularity (Hague *et al.,* 2002). The sponge causes the induction of a chronic granulomatous response including an intense angiogenesis and infiltration of inflammatory cells (Lage & Andrade 2000). Vascular growth into the sponge is assessed histologically by manual counting of blood vessels stained with Haematoxylin and Eosin. However, the differences in sponge materials used by others and the shape and size, makes direct data comparison difficult. Moreover, sponge implantation is associated with non-specific immune responses, which in turn, may cause a significant angiogenic response (Auberbach *et al.,* 2000).

The development of cre/lox technology has provided an important tool to manipulate gene expression in mice in a cell-type specific manner. This is eloquently demonstrated in the development of a transgenic mouse strain in which Cre recombinase expression is directed to endothelial cells by the mouse Tie2 promoter (Araki *et al.,* 1995). These mice are useful for cell lineage experiments and the incorporation of yellow fluorescent protein (YFP) into the Cre alleles allows these autofluorescent proteins to be visualised, when excited by UV light. Such a technique has been used to image tumours during progression and metastasis (Yang *et al.,* 2000; McCann 2001) and has recently been adapted for the study of *in vivo* tumour angiogenesis (Hoffman 2002). As fluorescence is directed to the endothelial cell, the potential examination of angiogenesis in adipose could be performed. The combination of sponge

implantation within the Tie2-Cre mouse would also allow the angiogenic response under different treatments and diets to be assessed. However, the main disadvantage with YFP is that its sensitivity may be limited due to light absorption by surrounding tissues.

8.2 Alternate methods of quantifying angiogenesis *in vivo*

8.2.1 Fluorescence detectable in implanted sponges in YFP mice

The fluorescent labelling of the endothelium (in mice with endothelium-specific expression of yellow fluorescent protein (YFP)), was hypothesised to improve detection and characterisation of angiogenic structures. Sponges implanted (see section 2.1.3.1) into YFP mice and excised after 21 days, were visualised under UV light. Sponge shape was clearly visible with signal achievable from adipose, which was left on from dissection on the corner of sponge (Figure 8.1).

8.2.2 Optical projection tomography (OPT) of implanted sponges in YFP mice did not generate fluorescent vessels

In addition to utilising conventional immunohistochemistry on sponge sections, the organisation of sponge vessel infiltration was attempted to be visualised in three dimensions by combining the genetic labelling of endothelial cells expressing yellow fluorescent protein (YFP) with optical projection tomography (OPT), a novel imaging technique particularly useful for 3D examination of organs. Sponges removed from YFP mice were subjected to OPT (see section 2.4.5). As an incorporated YFP endothelial cell specific signal would be detectable within vessels that infiltrate the sponge, then no additional antibodies would be required for OPT analysis. However, when these sponges were scanned the fluorescence emitted by the sponge itself did not allow any individual vessels to be observed or analysed (Figure 8.2).

8.2.3 No isolation of YFP positive endothelial cells by fluorescence activated cell sorting (FACS)

Manipulating directly YFP labelled endothelial cells present within adipose of Tie-2 YFP mice would allow the quantification of endothelial cell number and

give an indication of adipose angiogenesis. Thus, pooled subcutaneous adipose from six Tie-2 YFP mice was removed and the stromal vascular fraction (SVF) was isolated (see section 2.4.10). No antibody incubation was necessary as endothelial cells would fluoresce as they are genetically labelled with YFP. However, the YFP signal seemed very short-lived as although a clear YFP population was observed (Figure 8.3A), the YFP positive cells had disappeared (Figure 8.3B) and their signal shifted (Figure 8.3C). Therefore, isolation of YFP positive cells within the SVF was not achieved.

8.2.4 Endothelial cells within tube-like structures of aortic rings not fluorescently stained by Dil-Ac-LDL uptake

To assess whether the fluorescent staining of endothelial branches from aortic rings could be used as a measure of angiogenesis, aortic rings from C57BL/6J mice were incubated for 4 hours with fluorescently-labelled acetylated low-density lipoprotein (Dil-Ac-LDL) on Days 2, 4, 6, 8 and 10 after implantation (see section 2.3.5) (Figure 8.4). Although it was apparent from the black and white images (Figure 8.4 A & C) that there were numerous branches emanating from the ring, this was not evident when viewed by fluorescence microscopy (Figure 8.4B). However, there was indication of uptake of Dil-Ac-LDL uptake in the endothelial cells of the aortic ring itself (Figure 8.4 D).

8.2.5 Small enrichment of CD31 positive cells obtained from stromal vascular fraction by fluorescence activated cell sorting (FACS)

Isolation of CD31 positive cells has previously been used as an indication of angiogenesis (Asahara *et al.,* 1997). In order to check if we could isolate CD31 positive stained cells from a stromal vascular fraction obtained from adipose, fluorescence activated cell sorting was performed on pooled subcutaneous adipose from C57BL/6J mice (Figure 8.5) (see section 2.4.10). Although adipose from five mice was pooled, the enrichment of CD31 positive cells was only 5.1% (Figure 8.5C) compared to CD31 negative cells (Figure 8.5B), which was deemed not sufficient enough to warrant pooling of so many mice. Ungated cells are also shown (Figure 8.5A).

8.2.6 Subcutaneous sponge implantation assay: comparison of histology and haemoglobin content

The sponge implantation assay was used to assess vascularity throughout a 3 week period. Sponges were removed and weighed at 4, 7, 13 and 21 days. One half of the left implanted sponge was used for histological processing (Figure 8.6 A, B, C & D) and the other half for assessment of haemoglobin content (Figure 8.6 F) (see section 2.4.4). As time progressed, histological examination showed a gradual increase in blood vessel infiltration into the sponge (Figure 8.6 E). This increase in blood vessel density was mirrored by an increase in haemoglobin content from Day 4 to Day 21 (Figure 8.5 F). The haemoglobin method of analysing the extent of vessel infiltration was also examined in three month high fat fed C57BL/6J mice (Figure 8.7). However, high interference in spectrophotometry readings obtained from sponges excised from the high fat group was observed.

8.2.7 Non-specific CD31 staining within C57BL/6J subcutaneous adipose

To improve the assessment of blood vessel distribution in adipose tissue, immunohistochemistry was performed using a CD31 antibody (Figure 8.8). CD31, a member of the immunoglobulin superfamily, is commonly used as a cytoplasmic endothelial cell marker (Figure 8.8B). However, there was non-specific staining of the CD31 antibody observed (Figure 8.8C).

8.2.8 Investigation of angiomodulatory factors in primary adipocyte conditioned medium

It has become increasingly clear that adipocytes are a source of altered bioactive (e.g. adipokines) factors in obesity. In order to determine whether adipocytes were are key source of angiomodulatory factors, aortic rings were incubated in adipocyte conditioned medium. Aortic rings were cultured in the presence of conditioned medium (DMEM) taken from C57BL/6J mouse primary subcutaneous adipocyte cultures (see section 2.5.5) or basal DMEM as a control. The standard medium for used for growing aortic rings (Nicosia & Ottinetti

1990) basal EBM2, was used as an additional control, and is the normal medium optimised for the aortic ring assay.

8.2.8.1 Decreased tube-like structure (TLS) formation in aortic rings when exposed to basal DMEM and adipocyte-conditioned medium

Basal DMEM diminished TLS number in aortic rings compared to aortic rings incubated with basal EBM2 irrespective of whether it has been conditioned by adipocyte culture (Figure 8.9). Reduction in TLS formation was evident from Day 4. As there was no significant difference between basal DMEM and adipocyte conditioned medium, it could not be determined whether exposure to adipocyte had any additional effect upon growth.

8.3.1 Visualisation of fluorescent signal from sponges implanted in YFP mice indicates quenching of endothelial signal by adipose

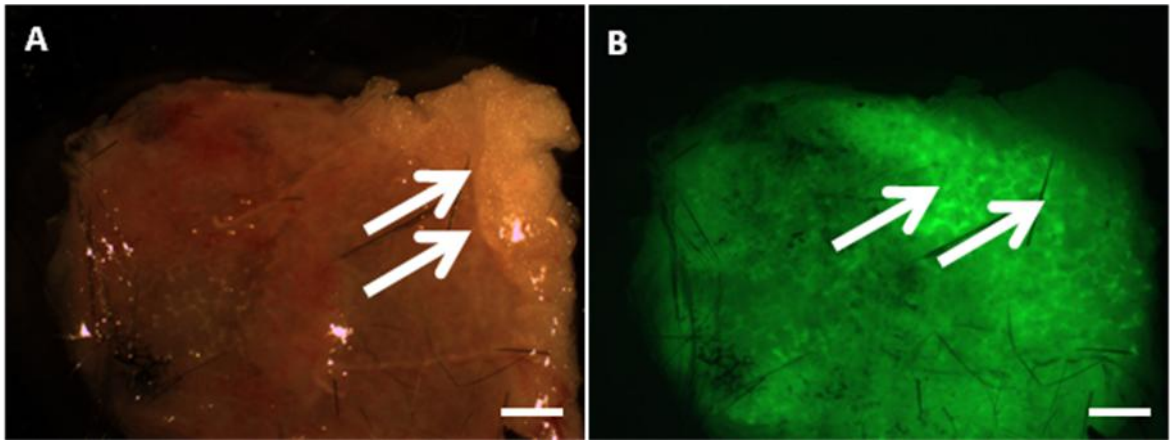

Figure 8.1: Visualisation of fluorescent signal from sponges implanted in YFP mice. (**A**) Sponge visualised under brightfield, with associated adipose visible on the top right edge of sponge (white arrow). (**B**) The same sponge visualised under UV light. The hexagonal shape of the sponge matrix is clearly visible, with a darkening of fluorescence from the top right edge of sponge (white arrow). Sponges excised 21 days after implantation from YFP mice and assessed under a fluorescent microscope Scale bar represents 0.25 mm; n=2; 7 week YFP mice.

8.2.2 Optical projection tomography (OPT) of implanted sponges in YFP mice does not show infiltrated blood vessels

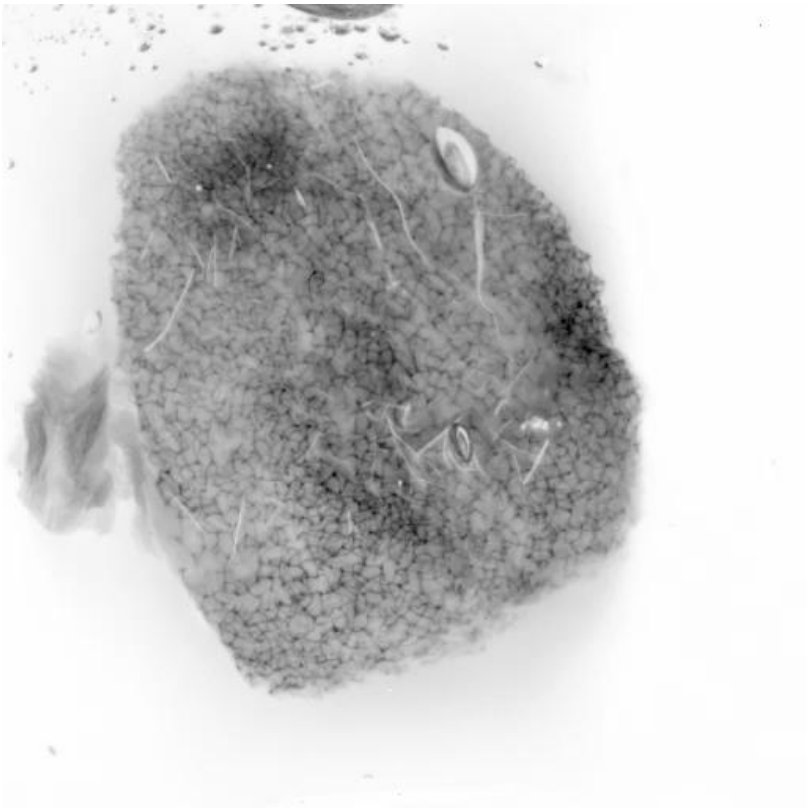

Figure 8.2: A still from optical projection tomography (OPT) of implanted sponges in YFP mice. Three dimensional video of sponge implanted in Tie-2 YFP mouse. Although clear visualisation of sponge architecture is evident, individual blood vessels that have infiltrated the sponge are not visible as the signal from sponge is too strong. Representative image from 3 sponges scanned.

8.2.3 Short lived YFP positive endothelial cell signal by fluorescence activated cell sorting (FACS)

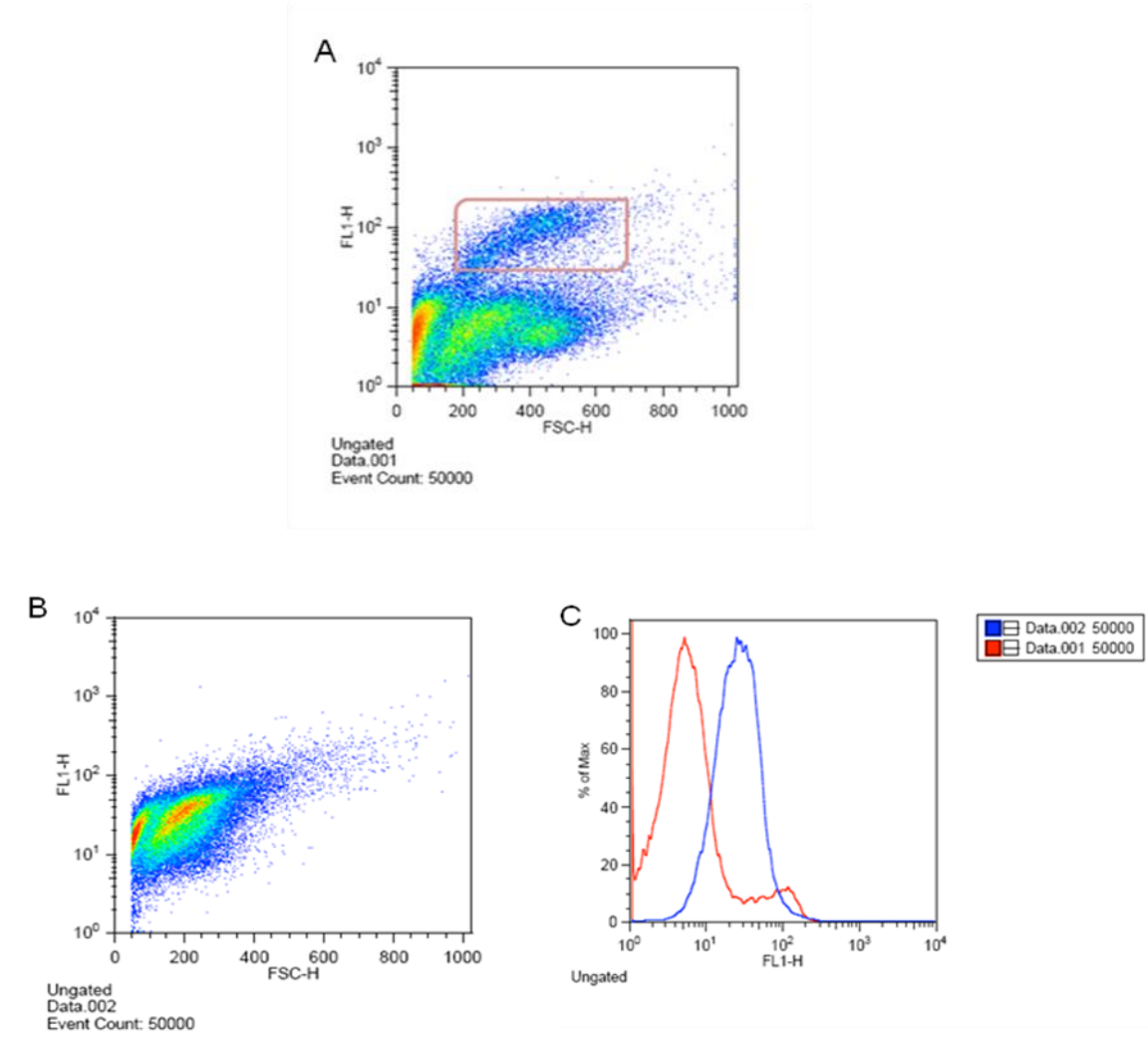

Figure 8.3: YFP positive endothelial cell signal by fluorescence activated cell sorting (FACS). Visualisation of the YFP population of the stromal vascular fraction of subcutaneous adipose from Tie-2 YFP mice. Clear YFP population observed (**A**), gated in pink. After a few hours incubation, this signal had disappeared (**B**) and the YFP signal shifted to the right (**C**), shown in blue. n=6.

8.2.4 No uptake of Dil-Ac-LDL into endothelial cells of aortic rings from C57BL/6J mice

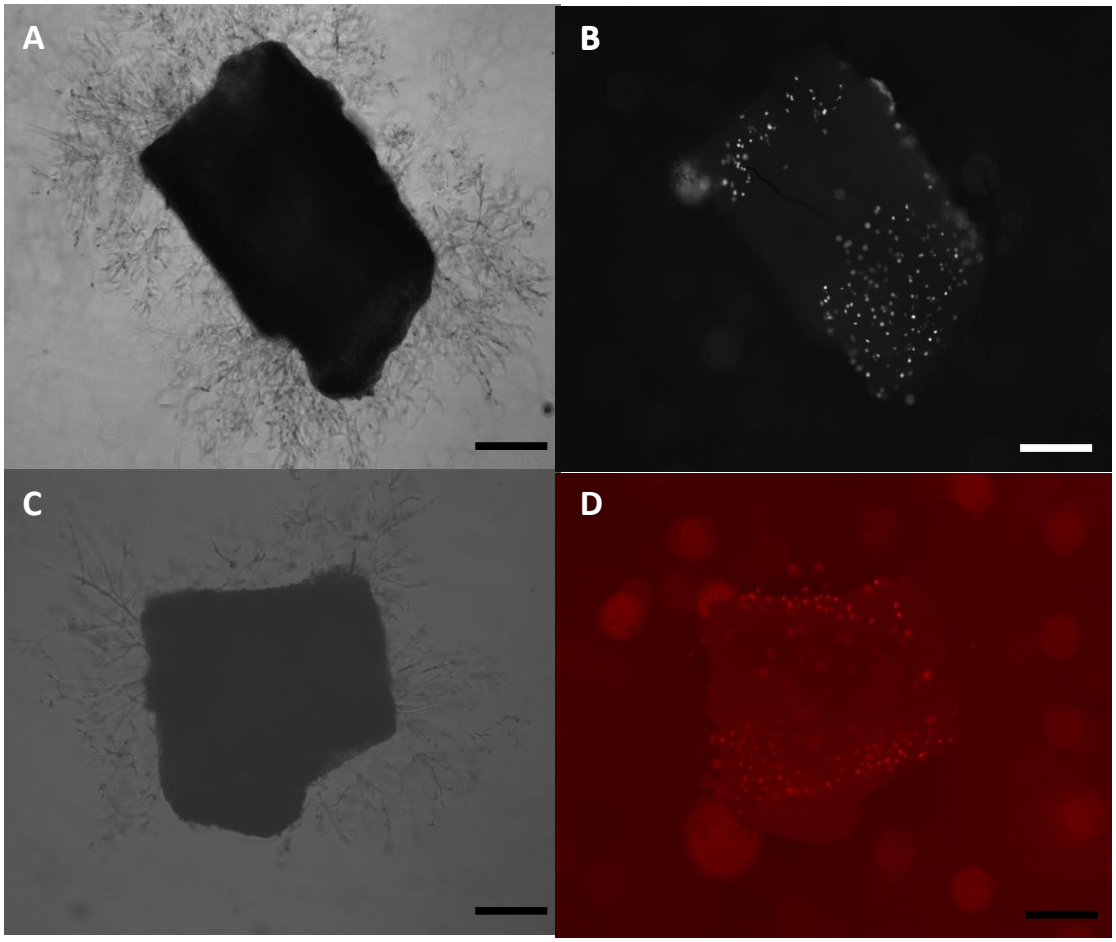

Figure 8.4: Dil-Ac-LDL uptake into endothelial cells of aortic rings. Black and white images show aortic rings on Day 8 of culture, with TLS branching from aortic ring (**A** & **C**) and fluorescent images show no visible TLS structures (**B** & **D**). However, there is clear incorporation of Dil-Ac-LDL into the aortic ring itself (**B** & **D**). Scale bar represents 200 μm. TLS formation was assessed under a fluorescent microscope; n=5; C57BL/6J; 7 weeks of age.

8.2.5 Marginal increase in CD31 positive cells from fluorescence activated cell sorting (FACS) of stromal vascular fraction

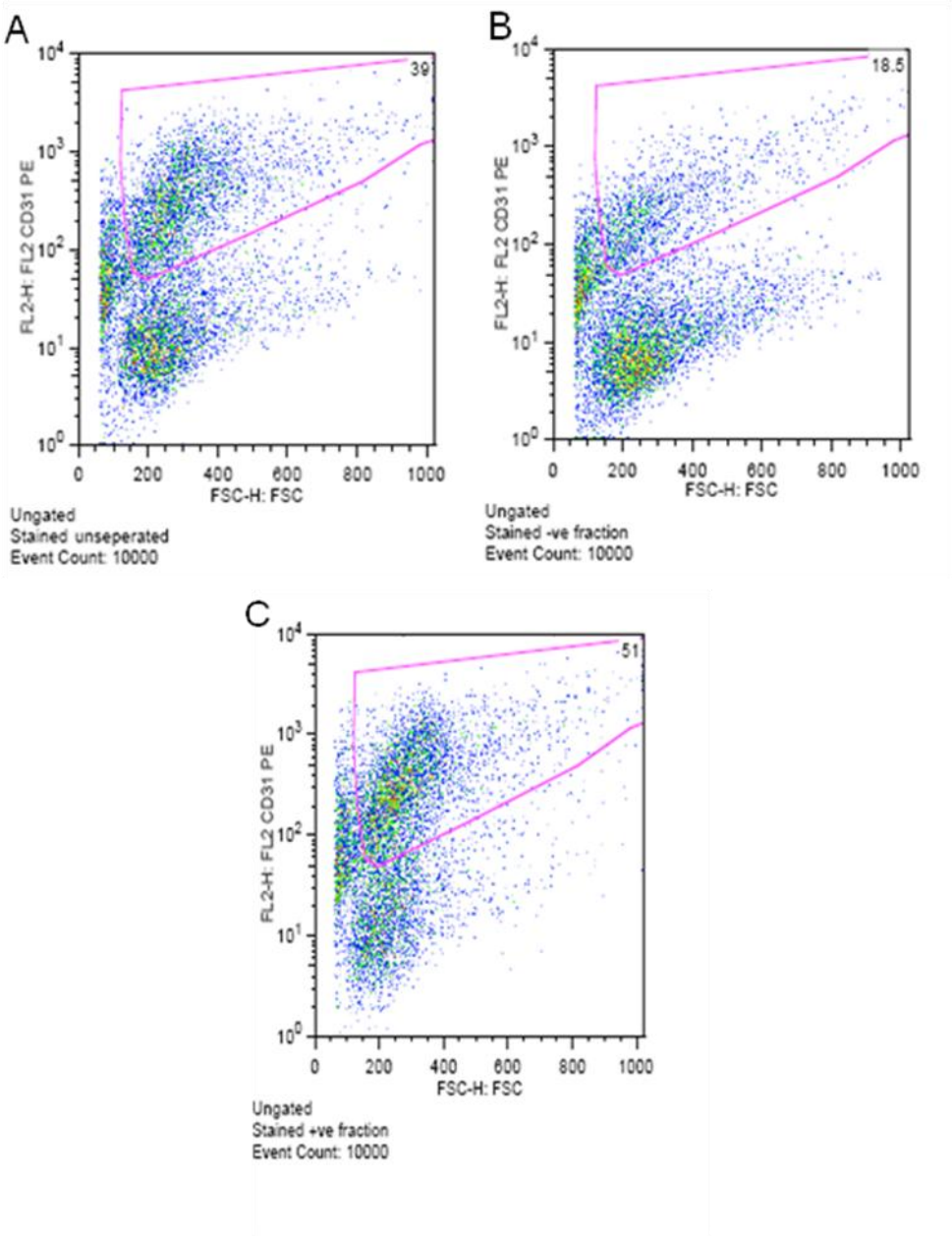

Figure 8.5: Fluorescence activated cell sorting (FACS) of stromal vascular fraction using CD31 antibody. Dot plot representation of CD31+ and CD31- populations in the stromal vascular fraction (SVF) of subcutaneous adipose from C57BL/6J mice. Ungated population of cells in SVF is shown in **A**. Negative CD31 cells were then gated (**B**) and CD31 positive cells (**C)** only exhibited 5.1 % enrichment.

8.2.6 Comparable results from subcutaneous sponge implantation using both histological and haemoglobin analysis

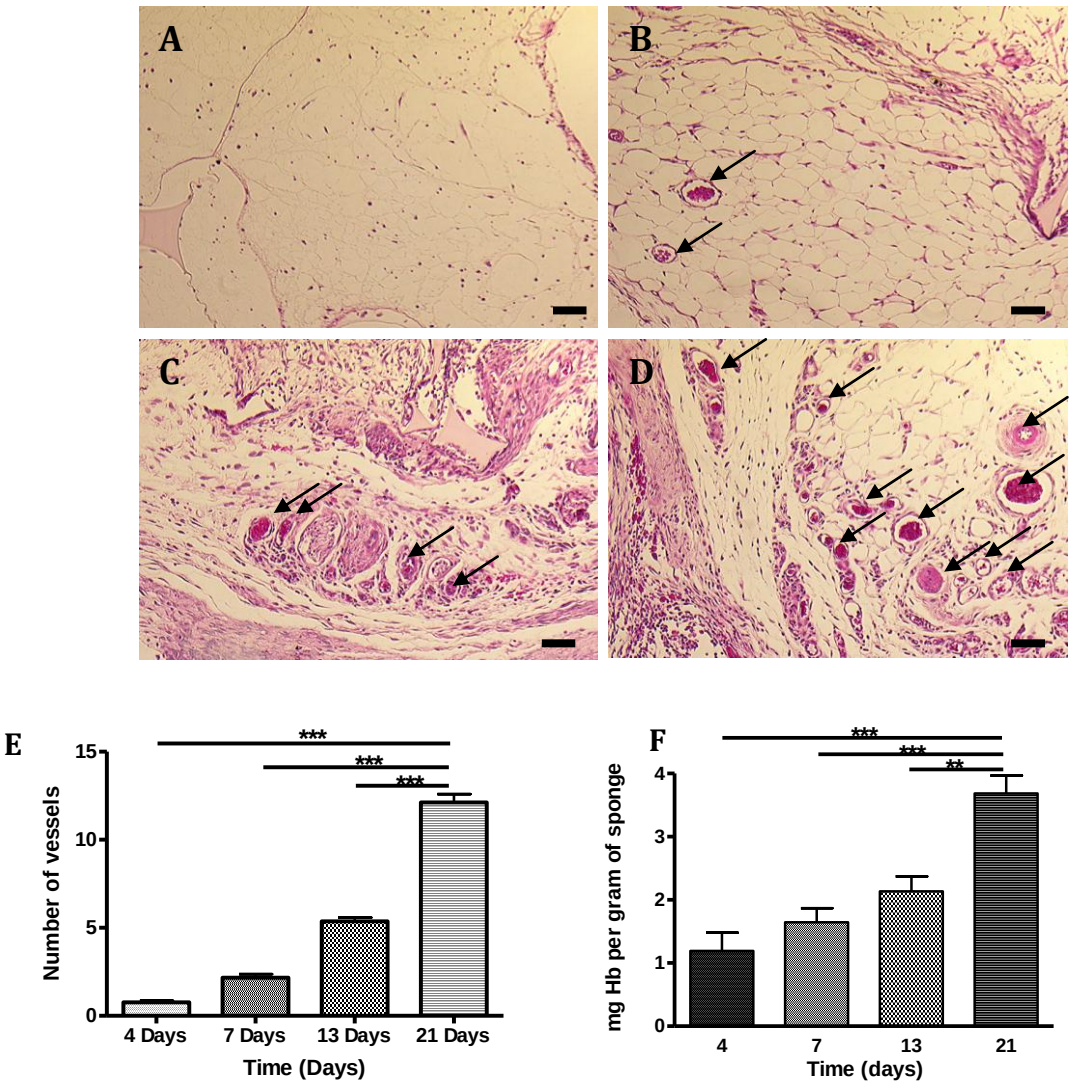

Figure 8.6: Analysis of vascularity in sponges implanted into C57BL/6J mice using both histological and haemoglobin assays. Photomicrographs (x 10) of H & E stained sponges from Day 4 (**A**), Day 7 (**B**), Day 13 (**C**) and Day 21 (**D**). Sponges excised on Days 4, 7, 13 and 21 all had significantly increased vascularity when compared to Day 4 (**F**). Blood vessels were identified morphologically, with or without erythrocytes present in the lumen and assessed by Chalkley counting. There was a similar increase in haemoglobin content with time assessed by colorimetric analysis (**E**). Data are expressed as mean ± SEM, n=6 for each time point. Data were analysed by one-way ANOVA followed by Bonferroni correction; *** $p<0.001$. Scale bar represents 50 μm. Arrows indicate blood vessels.

8.2.6 Variable haemoglobin content of sponges excised from 3 month high fat fed C57BL/6J mice

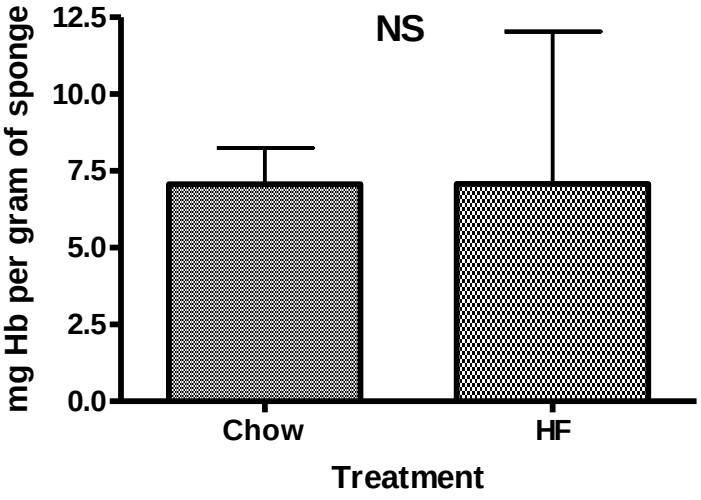

Figure 8.7: Haemoglobin content of sponges excised from 3 month high fat fed C57BL/6J mice. No difference in haemoglobin content in sponges excised from 3 month high fat fed and chow fed C57BL/6J mice, as assessed by colorimetric analysis. Data are expressed as mean ± SEM, n=6 for each time point. Data were analysed by one-way ANOVA followed by Bonferroni correction; NS; non-significant.

8.2.7 Patchy CD31 antibody staining within subcutaneous adipose from C57BL/6J mice

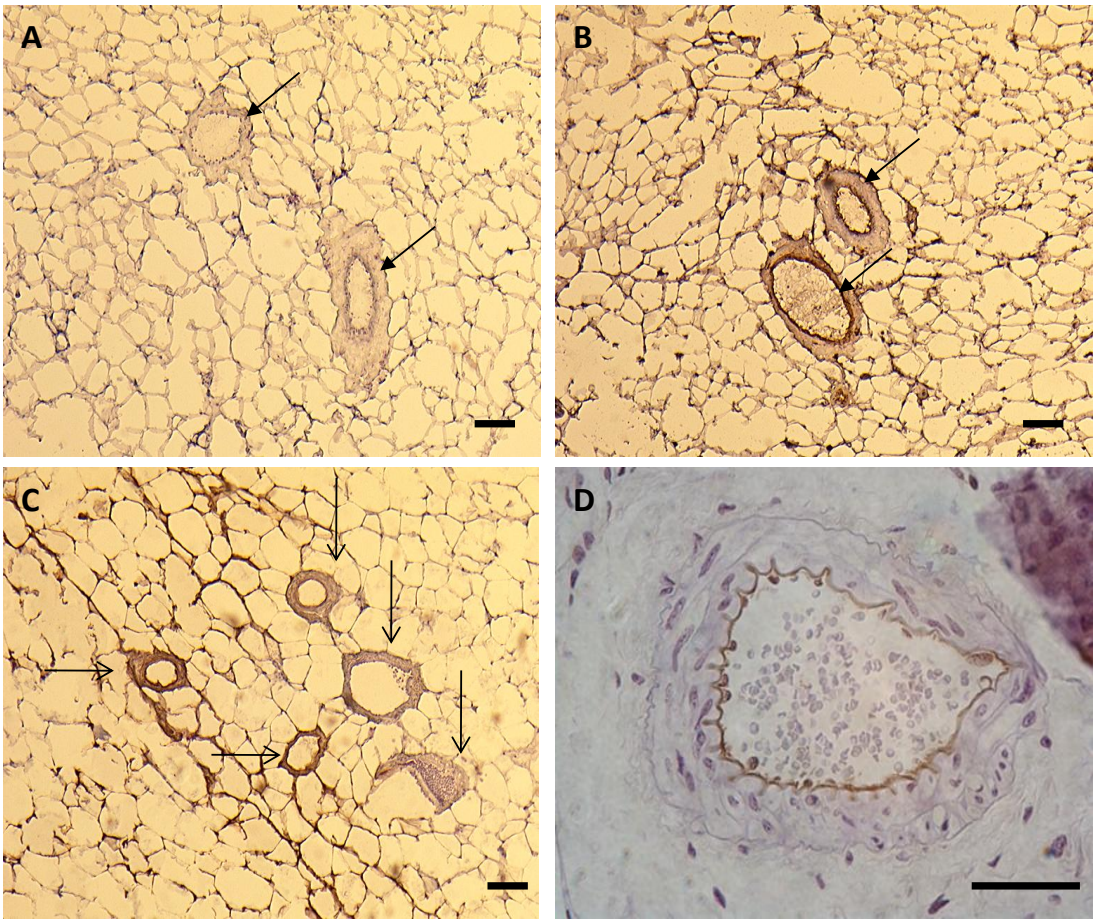

Figure 8.8: CD31 staining of blood vessels within subcutaneous adipose of C57Bl/6J mice. (**A**) No CD31 antibody control in adipose sections (x10). (**B**) CD31 expression in adipose sections with strong positivity in the endothelial cells lining blood vessels. (**C**) Patchy staining of CD31 antibody (horizontal arrows), in which there is clear staining of some blood vessels and not of others (vertical arrows). (**D**) Control staining of CD31 antibody of kidney glomeruli blood vessel from C57BL/6J mouse (X 40). Scale bars represent 50 μm. n=4; 10 week C57BL/6J mice.

8.2.8 Decreased tube-like structure (TLS) formation in aortic rings cultured in basal DMEM and adipocyte conditioned medium (ACM)

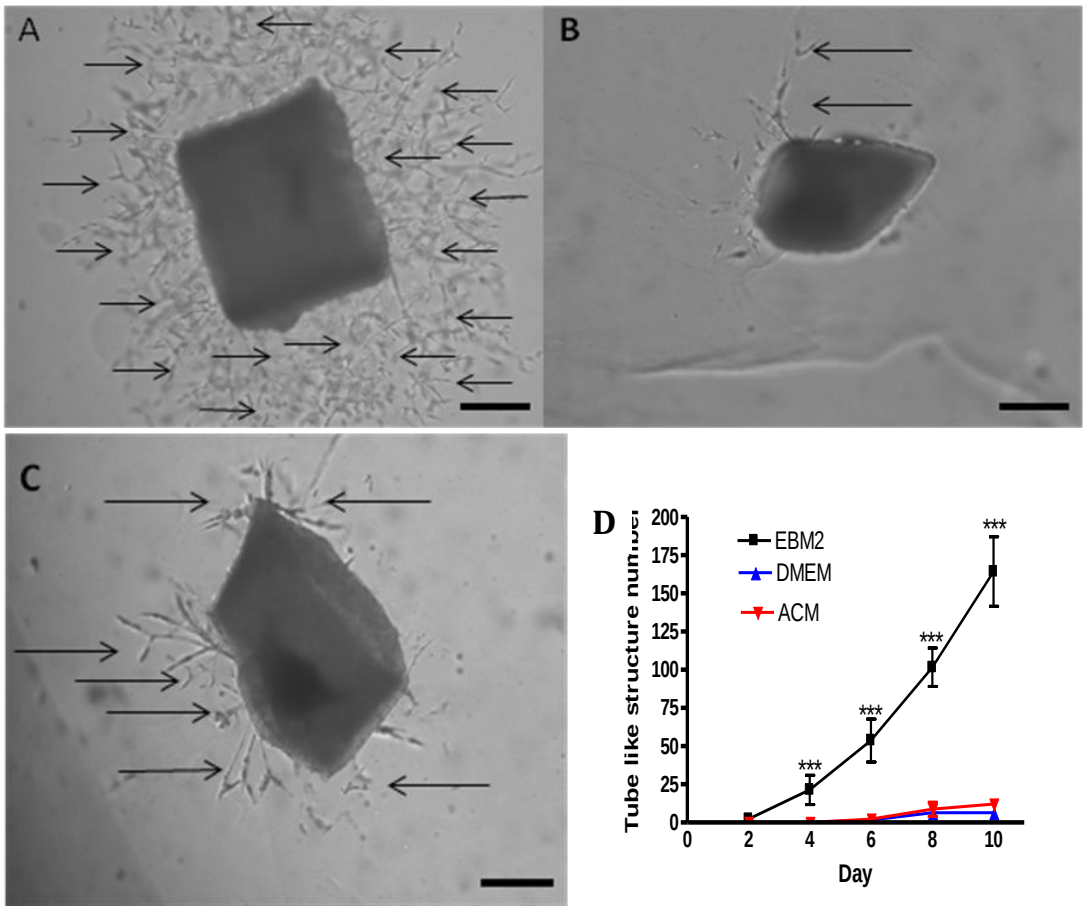

Figure 8.9: TLS formation in aortic rings in adipocyte conditioned medium and basal DMEM media compared to aortic rings cultured in EBM-2. TLS formation was assessed by manual counting under light microscopy of (**A**) Basal EBM2, (**B**) Adipocyte conditioned medium (ACM) and (**C**) Basal DMEM on Day 8. TLS formation was quantified over the 10 ten period (**D**). Scale bar represents 0.2 mm; n=3; C57BL/6J; 9 weeks of age.

8.3 Discussion

8.3.1 Evaluation of new methods of quantification of angiogenesis

8.3.1.1 Visualisation of YFP signal from endothelial cells from Tie-2 YFP mice

It was evident that a new model for the *in vivo* (and *ex vivo*) quantification of angiogenesis would be useful in alleviating some of the problems described above with the other techniques. The development of cre/lox technology has provided an important tool to manipulate gene expression in mice in a cell-type specific manner. As fluorescence will be directed to the endothelial cells, the examination of angiogenesis could be performed. Preliminary experiments were conducted with the implantation of sponges into Tie-2 Cre mice to observe whether any fluorescence could be detected from or within the sponge as angiogenesis progressed. Promising results were achieved with clear structures visible within the sponge. Unfortunately, when similar sponges were investigated using OPT, the sponge matrix was only visible and the YFP signal had not survived the fixation process and was not visible. Tie2-cre mice that were used in FACs analysis also produced some disappointing results. The number of animals pooled (6 mice) in order to obtain enough adipose, associated with colony difficulties, severely restricted this work: it was not always possible to obtain mice at the same age. These issues were also mirrored with the use of CD31 positive cell FACS isolation, whereby for the enrichment of positive cells observed, the amount of subcutaneous adipose needed was large.

8.3.1.2 Limited uptake of Dil-Ac-LDL by aortic rings

There is a large volume of analysis required with TLS counting in aortic rings, which naturally may introduce a margin of human error. It was therefore desirable to attempt other methods of assessing TLS formation. Acetylated-low density lipoprotein (Ac-LDL) is taken up by macrophages and endothelial cells via the "scavenger cell pathway" of LDL metabolism (Voyta *et al.,* 1984). Lipoproteins labelled with the fluorescent probe 1,1'-dioctadecyl-3,3,3',3'-tetramethyl-indocarbocyanine perchlorate (DiI) have been utilized to visualize

the uptake of lipoproteins by macrophages and arterial foam cells (Pitas *et al.,* 1983). Subsequently, it was hypothesied that Dil-Ac-LDL could be used to visualise endothelial TLS from aortic rings in culture. Although the results showed an accumulation of Dil-Ac-LDL within the aortic ring itself, there was no evidence of such an accumulation within the tube-like structures. TLS were visible from Day 4 of the experiment; however Dil-Ac-LDL fluorescence was not apparent until Day 8. It was believed that the fluorescence given from the aortic ring was too strong to examine individual TLS, however has been achieved by other groups (Blacher *et al.,* 2001). Therefore, this assay was not used for future analysis of aortic growth.

8.3.1.3 Haemoglobin vs. Histology

The subcutaneous implantation of a sponge encapsulates many of the advantages of other techniques in measuring angiogenesis, such as it is technically simple and inexpensive. However, vascular growth is assessed histologically and is very time consuming. We therefore attempted to develop a method of processing the sponges biochemically by measuring the haemoglobin content (Ferreira *et al.,* 2004). The pattern of increasing vascularity and increasing haemoglobin content of sponges taken at different points over a 21 day period was comparable between both methods. However, when the sponges were placed in mice placed fed a high fat diet for three months, there was associated interference observed in the spectrophotometer readings. We speculate that the high fat diet or increased adipose with high fat feeding may have a subsequent effect upon the assay and therefore, used histological staining and analysis of sponges for future sponge implantation experiments. However, this interpretation is hard to compare as has not been attempted in the literature.

8.3.1.4 Angiomodulatory factors present in primary adipocyte conditioned medium

Preliminarily experiments addressed the hypothesis that adipocytes regulate new blood vessel formation by releasing an angiogenic factor. The specific aim

was to use aortic rings to determine whether factors secreted by primary, mature adipocytes augment tube formation by aortic rings. Whilst the TLS assay is traditionally performed in a medium designed for endothelial cells (EBM-2), a version of the assay has also been reported using DMEM (Saiki *et al.,* 2006). As the latter is the medium of choice for culturing adipocytes, we assessed the influence of DMEM on TLS formation in our assay also. It became apparent that adipocyte conditioned medium and medium without exposure to any cell inhibited tube formation markedly. As eventual co-culture of adipocytes and endothelial cells would be desirable, we concluded that DMEM would not be optimal for both cell types.

8.4 Supplementary microarray information

8.4.1 Microarray analysis of subcutaneous adipose tissue from Fat and Lean mice

In order to identify changes in adipose tissue from Lean and Fat mice, with or without a further dietary obesity challenge, RNA was obtained from subcutaneous adipose (the most divergent in mass in response to diet: Morton *et al.,* 2005) and used for microarray analysis. Processed RNAs were hybridised to Affymetrix Mouse Exon 1.0 ST Arrays. Scanning was on an Affymetrix GeneChip scanner. The GeneChip Mouse Exon 1.0 ST Array core probeset had 16654 non-control probe sets. RNA quality control and processing were carried out by Ark Genomics, Roslin, Edinburgh. Further analysis and database preparation were by Dr Donald Dunbar of the Bioinformatics Team at the Centre for Cardiovascular Science (CVS). The criteria used for determining whether changes were significant was calculated by Limma and adjusted by Benjamini and Hochberg. Fold changes, greater than 1.5 and associated adjusted p-values less than 0.05, were used to select genes. The total number of genes that were differentially expressed on these criteria was 268. Angiogenesis gene ontology (Ashburner *et al.,* 2000) and KEGG pathway enrichment analysis was performed to identify pathways using Webgestalt (WEB-based Gene SeTAnalysis Toolkit) (Zhang *et al*., 2005) and DAVID (Database for annotation, visualisation and integrated discovery) (Dennis *et al.,* 2003; Huang *et al.,* 2009). The differential expression of genes were analysed for significant changes in a custom built MySQL database.

Genes that were strongly up to strongly down – regulated were investigated and these included macrophage inflammatory proteins- MIP-1α/ccl3, ccl2, ccl5 ccl19, complement receptor (cr2), toll-like receptors (tlr) 2, 4 and 13 (tlr2, tlr 4, tlr 13), serum amyloid A 3 (Saa3), prostaglandin D2 synthase (ptgds 2), thromboxane synthase (tbaxs1), osteopontin 1 (spp1), prostaglandin E2 receptor subtype 3 (ptger 3), platelet activating factor acetylhydrolase (pla2g7), carnitine palmityl trasnferase-1 (cpt1), pyruvate dehydrogenase kinase (pdk4),

retinol binding protein 4 and 7 (rbp 4, rbp 7), uncoupling binding proteins 1, 2 and 3 (ucp1, ucp2, ucp3) and paraoxnase (pon1).

8.4.2 Validation and confirmation of gene expression in adipose of Lean and Fat mice

To validate the gene expression changes seen in the microarray, qPCR was used by selecting genes that the arrays indicated ranged from being strongly up to strongly down – regulated.

RNA was extracted from subcutaneous adipose tissue from the complete cohort (n=6 from each strain and dietary constraint) in order to increase statistical power over the microarray (see section 2.2.1). The expression of the housekeeping gene, tata-binding protein (TBP) did not differ within and between groups when used (data not shown). Therefore, transcript levels of this gene were used for normalisation of most target genes.

Genes investigated included macrophage inflammatory proteins- MIP-1α/ccl3, ccl2, ccl5 ccl19, complement receptor (cr2), toll-like receptors (tlr) 2, 4 and 13 (tlr2, tlr 4, tlr 13), serum amyloid A 3 (Saa3), prostaglandin D2 synthase (ptgds 2), thromboxane synthase (tbaxs1), osteopontin 1 (spp1), prostaglandin E2 receptor subtype 3 (ptger 3), platelet activating factor acetylhydrolase (pla2g7), carnitine palmityl trasnferase-1 (cpt1), pyruvate dehydrogenase kinase (pdk4), retinol binding protein 4 and 7 (rbp 4, rbp 7), uncoupling binding proteins 1, 2 and 3 (ucp1, ucp2, ucp3) and paraoxnase (pon1).

8.4.2 Divergent gene expression responses in Fat versus Lean mice

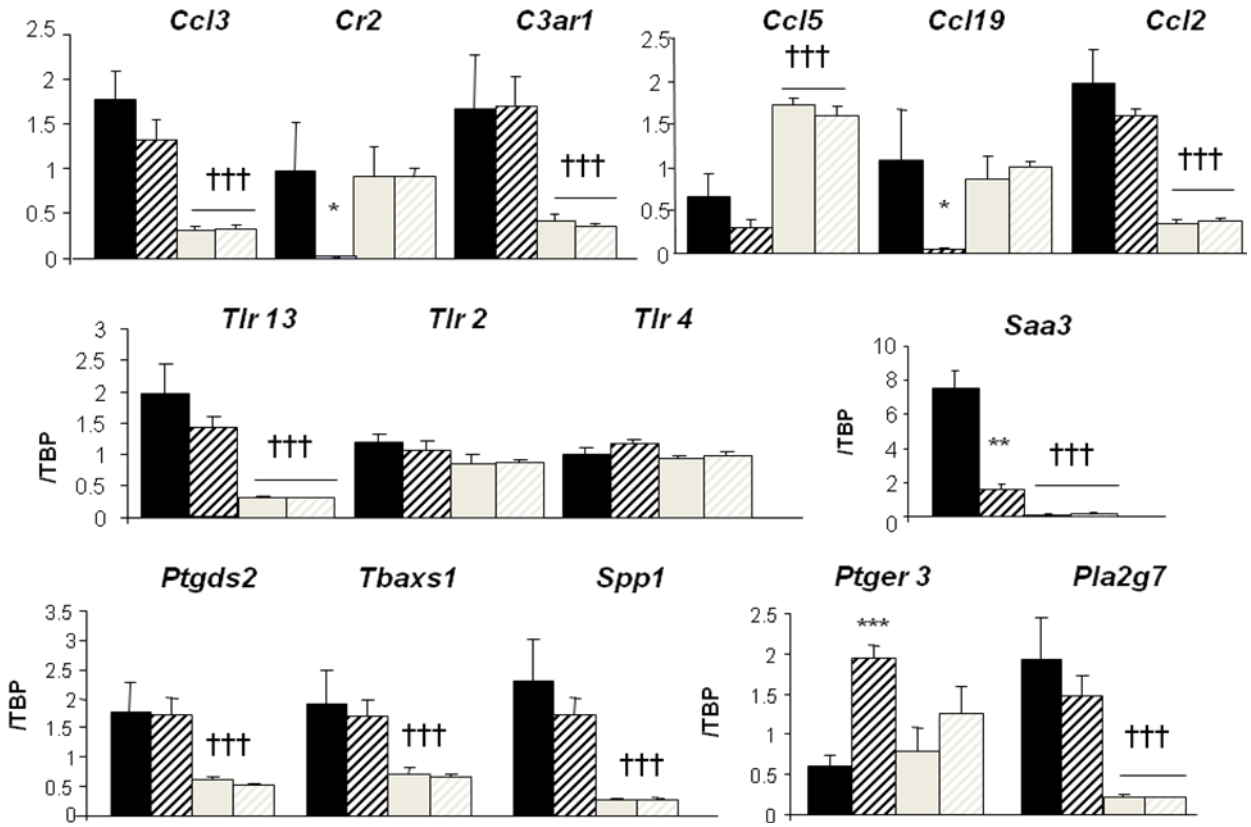

Figure 8.10: Divergent changes in expression of genes: real-time PCR analysis of cDNA from subcutaneous adipose tissue from Lean and Fat mice on control or high fat diet. Genes that were differentially expressed in the Fat mouse strain included macrophage inflammatory proteins (MIP-α/Ccl3 and Ccl2); (C3ar1); toll-like receptor 13 (Tlr13); prostagladin D2 synthase (Ptgds2); thromboxane synthase (Tbxas1); osteopontin 1 (Spp1) and platelet activating factor acetylhydrolase (Pla2g7). Genes that were differentially expressed in the Lean mouse strain included the macrophage inflammatory protein, Ccl5. No expression changes in toll-like receptors 2 and 4 (Tlr2 and 4). Black indicates control fed Fat mice (FC); black strip indicates Fat mice on high fat diet; grey colouring indicates Lean mice on control diet and grey strip is indicative of Lean mice on high fat diet. n=6. *p<0.05; **p<0.01; ***p<0.001; †††p<0.001. Two way ANOVA with *Bonferroni* post hoc test.

8.4.2 Divergent gene expression responses in Fat versus Lean mice

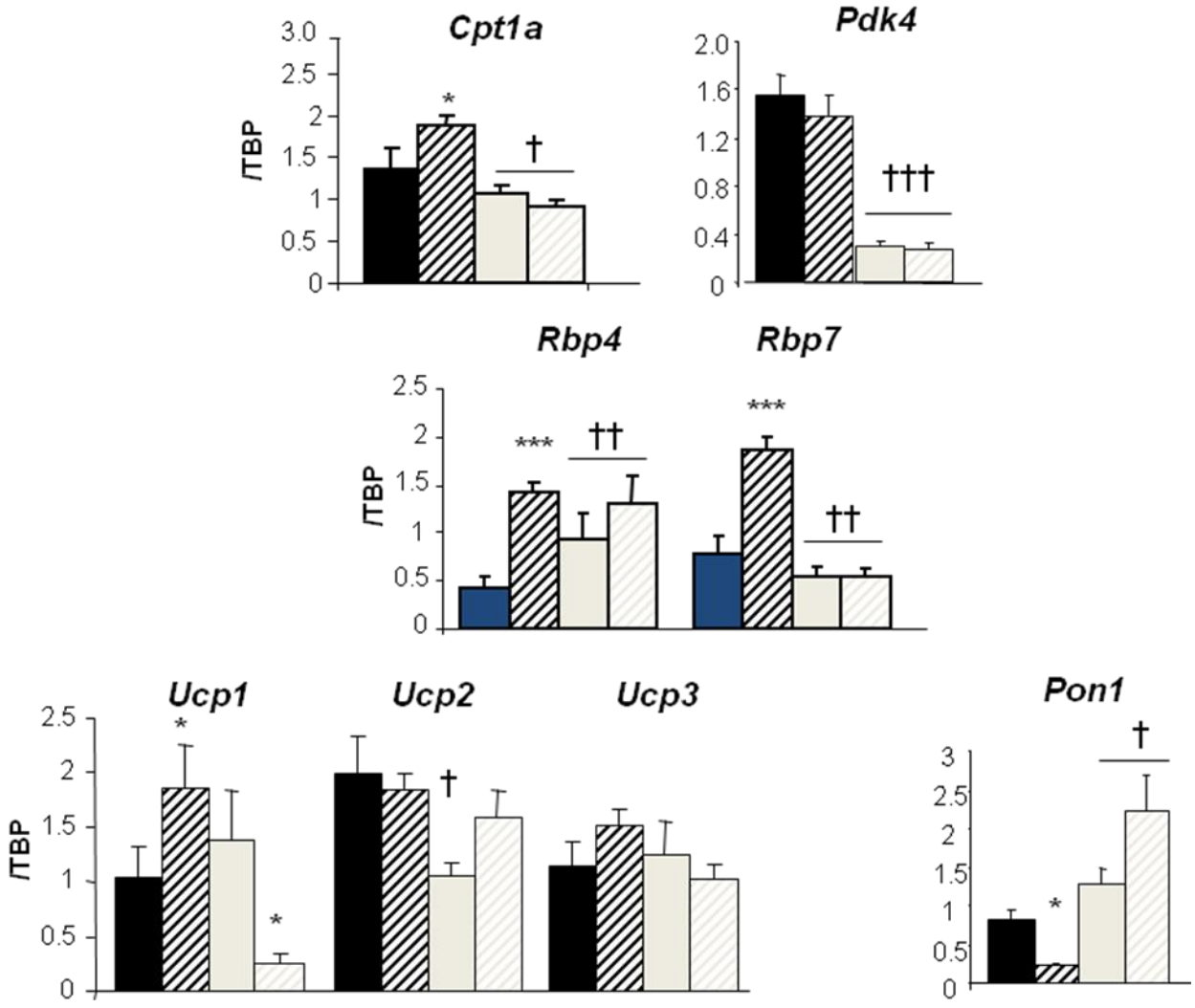

Figure 8.11: Divergent changes in expression of genes: real-time PCR analysis of cDNA from subcutaneous adipose tissue from Lean and Fat mice on control or high fat diet. Genes that were differentially expressed included carnitine palmityl trasnferase-1 (cpt1), pyruvate dehydrogenase kinase (pdk4), retinol binding protein 4 and 7 (rbp 4, rbp 7), uncoupling binding proteins 1 and 2 (ucp1, ucp2) and paraoxnase (pon1). No change in expression was in observed in uncoupling protein 3 (Ucp3). Black indicates control fed Fat mice (FC); black strip indicates Fat mice on high fat diet; grey colouring indicates Lean mice on control diet and grey strip is indicative of Lean mice on high fat diet. n=6. *p<0.05; **p<0.01; ***p<0.001; †††p<0.001. Two way ANOVA with *Bonferroni* post hoc test.

8.4.3 Top 20 genes whose expression was up-regulated in subcutaneous adipose of high fat fed Fat and Lean mice

Affymetrix Exon Gene ID	Name
6933072	Secreted phosphoprotein
6812214	Tubulin, beta 2A
6986031	Actin, alpha 1
6881092	Fibulin 7
6750546	Solute carrier family 11 (protein coupled divalent metal ion transporters), member 1
6762967	Proteoglycan 4 (megakarocyte stimulating factor, articular superficial zone protein)
6783044	RIKEN cDNA 1100001G20 gene
6985008	Dipeptidase 2
6945584	Thromboxane A synthase 1, platelet
6909083	UDP galactosyltransferase 8A
6751634	Glypican 1
6975367	Protein phosphatase 1, regulatory (inhibitor) subunit 3B
7019616	Brain expressed gene 1
6789316	ATPase, Na+/K+ transporting, beta 2 polypeptide
6841136	CD200 receptor 1
6947176	Regenerating islet-derived 1
6755210	CD84 antigen
7017134	Fibroblast growth factor 13
6958058	Glycogen synthase 2

Figure 8.12: Genes whose expressions were up-regulated in subcutaneous adipose tissue of Fat and Lean mice on high fat or control diet. n=6; Fold changes (>1.5) and p-values (<0.05) were calculated by Limma and adjusted, using Benjamini and Hochberg correction.

8.4.4 Top 20 genes were down regulated in their expression in subcutaneous adipose high fat fed Fat and Lean mice

Affymetrix Exon Gene ID	Name
6978332	Chemokine (C-C motif) ligand 22
6921229	Paired box gene5
6874979	Protein kinase C, theta
6939888	Ras association (RalGDS/AF-6), domain family member 6
6758691	Serine/theonine kinase 17b (apoptosis-inducing)
6862922	CD226 antigen
6779264	Pellino 1
6827943	G-protein coupled receptor 18
6868021	Fatty acid desaturase 1
6765166	Prospero-related homeobox 1
6814055	Zinc finger protein 874
6833100	Calcium channel, voltage dependent, beta 3 subunit
6943387	NEDD4 binding protein 2-like 1
6905422	Purinergic receptor P2Y, G-protein coupled 13
6921157	Suppression inducing transmembrane adaptor 1
6988701	CD3 antigen, delta polypeptide
6755216	SLAM family member 6
6910592	Interferon-induced protein 44
6803216	Serine peptidase inhibitor, clade A (alpha-1 antiproteinase, antitrypsin), member 10
6789359	Similar to Centaurin, beta 1

Figure 8.13: Genes whose expressions were down-regulated in subcutaneous adipose tissue of Fat and Lean mice on high fat or control diet. n=6; Fold changes (>1.5) and p-values (<0.05) were calculated by Limma and adjusted, using Benjamini and Hochberg correction.

8.4.5 Heatmap of angiogenic genes investigated in subcutaneous adipose of Fat and Lean mice

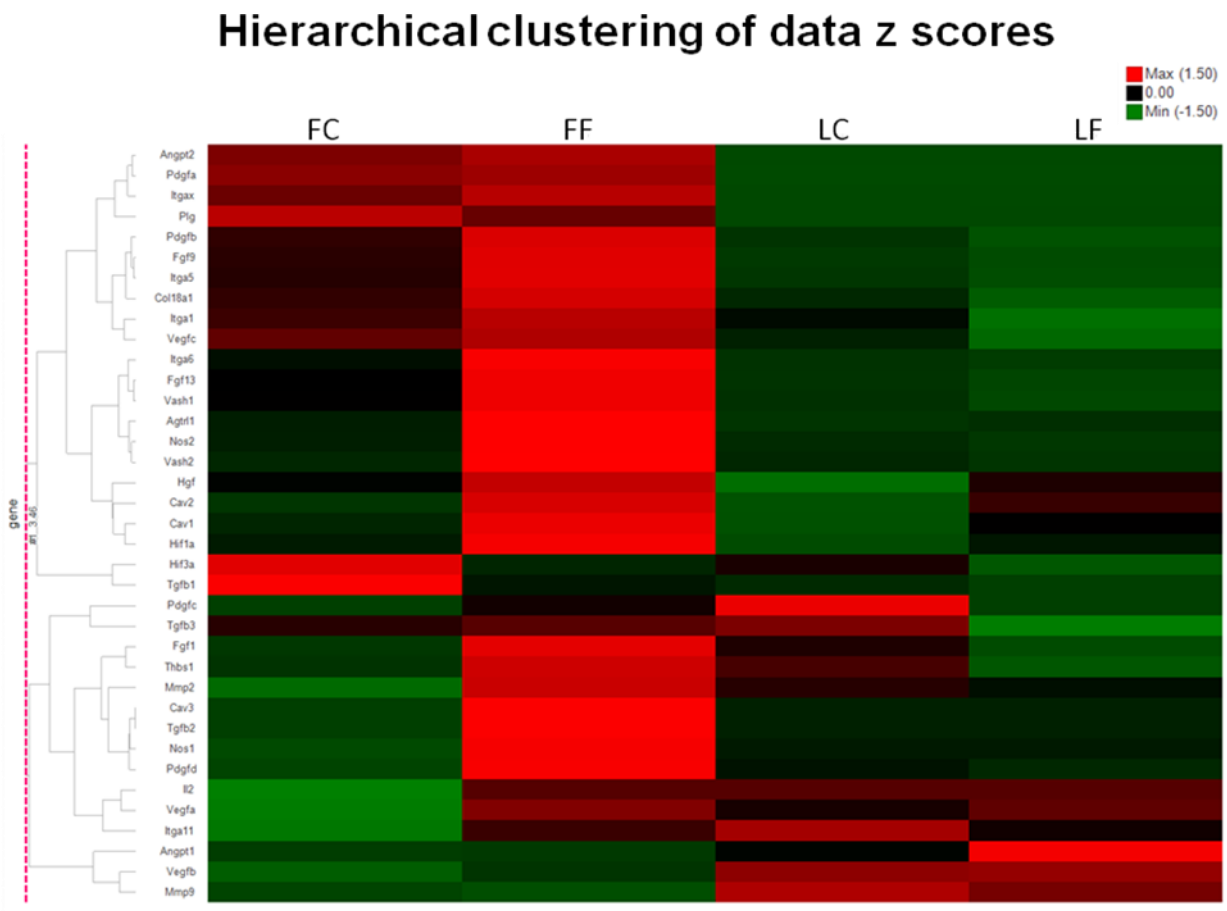

Figure 8.14: Heat map of angiogenic genes in Fat and Lean mice that have been high fat or control fed. Due to the high level of expression of vascular endothelial growth factor A (VEGFA), caveolin 1 (Cav1) and matrix metalloproteinase 2 (MMP2), the expression values have been transformed to a z score, allowing all the genes to be plotted on the same scale, with red indicating high levels of expression and green indicating low.

8.4.6 Full gene list of genes in which changed expression was observed in subcutaneous adipose of Fat and Lean mice

AFFYMETRIX EXON GENE ID	Name
6933072	secreted phosphoprotein 1
6812214	tubulin, beta 2A
6986031	actin, alpha 1, skeletal muscle
6881092	fibulin 7
6750546	solute carrier family 11 (proton-coupled divalent metal ion transporters), member 1
6762967	proteoglycan 4 (megakaryocyte stimulating factor, articular superficial zone protein)
6783044	RIKEN cDNA 1100001G20 gene
6803850	similar to creatine kinase, brain; predicted gene 12892; creatine kinase, brain
6768928	lanosterol synthase
6985008	dipeptidase 2
6945584	thromboxane A synthase 1, platelet
6909083	UDP galactosyltransferase 8A
6811689	histone cluster 1, H2ad; histone cluster 1, H2ae; histone cluster 1, H2ag; histone cluster 1, H2ah; histone cluster 1, H2ai; similar to histone 2a; histone cluster 1, H2an; histone cluster 1, H2ao; histone cluster 1, H2ac; histone cluster 1, H2ab
6751634	glypican 1
6975367	protein phosphatase 1, regulatory (inhibitor) subunit 3B
7019616	brain expressed gene 1
6972106	a disintegrin and metallopeptidase domain 8
6789316	ATPase, Na+/K+ transporting, beta 2 polypeptide
6841136	CD200 receptor 1
6947176	regenerating islet-derived 1
6755210	CD84 antigen
6930606	slit homolog 2 (Drosophila)
6777176	tryptophan hydroxylase 2
6787940	olfactory receptor 1396
6978869	similar to Chain A, D92n,D94n Double Point Mutant Of Human Nuclear Transport Factor 2 (Ntf2); predicted gene 10349; predicted gene 4682; nuclear transport factor 2; similar to nuclear transport factor 2; predicted gene 9386; predicted gene 10333
6872204	MAM domain containing 2
6843130	melanocortin 2 receptor accessory protein
7017134	fibroblast growth factor 13
6901634	solute carrier family 39 (metal ion transporter), member 8
6958058	glycogen synthase 2
6762197	PCTAIRE-motif protein kinase 3
6815558	predicted gene 8416; predicted gene 5593; cyclin B1; similar to cyclin B1; predicted gene 4870
6957059	complement component 3a receptor 1
6899682	cathepsin K
6813398	PDZ and LIM domain 7
6968778	mannosidase 2, alpha 2

6788851	epsin 2
6910173	cysteine rich protein 61
6775201	collagen, type XVIII, alpha 1
6849968	histocompatibility 2, class II antigen E beta2
6873065	cytochrome P450, family 2, subfamily c, polypeptide 70
6838417	predicted gene 7172; similar to tubulin, alpha 1; tubulin, alpha 1A
6874080	heat shock protein 12A
6803161	legumain
6957410	C-type lectin domain family 7, member a
6784564	mannose receptor, C type 2
6766372	microtubule-associated protein 7
6864813	sprouty homolog 4 (Drosophila)
6779843	SH3 and PX domains 2B
6784526	lin-52 homolog (C. elegans); predicted gene 7020
6775182	collagen, type VI, alpha 2
6974126	coagulation factor VII
6851324	EGF-like module containing, mucin-like, hormone receptor-like sequence 1
6981823	macrophage scavenger receptor 1
6763991	regulator of G-protein signaling 4
6861314	ENSMUSG00000063388
6879646	CD59b antigen
6977260	heme oxygenase (decycling) 1
6977656	uncoupling protein 1 (mitochondrial, proton carrier)
6866305	spire homolog 1 (Drosophila)
6882530	transformation related protein 53 inducible nuclear protein 2
6854419	tryptase alpha/beta 1
6878739	apelin receptor
6969698	monoacylglycerol O-acyltransferase 2
6958193	branched chain aminotransferase 1, cytosolic; similar to branched chain aminotransferase 1, cytosolic
6761687	transmembrane protein 37
6767613	popeye domain containing 3
6806791	CAP, adenylate cyclase-associated protein, 2 (yeast)
6946993	capping protein (actin filament), gelsolin-like
6778719	uridine phosphorylase 1
6834025	natriuretic peptide receptor 3
6871206	protein phosphatase 2, regulatory subunit B (B56), beta isoform
6868652	lactate dehydrogenase B; predicted gene 5514
6926948	retinol binding protein 7, cellular
6789325	CD68 antigen
6973527	leukocyte-associated Ig-like receptor 1
6833151	spermatogenesis associated, serine-rich 2
6951412	pyruvate dehydrogenase kinase, isoenzyme 4
6963534	microtubule associated monoxygenase, calponin and LIM domain containing 2

6899039	nestin
6757927	ankyrin repeat domain 23
6871009	RIKEN cDNA 2010003K11 gene
6970131	protein kinase C, delta binding protein
6980364	collagen, type IV, alpha 1
6986725	matrix metallopeptidase 3
6954269	prostaglandin D2 synthase 2, hematopoietic
7019615	transcription elongation factor A (SII)-like 5
6978290	metallothionein 2
6970944	cerebellar degeneration-related 2
6996438	anterior pharynx defective 1c homolog (C. elegans)
6855022	histocompatibility 2, class II antigen A, alpha; histocompatibility 2, class II antigen E alpha
6791229	plexin domain containing 1
6838578	chymotrypsin-like elastase family, member 1
6900994	breast cancer anti-estrogen resistance 3
6903360	predicted gene 5150; similar to SIRP beta 1 like 1 protein
6790294	chemokine (C-C motif) ligand 3
6764289	interferon activated gene 202B
6887520	SPC25, NDC80 kinetochore complex component, homolog (S. cerevisiae)
6760009	serine (or cysteine) peptidase inhibitor, clade E, member 2
7016678	apelin
6847556	a disintegrin-like and metallopeptidase (reprolysin type) with thrombospondin type 1 motif, 1
6782808	ArfGAP with dual PH domains 2
6760347	5-hydroxytryptamine (serotonin) receptor 2B
6937522	Wolfram syndrome 1 homolog (human)
6868058	solute carrier family 15, member 3
6792367	CD300 antigen like family member B
6809047	lipoma HMGIC fusion partner-like 2
6880393	thrombospondin 1; similar to thrombospondin 1
6919171	RIKEN cDNA B930041F14 gene
6768198	pterin 4 alpha carbinolamine dehydratase/dimerization cofactor of hepatocyte nuclear factor 1 alpha (TCF1) 1
6755896	dual specificity phosphatase 10
6870028	elongation of very long chain fatty acids (FEN1/Elo2, SUR4/Elo3, yeast)-like 3
6910621	nexilin
6807041	growth arrest and DNA-damage-inducible 45 gamma
6781515	microfibrillar-associated protein 4
6898138	pentraxin related gene
6993154	chemokine (C-C motif) receptor 5
6937227	spondin 2, extracellular matrix protein
6887282	growth factor receptor bound protein 14
6972750	paternally expressed 3; antisense transcript gene of Peg3
6942524	serine (or cysteine) peptidase inhibitor, clade E, member 1
6876543	NIMA (never in mitosis gene a)-related expressed kinase 6

6838694	keratin 79
6789540	smoothelin-like 2
6920713	sperm acrosome associated 1
6849595	cyclin-dependent kinase inhibitor 1A (P21)
6790536	glycerophosphodiester phosphodiesterase domain containing 1
6791069	beta-1,4-N-acetyl-galactosaminyl transferase 2
6803172	inositol 1,3,4-triphosphate 5/6 kinase
6876226	family with sequence similarity 129, member B
6918021	phospholipase A2, group IIE
6907246	histone cluster 2, H3b; histone cluster 1, H3f; histone cluster 1, H3e; histone cluster 2, H3c1; histone cluster 1, H3d; histone cluster 1, H3c; histone cluster 1, H3b; histone cluster 2, H3c2; histone cluster 2, H2aa1; histone cluster 2, H2aa2
6899756	hemochromatosis type 2 (juvenile) (human homolog)
6877909	dehydrogenase/reductase (SDR family) member 9
6920056	ATPase, H+ transporting, lysosomal V0 subunit D2
6806435	glucosaminyl (N-acetyl) transferase 2, I-branching enzyme
6972501	two pore segment channel 2
6813246	similar to NFIL3/E4BP4 transcription factor; nuclear factor, interleukin 3, regulated
6849951	myosin IF
6850834	triggering receptor expressed on myeloid cells 2
6978263	guanine nucleotide binding protein, alpha O
6998907	receptor transporter protein 3
6951783	protein phosphatase 1, regulatory (inhibitor) subunit 3A
6939130	OCIA domain containing 2
6875933	olfactomedin 1
6753068	RIKEN cDNA 5430435G22 gene
6772009	SAM and SH3 domain containing 1; predicted gene 2082
6893131	potassium voltage gated channel, Shab-related subfamily, member 1
6957185	CD9 antigen
6992493	doublecortin-like kinase 3
6964382	integrin alpha X
6944982	RIKEN cDNA 2310016C08 gene
6840357	HRAS-like suppressor
6957044	apolipoprotein B mRNA editing enzyme, catalytic polypeptide 1
6758435	solute carrier family 40 (iron-regulated transporter), member 1
6881028	acyl-Coenzyme A oxidase-like
6869293	lipase, gastric
6791520	mesenchyme homeobox 1
6913269	collagen, type XV, alpha 1
6975861	sorbin and SH3 domain containing 2
6986722	matrix metallopeptidase 12
6935074	transferrin receptor 2
6963854	transmembrane channel-like gene family 5
7019785	microrchidia 4

6876136	hemicentin 2
7011944	solute carrier family 6 (neurotransmitter transporter, creatine), member 8
6815739	regulator of G-protein signalling 7 binding protein
6983351	like-glycosyltransferase
6967059	serum amyloid A 3
6756386	lysophosphatidylglycerol acyltransferase 1
6949746	C-type lectin domain family 4, member d
6762784	regulator of G-protein signaling 2
6990216	similar to Annexin A2 (Annexin II) (Lipocortin II) (Calpactin I heavy chain) (Chromobindin-8) (p36) (Protein I) (Placental anticoagulant protein IV) (PAP-IV); annexin A2
6874000	actin filament associated protein 1-like 2
6988855	cell adhesion molecule 1
6896615	ubiquitin specific peptidase 13 (isopeptidase T-3)
6957046	growth differentiation factor 3
6751362	similar to UDP glycosyltransferase 1 family polypeptide A13; similar to UGT1.6; UDP glucuronosyltransferase 1 family, polypeptide A1; UDP glucuronosyltransferase 1 family, polypeptide A2; UDP glycosyltransferase 1 family, polypeptide A10; UDP glucuronosyltransferase 1 family, polypeptide A5; UDP glycosyltransferase 1 family, polypeptide A cluster; UDP glucuronosyltransferase 1 family, polypeptide A9; UDP glucuronosyltransferase 1 family, polypeptide A8; similar to UDP glycosyltransferase 1 family, polypeptide A8; UDP glucuronosyltransferase 1 family, polypeptide A7C; UDP glucuronosyltransferase 1 family, polypeptide A6A; similar to UDP glucuronosyltransferase 1 family, polypeptide A6B; UDP glucuronosyltransferase 1 family, polypeptide A6B
6972415	tumor necrosis factor receptor superfamily, member 22
6829971	transmembrane 7 superfamily member 4
6956867	ret proto-oncogene
6824763	solute carrier family 7 (cationic amino acid transporter, y+ system), member 8
6849237	protease, serine, 21
6897557	periostin, osteoblast specific factor
6959000	reticulon 2 (Z-band associated protein)
6864776	protocadherin 1
6784236	ATPase, H+ transporting, lysosomal V0 subunit A1
7015521	cytochrome b-245, beta polypeptide
6790670	noggin
6944966	leptin
7013185	toll-like receptor 13
6947987	fibulin 2
6950137	C-type lectin domain family 12, member a
6935402	diacylglycerol lipase, beta
7011394	four and a half LIM domains 1
6761998	zinc finger, RAN-binding domain containing 3
6892286	syntrophin, acidic 1
6767844	nephrocan
6822367	integrin, beta-like 1
6922541	multiple EGF-like-domains 9
7019519	galactosidase, alpha
6768479	early growth response 2
6946055	glycoprotein (transmembrane) nmb

6976472	microfibrillar-associated protein 3-like
6897908	purinergic receptor P2Y, G-protein coupled 1
6956497	oxytocin receptor
6850534	phospholipase A2, group VII (platelet-activating factor acetylhydrolase, plasma)
6946749	TNFAIP3 interacting protein 3
6820752	protocadherin 17
6921161	tropomyosin 2, beta
7011757	fragile X mental retardation syndrome 1 homolog
7016887	family with sequence similarity 122, member B
6856133	solute carrier family 5 (choline transporter), member 7
7014110	ring finger protein 128
6896351	arylacetamide deacetylase-like 1
6952601	solute carrier family 35, member B4
6854260	tumor necrosis factor receptor superfamily, member 12a
6941182	transmembrane protein 119
6917374	fatty acid binding protein 3, muscle and heart; similar to mammary-derived growth inhibitor
6997037	RIKEN cDNA 2310046A06 gene
6807609	RIKEN cDNA 2010111I01 gene
6758414	collagen, type V, alpha 2
6838809	integrin alpha 5 (fibronectin receptor alpha)
6964250	family with sequence similarity 57, member B
6968735	alanyl (membrane) aminopeptidase
6811046	ryanodine receptor 2, cardiac
6932509	starch binding domain 1
6875649	interleukin 1 receptor antagonist
6996448	tropomyosin 1, alpha
6932718	bone morphogenetic protein 3
7007379	isoamyl acetate-hydrolyzing esterase 1 homolog (S. cerevisiae)
6765218	activating transcription factor 3
6855071	mutS homolog 5 (E. coli)
6820040	lysyl oxidase-like 2
6769635	synaptonemal complex protein 3
6837144	similar to platelet-derived growth factor B chain; platelet derived growth factor, B polypeptide
6872783	lysosomal acid lipase A
6971277	nuclear protein 1
6938217	RIKEN cDNA 2310045A20 gene
6957412	oxidized low density lipoprotein (lectin-like) receptor 1
6850284	ubiquitin D
6767782	glycoprotein 49 A; leukocyte immunoglobulin-like receptor, subfamily B, member 4
6762796	regulator of G-protein signaling 1
6791528	dual specificity phosphatase 3 (vaccinia virus phosphatase VH1-related)
6891880	CD93 antigen
7010355	tissue inhibitor of metalloproteinase 1

6969838	purinergic receptor P2Y, G-protein coupled 2
6789609	olfactory receptor 380; hypothetical protein LOC100044155; olfactory receptor 75, pseudogene 1
6951302	tissue factor pathway inhibitor 2
7017520	gamma-aminobutyric acid (GABA) A receptor, subunit alpha 3
6993713	collagen, type V, alpha 3
6989861	lactase-like
6819442	fibroblast growth factor 9
6904303	transient receptor potential cation channel, subfamily C, member 3
6784845	potassium inwardly-rectifying channel, subfamily J, member 2
6871545	membrane-spanning 4-domains, subfamily A, member 7
6755054	regulator of G-protein signaling 5
6755055	regulator of G-protein signaling 5
6983162	neurocan; similar to Neurocan
7011263	PHD finger protein 6
7020800	toll-like receptor 8
6819602	ADP-ribosylation factor-like 11
6883184	solute carrier family 2 (facilitated glucose transporter), member 10
6885873	lipocalin 2
6927227	RIKEN cDNA 2810405K02 gene
6818696	lectin, galactose binding, soluble 3
6892190	dual specificity phosphatase-like 15
6855068	DNA segment, Chr 17, human D6S56E 5
6890205	DnaJ (Hsp40) homolog, subfamily C, member 17; predicted gene 6257
6974003	collagen, type IV, alpha 2
6819910	adrenergic receptor, alpha 1a
6932374	chemokine (C-X-C motif) ligand 1
6865100	dihydropyrimidinase-like 3
6760917	peptidylglycine alpha-amidating monooxygenase
6872791	solute carrier family 16 (monocarboxylic acid transporters), member 12
6882774	family with sequence similarity 83, member D
6807201	unc-5 homolog A (C. elegans)
6830505	DEP domain containing 6
6991383	procollagen lysine, 2-oxoglutarate 5-dioxygenase 2
6946004	ATPase, H+ transporting, lysosomal V0 subunit E2
6789397	B-cell CLL/lymphoma 6, member B
6792129	ATP-binding cassette, sub-family A (ABC1), member 5
6765276	glutathione S-transferase, pi 2; glutathione S-transferase, pi 1; similar to glutathione S-transferase pi class A; predicted gene 3934
6899378	S100 calcium binding protein A8 (calgranulin A)
6971758	a disintegrin and metallopeptidase domain 12 (meltrin alpha)
6994678	solute carrier family 37 (glycerol-3-phosphate transporter), member 2
6945831	olfactory receptor 438
6762804	regulator of G-protein signaling 18
7016409	family with sequence similarity 70, member A

6754867	family with sequence similarity 78, member B
6785111	ENSMUSG00000083237
6873179	secreted frizzled-related sequence protein 5
6852750	pleckstrin homology domain containing, family H (with MyTH4 domain) member 2
6935150	family with sequence similarity 20, member C
6819250	fat storage-inducing transmembrane protein 1
6856202	RIKEN cDNA 2310076L09 gene
6893558	prostate transmembrane protein, androgen induced 1; similar to Nedd4 WW binding protein 4
6978332	chemokine (C-C motif) ligand 22
6921229	paired box gene 5
6910648	ST6 (alpha-N-acetyl-neuraminyl-2,3-beta-galactosyl-1,3)-N-acetylgalactosaminide alpha-2,6-sialyltransferase 5
6874979	protein kinase C, theta
6939888	Ras association (RalGDS/AF-6) domain family member 6
6989238	cholinergic receptor, nicotinic, alpha polypeptide 5
6758691	serine/threonine kinase 17b (apoptosis-inducing)
6789359	similar to Centaurin, beta 1
6941780	ras homolog gene family, member f
6862922	CD226 antigen
6814044	zinc finger protein 874
6833100	calcium channel, voltage-dependent, beta 3 subunit
6779264	pellino 1
6943387	NEDD4 binding protein 2-like 1
6905422	purinergic receptor P2Y, G-protein coupled 13
6803216	serine (or cysteine) peptidase inhibitor, clade A (alpha-1 antiproteinase, antitrypsin), member 10
6800913	predicted gene 7511; polymerase (RNA) II (DNA directed) polypeptide H
6945066	family with sequence similarity 40, member B
6827943	G protein-coupled receptor 18
6921157	suppression inducing transmembrane adaptor 1
6906433	RIKEN cDNA D930015E06 gene
6926974	phosphatidylinositol 3-kinase catalytic delta polypeptide; RIKEN cDNA 2610208K16 gene
6992091	copine IV
6988701	CD3 antigen, delta polypeptide
6868021	fatty acid desaturase 1
6765166	prospero-related homeobox 1
6755216	SLAM family member 6
6960404	D site albumin promoter binding protein
6906721	Rhesus blood group-associated B glycoprotein
6971264	CD19 antigen
6910592	interferon-induced protein 44
6961289	family with sequence similarity 169, member B
6832005	GRB2-related adaptor protein 2
6900254	DENN/MADD domain containing 2D
6946021	GTPase, IMAP family member 8

6749835	CD28 antigen; similar to CD28 antigen
6814055	zinc finger protein 87
6850011	histocompatibility 2, O region alpha locus
6767468	sex comb on midleg-like 4 (Drosophila)
6803524	B-cell leukemia/lymphoma 11B
6945699	similar to protein tyrosine phosphatase domain containing 1 protein; protein tyrosine phosphatase domain containing 1; predicted gene 2719
6992920	predicted gene 9323; predicted gene 7516; ribosomal protein SA pseudogene; predicted gene 9819; predicted gene 6339; predicted gene 9083; ribosomal protein SA; predicted gene 13374; predicted gene 12595; similar to laminin receptor 1 (ribosomal protein SA); predicted gene 13208; predicted gene 12113; predicted gene 5498; similar to 40S ribosomal protein SA (p40) (34/67 kDa laminin receptor); predicted gene 7549
6995161	CD3 antigen, epsilon polypeptide
6901380	lymphoid enhancer binding factor 1
6983286	FCH domain only 1
6887081	lymphocyte antigen 75
6886953	cytohesin 1 interacting protein
6782286	integrin alpha E, epithelial-associated
6754681	selectin, lymphocyte
6828699	prolactin receptor
6977814	glutamic pyruvate transaminase (alanine aminotransferase) 2
6765321	TRAF3 interacting protein 3
6973937	tumor necrosis factor (ligand) superfamily, member 13b
6772829	A kinase (PRKA) anchor protein 7
6903056	interleukin 7
6965314	tetraspanin 32
6971341	septin 1
6850128	lymphotoxin B
6868909	RIKEN cDNA C030016D13 gene
6878045	Rap guanine nucleotide exchange factor (GEF) 4
6810688	predicted gene 8990; neuroepithelial cell transforming gene 1
6980089	Fc receptor, IgE, low affinity II, alpha polypeptide
6850177	corneodesmosin; hypothetical protein LOC100043961
6790288	chemokine (C-C motif) ligand 5
6910597	prostaglandin F receptor
6959279	cytochrome P450, family 2, subfamily f, polypeptide 2
6930006	hypothetical protein LOC665705
6867653	cardiotrophin-like cytokine factor 1
6845435	CD86 antigen
6769179	calponin 2
6848579	chemokine (C-C motif) receptor 6
6775762	similar to FEX2; stabilin 2
6792832	CD7 antigen
6764274	predicted gene 2785
7013205	purinergic receptor P2Y, G-protein coupled 10
7017601	Rho GTPase activating protein 4

7010644	dedicator of cytokinesis 11
6847190	SAM domain, SH3 domain and nuclear localization signals, 1
6811368	RIKEN cDNA A530099J19 gene
6764038	Fc receptor, IgG, low affinity IIb
6880987	dual specificity phosphatase 2
6989422	cytochrome P450, family 1, subfamily a, polypeptide 1
6769033	icos ligand
6943142	FMS-like tyrosine kinase 3
6863755	desmocollin 3
6958078	ST8 alpha-N-acetyl-neuraminide alpha-2,8-sialyltransferase 1
6848556	tubulin tyrosine ligase-like family, member 2; predicted gene, ENSMUSG00000079713
7017672	coagulation factor VIII
6844819	claudin 1
6868105	membrane-spanning 4-domains, subfamily A, member 6B
6993481	folate receptor 4 (delta)
6855088	lymphotoxin A
6963895	acyl-CoA synthetase medium-chain family member 3
6791310	chemokine (C-C motif) receptor 7
6759951	cDNA sequence BC035947
6960178	kallikrein related-peptidase 8
6950985	lymphoid-restricted membrane protein
6960144	natural killer cell group 7 sequence
6780570	hepatitis A virus cellular receptor 1
6908073	glutathione S-transferase, mu 7
6942960	BAI1-associated protein 2-like 1
6922301	AT-hook transcription factor
6836959	predicted gene 8221; apolipoprotein L 7c
6748889	interleukin 18 receptor 1
6791881	similar to epithelial protein lost in neoplasm; LIM domain containing 2
6871542	membrane-spanning 4-domains, subfamily A, member 1
6824838	transglutaminase 1, K polypeptide
6769159	complement factor D (adipsin)
6871509	CD5 antigen
6870971	cDNA sequence BC021614
7018531	predicted gene 614; interleukin 2 receptor, gamma chain
6977119	cDNA sequence BC049349
6760518	similar to ADP-ribosylation factor-like protein 7; ADP-ribosylation factor-like 4C
6838828	glycosylation dependent cell adhesion molecule 1
6838716	integrin beta 7
6946920	CD8 antigen, alpha chain
6857769	3-hydroxyanthranilate 3,4-dioxygenase
6947932	Kruppel-like factor 15
6919417	thymocyte selection-associated high mobility group box; similar to thymus high mobility group box protein TOX

6775151	glutathione S-transferase, theta 1
6952137	Ca2+dependent activator protein for secretion 2
6805430	cytidine monophospho-N-acetylneuraminic acid hydroxylase
6980090	C-type lectin domain family 4, member g
6766351	interleukin 22 receptor, alpha 2
6960382	branched chain aminotransferase 2, mitochondrial
6885432	ficolin A
6871471	fatty acid desaturase 2
7016321	septin 6
6898996	Fc receptor-like 1
6820472	epithelial stromal interaction 1 (breast)
6841187	B and T lymphocyte associated
6839897	UDP-GlcNAc:betaGal beta-1,3-N-acetylglucosaminyltransferase 5
6861458	adenomatosis polyposis coli down-regulated 1
6861776	melanocortin 5 receptor
6870489	programmed cell death 4
7014854	G protein-coupled receptor 64
6940646	macrophage activation 2 like
6988366	sodium channel, voltage-gated, type III, beta
7018687	zinc finger, DHHC domain containing 15
6805825	interferon regulatory factor 4
6800236	zinc finger protein 277
6822443	deoxyribonuclease 1-like 3
7011413	CD40 ligand
6841201	germinal center expressed transcript 2
6782102	macrophage galactose N-acetyl-galactosamine specific lectin 2
6754799	CD247 antigen
6747472	alcohol dehydrogenase, iron containing, 1
6964163	interleukin 21 receptor
6925575	lymphocyte protein tyrosine kinase
6785114	RAB37, member of RAS oncogene family
6932571	chemokine (C-X-C motif) ligand 13
6965115	cytochrome P450, family 2, subfamily e, polypeptide 1
6784205	2',3'-cyclic nucleotide 3' phosphodiesterase
6871117	cathepsin W
6866852	solute carrier family 14 (urea transporter), member 1
6870980	TBC1 domain family, member 10c
6769181	histocompatibility (minor) HA-1
6924750	fatty acid amide hydrolase
6867646	protein tyrosine phosphatase, receptor type, C polypeptide-associated protein
6984372	expressed sequence AU018778
6763295	Ral GEF with PH domain and SH3 binding motif 2
6849761	similar to axonemal dynein heavy chain 8 long form; similar to dynein, axonemal, heavy chain 8; dynein, axonemal, heavy chain 8

6988706	myelin protein zero-like 2
6859850	calcium/calmodulin-dependent protein kinase IV
6992950	predicted gene 9811; ribosomal protein L14
6960301	interleukin 4 induced 1
6844373	immunoglobulin lambda chain, constant region 2; immunoglobulin lambda chain, constant region 1; immunoglobulin lambda chain, variable 1
6902179	mucolipin 3
6966327	hepcidin antimicrobial peptide
6782989	schlafen 1
6828417	ribosomal protein L37
6980091	CD209a antigen
6941029	peroxisomal membrane protein 2
6817903	choline dehydrogenase
6937056	solute carrier family 5 (sodium-dependent vitamin transporter), member 6
6855981	special AT-rich sequence binding protein 1
6907624	CD2 antigen
6959165	CD79A antigen (immunoglobulin-associated alpha)
6886021	TNF receptor-associated factor 1
6891879	thrombomodulin
6960140	sialic acid binding Ig-like lectin G
6939076	TXK tyrosine kinase
6902183	mucolipin 2
6900279	expressed sequence AI504432
6917630	UBX domain protein 11
6968314	multiple C2 domains, transmembrane 2
6915847	leptin receptor
6753067	cathepsin E
6771794	RIKEN cDNA 5830405N20 gene
6749852	inducible T-cell co-stimulator; similar to activation-inducible lymphocyte immunomediatory molecule AILIM
6819887	similar to clusterin; clusterin
6912477	BTB and CNC homology 2
6766839	thymocyte selection pathway associated
6837013	thiosulfate sulfurtransferase, mitochondrial
6763706	ATPase, Na^+ transporting, beta 1 polypeptide
6918015	phospholipase A2, group IID
6778784	IKAROS family zinc finger 1
6878712	solute carrier family 43, member 1
6876740	Rho GTPase activating protein 15
6844316	proline dehydrogenase
6850645	nuclear factor of kappa light polypeptide gene enhancer in B-cells inhibitor, epsilon
6919497	carbonic anhydrase 8; similar to Carbonic anhydrase-related protein (CARP) (CA-VIII)
6812261	RIKEN cDNA 1810022C23 gene
6970445	lymphatic vessel endothelial hyaluronan receptor 1
6846386	centrosomal protein 97

6827944	G protein-coupled receptor 183
6950170	killer cell lectin-like receptor, subfamily D, member 1
6922324	tumor necrosis factor (ligand) superfamily, member 8
6779827	neuron specific gene family member 2
6988722	FXYD domain-containing ion transport regulator 6
6810063	ELOVL family member 7, elongation of long chain fatty acids (yeast)
6879140	carbohydrate (keratan sulfate Gal-6) sulfotransferase 1
6849771	ubiquitin associated and SH3 domain containing, A
6980107	similar to SIGNR2; CD209c antigen
7011124	RIKEN cDNA 2610018G03 gene
6845933	SID1 transmembrane family, member 1
6778057	diacylglycerol kinase, alpha
6923313	predicted gene 12669; glutaredoxin 3
6953424	similar to immunity-associated nucleotide 4; GTPase, IMAP family member 3
6983819	interleukin 27 receptor, alpha
6929144	predicted gene 9209; armadillo repeat containing 10
6991264	cathepsin H
6953810	indolethylamine N-methyltransferase
6791914	CD79B antigen
6883125	matrix metallopeptidase 9
6957051	solute carrier family 2 (facilitated glucose transporter), member 3
6890068	RAS guanyl releasing protein 1
6846497	ST3 beta-galactoside alpha-2,3-sialyltransferase 6
6764349	regulator of G protein signaling 7
6775471	sphingosine-1-phosphate receptor 4
6995158	CD3 antigen, gamma polypeptide
6971280	sulfotransferase family 1A, phenol-preferring, member 1
6814050	zinc finger protein 58
6971287	coronin, actin binding protein 1A
6900141	protein tyrosine phosphatase, non-receptor type 22 (lymphoid)
6998930	mutL homolog 1 (E. coli)
6981328	adrenergic receptor, beta 3
6984452	RIKEN cDNA 9330175E14 gene
6787769	IL2-inducible T-cell kinase
6915567	hook homolog 1 (Drosophila)
6798334	a disintegrin and metallopeptidase domain 6B
6761701	macrophage receptor with collagenous structure
6954000	family with sequence similarity 13, member A
6850135	histocompatibility 2, D region; histocompatibility 2, D region locus 1
6787918	protease (prosome, macropain) 28 subunit beta B, pseudogene; similar to Proteasome activator complex subunit 2 (Proteasome activator 28-beta subunit) (PA28beta) (PA28b) (Activator of multicatalytic protease subunit 2) (11S regulator complex beta subunit) (REG-beta); proteasome (prosome, macropain) 28 subunit, beta; predicted gene 7928
6848553	similar to T-cell activation Rho GTPase-activating protein; T-cell activation Rho GTPase-activating protein; T-cell activation GTPase activating protein 1

6989054	POU domain, class 2, associating factor 1
6867853	mitogen-activated protein kinase kinase kinase kinase 2
6748662	zeta-chain (TCR) associated protein kinase
6989015	interleukin 18
6764036	Fc receptor-like A
6765460	complement receptor 2
6755378	kynurenine 3-monooxygenase (kynurenine 3-hydroxylase)
6969832	RELT tumor necrosis factor receptor
6988713	sodium channel, voltage-gated, type II, beta
6850149	histocompatibility 2, Q region locus 10
6825311	B lymphoid kinase
6868091	membrane-spanning 4-domains, subfamily A, member 4C
6946912	CD8 antigen, beta chain 1
6940658	ATP-binding cassette, sub-family G (WHITE), member 3
6762147	Ras association (RalGDS/AF-6) domain family member 5
6768827	protocadherin 15
6871511	CD6 antigen
6807882	zinc finger protein 273
6993142	chemokine (C-X-C motif) receptor 6
6919212	tumor necrosis factor receptor superfamily, member 18
6788172	transcription factor 7, T-cell specific
6959616	suprabasin
6928871	sema domain, immunoglobulin domain (Ig), short basic domain, secreted, (semaphorin) 3A; hypothetical protein LOC100044161
6971260	linker for activation of T cells
6966320	free fatty acid receptor 1
6889891	gremlin 1
6970166	hypothetical protein LOC100044265; predicted gene 4759
6885855	family with sequence similarity 78, member A; hypothetical protein LOC100047386
6777310	lysozyme 1
6995099	chemochine (C-X-C motif) receptor 5
6868096	membrane-spanning 4-domains, subfamily A, member 4B
6966322	CD22 antigen; hypothetical protein LOC100047973
6860035	prenatal ethanol induced mRNA, pseudogene
6780572	T-cell immunoglobulin and mucin domain containing 4
6998434	acid phosphatase, prostate
6835353	angiopoietin 1
6951396	paraoxonase 1
6785865	insulin-like growth factor binding protein 3
6957141	CD4 antigen

Figure 8.17: Gene set enrichment list of genes differentially expressed in subcutaneous adipose tissue of Fat and Lean mice on high fat or control diet. n=6; Fold changes (>1.5) and p-values (<0.05) were calculated by Limma and adjusted, using Benjamini and Hochberg correction.

References

Aarden LA (1989). Hybridoma growth factor. Annals of the New York Academy of Sciences 557: 192-198.

Abumrad NA, el Maghrabi MR, Amri EZ, Lopez E, Grimaldi PA (1993). Cloning of a rat adipocyte membrane protein implicated in binding or transport of long chain fatty acids that is induced during preadipocyte differentiation. Homology with human CD36. Journal of Biological Chemistry. 268: 17665-17668.

Adams JC (2001). Thrombospondins: multifunctional regulators of cell interactions. Annual Reviews Cell and Developmental Biology 17, 25-51.

Aitman TJ, Glazier Am, Wallace CA, Cooper LD, Norsworthy PJ, Wahid FN, Majali KM, Trembling PM, Mann CJ, Shoulders CC, Graf D, Lezin E, Kurtz RW, Kren V, Pravenec M, Ibrahimi A, Abumrad NA, Stanton LW, Scott J (1999). Identification of CD36 (Fat) as an insulin resistance gene causing defective fatty acid and glucose metabolism in hypertensive rats. Nature Genetics. 21: 76-83.

Agah A, Kyriakides TR, Lawler J, Bornstein P (2002). The lack of thrombospondin-1 (TSP-1) dictates the course of wound healing in double TSP-1/TSP-2 null mice. American Journal of Pathophysiology 161: 831-839.

Ailhaud G, Grimaldi P, Negrel R (1992). Cellular and molecular aspects of adipose tissue development. Annual Reviews of Nutrition 12: 207-233.

Andersson K, Gaudiot N, Ribiere C, Elizalde M, Giudicelli Y and Arner P (1999). A nitric oxide-mediated mechanism regulates lipolysis in human adipose tissue *in vivo*. British Journal of Pharmacology 126: 1639-1645.

Andrade S, Fan TP, Lewis GP (1987). Quantitative in-vivo studies on angiogenesis in a rat sponge model. British Journal of Experimental Pathology 68:755–766.

Aoki S, Toda S, Sakemi T, Sugihara H (2003). Coculture of endotheial cells and mature adipocytes actively promotes immature preadipocyte developmnent *in vitro*. Cell Structure and Function **28**:55-60.

Araki K, Araki M, Miyazaki J, Vassalli P (1995). Site-specific recombination of a transgene in fertilized eggs by transient expression of Cre recombinase. Proceedings of the National Academy of Sciences USA 92: 160-164.

Archer S (1993). Measurement of nitric oxide in biological models. ASEB Journal 7: 349-360.

Arkan Mc, Hevener AL, Greten FR, Arkan M, Hevener AL, Greten FR, Maeda S, Li Z, Long J, Wynshaw-Boris A, Poli G, Olefsky J, Karin M (2005). IKK-beta links inflammation to obesity-induced insulin resistance. Nature Medicine 11:191-198.

Armstrong LC and Bornstein P (2003). Thrombospondin 1 and 2 function as inhibitors of angiogenesis. Matrix Biology 22, 63-71.

Arner P (1996). Regulation of lipolysis in fat cells. Diabetes Review 4: 450-463.

Arner E, Westermark PO, Spalding KL, Britton T, Ryden M, Frisen J, Bernard S, Arner P (2009). Adipocyte turnover: relevance to human adipose tissue morphology. Diabetes 59: 105-9.

Asahara T, Murohara T, Sullivan A, Silver M, van der zee R, Li T, Witzenbichler B, Schatteman G, Isner J (1997). Isolation of putative progenitor endothelial cells for angiogenesis. Science 275: 964-966.

Asano A, Irie Y, Saito M (2001). Isoform-specific regulation of vascular endothelial growth factor (VEGF) family RNA expression in cultured mouse brown adipocytes. Molecular and Cellular Endocrinology 174: 71-76.

Ashburner M, Ball CA, Blake JA, Botstein D, Butler H, Cherry JM, Davis AP, Dolinski K, Dwight SS, Eppig JT, Harris MA, Hill DP, Issel-Tarver L, Kasarskis A, Lewis S, Matese JC, Richardson JE, Ringwald M, Rubin GM, Sherlock G. (2000) Gene ontology: tool for the unification of biology. The Gene Ontology Consortium. Nature Genet 25: 25-29.

Assimacopoulos-Jeannet F, Brichard S, Rencurel F, Cusin I, Jeanrenaud B (1995). *In vivo* effects of hyperinsulinemia on lipogenic enzymes and glucose transporter expression in rat liver and adipose tissues. Metabolism 44: 228-233.

Auberbach R, Akhtar N, Lewis RL, Shinners BL (2000). Angiogenesis assays: problems and pitfalls. Cancer Metastasis Reviews 19: 167-172.

Auerbach, R., Lewis, R., Shinners, B., Kubai, L., Akhtar, N. (2003) Angiogenesis Assays: A Critical Overview. Clinical Chemistry 49*:* 32-40*.*

Bai Y, Zhang S, Kim KS, Lee JK and Kim KH (1996). Obese gene expression alters the ability of 3OA5 preadipocytes respond to lipogenic hormones. Journal of Biological Chemistry 271: 13939-13942.

Banerjee RR, Rangwala SM, Shapiro JS, Rich AS, Rhoades B, Qi Y, Wang J, Rajala MW, Pocai A, Scherer PE, Steppan CM, Ahima RS, Obici S, Rossetti L, Lazar MA (2004). Regulation of fasted blood glucose by resistin. Science 303: 1195-1198.

Baranova A, Schlauch K, Gowder S, Collantes R, Chandhoke V, Younossi ZM (2005). Microarray technology in the study of obesity and non-alcoholic fatty liver disease. Liver International 25: 1091-1096.

Barros LF, Young M, Saklatvala J, Baldwin SA (1997). Evidence of two mechanisms for the activation of the glucose transporter GLUT1 by anisomycin:

p38 (MAPK kinase) activation and protein synthesis inhibition in mammalian cells. Journal of Physiology 504: 517-525.

Bayraktar M, Dundar S, Kirazli S, Teletar F (1994). Platelet factor 4, beta-thromboglobulin and thrombospondin levels in type I diabetes mellitus patients. Journal of International Medical Research 22: 90-94.

Beck L Jr. and D'Amore PA (1997). Vascular development: cellular and molecular regulation. Faseb Journal 11(5): 365-73.

Bell LN, Cai L, Johnstone BH, Traktuev DO, March KL, Considine RV (2007). A central role for hepatocyte growth factor in adipose tissue angiogenesis. American Journal of Physiolgy and Endcrinology Metabolism 294: E336-344.
Bender JE, Vishwanath K, Moore LK, Brown JQ, Chang V, Palmer GM, Ramanujam N (2009). A robust Monte Carlo model for the extraction of biological absorption and scattering *in vivo*. Biomedical Engineering (IEEE Transactions) 56: 960-968.

Benelli R, Albini A (1999). In vitro models of angiogenesis: the use of Matrigel. International Journal of Biological Markers 14: 243-246.

Benny O, Fainaru O, Adini A, Cassiola F, Bazinet L, Adini I, Pravada E, Nahmias Y, Koirala S, Corfas G, D'Amato RJ, Folkman J (2008). An orally delivered small-molecule formulation with antiangiogenic and anticancer activity. Nature Biotechnoloigy 26: 799-807.

Berger R, Albelda SM, Berd D, Ioffreda M, Whitaker D, Murphy GF (1993). Expression of platelet-endothelial cell adhesion molecule-1 (PECAM-1) during melanoma-induced angiogenesis *in vivo*. Journal of Cutaneous Pathology 20:399-406.

Bernstein E, Caudy A, Hammond S, Hannon G (2001). Role of bidentate ribonuclease in the initiation step of RNA interference. Nature 409: 363-366.

Bezaire V and Langin D (2009). Regulation of adipose tissue lipolysis revisted. Proceedings of the Nutrition Society 68: 350-360.

Birgel M, Gottschling-Zeller H, Röhrig K, Hauner H (2000). Role of cytokines in the regulation of plasminogen activator inhibitor-1 expression and secretion in newly differentiated subcutaneous human adipocytes. Arteriosclerosis, Thrombosis and Vascular Biology**;** 20: 1682-1687.

Bischoff J (1997). Cell adhesion and angiogenesis. Journal of Clinical Investigation 100: S37-9.

Blacher S, Devy L, Burbridge MF, Roland G, Tucker G, Noel A, Foidart JM (2001). Improved quantification of angiogenesis in the rat aortic ring assay 4:2: 133-142.

Black MA, Heick HM, Begin-Heick N (1988). Abnormal regulation of cAMP accumulation in pancreatic islets of obese mice. American Journal of Physiology 255(6 Pt 1): E833-8.

Bjorntorp P, Berchtold P, Berchtold P, Holm J, Larsson B (1971). The glucose uptake of human adipose tissue in obesity. European Journal of Clinical Investigation 1: 480-5.

Bjorntorp P, Karlsson M and Pettersson P (1982). Expansion of adipose tissue storage capacity at different ages in rats. Metabolism 31: 366-373.

Boden G (2001). Pathogenesis of type 2 diabetes, insulin resistance. Endocrinology Metabolism Clinical North AM 30: 801-815.

Bonen A, Luiken JJFP, Liu S, Dyck DJ, Kiens B, Kristiansen S, Turcotte LP, Van der Vusse GJ, Glatz JFC (1998). Palmitate transport and fatty acid transporters in red and white muscles. American Journal of Physiology Endocrinology Metabolism 275: 471-478.

Bonnefoy A, Moura R, Hoylaerts MF (2008). The evolving role of thrombospondin-1 in haemostasis and vascular biology. Cell Molecular Life Sciences 65: 713-727.

Bornstein P (1992). Thrombospondins: structure and regulation of expression. The Journal of the Federation of American Societies for Experimental Biology (FASEB) Journal 6: 3290-3299.

Bornstein P (1995). Diversity of function is inherent in matricellular proteins: an appraisal of thrombospondin 1. Journal of Cellular Biology 130: 503-506.

Bornstein P (2001). Thrombospondins as matricellular modulators of cell function. Journal of Clinical Investigation 107:927-934.

Borradaile NM, Han X, Harp JD, Gale SE, Ory DS, Schaffer JE (2006). Disruption of endoplasmic reticulum structure and integrity in lipotoxic cell death. Journal of Lipid research 12: 2726-2737.

Bouloumie A, Lolmede K, Sengenes C, Galitzky J, Lafontan M (2002). Angiogenesis in adipose tissue. Annales d'Endocrinologie (Paris) 63:91-95.

Bouwmeester T, Baunch A, Ruffner H, Angrand PO, Bergamini G, Croughton K, Cruciat C, Eberhard D, Gagneur J, Ghidelli S (2004). A physical and functional map of the human TNF-alpha/NF-kappa B signal transduction pathway. Nature Cell Biology 6: 97-105.

Bouskila M, Pajvani B, Scherer PE (2005). Adiponectin:a relevant player in PPARgamma-agonist-mediated improvements in hepatic insulin sensitivty? Interantional Journal of Obesity 29:S17-S23.

Brakenhielm E, Cao R, Gao B, Angekin B, Cannon B, Parini P, Cao Y (2004). Angiogenesis inhibitor, TNP-470, prevents diet-induced and genectic obesity in mice. Circulation Research 94:1579-1588.

Brakenhielm E, Veitonmaki N, Cao R, Kihara S, Matsuzawa Y, Zhivotovsky B, Funahashi T, Cao Y (2004). Adiponectin-induced antiangiogenesis and antitumor activity involve caspase-mediated endothelial cell apoptosis. Proceedings of the National Academy of Sciences of the United States of America 101: 2476-2481.

Brasaemle DL, Levin DM, Adler-Wailes DC, Londos C (2000). The lipolytic stimulation of 3T3-L1 adipocytes promotes the translocation of hormone-sensitive lipase to the surfaces of lipid storage droplets. Biochimica et Biophysica Acta (BBA) - Molecular and Cell Biology of Lipids 1483(2): 251-262.

Breier G, Breviario F, Caveda L, Berthier R, Schnurch H, Gotsch U, Vestweber D, Risau W, Dejana E (1996). Molecular cloning and expression of murine vascular endothelial-cadherin in early stage development of the cardiovascular system. Blood 87:630-641.

Breitling R, Armengaud P, Amtmann A, Herzyk P. (2004) Rank products: a simple, yet powerful, new method to detect differentially regulated genes in replicated microarray experiments. Federation of European Biochemical Societies Letters 573: 83-92.

Brodsky SV, Gealekman O, Chen J, Zhang F, Togashi N, Crabtree M, Gross SS, Nasjletti A, Goligorsky MS (2004). Prevention and reversal of premature endothelial cell senescence and vasculopathy in obesity-induced diabetes by ebselen. Circulation Research 94: 377-384.

Brown JQ, Wilke LG, Geradts J, Kennedy SA, Palmer GM, Ramanujam N (2009). Quantitative optical spectroscopy: a robust tool for direct measurement of breast cancer vascular oxygenation and total haemoglobin content *in vivo*. Cancer Research 69: 2919-2926.

Brown PO, and Botstein D (1999). Exploring the new world of the genome with DNA microarrays. Nature Genetics 21: 33-37.

Brown WV, Fujioka K, Wilson PW, Woodworth KA (2009). Obesity: why be concerned? American Journal of Medicine 122: S4-11.

Browne PV, Mosher DF, Steinberg MH, Hebbel RP (1996). Disturbance of plasma and platelet thrombospondin levels in sickle cell disease. American Journal of Haematology 51: 296-301.

Brun RP, Kim KP, HU E, Altiok S, Speigelman BM (1996). Adipocyte differentiation: a transcriptional regulatory cascade. Current Opinions in Cell Biology 8: 826-832.

Bunger L and Hill WG (1999). Inbred lines of mice derived from long-term divergent selection on fat content and body weight. Mammalian Genome 10**:** 645-648.

Burch J, Mckenna, Palmer S, Norman G, Glanville J, Sculpher M, Woolacott N (2009). Rimonabant for the treatment of overweight and obese people. Health Technology Assessment 13: 13-22.

Bussolino F, Renzo MFD, Ziche M, Bocchietto E, Olivero M, Naldini L, Gaudino G, Tamagnore L, Coffer A, Comoglio PM (1992). Hepatocyte growth factor is a potent angiogenic factor which stimulates endothelial cell motility and growth. The Journal of Cell Biology 119: 629-641.

Camenisch G, Stroka DM, Gassmann M, Wenger RH (2001). Attenuation of HIF-1 DNA binding activity limits hypoxia-inducible endothelial-1 expression. Pflugers Archive European Journal of Physiology 443: 240-249.

Cao R, Brakenhlem E, Wahlestedt C, Thyberg J, Cao Y (2001a). Leptin induces vascular permeability and synergistically stimulates angiogenesis with FGF-2 and VEGF. The Proceedings of the National Academy of Sciences 98: 11: 6390-6395.

Cao W, Medvedev AV, Daniel KW, Collins S (2001b). B-Adrenergic activation of p38 MAP kinase in adipocytes. The Journal of Biological Chemistry 276: 27077-27062.

Campbell IL, Abraham CR, Masliah E, Kemper P, Inglis JD, Oldstone MB, Mucke L (1993). Neurologic disease induced in transgenic mice by cerebral overexpression of interleukin-6. Proceedings of the National Academy of Sciences of the United States 90: 10061-10065.

Campbell NE, Greenaway J, Henkin J, Moorehead RA, Petrik J (2010). The thrombospondin-1 mimetic ABT-510 increases the uptake and effectiveness of cisplatin and paclitaxel in a mouse model of epithelial ovarian cancer. Neoplasia 3: 275-283.

Carlson T, Feng Y, Maisonpierre P, Mirksich M, Morla A (2001). Direct cell adhesion to the angiopoietins mediated by integrins. Journal of Biological Chemistry 276: 26516-26525.

Carmeliet P, Ferreira V, Breier G, Pollefeyt S, Kieckens L, Gertsenstein M, Fahrig M, Vandenhoeck A, Harpal K, Eberhardt C, Declerc C, Pawling J, Moons L, Collen D, Risau W, Nagy A (1996). Abnormal blood vessel development and lethality in embryos lacking a single VEGF allele. Nature 380; 435-439.

Carmeliet P, Lampugnani MG, Moons L, Breviario F, Compernolle V, Bono F, Balconi G, Spagnuolo R, Oosthuyse B, Dewerchin M, Zanetti A, Angellilo A, Mattot V, Nuyens D, Lutgens E, Clotman F, de Ruiter MC, Gittenberger-de Groot A, Poelmann R, Lupu F, Herbert JM, Collen D and Dejana E (1999). Targeted

deficiency or cytosolic truncation of the VE-cadherin gene in mice impairs VEGF-mediated endothelial survival and angiogenesis. Cell 98, 147–157.

Carmeliet P & Jain RK (2000). Angiogenesis in cancer and other diseases. Nature 407: 249-257.

Carmen GY and Victor SM (2006). Signalling mechanisms regulating lipolysis. Cell Signalling 18(4): 401-8.

Carnicero HH (1984). Changes in the metabolsim of long chain fatty acids during adipose differentiation of 3T3L1 cells. The Journal of Biological Chemistry 259: 3844-3850.

Castan I, Wijkander J, Manganiello V, Degerman E (1999). Mechanism of inhibtion of lipolysis by insulin, vandate and perovanadate in rat adipocytes. Biochemical Journal 339: 281-289.

Ceddia RB, Somwar R, Maida A, Fang X, Bikopoulos G and Sweeney G (2005). Globular adiponectin increases GLUT4 translocation and glucose uptake but reduces glycogen synthesis in rat skeletal muscle cells. Diabetologia 48:132-139.

Cinti S, Mitchell G, Barbatelli G, Murano I, Ceresi E, Faloia E, Wang S, Fortier M, Greenberg As, Obin MS (2005). Adipocyte death defines macrophage localisation and function in adipose tissue of obese mice and humans. Journal of Lipid Research 46: 2347-2355.

Chagnon YC, Rankinen T, Snyder EE et al (2002). The human obesity gene map: the 2002 update. Obesity Research 11: 313.

Chaldakov GN, Stankulov IS, Hristova M, Ghenev PI (2003). Adipobiology of disease: Adipokines and adipokine-targeted pharmacoclogy. Current Pharmaceutical Design **9:**1023-1031.

Cho CH, Ju JH, Kim HR, Oh HJ, Kang CM, Jhun JY, Lee SY, Park MK, Min JK, Park SH, Lee SH (2007). Angiogenic role of LYVE-1- postive macrophages in adipose tissue. Circulation Research 100: e47-e57.

Chomczynski P and Sacchi N (1987). Signal step method of RNA isolation by acid guanidinium thiocyanate phenol chloroform extraction. Analytical Biochemistry 162: 156-159.

Christiaens V, Voros G, Scroyen I, Lijnen HR (2007). On the role of placental growth factor in murine adipogenesis. Thrombosis Research 120(3): 399-405.

Coburn CT, Knapp FF, Febbraio M, Beets AL, Silverstein RL, Abumrad NA (2000). Defective uptake and utilsation of long chain fatty acids in muscle and adipose tissues of CD36 knockout mice. The Journal of Biolocial Chemistry 275: 32523-32529.

Cohen B, Barkan D, Levy Y, Goldberg I, Fridman E, Kopolovic J, Rubinstein M (2001). Leptin induces angiopoietin-2 expression in adipose tissues. The Journal of Biological Chemistry 276: 7697-7700.

Cohen AW, Razani B, Schubert W, Williams TM, Wang XB, Lyengar P, Brasaemle DL, Scherer PE, Lisanti M (2004). Role of caveolin-1 in the modulation of lipolysis and lipid droplet formation. Diabetes 53: 1261-1270.

Colman RJ, Anderson RM, Johnson SC, Kastman EK, Kosmatka KJ, Beasley TM, Allison DB, Cruzen C, Simmons HA, Kemnitz JW, Weindruch R (2009). Caloric restriction delays disease onset and mortality in rhesus monkeys. Science 325: 201-204.

Conway EM, Collen D, Carmeliet P (2001). Molecular mechanisms of blood vessel growth. Cardiovascular Research *1*49:507-521.

Cook JA and Mitchell JB (1989). Viability measurements in mammalian cell systems. Annuals in Biochemsity 15: 179: 1-7.

Coort SL, Willems J, Coumans WA, van der Vusse GJ, Bonen A, Glatz JF, Luiken JJ (2002). Sulfo-N-succinimidyl esters of long chain fatty acids specifically inhibit fatty acid translocase (FAT/CD36) mediated cellular fatty acid uptake. Molecular Cell Biochemistry 239: 213-219.

Coppack SW, Patel JN, Lawernce VJ (2001). Nutritional regulation of lipid metabolism in human adipose tissue. Experimental Clinical Endocrinology Diabetes 109: S202-214.

Corton JM, Gillespie JG, Hawley SA, Hardie DG (1995). 5-aminoimidazole-4-carboxamide ribonucleoside. A specific method for activating AMP-activated protein kinase in intact cells? European Journal of Biochemistry 229(2): 558-65.

Coussens LM, Fingleton B, Matrisian LM (2002). Matrix metalloproteinase inhibitors and cancer: trials and tribulations. Science 295*:*2387–2392*.*

Crandall DL, Hausman GJ, Kral JG (1997). A review of the microcirculation of adipose tissue: anatomic, metabolic, and angiogenic perspectives. Microcirculation 4:211-232.

Crawford SE, Stellmach V, Murphy-Ullrich JE, Ribeiro SMF, Lawler J, O'Hynes R, Boivin GP, Bouck N (1998). Thrombospondin-1 is a major activator of TGFβ-1 in vivo. Cell 93: 1159-1170.

Crandall DL (2006). Modulation of adipose tissue development by pharmacological inhibition of PAI-1. Arteriosclerosis, Thrombosis and Vascular Biology 2209-2215.

Crichton MB, Nicholas JE, Zhao Y, Bulun SE, Simpson ER (1996). Expression of transcripts of interleukin-6 and related cytokines by human breast tumors,

breast cancer cells, and adipose stromal cells. Molecular and Cellular Endocrinology 118: 215-220.

Croissandeau G, Chretien M, Mbikay M (2002). Involvement of matrix metalloproteinases in the adipose conversion of 3T3L1 preadipocytes. Journal of Biochemistry 15: 739-746.

Crujeiras AB, Goyenechea E, Abete I, Lage M, Carreira MC, Martinez JA, Casanueva FF (2010). Weight regain after a diet-induced weight loss is predicated by higher baseline leptin and lower ghrelin plasma levels. Journal of Clinical Endocrinology and Metabolism 11: 5037-5044.

Curfman GD, Morrissey S, Drazen JM (2010). Sibutramine- another flawed diet pill. The New England Journal of Medicine 363: 972-974.

Dallabrida SM, Zurakowski D, Shih SC, Smith LE, Folkman J, Moulton KS, Rupnick MA (2003). Adipose tissue growth and regression are regulated by angiopoietin-1. Biochemical Biophysical Research Communications 311: 563-571.

D'Amato RJ, Loughnan MS, Flynn E, Folkman J (1994). Thalidomide is an inhibitor of angiogenesis. Proceedings of the National Academy of Sciences of the United States of America 26: 4082-4085.

Darland DC and D'Amore PA (1999). Blood vessel maturation: vascular development comes of age. Journal of Clinical Investigation 103(2): 157-8.

Dawson DW, Pearce SFA, Zhong R, Silverstein RL, Frazier WA, Bouck NP (1997). CD36 mediates the in vitro inhibitory effects of thrombopsonind-1 on endothelial cells. The Journal of Cell Biology 138: 707-717.

Dawson DW, Volpert OV, Pearce FS, Schneider AJ, Silverstein RL, Henkin J, Bouck NP (1999). Three distinct D-amino acid substitutes confer potent antiangiogenic activity on an inactive peptide derived from thrombospodin-1 repeat. Molecular Pharmacology 55: 332-338.

Dellian M, Witwer BP, Salehi HA, Yuan F, Jain RK (1996). Quantitation and physiological characterization of angiogenic vessels in mice: effect of basic fibroblast growth factor, vascular endothelial growth factor/vascular permeability factor, and host microenvironment. American Journal of Pathology 149(1): 59-71.

Dennis G Jr, Sherman BT, Hosack DA, Yang J, Gao W, Lane HC, Lempicki RA. (2003) DAVID: Database for Annotation, Visualization, and Integrated Discovery. Genome Biology 4(5):P3.

Denzel MS, Hebbard LW, Shostak G, Shapiro I, Cardiff RD, Ranscht B (2009). Adiponectin deficiency limits tumor vascularisation in the MMTV-PyV-mT mouse model of mammary cancer. Clinical Cancer Research 15: 3256-3264.

Deslex S, Negrel R, Vannier C, Etienne J, Ailhaud G (1987). Differentiation of human adipocyte precursors in a chemically defined serum-free medium. International Journal of Obesity 11: 19-27.

Desreumaux P, Dubuquoy L, Nutten S, Peuchmaur M, Englaro W, Schoonjans K, Derijard B, Desvergne B, Wahli W, Chambon P, Leibowitz MD, Colombel JF, Auwerx J (2001). Attenuation of colon inflammation through activators of the retinoid X receptor (RXR)/peroxisome proliferator-activated receptor gamma (PPARgamma) heterodimer. A basis for new therapeutic strategies. Journal of Experimental Medicine 193(7): 827-38.

De Souza CJ, Hirshman MP, Horton ES (1997). CL 316, 243 a beta 3 specific adrenoceptor agonist enhances insulin-stimulated glucose disposal in nonobese rats. Diabetes 48: 1257-1263.

Devy L, Blacher S, Grignet-Debrus C, Bajou K, Masson V, GerardRD, Gils A, Carmeliet G, Carmeliet P, Declerck PJ, Noel A, Foidart JM (2002). The pro or antiangiogenic effect of plasminogen activator inhibitor 1 is dose dependent. Federation of American Societies for Experimental Biology **16:** 147-154.

Dings RPM, Yokoyama Y, Ramakrishnan S, Griffioen AW, Mayo KH (2003). The designed angiostatic peptide anginex synergistically improves chemotherapy and antiangiogenesis therapy with angiostatin. Cancer Research 63; 382-385.

DiPietro LA, Polverini PI (1994). Angiogenic macrophages produce the angiogenesis inhibitor thrombospondin 1. American Journal of Pathology **143**:678-684.

DiPietro LA, Nebgen DR, Polverini PI (1994). Downreguaktion of endotheial cell thrombospodin 1 enhances in vitro angiogenesis. Journal of Vascular Research 31: 178-185.

Drab M, Verkade P, Elger M, Kasper M, Lohn M, Lauterbach B, Menne J, Lindschau C, Mende F, Luft FC, Schedl A, Haller H, Kurzchalia TV (2001). Loss of caveolae, vascular dysfunction, and pulmonary defects in caveolin-1 gene-disrupted mice. Science 293: 2449-2452.

Dubois M, Kerr-Conte J, Gmyr V, Bouckenooghe T, Muharram G, D'Herbomez M, Martin-Ponthieu A, Vantyghem C, Vandwalle B and Pattou F (2004). Non-esterified fatty acids are deleterious for human pancreatic islet function at physiological glucose concentration. Diabetologia 47:463-469.

Ebbinghaus S, Hussain M, Tannir N, Gordon M, Desai AA, Kinght RA, Humerickhouse RA, Qian J, Gordon GB, Eiglin R (2007). Phase 2 study of ABT-510 in patients with previously untreated advanced renal carcinoma. Cancer Research 13: 6689-6695.

Egan JJ, Greenberg AS, Chang MK, Wek SA, Moos MC Jr, Londos C (1992). Mechanism of hormone-stimulated lipolysis in adipocytes: translocation of hormone-sensitive lipase to the lipid storage droplet. Proceedings of the National Academy of Sciences U S A 89(18): 8537-41.

Elmquist JK, Ahima RS, Elias CF, Flier JS and Saper CB (1998). Leptin activates distinct projections from the dorsomedial and ventromedial hypothalamic nuclei. Proceedings of the National Academy of Sciences USA 95:741-746.

Engelman JA, Lisanto MP, Scherer PE (1998). Specific inhibitors of p38 Mitogen-activated protein kinase block 3T3L1 adipogenesis. The Journal of Biologcial Chemistry 48: 3211-32120.

Engerman R L, Pfaffenbach D, Davis MD (1967). Cell turnover of capillaries. Laboratory Investigations 17(6): 738-43.

Eriksson P, Reynisdottir S, Lönnqvist F, Stemme V, Hamsten A and Arner P (1998). Adipose tissue secretion of plasminogen activator inhibitor-1 in non-obese and obese individuals. Diabetologia; 41: 65-71.

Etoh T, Inoe H, Tanaks S, Barnard GF, Kitano S, Mon M (2001). Angiopoietin-2 is related to tumor angiogenesis in gastric carcinoma possible in vivo regulation via induction of proteases. Cancer Research 61: 2145-2154.

Etherton TD (2000). The biology of somatotropin in adipose tissue growth and nutrition partitioning. The Journal of Nutrition 130: 2623-2625.

Fajas L, Schoonjans K, Gelman L, Kim JB, Najib J, Martin G, Fruchart JC, Briggs M, Speigelman BM, Auwerx J (1999). Regulation of perixsome proliferator-activated receptor γ expression by adipocyte differentiation and determination factor1/sterol regulatory element binding protein 1: implications for adipocyte differentiation and metabolism. Molecular Cellular Biology 19: 5495-5503.

Faust LM, Miller WH, Sclafani A, Aravich F, Triscari J and Sullivan AC (1984). Diet-dependent hyperplastic growth of adipose tissue in hypothalamic obese rats. American Journal of Physiology 247: R1038-R1046.

Febbraio M, Abumrad NA, Hajjar DP, Sharma K, Cheng W, Pearce SF, Silverstein RL (1999). A null mutation in murine CD36 reveals an important role in fatty acid and lipoprotein metabolism. Journal of Biological Chemistry 2: 274: 19055-19062.

Febbraio M, Hajjar DP, Silverstein RL (2001). CD36: a class B scavenger receptor involved in angiogenesis, atherosclerosis, inflammation and lipid metabolism. Journal of Clinical Investigation 108: 785-791.

Feingold KR, Doerrir W, Dinarello CA, Fiers W, Grunfield C (1992). Stimulation of lipolysis in cultured fat cells by tumor necrosis factor, interleukin-1 and the

interferons are blocked by the inhibition of prostaglandin synthesis. Endocrinology 130: 10-16.

Ferreira M, Barcelos LS, Campos PP, Vasconcelos AC, Teixeira MM, Andrade SP (2004). Sponge-induced angiogenesis and inflammation in PAF receptor-deficient mice (PAFR-KO). British Journal of Pharmacology 141: 1185-1192.

Fidler IJ and Ellis LM (2000). Chemotherapeutic drugs-more really is not better. Nature Medicine 5: 500.

Fitzpatrick TE, Graham CH (1998). Stimulation of plasminogen activator inhibitor-1 expression in immortalised human trophoblast cells cultured under low levels of oxygen. Exp Cell Research 245: 155-162.

Folkman J (1985). Angiogenesis and its inhibitors. Important Advancements in Oncology 42-62.

Folkman J (1986). How is blood vessel growth regulated in normal and neoplastic tissue? Cancer Research 46: 467-473.

Folkman J (1989). Successful treatment of an angiogenic disease. New England Journal of Medicine. 320: 1211-1212.

Folkman, J. (1997) in *Cancer*, eds. DeVita, V., Jr., Hellman, S. & Rosenberg, S. (Lippincott, Philadelphia), pp. 3075–3085.

Folkman J (1995). Angiogenesis in cancer, vascular, rheumatoid and other disease. Nature Medicine 1: 27-31.

Forsythe JA, Jiang BH, Iyer NV, Againi F, Leung SW, Koos RD, Semenza GL (1996). Activation of vascular endothelial growth factor gene transcription by hypoxia-inducible factor 1. Molecular Cellular Biology 16: 4604.

Fox SB, Leek RD, Weekes MP, Whitehouse RM, Gatter KC, Harris AL (1995). Quantitation and prognostic value of breast cancer angiogenesis: comparison of microvessel density, Chalkley count, and computer image analysis. The Journal of Pathology 177: 275-283.

Frazier WA (1991). Thrombospondins. Current Opinions Cell Biology 3: 792-799.

Fredrikson G, Stralfors P, Nilsson NO, Belfage P (1981). Hormone-sensitive lipase of rat adipose tissue. Purification and some properties. The Journal of Biological Chemistry 256: 6311-6320.

Fried SK, Bunkin DA, Greenberg AS (1998). Omental and subcutaneous adipose tissues of obese subjects release interleukin-6: depot difference and regulation by glucocorticoid. Journal of Clinical Endocrinolgy Metabolism 83: 847-850.

Friedman JM, Halaas JL (1998). Leptin and the regualtion of body weight in mammals. Nature 395: 673-770.

Fuchtenbusch M, Standi E, Schatz H (2000). Clinical efficacy of new thiazolidinediones and glinides in the treatment of type 2 diabates mellitus. Experimental Clinical Endocrinology Diabetes 108: 151-163.

Fugel-Koch C, Phimann A, Fuchshofer R, Weige-Lussen U, Tamm E (2004). Thrombospondin-1 in the trabecular network: localisation in normal and glaucomatous eyes, and induction by TGF-β1 and dexamethasone in vitro. Experimental Eye Research 79: 649-663.

Fujimoto T, Kogo H, Ishiguro K, Tauchi, K, Nomura R (2001). Caveolin-2 is targeted to lipid droplets, a new "membrane domain" in the cell. Journal of Cell Biology 152(5): 1079-85.

Fukumura D, Ushiyama A, Duda DG, Xu L, Tam J, Chatterjee VKK, Garkavtsev I and Jain RK (2003). Paracrine regualtion of angiogenesis and adipocyte differentiation during *in vivo* adipogenesis. Circulation Research 93: E88-E97.

Galic S, Oakhill JS, Steinberg,GR (2010). Adipose tissue as an endocrine organ. Mol Cell Endocrinology 316(2): 129-39.

Galis Z, Sukhova GK, Kranzhofer R, Clark S, Libby P (1994). Macrophage foam cells from experimental atheroma constitutively produce matrix-degrading proteinases. The Proceeding of the National Academy of Sciences 92: 402-406.

Gao AG, Lindberg FB, Finn SD, Blystone EJ, Brown EJ, Frazier WA (1996). Integrin-associated protein is a receptor for the COOH-terminal domain of thrombospondin. The Journal of Biological Chemistry 271: 21-24.

Gao L, Mann GE (2009). Vascular NAD(PH) oxidase activation in diabetes: a double-edged sword in redox signalling. Cardiovascular Research 82 (1); 9-20.

Garg A (2004). Acquired and inherited lipodystrophies. New England Journal of Medicine 350:1220-1234.

Gaudiot N, Jaubert AM, Charbonnier E, Sabourault D, Lacasa D, Giudicelli Y, Ribiere C (1998). Modualtion of white adipose tissue lipolysis by nitric oxide. Journal of Biological Chemistry 273: 13475-13481.

Gaudiot N, Ribiere C, Jaubert AM, Giudicelli Y (2000). Endogenous nitric oxide is implicated in the regualtion of lipolysis through anti-oxidant-related effect. Cell Physiology 279: C1603-C1610.

Gealekman O, Burkart A, Chouinard M, Nicoloro SM, Straubhaar J, Corvera S (2008). Enhanced angiogenesis in obesity and in response to PPARγ activators through adipocyte VEGF and ANGPL4 production. The American Journal of Physiology Endocrinology Metaboilsm 295: E1056-E1064.

Ghorbani M, Himms-Hagen J (1998). Treatment with Cl 316, 243, a beta3 specific adrenoceptor agonist, reduces serum leptin in rats with diet or aging

associated obesity, but not in Zucker rats with genetic (fa/fa) obesity. International Journal of Obesity 22: 63-65.

Gill T (2006). Epidemiology and health impact of obesity: an Asia Pacific perspctive. Asia Pacific Journal of Clinical Nutitition 15: 3-14.

Gimeno RE and Klaman LD (2005). Adipose tissue as an active endocrine organ:recent advances. Current Opinion in Pharmacology 5:122-128.

Ginsberg HN (1991). Lipoprotein physiology in nondiabetic and diabetic states. Relationship to atherogenesis. Diabetes Care 14: 893-855.

Go RS and Owen WG (2003). The rat aortic ring assay for *in vivo* study of angiogenesis. Novel Anticancer Drug Protocols; Methods in Molecular Medicine 85: 59-64.

Gonzalez RP, Soares FS, Farias RF, Pessoa C, Leyva A, de Barros Viana GS, Moraes MO (2001). Demonstration of inhibitory effect of oral shark cartilage on basic fibroblast growth factor-induced angiogenesis in the rabbit cornea. Biol Pharm Bull 24: 151-154.

Good DJ, Polverini PJ, Rastinejad F, Le Beau MM, Lemons RS, Frazier WA, Bouck NP (1990). A tumor suppressor dependent inhibitor of angiogenesis is immunologically and functionally indistinguishable from a fragment of thrombospodin. Proc Natl Acad Sci USA 87: 6624-6628.

Gordon S (1998). The role of the macrophage in immune regulation in immune regulation. Research in Immunology 149; 685-688.

Granneman JG, Moore HP, Granneman RL, Greenberg AS, Obin MS, Zhu Z (2007). Analysis of lipolytic protein trafficking and interactions in adipocytes. Journal of Biological Chemistry 282(8): 5726-35.

Grant DS (1994). The role of basement membrane in angiogenesis and tumor growth. Pathology Research and Practice 190: 854-863.

Green A, Dobias SB, Walters DJ, Braiser AR (1994). Tumor necrosis factor increase the rat eof lipolysis in primary cultures of adipocytes without altering levels of hormone sensitive lipase. Endocrinology 134: 2581-2588.

Greenberg AS, Egan JJ, Wek SA, Moos MC Jr, Londos C, Kimmel AR (1993). Isolation of cDNAs for perilipins A and B: sequence and expression of lipid droplet-asscoiated proteins of adipocytes. The Proceedings of the National Academy of Sciences USA 90: 12035-12039.

Greenberg As, Nordan RP, McIntosh J, Calvo JC, Scow RO, Jablons D (1992). Interleukin 6 reduces lipolprotein lipase activity in adipose tissue of mice in vivo and in 3T3L1 adipocytes: a possible role for interleukin 6 in cancer cachexia. Cancer Research 52: 4113-4116.

Greenaway J, Lawler J, Moorehead R, Bornstein P, Lamarre J, Petrik J (2007). Thrombospondin-1 inhibits VEGF levels in the ovary directly by binding and internalisation via the low density lipoprotein receptor related protein (LRP1). Journal of Cellular Physiology 210: 807-818.

Greenway J, Henkin J, Lawer J, Moorehead, Petrik J (2009). ABT-510 induces tumor cell apoptosis and inhibits ovarian tumor growth in an orthotopic, syngeneric model of epitheial ovarian cancer. Molecular Cancer Therapy 8: 64-74.

Gregoire FM, Johnson PR and Greenwood MR (1995). Comparison of the adipoconversion of preadipocytes derived from lean and obese Zucker rats in serum free cultures. International Journal of Obesity Realted Metabolic Disorders 19: 664-670.

Gregoire FM, Smas CM, Sui HS (1998). Understanding adipocyte differentiation. The American Physiological Society. 78: 783-809.

Grimble RF (2002). Inflammatory status and insulin resistance. Current Opinion in Clinical Nutrition and Metabolic Care **5**:551-559.

Grober J, Lucas S, Sorhede-Winzell M, Zaghini I, Mairal A, Contreras JA, Besnard P, Holm C, Langin D (2003). Hormone-sensitive lipase is a cholesterol esterase of the intestinal mucosa. The Journal of Biological Chemistry 256: 6311-6320.

Griffioen AW, Molema G. (2000) Angiogenesis: Potentials for Pharmacologic Intervention in the Treatment of Cancer, Cardiovascular Diseases, and Chronic Inflammation. Pharmacological reviews 52*:237-268.*

Groetzinger J, Kernebeck T, Kallen KJ, Rose-John S (1999). IL-6 type cytokine receptor complexes: hexamer, tetramer or both? The Journal of Biological Chemistry 380: 803-813.

Guh DP, Zhang W, Bansback N, Amarsi Z, Birmingham CL, Anis AH (2009). The incidence of co-morbidities related to obesity and overweight: a systematic review and meta-analysis. BMC Public Health 9; 88.

Gutkind JS (1998). The pathways connecting G protein-coupled receptors to the nucleus through divergent mitogen-activated protein kinase cascades. The Journal of Biological Chemistry 273: 1839-1842.

Guthman F, Haupt R, Looman C, Spener F, Rustow B (1999). Fatty acid translocase/CD36 mediates the uptake of palmitate by type II pneumocytes. American Journal of Physiology Lung Cell Molecular Physiology 277: 191-196.

Haddad JJ (2002) Antioxidant and prooxidant mechanisms in the regulation of redox (y)-sensitive transcription factors. Cellular Signaling ***14:****879-897.*

Haddad, JJ, Harb HL (2005) Cytokines and the regulation of hypoxia-inducible factor (HIF) -1α. International Immunopharmacology ***5:****461-483*

Haemmerle G, Lass A, Zimmermann R, Gorkiewicz G, Meyer C, Rozman,J, Heldmaier G, Maier R, Theussl C, Eder S, Kratky D, Wagner EF, Klingenspor M, Hoefler G, Zechner R (2006). Defective lipolysis and altered energy metabolism in mice lacking adipose triglyceride lipase. Science 312(5774): 734-7.

Hague S, MacKenzie IZ, Bicknell, R., Rees, M.C.P. (2002**)** In-vivo angiogenesis and progestogens. Human Reproduction 17: 786-793.

Hamilton JA (1998). Fatty acid transport: difficult or easy? Journal of Lipid Research 39: 467-481.

Hauner H, Entenmann M, Wabitsch D, Gillard G, Alihaud R, Negrel R, Pfeiffer EF (1989). Promoting effect of glucocorticoids on the differentiation of human adipocyte precursor cells cultured in a chemically defined medium. Journal Clinical Investigation 84: 1663-1670.

Hauner H, Wabitsch M, Braun S, Heinze E, Ilondo MM, Shymko R, De Meyts P, Teller WM (1997). Mitogenic and antiadipogenic properties of human growth hormone in differentiating human adipocyte precursor cells in primary culture. Pediatric Research 40: 450-456.

Hauner H (2005). Secretory factors from human adipose tissue and their functional role. Proceedings of the Nutrition Society 64: 163-169.

Hausdorff SF, Fingar DC, Morioka K, Garzia LA, Whiteman El, Summers SA, Birnbaum MJ (1999). Identification of wortmannin-sensitive targets in 3T3L1 adipocytes: dissociation of insulin-stimulated glucose uptake and GLUT4 translocation. Journal of Biological Chemistry 274: 24677-24684.

Hausman DB, DiGirolamo M, Bartness TJ, Hausman GJ, Martin RJ (2001). The biology of white adipocyte proliferation. Obesity Reviews 2:239-254.

Haviv F, Bradley MF, Kalvin DM, Schneider AJ, Davidson DJ, Majest SM, McKay LM, Haskell CJ, Bell RJ, Nguyen B, Marsh KC, Henkin J (2005). Thrombospondin-1 mimetic peptide inhibiotrs of angiogenesis and tumor growth: design, synthesis, and optimisation of pharmacokinetics and biologival activites. The Journal of Medical Chemistry 48: 2838-2846.

Heilbronn LK, Smith SR, Ravussin E (2003). The insulin-senitising role of the fat derived hormone adiponectin. Current Pharmaceutical Design 9:1411-1418.

Heldin, C.H., Ostman, A., Ronnstrand, L (1998). Signal transduction via platelet-derived growth factor receptors. Biochem Biophys Acta 1378: *F79–F113.*

Hida K, Wada J, Zhang H, Hiragushi K, Tsuchiyama Y, Shikata K, Makino (2000) H. Identifcation of genes specifically expressed in the accumlated visceral adipose tissue of OLETF rats. The Journal of Lipid Research 41: 1615-1622.

Hirosumi J, Tuncman G, Chang L, Görgün GZ, Teoman Uysal K, Maeda K, Karin M, Hotamisligil G (2002). A central role for JNK in obesity and insulin resistance. Nature 420:333-336.

Hobson B and Denekamp J. (1984) Endothelial proliferation in tumours and normal tissues: continuous labeling studies. British Journal of Cancer 49:405–413.

Hoekstra R, de Vos FY, Eskens F, Gietema JA, Gaast A, Groen h, Knight R, Carr RA, Humerickhouse RA, Verweij J, de Vries EGE (2005). Phase I safety, pharmakinetic, and pharmacodynamic study of the thrombospondin-1-mimietic angiogenesis inhibitor ABT-510 in patients with advanced cancer. The Journal of Clinical Oncology 23: 5188-5197.

Hoffman RM (2002). Green fluorescent protein imaging of tumor growth, metastasis and angiogenesis in mouse models. Lancet Oncology 3: 546-556.

Hoffstedt J, Lonnqvist F, Shimizu M, Black E, Arner P (1996). Effects of putative β_3-adrenoceptor agonists on lipolysis in human omental adipocytes. International Journal of Obesity 20; 428-434.

Holash J, Wiegand SJ and Yancopoulos GD (1999). New model of tumour angiogenesis: dynamic balance between vessel regression and growth mediated by angiopoietins and VEGF. Oncogene 18: 5356-5362.

Holm C, Belfrage P, Fredrikson G (1987). Immunological evidence for the presence of hormone-sensitive lipase in rat tissues other than adipose tissue. Biochemical and Biophysical Research Communications 148: 99-105.

Holm C (2003). Molecular mechanisms regulating hormone-sensitive lipase and lipolysis. Biochem Soc Trans 31(Pt 6): 1120-4.

Horvat S, Bünger L, Falconer VM, Mackay P, Law A, Bulfield G, Keightly PD (2000). Mapping of obesity QTLs in a cross between mouse lines divergently selected on fat content. Mammalian Genome 11:2-7.

Horvath C, Preiss BA, Lipsky SR (1967). Fast liquid chromatography. Investigation of operating parammeters and the separation of nucleotides on pellicular ion exchanges. Analytical Chemistry 39: 1422-1428.

Hotamisligil GS, Shargill NS, Spiegelman BM (1993). Adipose expression of tumor necrosis factor-alpha: direct role in obesity-linked insulin resistance. Science 259(5091):87–91.

Hotamisligil GS, Peraldi P, Budavari A, Ellis R, White MF, Spiegelman BM (1996). IRS-1 mediated inhibition of insulin receptor tyrosine kinase activity in TNF-α and obesity induced insulin resistance. Science 271: 665-668.

Hotta K, Funahashi T, Arita Y, Takahashi M, Matsuda M, Okamoto Y, Iwahashi H, Kuriyama H, Ouchi N, Maeda K, Nishida M, Kihara S, Sakai N, Nakajima T,

Hasegawa K, Muraguchi M, Ohmoto Y (2000). Plasma concentrations of a novel, adipose-specific protein, adiponectin, in type 2 diabetic patients. Arteriosclerosis, Thrombosis and Vascular Biology 20: 1595-1599.

Howell LP (1993). Diagnosis of palpable breast cancer by FNA: a changing role? Diagnostic Cytopathology 6: 611-612.

Hu DE, Hiley CR, Smither RL, Gresham GA, Fan TP (1995). Correlation of 133Xe clearance, blood flow and histology in the rat sponge model for angiogenesis. Further studies with angiogenic modifiers. Laboratory Investigations 72*: 601–610*

Hua X, Yokoyama C, Wu J, Briggs MR, Brown MS, Goldstein JL, Wang X (1993). SREBP-2, a second basic-helix-loop-helix-leucine zipper protein that stimulates transcription by binding to a sterol regulatory element. The Proceedings of the National Academy of Sciences USA 190: 11603-11607.

Huang L and Li C (2000). Leptin: a multifunctional hormone. Cell Research 10: 81-92.

Huang DW, Sherman BT, Lempicki RA. (2009) Systematic and integrative analysis of large gene lists using DAVID Bioinformatics Resources. Nature Protocols 4(1):44-57.

Huber J, Loffler M, Bilban M, Reimers M, Kadl A, Todoric J, Zeyda M, Geyeregger R, Schreiner M, Weichhart T, Leitinger N, Waldhausl W, Stunlig TM (2006) Prevention of high-fat diet-induced adipose tissue remodelling in obese diabetic mice by n-3 polyunsaturated fatty acids. International Journal of Obesity 31: 1004-1013.

Hursting SD, Lavigne JA, Berrigan D, Perkins SN, Barrett C (2003). Energy restriction, aging and cancer prevention: mechanism of action and applicability to humans. Annual Review of Medicine 54: B1-152.

Hursting SD, Lashinger LM, Colbert LH, Rogers CJ, Wheatley KW, Nunez NP, Mahabir S, Barrett JC, Forman MR, Perkins SN (2007). Energy balance and carcinogenesis underlying pathways and targets for intervention. Current Cnacer Drug Tragets 7: 484-491.

Hutley LJ, Herington AC, Shurety W, Cheung C, Vesey DA, Cameron DP and Prins JB. (2001). Human adipose tissue endotheial cells promote preadipocyte proliferation. American Journal of Physiology-Endocrinolgy and Metabolism **281**:E1037-E1044

Ibrahimi A, Sfeir Z, Magharaie H, Amri EZ, Grimaldi P, Aumrad NA (1996). Expression of the CD36 homolog (FAT) in fibroblast cells: effects on fatty acid transport. Proc Natl Acad Sci USA 93: 2646-2651.

Ignarro LJ (1990). Nitric oxide: a novel signal transduction mechanism for transcellular communication. Hypertension 16: 477-483.

Inoue K, Chikazawa M, Fukata S, Yoshikawa C, Shuin T (2003). Docetaxel enhances the therapeutic effect of the angiogenesis inhibitor TNP-470 (AGM-1470) in metastatic human transitional cell carcinoma. Clinical Cancer Research 9: 886-899.

Iruela-Arispe ML, Bornstein P, Sage H (1991). Thrombospondin exerts an antiangiogenic effect on cord formation by endotheial cells in vitro. Proceedings of the National Academy of Sciences of the United States of America 88: 7844-7848.

Iruela-Arispe ML, Lombardo M, Krutzsch HC, Lawler J, Roberts DD (1999). Inhbition of angiogeneis by thrombospondin 1 is mediated by two independent regions within the type 1 repeats. Circulation 100, 1423-1431.

Isenberg JS, Ridnour LA, Perruccio EM, Espey MG, Wink DA, Roberts DD (2005). Thrombospondin-1 inhibits endotheial cell responses to nitric oxide in a cGMP-dependent manner. Proceedings of the National Academy of Sciences of the United States of America 102: 13141-13146.

Isenberg JS, Wink DA, Roberts DD (2006). Thrombosponin-1 antagonises nitric-oxide stimulated vascular smooth mucsle cell responses. Cardiovascular Research 71: 785-793.

Isenberg JS, Jia Y, Fukuyama J, Switzer CH, Wink DA, Roberts DD (2007). Thrombospondin-1 inhibits nitric oxide signalling via CD36 by inhibiting myrsitic acid uptake. The Journal of Biological Chemistry 282: 15404- 15415.

Isenberg JS, Frazier WA, Roberts DD (2008). Thrombospondin-1: a physiological regulator of nitric oxide signalling. Cellular and Molecular Life Sciences 65: 728-742.

Jain, N., K. C. Catania, Kaas JH (1997). Deactivation and reactivation of somatosensory cortex after dorsal spinal cord injury. Nature 386(6624): 495-8.

Jain RK, Safabakhsh N, Sckell A, Chen Y, Jiang P, Benjamin L, Yuan F, Kesh E (1998). Endothelial cell death, angiogenesis, and microvascular function after castration in an androgen-dependent tumor: role of vascular endothelial growth factor. Proceedings of the National Academy of Sciences USA 95, 10820–10825.

Jensen MD, Rogers PJ, Ellman MG, Miles JM (1988). Choice of infusion-sampling modelf ro tracer studies of free fatty acid metabolism. American Journal of Physiology and Metabolism 242: E562-E565.

Jensen MD, Haymond MW, Rizza RA (1989). Influence of body fat disrtrubution on free fatty acid metabolism in obesity. Journal of Clinical Investigation 83: 1168-1173.

Jimenez B, Volpert OV, Crawford E, Febbraio M, Silverstein RL, Bouck N (2000). Signals leading to apoptosis dependent inhibition of neovascularisation by thrombopondin-1. Nature Medicine 6: 41 -48.

Jimenez B, Volpert OV (2001). Mechanistic insights on the inhibition of tumor angiogenesis. Journal of Molecular Medicine 78: 6636-6672.

Jimenez B, Volpert OV, Reiher F, Chang L, Munoz A, Karin M, Bouck N (2001). C Jun N terminal kinase activation is required for the inhibition of neovascularisation by thrombospondin 1. Oncogene 20: 3443-3448.

Jones DC, Ding X, Zhang TY, Daynes RA (2003). Peroxisome proliferator-activated receptor alpha negatively regulates T-bet transcription through suppression of p38 mitogen-activated protein kinase activation. Journal of Immunology 171(1): 196-203.

Jung C, Frutzenwanger M, Fischer N, Figulla HR (2009). Hepatocyte growth factor is elevated in obese adolescents. Journal of Paediatric Endocrinology Metabolism 22: 645-651.

Kaestner KH, Flores-Riveros JR, McLenithan JC, Janicot M, Lane MD (1991). Transcriptional repression of the mouse insulin-responsive glucose transporter (GLUT4) gene by cAMP. The Proceedings of the National Academy of Sciences 88: 1933-1937.

Kanda S, Landgren E, Ljungsrom M, Claesson-Welsh L (1996). Fibroblast growth factor receptor 1-induced differentiation of endothelial cell line established from tsA58 large T transgenic mice. Cell Growth Differentiation 7: 383-395.

Kapur S, Marcotte B, Marette A (1999). Mechanism of adipose tissue iNOS induction in endotoxemia. American Journal of Physiology 276: E635-E641.

Kawanami D, Maemura K, Takeda N, Harada T, Nojiri T, Imai Y, Manabe I, Utsunomiya K, Nagai R (2004). Direct reciprocal effects of resistin and adiponectin on vascular endotheial cells: a new insight into adipocytokine-endothelial cell interactions. Biochemical and Biophysical Research Communications 314: 2: 415-419.

Kern PA, Ranganathan S, Li C, Wood L, Ranganathan G (2001). Adipose tissue tumor necrosis factor and interleukin-6 expression in human obesity and insulin resistance. American Journal of Physiology and Endocrinology Metabolism 280(5): E745-51.

Kershaw EE and Flier JS (2004). Adipose tissue as an endocrine organ. Journal of Clinical Endocrinology and Metabolism 89:2548-2556.

Kersten S, Desvergne B, Wahli W (2000). Roles of PPARs in health and disease. Nature 405, 421-424.

Khurana R, Simmons M, Martin JF, Zachary IC (2005). Role of angiogenesis in cardiovascular disease. A critical appraisal. Circulation 112: 1813-1824.

Kim JK, Gavrilova O, Chen Y, Reitman ML, Shulman GI (2000). Mechanism of insulin resistance in A-ZIP/F-1 fatless mice. The Journal of Biological Chemistry 275: 8456-8460.

Kirkland JL, Hollenberg CH and Gillon WS (1990). Age, anatomic site and the replication and differentiation of adipocyte precursors. American Journal of Physiology 258: C206-C2010.

Klatt P, Cacho J, Crespo MD, Herrera E, Ramos P (2000). Nitric oxide inhibits isoproterenol-stimulated adiopocyte lipolysis through oxidative inactivation of the β-agonist. Biochemical Journal 351:485-493.

Kobliztek T, Weiss C, Yancopoulos GP, Deutsch U, Risau W (1998). Angiopoitin-1 induces sprouting angiogenesis in vitro (1998). Current Biology 8: 529-532.

Kolditz CL and Langin D (2010). Adipose tissue lipolysis. Current Opinions in Clinical Nutrition & Metabolic Care 13: 377-81.

Kolonin MG, Saha PK, Chan L, Pasqualini R and Arap W (2004). Reversal of obesity by targeted ablation of adipose tissue. Nature Medicine 10: 625-632.

Kritchesky D (2003). Diet and cancer: what's next? Journal of Nutrirtion 133: 3827S-3829S.

Krotkiewski M, Bjorntorp P, Sjostrom L, Smith U (1983). Impact of obesity on metabolism in men and women. Importance of regional adipose tissue distribution. Journal of Clinical Investigation 72(3): 1150-62.

Kusaka M, Sudo K, Matsutani E, Kozai Y, Marui S, Fujita T, Ingber D, Folkman J (1994). Cytostatic inhibition of endotheial cell growth by the angiogenesis inhibitor TNP-470 (AGM-1470). British Journal of Cancer 69: 212-216.

Lafontan M and Berlan M (1995). Fat cell a2-adrenoceptors: the regulation of fat cell function and lipolysis. Endocrine Reviews 16: 716-738.

Lafontan M, Moro C, Sengenes C, Galitzky J, Crampes F, Berlan M (2005). An unsuspected metabolic role for atrial natriuretic peptides; the control of lipolysis, lipid mobilisation, and systemic non-esterified fatty acids levels in humans. Arteriosclerosis, Thrombosis and Vascular Biology 25: 2032-2042.

Lage AP and Andrade SP (2000). Assessment of angiogenesis and tumor growth in conscious mice by a fluorimetric method. Microvascular Research 59**,** 278–285.

Lago F, Dieguez C, Go´mez-Reino J, Gualillo O (2007). The emerging role of adipokines as mediators of inflammation and immune responses. Cytokine & Growth Factor Reviews 18: 313–325.

Lahav J (1993). The functions of thrombospondin and its involvement in physiology and pathology. Biochemica Biophysica Acta 1182: 1-14.

Landskroner-Eiger S, Qian B, Muise ES, Nawrocki AR, Berger JP, Fine EJ, Koba W, Yingfeng D, Pollard JW, Scherer PE (2009). Proangiogenic contribution of adiponectin toward mammary tumor growth *in vivo*. Clinical Cancer Research 15: 3265-3276.

Large V, Reynisdottir S, Langin D, Fredby K, Klannemark M, Holm C, Arner P (1999). Decreased expression and function of adipocyte hormone-sensitive lipase in subcutaneous fat cells of obese subjects. Journal of Lipid Research 40: 2059-2066.

Largis EE, Burns MG, Muenekl MA, Dolan JA, Claus TH (1994). Antidiabetic and antiobesity effects of a highly selective β_3- adrenoceptor agonist (CL 316, 243). Drug Development Research 32: 69-76.

Lass A, Zimmermann R, Haemmerle G, Riederer M, Schoiswohl G, Schweiger M, Kienesberger P, Strauss JG, Gorkiewicz G, Zechner R (2006). Adipose triglyceride lipase-mediated lipolysis of cellular fat stores is activated by CGI-58 and defective in Chanarin-Dorfman Syndrome. Cell Metabolism 3(5): 309-19.

Laurencikiene J, van Harmelen V, Nordstrom EA, Dicker A, Blomqvist L, Naslund E, Langin D, Arner P, Ryden M (2007). NF-κB is important for TNF-α induced lipolysis in human adipocytes. Journal of Lipid Research 48: 1069-1077.

Lazar MA (2005). How obesity causes diabetes: not a tall tale. Science 307: 373-375.

Lee YH, Nair S, Rousseau E, Allison DB, Page GP, Tataranni PA, Bogardus C, Permana A (2004). Microarray profiling of isolated abdominal subcutaneous adipocytes from obese vs non-obese Pima Indians: increased expression of inflammation-related genes. Diabetologia 9: 1776-1783.

Lee JW, Shahzad MM, Lin YG, Armaiz-Pena G, Mangala LS, Han HD, Kim HS, Nam EJ, Jennings NB, Halder J, Nick AM, Stone RL, Lu C, Lutgendorf SK, Cole SW, Lokshin AE, Sood AK (2009). Surgical stress promotes tumor growth in ovarian carcinoma. Clinical Cancer Research 15(8): 2695-702.

Liekens S, De Clercq E, Neyts J (2001) Angiogenesis: regulators and clinical applications. Biochemical Pharmacology 61:253-270.

Lien CC, Au LC, Tsai YL, Ho LT, Juan CC (2009). Short term regulation of tumor necrosis factor α induced lipolysis in 3T3L1 adipocytes is mediated through the inducible nitric oxide synthase/nitric oxide dependent pathway. Endocrinology 150: 4892-4900.

Lijnen HR, Demeulemeester D, Van Hoef B, Collen D, Maquoi E (2003). Deficiency of tissue inhibitor matrix metalloproteinase 1 (TIMP-1) impairs

nutritionally induced obesity in mice. The Journal of Thrombosis and Haemostasis 89: 249-255.

Lijnen HR, Christiaens V, Scroyen I, Voros G, Tjwa M, Carmeliet P, Collen D (2006). Impaired adipose tissue development in mice with inactivation of placental growth factor function. Diabetes 55: 2698-2704.

Lijnen, HR (2011). Murine models of obesity and hormonal therapy. Thrombosis Research 127S3: S17-S20.

Lillioja S, Bogardus C (1988). Obesity and insulin resistance: lessons learned from the Pima Indians. Diabetes Metabolic Reviews 4: 517-540.

Liu J, Ranzani B, Tang S, Terman BI, Ware A, Lisanti MP (1999). Angiogenesis activators and inhibiotrs differentially regulate caveoilin-1 expression and caveolae formation in vascular endotheil cells. The Journal of Biological Chemistry 274: 15781-15785.

Liu X, Perusse F, Bukowicki LJ (1998). Mechanisms of the anti-diabetic effects of the β3 adrenergic agonist Cl 316, 243 in obese Zucker (ZDF) rats. American Journal of Physiology 274: R1212-R1219.

Liu Y, Wan Q, Guan L, Gao L, Zhao J (2006). High-fat diet feeding impairs both the expression and activity of AMPKa in rats' skeletal skeletal muscle. Biochemical and Biophysical Research Communications 339:701-707.

Low S, Chin MC, Deurenberg-Yap M (2009). Review on the epidemic of obesity. Annals of Academy of Medicine Singapore 38: 57-59.

Lundgren M, Svensson M, Lindmark S, Renstrom F, Ruge T, Eriksson JW (2007). Fat cell enlargement is an independent marker of insulin resistance and 'hyperleptinaemia'. Diabetologia 50(3): 625-33.

Luscinskas FW and Lawler F (1994). Integrins as dynamic regulators of vascular function. Federation of American Societies for Experimental Biology 8:929-938.

Madamanchi NR, Vendrov A, Runge MS (2005). Oxidative stress and vascular disease. Arteriosclerosis Thrombosis Vascular Biology 25: 29-38.

Madri JA, Pratt BM, Tucker AM (1988). Phenotypic modulation of endothelial cells by transforming growth factor-β depends upon the composition and organisation of the extracellular matrix. Journal of Cell Biology 106: 1375-1384.

Majima M, Isono M, Ikeda Y, Hayashi I, Hatanaka K, Haraday y, Katsumata O, Yamashina S, Katori M, Yamamoto S (1997). Significant roles of inducible cyclooxygenase (COX)-2 in angiogenesis in rat sponge implants. Journal of Pharmacology 75: 105-114.

Man K, Ng KT, Xu A, Cheng Q, Lo CM, Xiao JW, Sun BS, Lim ZX, Cheung JS, Wu EX, Sun CK, Poon RT, Fan ST (2010). Suppression of liver tumor growth and metastasis by adiponectin in nude mice through inhibition of tumor angiogenesis and downregulation of Rho kinase/IFN-inducible protein 10/matrix metalloproteinase 9 signaling. Clinical Cancer Research 16(3): 967-77.

Maquoi E, Demeulemeester D, Voros G, Collen D, Lijnen HR (2003). Enhanced nutritionally induced adipose tissue development in mice with stromelysin-1 gene inactivation. Journal of Thrombosis and Haemostasis 89: 696-704.

Markovic SN, Suman VJ, Rao RA, Ingle JN, Kaur JS, Erickson LA, Pitot HC, Croghan GA, McWillaims RR, Merchan J, Kottschade LA, Creagan ET (2007). A phase II study of ABT-510 (thrombospondin-1 analogue) for the treatment of metastatic melanoma. American Journal of Oncology 30: 303-309.

Maxwell PH (2005). Hypoxia-inducible factor as a physiological regulator. Experimental Physiology 90: 7910797.

McCann J (2001) Jellyfish protein gives new glow to tumor imaging. Journal of the National Cancer Institute 93, 976–977.

McGarry JD and Dobbins RL (1999). Fatty acids, lipotoxicity and insulin secretion. Diabetologia 42: 128-138.

Melillo G, Musso T, Sica A, Taylor LS, Cox GW, Varesio L (1995). A hypoxia-responsive element mediates a novel pathway of activation of the inducible nitric oxide synthase promoter. The Journal of Experimental Medicie 182: 1683.

Michelle FL, Poon V, Klip A (2003). GLUT4 activation: thoughts on possible mechanism. Acta Physiologica Scandinavia 178: 287-296.

Mick GJ, Wang X, McCormick K (2002). White adipocyte vascular endothelial growth factor: regulation by insulin. Endocrinology 143: 948-953.

Miller WH, Fuat IM, Hirsch J (1984). Demonstartion of de novo production of adipocytes in adult rats by biochemical and radioautographic techniques. Journal of Lipid Reserach 25: 336-347.

Mirochnik Y, Kwiatek, Volpert OV (2008). Thrombospondin and apoptosis: molecular mechanisms and use for design for complementation treatments. Current Drug Targets 9: 851-862.

Miyaoka K, Kuwasako T, Hirano K, Nozaki S, Yamashita S, Matsuzawa Y (2001). CD36 deficiency is associated with insulin resistance. Lancet 357: 686-687.

Miyazawa-Hoshimoto S, Takahashi K, Bujo H, Hashimoto N, Saito Y (2003). Elevated serum vascular endothelial growth factor is associated with visceral fat accumulation in human obese subjects. Diabetologia 46: 1483-1488.

Mohamed-Ali V, Goodrick S, Rawesh A, Katz DR, Miles JM, Yudkin JS, Klein S, Coppack SW (1997). Subcutaneous adipose tissue releases interleukin-6, but not tumor necrosis factor-alpha, in vivo. Journal of Clinical Endocrinology Metabolism 82: 4196-4200.

Mokdad AH, Ford ES, Bowman BA, Dietz WH, Vinicor F, Bales VS, Marks JS (2003). Prevalence of obesity, diabetes, and obesity-related health risk factors. Journal of American Medical Association 289: 76-79.

Moncada S, Higgs EA (1991). Endogenous nitric oxide: physiology, pathology and clinical relevance. European Journal of Clinical Investigation 21: 361-374.

Morabito A, De Maio A, Di Maio M, Normanno N, Perrone F (2006). Tyrosine Kinase Inhibitors of Vascular Endothelial Growth Factor Receptors in Clinical Trials: Current Status and Future Directions. The Oncologist: **7**:753-764.

Moreno MJ, Marti A, Garcia-Foncillas J, Martinez JA (2001). DNA hybridisation arrays: a powerful technology for nutritional and obesity research. British Journal of Nutrition 86: 119-122.

Morton NM, Holmes MC, Fievet C, Staels B, Tailleux A, Mullins JJ, Seckl JR (2001). Improved lipid and lipoprotein profile, hepatic insulin sensitivity, and glucose tolerance in 11beta-hydroxysteroid dehydrogenase type 1 null mice. Journal of Biological Chemistry 2: 276: 41293-41300.

Morton NM, Densmore V, Wamil M, Ramage L, Nichol K, Bünger L, Seckl JR and Kenyon CJ (2005). A polygenic model of the metabolic syndrome with reduced circulating and intra-adipose glucocorticoid action. Diabetes 54: 3371-3378.

Morton N, Seckl J (2008). 11B-Hydroxysteroid dehydrogenase type 1 and obesity. Obesity and Metabolism 36: 146-164.

Moto C, Crampes F, Sengenes C (2004). Atrial natriuretic peptide contributes to physiological control of lipid mobilisation in humans. FASEB Journal 18: 908-910.

Motojima K, Passilly P, Peters JM, Gonzalez FJ, Latruffe N (1998). Expression of putative FA transporter genes are regulated by peroxisome proliferator activated receptor alpha and gamma activators in a tissue and inducer specific manner. Journal of Biological Chemistry 273: 16710-16714.

Mottillo EP, Shen XJ, Granneman JS (2010). B3-adrenergic receptor induction of adipocyte inflammation requires lipolytic activation of stress kinases p38 and JNK. Bichimica et Biophysica Acta 1801: 1048-1055.

Mu H, Ohashi R, Yan S, Chai H, Yang H, Lin P, Yao Q, Chen C (2006). Adipokine resisitin promotes in vitro angiogenesis of human endothelial cells. Cardiovascular Research 70: 146-157.

Mukherjee P, Abate LE, Seyfried TN (2004). Antiangiogenic and proapoptotic effects of dietary restriction on experimental mouse and human brain tumours. Clinical Cancer Research 10: 5622-5629.

Muller-riemenschneider F, Reinhold T, Berghofer A, Willich SN (2009). Health-economic burden of obesity in Europe. European Journal of Epidemiology 23: 499-509.

Murohara T, Asahara T, Silver M, Bauters C, Masuda H, Kalka C, Kearney M, Chen D, Symes JF, Fishman MC (1998). Nitric oxide synthase modulates angiogenesis in response to tissue ischemia. The Journal of Clinical Investigation 101: 2567-2578.

Muzzin P, Revelli JP, Kuhne F, Gocayne JD, mcCombie WR, Venter JC, Giacobino JP, Fraser CM (1991). An adipose tissue-specific beta-adrenergic receptor: molecular cloning and down-regulation in obesity. The Journal of Biological Chemistry 15: 24053-24058.

Nabors LB, Suswam E, Huang Y, Yang X, Johnson MJ, King PH (2003). Tumor necrosis factor alpha induces angiogeneic factor up-regulation in malignant glioma cells: a role for RNA stabilisation and HuR. Cancer Research 66 (23) 11125-11130.

Nakae J, Accilli D (1999). The mechanisms of insulin action. Journal of Endocrinology Metabolism 3: 721-731.

Nassir F, Wilson B, Han X, Gross RW, Abumrad NA (2007). CD36 is important for fatty acid and cholesterol uptake by the proximal but not distal intestine. The Journal Biological Chemistry 282: 19493-19501.

Nathan FE, Hernandez E, Dunton CJ, Treat J, Switalska HI, Joseph RR, Tusynski GP (1994). Plasma thrombospondin levels in patients with gynaecologic malignancies. Cancer 73: 2853-2858.

Nechad M, Kussela P, Carneheim C, Bjorntorp P, Nedergaard J, Cannon B (1983). Development of brown fat cells in monolayer culture: morphological and biochemical distinction from white fat cells in culture. Experimental Cell Research 149: 105-118.

Nicosia RF and Ottinetti A (1990). Growth of microvessels in serum-free matrix culture of rat aorta: A quantitative assay of angiogenesis in vitro. Laboratory Investigations. **63**, 115–122.

Nilsson MB, Langley RR, Fidler IJ (2005). Interleukin-6 secreted by human ovarian carcinoma cells, is a potent proangiogenic cytokine. Cancer Research 65: 10794-10800.

Nisoli E, Clementi E, Tonello C, Sciorati C, Briscini L, Carruba MO (1998). Effects of nitric oxide on proliferation and differentiation of rat brown adipocytes in primary cultures. British Journal of Pharmacology 125: 888-894.

Ng QS, Goh V, Milner J, Stratford MR, Folkes LK, Tozer GM, Saunders MI, Hoskin PJ (2007). Effect of nitric oxide synthesis on tumour blood volume and vascular activity. A phase I study. Lancet Oncology 8: 111-118.

Nor JE, Mitra RS, Sutorik MM, Mooney DJ, Castle VP, Polverini PJ (2000). Thrombospondin-1 induces endothelial cell apoptosis and inhibits angiogenesis by activating caspase death pathway. The Journal of Vascular Research 37: 209-218.

Old LJ (1985). Tumor necrosis factor (TNF). Science 230: 630-632.

Okada T, Kawano Y, Sakakibara T, Hazeki O, Ui M (1994). Association between a cytochrome P450 CYPIA1 genotype and incidence of lung cancer. The Journal of Biological Chemistry 269: 3568-3573.

O'Reilly MS, Boehm T, Shing Y, Fukai N, Vasios G, Lane WS, Flynn E, Birkhead JR, Olsen BR, Folkman J (1997). Endostatin: An endogenous inhibitor of angiogenesis and tumor growth. Cell 88: 277-285.

Ostermeyer AG, Paci JM, Zeng Y, Lublin DM, Munro S, Brown DA (2001). Accumulation of caveolin in the endoplasmic reticulum redirects the protein to lipid storage droplets. J Cell Biology 152(5): 1071-8.

Ouchi N, Kihara S, Arita Y, Maeda K, Kuriyama H, Okamoto Y, Hotta K, Nishida M, Takahashi M, Nakamura T, Yamashita S, Funahashi T and Matsuzawa Y (1999). Novel modulator for endothelial adhesion molecules; adipocyte-derived plasma protein adiponectin. Circulation 100; 2473-2476.

Pang C, Gaol Z, Yin J, Zhang J, Jia W, Ye J (2008). Macrophage infiltration into adipose tissue may promote angiogenesis for adipose tissue remodelling in obesity. American Journal of Endocrinology Metabolism 295: E313-E322.

Park HY, Kwon HM, Lim HJ, Hong BK, Lee JY, Park BE, Jang Y, Cho SY, Kim HS (2001). Potential role of leptin in angiogenesis: leptin induces endothelial cell proliferation and expression of matrix metalloproteinase in vivo and in vitro. Experimental and Molecular Medicine 30: 95-102.

Parton RG, Hanzal-Bayer M, Hancock JF (2006). Biogenesis of caveolae: a structural model for caveolin-induced domain formation. Journal of Cell Science 119(Pt 5): 787-96.

Pasarica M, Sereda OR, Redman LM, Albarado DC, Hymel DT, Roan LE, Rood JC, Burk DH, Smith SR (2008). Reduced adipose tissue oxygenation in human obesity: evidence for rarefaction, macrophage chemotaxis and inflammation without an angiogenic response. Diabetes 58: 18-25.

Passanitia A, Taylor RM, Pili R, Guo Y, Long PV, Haney JA, Pauly RR, Grant DS and Martin GR (1992). Methods in laboratory investigation: A simple, quantitative method for assessing angiogenesis and antiangiogenic agents using reconstituted basement membrane, heparin, and fibroblast growth factor. Laboratory Investigations 67(4):519-28.

Patel HH, Murray F and Insel PA (2008). Caveolae as organisers ofpharmacologically relevant signal transduction molecules. Annual Reviews Pharmacology Toxicology 48: 359-391.

Patel BP, Safdar A, Raha S, Tarnopolsky M, Hamadeh MJ (2010). Caloric restriction shortens lifespan through an increase in lipid peroxidation, inflammation and apaotosis in the G93A mouse, and animal model of ALS. PLoS ONE 5 (2); e9386.

Parton RG, Hanzal-Bayer M and Hancock JF (2006). Biogenesis of caveolae: a structural model for caveolin-induced domain function. Joournal of Cell Science 119: 787-796.

Perman PA, Menge C, Reaven PD (2006). Macrophage-secreted factors induce adipocyte inflammation and insulin resistance. Biochemical and Biophysical Research Communications 341:507-514.

Permana PA, Del Parigi A, Tataranni PA (2004). Microarray gene expression profiling in obesity and insulin resistance. Nutrition 20: 134-138.

Pitas RE, Innerarity TL, Mahley RW (1983). Foam cells in explants of atherosclerotic rabbit aortas have recepotrs for β–very low density lipoproteins and modified low density lipoproteins. Arteriosclerosis 3: 2-12.

Pohl, Ring A, Ehehalt R, Schulze-Bergkamen H, Schad A, Verkade P, Stremmel W (2004). Long chain fatty acid uptake into adipocytes depends on lipid raft function. Biochemistry 43: 4179-4187.

Pol, A, Luetterforst R, Lindsay M, Heino S, Ikonen E, Parton RG (2001). A caveolin dominant negative mutant associates with lipid bodies and induces intracellular cholesterol imbalance. Journal of Cell Biology 152(5): 1057-70.

Popkin BM (2001). The nutrition transition and obesity in the devlopeing world. Journal of Nutrition. 131: 871-873.

Poskitt EM (2009). Countries in transition: underweight to obesity non-stop? Annals of Tropical Paediatrics 29: 1-11.

Pravenec M, Lands V, Zidek V, Musilova A, Kazdova L, Qi N, Wang J, Lenzin E, Kutz TW (2003). Transgenic expression of CD36 in the spontaneously hypertensive rat is associated with amelioration of metabolic disturbances but has no effect on hypertension. Physiologcial Research 52: 681-688.

Punekar S, Zak S, Kalter VG, Dobransky L, Punekar I, Lawler JW, Gutierrez LS (2007). Thrombospondin-1 and its mimetic peptide ABT-510 decrease angiogenesis and inflammation in a murine model of inflammatory bowel disease. Pathobiology 75: 9-21.

Qi Y, Nie Z, Lee YS, Singhal NS, Scherer PE, Lazar MA, Ahima RS (2006). Loss of resistin improves glucose homeostasis in leptin deficiency. Diabetes 55(11): 3083-90.

Quesada AJ, Neaius T, Yap R, Zaichuk TA, Alfranca A, Filleur S, Volpert OV, Redondo JM (2005). In vivo upregualtion of CD95 and CD95L causes synergistic inhibition of angiogenesis by TSP1 peptide and metronomic doxorubicin treatment. Cell Death and Differentiation 2: 649-658.

Rahn T, Ridderstrale M, Tornquist H, Manganiello V, Friedkson G, Belfage P, Degerman E (1994). Esseential role of phospatidylinositol 3-kinase in insulin-induced activation and phosphorylation of the cGMP-inhibited cAMP phosphodiesterase in rat adipocytes. Studies using the selective inhibitor Wortmannin. FEBS Letters 350, 314-318.

Rankinen T, Zuiben A, Chagnon YC, Weisnagel SJ, Argyropoulos G, Watts B, Perusse L, Bouchard C (2006). The human obesity gene map: the 2005 update. Obesity: 14: 529-644.

Rausch ME, Weisberg S, Vardhana P, Tortoriello DV (2008). Obesity in C57BL/6J mice is characterized by adipose tissue hypoxia and cytotoxic T-cell infiltration. International Journal of Obesity (Lond) 32(3): 451-63.

Reaven GM (1993). Role of insulin resistance in human disease (Syndrome X): An expanded definition. Annual Review of Medicine 44: 121-131.

Rehman JD, Traktuev J, Li S, Merfeld-Clauss CJ, Temm-Grove JE, Bovenkerk CL, Pell BH, Johnstone RV (2004). Secretion of angiogenic and antiapoptotic factors by human adipose stromal cells. Circulation 109**:**1292-1298.

Reiher FK, Volpert OV, Jimenez B et al (2002). Inhibition of tumor growth by systemic treatment with thrombopsonin-1 peptide mimetics. International Journal of Cancer 98: 682-689.

Reynisdottir S, Langin D, Carlstrom K, Holm C, Rossner S, Arner P (1995). Effects of weight reduction on the regulation of lipolysis in adipocytes of women with upper-body obesity. Clinical Science 89: 421-429.

Ribiere C, Jaubert AM, Gaudiot N, Sabourault D, Marcus ML, Boucher JL, Denishenriot D and Gludicelli Y (1996). White adipose tissue nitric oxide synthase: A potential source for NO production. Biochemical and Biophysical Research Communications 222: 706-712.

Ronti T, Lupattelli G and Mannarino E (2006). The endocrine function of adipose tissue: an update. Clinical Endocrinology 64: 355-365.

Rosell S and Belfrage E (1979). Blood circulation in adipose tissue. Physiological Reviews 59:1078-1104.

Rosen ED, Arraf P, Troy AE, Bradwin G, Moore K, Milstone DS, Spiegelman BM, Mortensen RM (1999). PPARγ is required for the differentiation of adipose tissue in vivo and in vitro. Molecular Cell 4: 611-617.

Rotter V, Nagaev I, Smith U (2003). Interleukin-6 (IL-6) induces insulin resistance in 3T3-L1 adipocytes and is, like IL-8 and tumor necrosis factor-alpha, over expresses in human fat cells from insulin-resistant subjects. The Journal of Biological Chemistry 14: 45777-45784.

Rou P (1914). The influence of diet on transplanted and spontaneous mouse tumours. Journal of Experimental Medicine 20: 433-451.

Rupnick MA, Panigraphy D, Zhang CY, Dallabrida SM, Lowell BB, Langer R and Folkman MJ (2002). Adipose tissue mass can be regulated through the vasculature. Proceedings of the National Academy of Sciences U.S.A *99*:10730-10735.

Rusk A, Cozzi E, Stebbins M, Vai D, Graham J, Va V, Henkin J, Sharpee R, Khana C (2006). Cooperative activity of cytotoxic chemotherapy with antiangiogenic thrombospondin-1 peptides, ABT-526 in pet dogs with relapsed lymphoma. Cancer Reserach 12: 7456-7564.

Ryan TJ (1995). Lymphatics and adipose tissue. Clinical Dermatology 13:493-498.

Saiki A, Watanabe F, Murano T, Miyashita Y and Shirai K (2006). Hepatocyte growth factor secreted by cultured adipocytes promotes tube formation of vascular endothelial cells *in vitro*. International Journal of Obesity 30: 1676–1684.

Saglio SD, Slayter HS (1982). Use of radioimmunoassay to quantify thrombospondin. Blood 59: 162-166.

Sanges, R, Cordero F, Calogero RA (2007). oneChannelGUI: a graphical interface to Bioconductor tools, designed for life scientists who are not familiar with R language. Bioinformatics 23(24): 3406-8.

Scannell G, Waxman K, Vaziri ND, Zhang J, Kaupe CJ, Jalai M, Hecht CC (1995). Hypoxia-induced alterations of nutrophil membrane receptors. Journal of Surgical Research 59: 141-145.

Schafer K, Fujisawa K, Konstantinides S, Loskutoff DJ (2001). Disruption of the plasminogen activator inhibitor 1 gene reduces the adiposity and improves the metabolic profile of genetically obese and diabetic ob/ob mice. Federation of American Societies for Experimental Biology **15**:1840-1842.

Schaffer JE (2003). Lipotoxicity:when tissues overeat. Current Opinion in Lipidology 14: 281-287.

Schneiter P, Tappy L (1998). Kinetics of dexamthasone-induced alterations of glucose metabolism in healthy humans. American Journal of Physiology 275: E806-E13.

Shojima N, Sakoda H, Ogihara T, Fujishiro M, Katagiri H, Anai M, Onishi Y, Ono H, Inukai K, Abe M, Fukushima Y, Kikuchi M, Oka Y, Asano T (2002). Humoral regulation of resistin expression in 3T3-L1 and mouse adipose cells. Diabetes 51(6): 1737-44.

Schoonjans K, Peinado-Onsurbe J, Lefebvre Am, Heyman RA, Briggs M, Deeb S, Staels B, Auwerx J (1996). PPAR alpha and PPAR gamma activators direct a distinct tissue-specific transcriptional response via a PPRE in the lipoprotein lipase gene. EMBO Journal 15: 5336-5348.

Sekar N, Li J, Shechter Y (1996). Vanadium salts as insulin substitutes: mechanisms of action, a scientific and therapeutic tool in diabetes mellitus research. Critical Reviews in Biochemistry and Molecular Biology 31: 339-359.

Semenza GL, Agani F, Booth G, Forsythe J, Iyer N, Jiang BH, Lueng S, Roe R, Wiener C, Yu A (1997). Kidney International 51: 553-555.

Sengenes C, Berlan M, De Glisezinski I, Lafontan M, Galitzky J (2000). Natriuretic peptides: a new lipolytic pathway in human adipocytes FASEB Journal 14: 1345-1351.

Sethi JK and Vidal-Puig JV (2007). Adipose tissue function and plasticity orchestrate nutrional adaptation. Journal of Lipid Research 48: 1253-1262.

Shaked Y, Bertolini F, Man S, Rogers MS, Cervi D, Foutz T, Rawn K, Voskas D, Dummont DJ, Lawler J, Henkin J, Hicklin DJ, D'Amato RJ, Kerbel RS (2005). Genetic heterogeneity of the vasculogenic phenotype parallels angiogenesis. Cancer Cell 7: 101-111.

Sharpe J, Ahlgren U, Perry P, Hill B, Ross A, Hecksher-Sorensen J, Baldock R, Davidson D (2002). Optical projection tomography as a tool for 3D microscopy and gene expression studies. Science. 296: 541-545.

Shih CM, Lee YL, Chiou HL, Chen W, Chang GC, Chou MC et al (2006). Association of TNF-alpha polymorphism with susceptibility to and severity of non-small cell lung cancer. Lung Cancer 52: 15-20.

Shulman (2000). Cellular mechanisms of insulin resistance. Journal of Clinical Investigation 106: 171-176.

Siegrist-Kaiser CA, Pauli V, Juge-Aubry CE, Boss O, Pernin A, Chin WW, Cusin I, Rohner –Jeanrenaud F, Burger AG, Zapf J, Meier CA (1997). Direct effects of

leptin on brown and white adipose tissue. Journal of Clinical Investigations 100(11): 2858-2864.

Sierra-Honigmann, M. R., A. K. Nath, C. Murakami, G. Garcia-Cardena, A., Papapetropoulos, W. C. Sessa, L. A. Madge, J. S. Schechner, M. B. Schwabb, P., J. Polverini, and J. R. Flores-Riveros (1998). Biological action of leptin as an angiogenic factor. Science 281:1683-1686.

Silha JV, Krsek M, Sucharda P and Murphy LJ (2005). Angiogenic factors are elevated in overweight and obese individuals. International Journal of Obesity 29: 1308-1314.

Simantov R, Silverstein RL (2003). CD36: a critical anti-angiogenic receptor. Front Bioscience 8: 874-882.

Silverman KJ, Lund DP, Zetter BR, Lainey LL, Shahood JA, Freiman DG, Folkman J and Barger AC. (1988). Angiogenic activity of adipose tissue. Biochemical and Biophysical Research Communications **153,** 347–352.

Singhal S, Vachani A, Antin-Ozerkis D, Kaiser LR, Albelda SM (2005). Prognostic implications of cell cycle, apoptosis and angiogenesis biomarkers in non-small cell lung cancer: A Review. Clinical Cancer Research 11: 3974-3986.

Skala MC, Palmer GC, Vrotsos KM, Gendron-Fitzpatrick A, Ramanujam N (2007). Comparison of a physical model and principal component analysis for the diagnosis of epithelial neoplasias in vivo using diffuse reflectance spectroscopy. Optical Express 15: 7863-7875.

Skobe M and Detmar M (2000). Structure, function, and molecular control of the skin lymphatic system. Journal of Investigative Dermatology Symposium Proceedings 5: 14-19.

Small GR, Hadoke PWF, Sharif I, Dover AR, Armour D, Kenyon CJ, Gray GA and Walker BR (2005). Preventing local regeneration of glucocorticoids by 11-hydroxysteroid dehydrogenase type 1 enhances angiogenesis. Proceedings of the National Academy of Science 102 (34), 12165–12170.

Spalding KL, Arner E, Westermark PO, Bernard S, Buchholz BA, Bergmann O, Blomqvist L, Hoffstedt J, Naslund E, Britton T, Concha H, Hassan M, Ryden M, Frisen J, Arner P (2008). Dynamics of fat cell turnover in humans. Nature 453(7196): 783-7.

Soukas A, Socci ND, Saatkamp BD, Novelli S, Friedman JM (2001). Distinct transcriptional profiles of adipogenesis in vivo and in vitro. Journal of Biological Chemistry 276: 34167-34174.

Souza SC, Yamamoto MT, Franciosa MD, Lien P, Greenberg AS (1998). BRL 49653 blocks the lipoltic actions of tumor necrosis factor α- a potential new insulin-sensitising mechainsm for thiazolidnediones. Diabetes 47: 691-695.

Staton CA, Stribbling SM, Tazzyman S, Huges R, Brown NJ, Lewis CL (2004). Current methods for assaying angiogenesis *in vitro* and *in vivo*. International Journal of Experimental Pathology 85: 223-248.

Stenina OI, Krukovets I, Wang K, Zhou Z, Forudi F, Penn MS, Topol EJ, Plow EF (2003). Increased expression of thrombospondin-1 in vessel wall of diabetic Zucker rat. Circulation 107: 3209-3215.

Steppan CM, Bailey ST, Bhat S, Brown EJ, Banerjee RR, Wright CM, Patel HR, Ahima RS, Lazar MA (2001). The hormone resistin links obesity to diabetes, Nature 409: 307-312.

Stern JS, Batchelor BR, Hollander N, Cohn CK, Hirsch J (1972). Adipose-cell size and immunoreactive insulin levels in obese and normal-weight adults. Lancet 2(7784): 948-51.

Stich V, De Glisezinski I, Crampes F, Hejnova J, Cottet-Emad JM, Galitzky J, Lafonatn M, Riviere D, Berlan M (2000). Activation of a2-adrenergic receptors impairs exercise-induced lipolysis in SCAT of obese subjects. American Journal of Physiology 279: 499-504.

Straczkowski M, Dzienis-Straczkowska, Stepien A, Kowalska I, Szlachowska M, Kinalska I (2002). Plasma interleukin-8 concnetrations are increased in obese subjects and related to fat mass and tumor necrossi factor-α system. The Journal of Clinical Endocrinology and Metabolism 87: 4602-4606.

Streit M, Veasco P, Riccardi L, Spencer L, Brown LF, Janes L, Lange-Asschenfeldt B, Yano K, Hawighorst T, Iruela-Arispe L, Detmar M (2000). Thrombospondin-1 suppresses wound healing and granulation tissue formation in the skin of transgenic mice. EMBO Journal 19: 3272-3282.

Strissel KJ, Stancheva Z, Miyoshi H, Perfield JW, Greenberg AS, Obin AS (2007). Adipocyte death, adipose tissue remodeling, and obesity complications. Diabetes 56: 2910-2918.

Stump DD, Fan X, Berk PD (2001). Oleic acid uptake and binding by rat adipocytes define dual pathways for cellular fatty acid uptake. Journal of Lipid Research 42: 509-520.

Subramanian V, Garcia A, Sekowski A, Brasaemle DL (2004). Hydrophobic sequences target and anchor perilipin A to lipid droplets. Journal of Lipid Research 45(11): 1983-1991.

Suganami E, Takagi H, Ohashi H, Suzuma K, Suzuma I, Oh H, Watanabe D, Ojima T, Suganami T, Fujio Y, Nakao K, Ogawa Y, Yoshimura N (2004). Leptin stimulates ischemia-induced retinal neovascularisation: possible role of vascular endothelial growth factor expresses in retinal endothelial cells. Diabetes 53: 2443-2448.

Sullivan JE, Carey F, Carling D, Beri RK (1994). Characterisation of 5'-AMP-activated protein kinase in human liver using specific peptide substrates and the effects of 5'-AMP analogues on enzyme activity. Biochemical Biophysical Research Communication 200(3): 1551-6.

Sumi M, Sata M, Toya N, Yanaga K, Ohki T, Nagai R (2007). Transplantation of adipose stromal cells, but not mature adipocytes, augments ischemia-induced angiogenesis. Life Sciences 80: 559-565.

Sunderkotter C, Goebeler M, Schulze-Osthoff K, Bhardwaj R, Sorg C (1991). Macrophage- derived angiogenesis factors. Pharmacology Therapeutics 51: 195-216.

Szabo KA, Ablin RJ, Singh G (2004) Matrix metalloproteinases and the immune response. Clinical and Applied Immunology Reviews 4*:295-319.*

Tada H, Kuboki K, Nomura K, Inokuchi T (2001). High glucose levels enhance TGF-beta-thrombospondin-1 pathway in cultured human mesangial cells via mechanisms dependent on glucose-induced PKC activation. Journal of Diabetes Complications 15: 193-197.

Tappy L, Randin D, Vollenweider P, Vollenweider L, Paquot N, Scherrer U, Scneiter P, Nicod P, Jequier E (1994). Mechanisms of dexamthasone-induced insulin resistance in healthy humans. Journal of Clinical Endocrinology Metabolism 79: 1063-1069.

Taraboletti G, Roberst D, Liotta LA, Giavazzi R (1990). Platelet thrombospondin modulates endothelial cell adhesion, motility and growth: a potential angiogenesis regulatory factor. Journal of Cell Biology 111:765-772.

Taraboletti G, Belotti D, Giavazzi R (1992). Thrombospondin modulates basic fibroblast growth factor activates on endothelial cells. Angiogenesis Key Principles. Birkhauser Verlag, Basel, Switzerland 210-213.

Thaker PH, Han LY, Kamat AA, Arevalo JM, Takahashi R, Lu C, Jennings NB, Armaiz-Pena G, Bankson JA, Ravoori M, Merritt WM, Lin YG, Mangala LS, Kim TJ, Colman RL, Landen CN, Li Y, Felix E, Sanguino AM, Newman RA, Lloyd M, Gershenson D, Cole SW, Sood AK (2006). Chronic stress promotes tumor growth and angiogenesis in a mouse model of ovarian carcinoma. Nature Medicine 12(8): 939-44.

Thorn H, Stenkula KG, Karlsson M (2003). Cell surface orifices of caveolae in adipocytes. Molecular Biology Cell 14: 3967-3976.

Tigno XT, Selaru IK, Angeloni SV, Hansen BC (2003). Is microvascular flow rate related to ghrelin, leptin and adiponectin levels? Clinical Hemorheology Microcirculation 29: 409-416.

Tolsma SS, Volpert OV, Good DJ, Frazier WA, Polverini PJ, Bouck N (1993). Peptides derived from 2 separate domains of the matrix protein thrombospondin-1 have anti-angiogenic actiivty. Journal of Cell Biology 122: 497-511.

Tolsma SS, Stack MS, Bouck N (1997). Lumen formation and other angiogenic activation of cultured capillary endotheial cells are inhibited by thrombospondin 1. Mircovascular Research 54: 13-26.

Tontonoz P, Kim JB, Graves RA, Spiegelman BM (1993). ADDI: a novel helix-loop-helix transcription factor associated with adipocyte determination and differentiation. Molecular Cellular Biology 13: 4753-4759.

Tontonoz P, Hu E, Spiegelman BM (1994). Stimulation of adipogenesis in fibroblasts by PPAR gamma 2, a lipid activated transcription factor. Cell 79: 1147-1156.

Trayhurn P and Wood IS (2005). Signalling role of adipose tissue: adipokines and inflammation in obesity. Biochemical Society Transactions 33: 1078–81.

Trayhurn P (2005). Endocrine and signalling role of adipose tissue:new perspectives on fat. Acta Physiologica Scandinavica 184:285-293.

Trayhurn P, Wand B, Wood IS (2008). Hypoxia and the endocrine and signalling role of white adipose tissue. Arch Physiol Biochem 114: 267-276.

Trigatti BL, Anderson RG and Gerber GE (1999). Identification of caveolin-1 as a fatty acid binding protein. Biochem Biophys Research Communication 255: 34-39.

Thurston G, Rudge JS, Ioffe E, AHou H, Ross L, Croll SD, Glazer N, Holash J, McDonald DM, Yancopoulos GD (2000). Angiopoietin-1 protects the adult vasculature against plasma leakage. Nature Medicine 6: 460-463.

Unger RH (1995). Lipotoxicty in the pathogenesis of obesity-dependent NIDDM, Genetic and clinical implications. Diabetes 44: 8: 863-870.

Uysal KT, Wiesbrock SM, Marino MW, Hotamisligil GS (1997). Protection from obesity-induced insulin resiatnce in mice lacking TNF-alpha function. Nature 389:610-614.

Van Belle E, Witzenbichler B, Chen D, Silver M, Chang L, Schwall R, Isner JM (1998). Potentiated angiogenic effect of scatter factor/hepatocyte growth factor via induction of vascular endothelial growth factor: the case for paracrine amplification of angiogenesis. Circulation 97: 381-390.

VanBiesen T, Luttrell LM, Hawes BE, Lefkowitz RJ (1996). Endocrinology Reviews 17: 698-714.

van Dam M, Mullberg J, Schooltink H, Stoyan T, Brakenhoff JP, Graeve L, Heinrich P, Rose-John S (1993). Structure-function analysis of interleukin-6 utilizing human/murine chimeric molecules. Involvement of two separate domains in receptor binding. Journal of Biological Chemistry 68(20): 15285-90.
Varma V, Ya-Borengasser A, Bodles A, Rasouli N, Phanavah B, Nolen GT, Kern EM, Nagarajan R, Spencer HJ, Lee MJ, Fried SK, McGehee RE, Peterson CA, Kern PA (2008). Thrombospondin-1 is an adipokine associated with obesity, adipose inflammation, and insulin resistance. Diabetes 57: 432-439.

Vidal-Puig AJ, Considine RV, Jimenez-Linan M, Werman A, Pories WJ, Caro JF, Filer JS (1997). Peroxisome prolifertor-activated receptor gene expression in human tissues. Effects of obesity, weight loss, and regulation by insulin and glucocorticoids. The Journal of Clinical Investigation 99: 2416-2422.

Villena JA, . Viollet B, Andreelli F, Kahn A, Vaulont S, Sul HS (2004). Induced adiposity and adipocyte hypertrophy in mice lacking the AMP-activated protein kinase-alpha2 subunit. Diabetes 53(9): 2242-9.

Vishwanath K, Yuan H, Moore L, Bender J, Dewhirst M, Ramanujam N (2008). Longitudinal monitoring of 4TI-tumor physiology in vivo with doxorubicin treatment via diffuse optical spectroscopy. Biomedical optics/digital holography and three-dimensional imaging/laser applications to chemical, security and environment analysis. The Optical Society of America 21: 157-168.

Vogel T, Guo NH, Krutsch HC, Blake DA, Hartman J, Mendelovitz S, Panet A, Roberts DD (1993). Modulation of endothelial cell proliferation, adhesion, and motility by recombinant heparin-binding domain and synthetic peptides from the Type I repeats of thrombospondin. Journal Cell Biochemistry 53: 74-84.

Vohl MC, Sladek R, Robiytallie J, Gurd S, Marceau P, Richard D, Hudson TJ, Tchernof A (2004). A survey of genes differentially expressed in subcutaneous and visceral adipose tissue in men. Obesity Research 12: 1217-1222.

Volin MV, Harlow LA, Woods JM, Campbell PL, Amin MA, Tokuhira M, Koch AE (1999). Treatment with sulfasalazine or sulfapyridine, but not 5-aminosalicyclic acid, inhibits basic fibroblast growth factor-induced endothelial cell chemotaxis. Arthritis Rheumatism 42: 1927-1935.

Volpert OV, Tolsma SS, Pllerin S, Feige JJ, Chen H, Chen DF (1995). Inhibition of angiogenesis by thrombospodin-2. Biochemical and Biophysical Research Communications 217: 326-332.

Volpert OV, Lawler J, Bouck NP (1998). A human fibrosarcoma inhibits systemic angiogenesis and the growth of experimental metastases via thrombospondin-1. Proceedings of the National Academy of Sciences USA 95: 6343-6348.

Voros G, Maquoi E, Demeulemeester D, Clerx N, Collen D, Lijnen HR (2005). Modulation of angiogenesis during adipose tissue development in murine models of obesity. Endocrinology 146: 4545-4554.

Vossler MR, Yao H, York RD, Pan MG, Rim CS, Stork PJ (1997). cAMP activates MAP kinase and ELK-1 through a B-Raf- and Rap1-dependent pathway. Cell 89: 73-82.

Voyta JC, Via DP, Butterfield CE, Zetter BR (1984). Identification and isolation of endothelial cells based on their increased uptake of acetylated-low density lipoprotein. The Journal of Cell Biology 99: 2034-2040.

Wadden TA (1993). Treatment of obesity by moderate and server caloric restriction. Results of clinical research trials. Annals of Internal Medicine 119: 688-693.

Wajchenberg BL (2000). Subcutaneous and visceral adipose tissue: their relation to the metabolic syndrome. Endocrine Reviews 21: 697-738.

Wang D and Sul HS (1997). Upstream stimulatory factor binding to the E-box at -65 is required for insulin regulation of the fatty acid synthase promoter. The Journal of Biological Chemistry 274: 18243-18251.

Wang S, Soni KG, Semache M, Casavant S, Fortier M, Pan L, Mitchell GA (2008). Lipolysis and the integrated physiology of lipid energy metabolism. Molecular Genetics and Metabolism 95: 117-126.

Wang D, Oparil S, Feng JA, Li P, Perry G, Chen LB, Dai M, John SW, Chen YF (2003). Effects of pressure overload on extracellular matrix expression in the heart of the atrial natriuretic peptide null mouse. Hypertension 42: 88-95.

Watanabe K, Hasegawa Y, Shimizu K, Ding Y, Abe M, Ohta H, Imagawa K, Hojo K, Maki H, Sonoda H, Sato Y (2004). Vasohibin as an endothelium-derived negative feedback regulator of angiogenesis. The Journal of Clinical Investigation 114: 898-907.

Weindruch R, Naylor PH, Goldstein AL, Walford RL (1988). Influences of aging and dietary restriction on serum thymosin alpha 1 levels in mice. J Gerontol 43(2): B40-2.

Weisberg SP, McCann D, Desai M, Rosenbaum M, Leibel RL, Ferrante AW (2003). Obesity is associated with macrophage accumulation in adipose tissue. Journal of Clinical Investigation 112: 1796-1808.

Weisberg SP, Hunter D, Huber R, Lemieux J, Slaymaker S, Vaddi K, Charo I, Leibel RL, Ferrant AW (2006). CCR2 modulates inflammatory and metabolic effects of high fat feeding. Journal of Clinical Investigation 116:115-124.

Wettenhall JM and Smyth GK (2004). limmaGUI: a graphical user interface for linear modeling of microarray data. Bioinformatics 20(18): 3705-6.

Westpha JR (2004). Technology evaluation: ABT-510. Abbott Current Opinions Molecular Therapy 6: 451-457.

Weyer C, Taaranni PA, Snitker K, Danforth E (1998). Increase in insulin action and fat oxidation following treatment with CL 316, 243, a highly selective beta-3 adrenoceptor agonist in humans. Diabetes 47: 1555-1561.

Winder WW, Arogyasami J , Elayan IM, Cartmill D (1990). Time course of exercise-induced decline in malonyl-CoA in different muscle types. American Journal of Physiology 259(2 Pt 1): E266-71.

Winder WW (1998). Intramuscular mechanisms regulating fatty acid oxidation during exercise. Advances in Experimental Medicine Biology 441: 239-48.

Winzell MS, Ahren B (2004). The high-fat fed mouse: a model for studying mechanisms and treatment of impaired glucose tolerance and type 2 diabetes. Diabetes 53: S215-S219.

Wu D, Ren Z, Pae M, Guo W, Merrill AH, Meydani SN (2007). Aging up regulates expression of inflammatory mediators in mouse adipose tissue. Journal of Immunology 179: 4829-4839.

Xi L, Qian Z, Xu G, Zhou C, Sun S (2007). Crocetin attenuates palmitate-induced insulin insensitivity and disordered tumor necrosis factor-alpha and adiponectin expression in rat adipocytes. British Journal of Pharmacology 151(5): 610-7.

Xu H, Barnes GT, Yang Q, Tan G, Yang D, Chou CJ, Sole J, Nicholas A, Ross JS, Tartaglia LA, Chen H (2003). Chronic inflammation in fat plays a crucial role in the development of obesity related insulin resistance. Journal of Clinical Investigation 112:1821-1830.

Xue Y, Lim S, Brakenhielm E, Cao Y (2010). Adipose angiogenesis: quantitative methods to study microvessel growth, regression and remodelling in vivo. Nature Protocols 5: 912-920.

Yao JS, Zhai W, Young WL, Yang GY (2006). Interleukin-6 triggers human cerebral endothelial cells proliferation and migration: the role for KDR and MMP-9. Biochemical and Biophysical Research Communications 342: 1396-1404.

Yamaguchi T, Omatsu N, Matsushita S, Osumi T (2004). CGI-58 interacts with perilipin and is localized to lipid droplets. Possible involvement of CGI-58 mislocalization in Chanarin-Dorfman syndrome. Journal of Biological Chemistry 279(29): 30490-7.

Yamauchi M, Imajoh Ohmi S, Shibuya M (2007). Novel antiangiogenic pathway of thrombospondin-1 mediated by suppression of the cell cycle. Cell Science 98: 1491-1497.

Yancopoulos GD, Davis S, Gale NW, Rudge JS, Wiegand SJ, Holash J (2000). Vascular specific growth factors and blood vessel formation. Nature 14:407: 242-248.

Yang M, Baranov E, Jiang P, Sun F, Li X, Li L, Hasegawa S, Bouvet M, Al-Tuwaijri M, Chishima T, Shimada H, Moossa A, Penman S and Hoffman RM (2000). Whole-body optical imaging of green fluorescent protein-expressing tumors and metastases. Proceedings of the National Academy of Sciences USA 97, 1206–1211.

Ye J, Gao Z, Yin J, He Q (2007). Hypoxia is a potential risk factor for chronic inflammation and adiponectin reduction in adipose tissue of ob/ob and dietary obese mice. American Journal of Endocrinology Metabolism 293: E118-E1128.

Yeaman SJ (2004). Hormone-sensitive lipase--new roles for an old enzyme. Biochemical Journal 379(1): 11-22.

Yin D, Clarke SD, Peters JL, Etherton TD (1998). Somatotropin-dependent decrease in fatty acid synthase mRNA abundance in 3T3L-F442A adipocytes is the result of a decrease in both gene trancription and mRNA stability. Biochemical Journal 331: 815-820.

Yokoyama C, Wang X, Briggs MR, Admon A, Wu J, Hua X, Goldstein JL, Brown MS (1993). SREBP-1, a basic-helix-loop-helix-leucine zipper protein that controls transcription of the low density lipoprotein receptor gene. Cell 75: 187-197.

Yu J, Cao Q, Mehra R, Laxman B, Yu J, Tomlins SA, Creighton CJ, Dhanasekaran SA, Shen R, Chen G, Morris DS, Marquez VE, Shah RB, Ghosh D, Varmabally, Chinnaiyan AM (2007). Integrative genomics analysis reveals silencing of β-adrenergic signalling by polycomb in prostate cancer. Cancer Cell 12: 419-430.

Yu GY, Lee KJ, Gao L, Lai MM (2006). Palmitoylation and polymerization of hepatitis C virus NS4B protein. Journal of Virology 80(12): 6013-23.

Zardi EM, Zardi DM, Cacciapaglia F, Dobrina A, Amoroso A, Picardi A, Afeltra A (2005) Endothelial dysfunction and activation as an expression of disease: role of prostacyclin analogs. International Immunopharmacology 5*:437-459*

Zechner R, Strauss JG, Haemmerle G, Lass A, Zimmermann R (2005). Lipolysis: pathway under construction. Current Opinions in Lipidology 16(3): 333-40.

Zhang QX, Magovern CJ, Mack CA, Budenbender KT, Ko W, Rosengart TK (1997). Vascular endothelial growth factor is the major angiogenic factor in omentum: mechanism of the omentum-mediated angiogenesis. Journal of Surgical Research 67:147-154.

Zhang, HH, Halbleib, M, Ahmad, F, Manganiello, VC, Greenberg, AS (2002). Tumor necrosis factor-alpha stimulates lipolysis in differentiated human adipocytes through activation of extracellular signal-related kinase and elevation of intracellular cAMP. Diabetes 51**:**2929-2935.

Zhang B, Kirov S, Snoddy J (2005) WebGestalt: an integrated system for exploring gene sets in various biological contexts. Nucleic Acids Res 1;33 (Web Server issue):W741-8.

Zhu W and Smart EJ (2005). Myristic acid stimulates endothelial nitric-oxide synthase in a CD36- and an AMP kinase dependent manner. The Journal of Biological Chemistry 280: 29543-29550.

Zimmermann R, Strauss JG, Haemmerle, G, Schoiswohl, G, Birner-Gruenberger R, Riederer M, Lass A, Neuberger G, Eisenhaber F, Hermetter A, Zechner R (2004). Fat mobilization in adipose tissue is promoted by adipose triglyceride lipase. Science 306(5700): 1383-6.

Zweier JL, Wang P, Samouilov A, Kuppusamy P (1995). Enzyme-independent formation of nitric oxide in biological tissues. Nature Medicine 1(8): 804-9.